The *Ostm1* osteopetrotic gene modulates lymphoid lineages

By

Marie S. Mutabaruka, M.Sc.

Division of Experimental Medicine
Faculty of Medicine
McGill University, Montréal

A thesis submitted to the Faculty of Graduate Studies and Research of McGill University in partial fulfillment of the requirements for the degree of Doctor of Philosophy in Experimental Medicine

Supervisor: Dr. Jean Vacher
Laboratory of Cellular Interactions and Development
Institut de Recherches Cliniques de Montréal

Montréal, Québec, Canada

March, 2016

To Mom, Dad, all Mutens and my family up there…

…

ABSTRACT

A null spontaneous mutation of the *Ostm1* (Osteopetrosis associated transmembrane protein 1) gene is responsible for the most severe form of the autosomal recessive osteopetrotic phenotype in the grey lethal (*gl/gl)* mouse and the human patient. *gl/gl* mice are characterized by non-functional bone-resorbing cells (osteoclasts), altered T-lymphoid differentiation, and decreased B-cell populations. When transgenesis was used to rescue these osteopetrosis-associated phenotypes; only PU-1-*Ostm1gl/gl* transgenic animals demonstrated rescue of osteopetrotic and hematopoietic B and T cells defects. These data indicated that *Ostm1* gene may either have an unknown function in other hematopoietic cells and may be involved in a crosstalk mechanism between hematopoietic cells for osteoclast activation.

The research goal of my thesis was to determine the role of the *Ostm1* gene mutation in the defective T cell and B cell homeostasis of the osteopetrotic *gl/gl* mouse model. To this end, *in vivo* studies in *gl/gl* hematopoietic tissues such as the thymus, spleen, and bone marrow allowed me to further characterize the osteopetrotic T cell and B cell phenotype.

My studies revealed the expression pattern of *Ostm1* from early to mature T cell populations, supporting a potential unknown role for the *Ostm1* gene in thymic homeostasis. Furthermore, flow cytometry experiments allowed me to identify the early and time-dependent T cell developmental arrest exhibited by the severe deficit of DP ($CD4^+CD8^+$) cells and the lower percentage of early T cell populations in *gl/gl* thymi. *Ostm1* expression was also ectopically expressed from early to mature T cell populations under the control of the CD2 promoter. CD2-*Ostm1* transgene expression was mainly detected in the thymus, spleen, and bone marrow of transgenic animals. Interestingly, flow cytometry analysis showed a rescue in the distribution of T cells in all CD2-*Ostm1gl/gl* transgenic mice, but these mice maintained compromised bone marrow cavities, bone defect and premature death. Together, these data demonstrate the early cell-autonomous role for *Ostm1* in the thymus-dependent T cell development

RNA sequencing illustrated differential transcriptome profiles between early T populations of *gl/gl* thymi compared to control, with significant expression differences in genes involved in cell migration. Importantly, these transcriptome variations were corrected in early T population of CD2-*Ostm1 gl/gl* thymus, indicating an *Ostm1* function in early T cell trafficking.

This study also investigated on the B cell phenotype associated with *gl/gl* osteopetrosis. In this case, the *Ostm1* mutation results in a total B cell deficit detected in the *gl/gl* spleen a few days after birth. This total B cell deficit also correlated with a significant reduction in immature and mature B subsets which also corresponded to early B cell development arrest. Surprisingly, expression of *Ostm1* gene exclusively in the B cell lineage under the control of the CD19 promoter did not rescue the *gl/gl* B cell defect, implicating the contribution of the compromised bone marrow in the phenotype of B lineage in the *gl/gl* spleen. Furthermore, the Mb1-Cre mediated deletion of *Ostm1* in early B cells showed no B cell phenotype. Therefore, both assays strongly indicate an indirect function of *Ostm1* in the defective B cell physiology of the osteopetrotic *gl/gl* mouse, possibly through regulation of bone marrow homeostasis.

Collectively, these data demonstrate the intrinsic role of *Ostm1* in the abnormal distribution of the T cell lineage and its indirect function in the depletion of the B cell population of *gl/gl* animals. These findings are the first to link the *Ostm1* mutation to the higher susceptibility to infections depicted in most osteopetrotic patients. Moreover, these data illustrate another promising characteristic of the *gl/gl* mouse as an animal model in osteoimmunology studies.

Keywords: *Ostm1*, osteopetrosis, *grey-lethal*, T cell, B cell, transgenic, Cre, lox, knockout, osteoimmunology

RÉSUMÉ

La mutation spontanée du gène *Ostm1* (Osteopetrosis associated transmembrane protein 1) est responsable du plus sévère phénotype d'ostéopétrose autosomale récessive chez le modèle de souris *grey-lethal* (*gl/gl*) et le patient humain. Les souris *gl/gl* se caractérisent par des cellules résorbant la matrice osseuse (ostéoclastes) qui ne sont pas fonctionnelles, une différenciation des cellules T altérée ainsi qu'un déficit de la population des cellules B. Lorsque la transgénèse a été utilisée pour corriger les phénotypes associés à l'ostéopétrose de la souris *gl/gl,* seul les animaux transgéniques PU-1-*Ostm1 gl/gl* ont démontrés une complémentation de l'ostéopétrose et des défauts des cellules B et T. Ces données nous ont indiqués que le gène *Ostm1* peut avoir une fonction inconnue dans d'autres cellules hématopoïétiques et/ou peut être impliqué dans un mécanisme bidirectionnel entre les cellules hématopoïétiques et l'activité des ostéoclastes.
L'objectif de recherche de ma thèse était de déterminer le rôle de la mutation du gène *Ostm1* dans le défaut d'homéostasie des cellules B et T détecté dans le model de souris ostéopétrotique *gl/gl*. À cette fin, des études *in vivo* ciblant les organes hématopoïétiques tels que le thymus, la rate, et la moelle osseuse m'ont permis de caractériser davantage le phénotype des cellules B et T ostéopétrotiques.

Mes études ont révélées le profil d'expression du gène *Ostm1* à partir de la population T précoce aux cellules matures, supportant un potentiel rôle inconnue du gène *Ostm1* dans l'homéostasie thymique. Des expériences de cytométrie en flux m'ont permis d'identifier un arrêt précoce et temps-dépendant de la différenciation des cellules T, qui est à la fois démontré par un déficit sévère des cellules DP ($CD4^+CD8^+$) et le faible pourcentage des cellules T précoces dans les thymus *gl/gl*. D'autre part, l'expression d'*Ostm1* a été rétablie dans les cellules précoces jusqu'aux populations T matures sous le contrôle du promoteur CD2. L'expression du transgène CD2-*Ostm1* a été principalement détectée dans le thymus, la rate, et la moelle osseuse des animaux transgéniques. Surprenamment, les analyses par cytométrie ont montrés une correction de la distribution de la population T dans toutes les souris transgéniques CD2-*Ostm1 gl/gl*, mais ces souris ont maintenu des cavités de moelle osseuse anormales, une résorption osseuse défectueuse et une mort précoce. Ensemble, ces données ont démontrés un rôle intrinsèque d'*Ostm1* très tôt dans le développement des cellules T dépendant du thymus.

Le séquençage d'ARN a illustré des profils de transcriptome différents entre les cellules T précoces des souris *gl/gl* comparé aux contrôles, avec des différences d'expression significatives dans les gènes impliqués dans la migration cellulaire. De manière intéressante, ces variations au niveau du transcriptome ont été corrigées dans la population T précoce des thymus CD2-*Ostm1 gl/gl* transgéniques, indiquant une fonction d'*Ostm1* dans le trafic des cellules T précoces.

Cette étude s'est aussi intéressée au phénotype des cellules B qui est associé avec l'ostéopétrose de *gl/gl*. Dans ce cas, la mutation d'*Ostm1* a induit une déplétion de la totalité des cellules B détectée dans la rate *gl/gl* peu après la naissance. De plus, ce déficit corrélait également avec une réduction significative des cellules B immatures et matures ainsi qu'un arrêt de la différenciation de la population B précoce dans la rate *gl/gl.* Surprenament, l'expression du gène *Ostm1* exclusivement dans la lignée B sous contrôle du promoteur CD19 n'a pas corrigé le défaut des cellules B de *gl/gl*, ce qui implique une contribution du défaut de la moelle osseuse dans le phenotype de la lignée B dans la rate *gl/gl*. D'autre part, l'ablation d'*Ostm1* médié par la Mb1-Cre a généré une population B sans phénotype apparent. Ainsi, ces deux tentatives ont fortement suggéré une fonction indirecte de la mutation *Ostm1* dans le défaut physiologique des cellules B dans la souris ostéopétrotique *gl/gl*, possiblement à travers la régulation de l'homéostasie de la moelle osseuse.

Collectivement, ces données démontrent un rôle intrinsèque du gène *Ostm1* dans la distribution anormale de la lignée des cellules T et sa fonction indirecte dans la déplétion de la population des cellules B dans les animaux ostéopétrotique *gl/gl*. Ces découvertes constituent un premier lien entre la mutation d'*Ostm1* et la forte susceptibilité aux infections qui a été rapportée chez la plupart des patients ostéopétrotiques. De plus, ces données illustrent une caractéristique prometteuse de la souris *gl/gl* en tant que modèle animal pour des études en ostéoimmunologie.

Mots-clés: Ostm1, osteopétrose, *grey-lethal*, cellules T, cellules B, transgénèse, Cre, lox, knockout, osteoimmunologie

ACKNOWLEDGEMENTS

I would like to express my sincere gratitude to Dr. Jean Vacher for his unlimited support during this entire journey. Jean has been an excellent mentor during my degree by providing constant encouragement, detailed and frequent supervisory advices, and financial support. He has also exemplified the professional attitude, work ethic and discipline to succeed any project. Thank you so much for these life and scientific lessons, your trust, and for allowing me to freely manage these interesting projects and to learn science communication during several national and international meetings.

I am also very grateful to Monica Pata who has been a very lovely and helpful lab sister from the first day. Thank you for your mentorship and complicity in several areas including research techniques and analysis, time organization, work ethic, and nutrition habits ☺ as well as work and personal life balance.

Jean and Monica have been understanding, encouraging and inspiring labmates. Their love for science and insatiable curiosity has fueled my scientific growth and eased the difficult steps.

I would also like to acknowledge both past and present members of the lab: Adam Griffith, Dr. Maya Boudiffa, and Sana Ghani, for their contribution to my scientific growth with many brainstorming sessions and for the improvement of my analytical and communication skills; Dr. Murthy, Eric Migeon, Joris Zhou, Prabhas Chaudhari, Veronica Nguyen, Daniella, Hailey Kim, and Eva Lee, for their support and help with experiments, Dr. Lina Saad, Billy Liu, and Cameron Bauer, for their kind words of encouragements during the thesis writing.

My research progress has been tremendously stimulated by the kind suggestions, fresh ideas, and regular feedback from members of my advisory thesis committee, including Dr. Javier Di Noia, Dr. John DiBattista, and Dr. Éric Lécuyer. Thank you all for your unlimited time and constant encouragements. I would especially like to thank Dr. Nathalie Labrecque, who has provided reagents and for her generous and stimulating input for immunology experiments.

The past six years and half at Institut de Recherches Cliniques de Montréal (IRCM) have been blessed with unexpected friendships, complicity, fun memories, kindness, smiles, and countless supportive gestures from the IRCM community. I would like to acknowledge Éric Massicotte and Julie Lord (Flow cytometry) for the technical help and data analysis; members of Dr. Tarik Moroy laboratory, especially Marissa, Charles, Jennifer, Hugues and other present and past members for their generous technical assistance, laughs and support, my colleagues from Dr. Marie Trudel, Dr. Nabil Seidah, Dr. Jean-François Côté, Dr. DiNoia, and Dr. Jacques Archambault laboratories for sharing reagents, technical assistance, scientific discussions, and life lessons; the Sodexo team (Marc, Chantal, Monique, and Bérénika) for the yummy dishes which have completely transformed my diet habits, Johanne Langevin and Virginie Leduc for their guidance; Stéphane Létourneau for informative discussions, as well as Dr. Dominic Maier, Rénée, Lise, and Linda.

A huge thank you to: Manishha, Marissa, Scott, Brandon, and Nicole for helping in the formatting and the editing of my thesis.

Research is comparable to a marathon and there is no better training for perseverance than regular exercising! Thanks to Steve Morin for his contagious energy and for introducing me to running, and to my past and present training partners including Julie Lord, Léa Lepelletier, Jennifer Alvarez, Claude and Xuan Nguyen.

Thank you to these amazing and inspiring women who have taught me what is being courageous, dedicated to my dreams, perseverant, outspoken, curious, and hard-working: Dr. Marie Trudel, Dr. Anik Prat, Ann Chamberland, Dr. Amélie Fradet-Turcotte and Dr. Manishha Patel.

I would like to recognize the IRCM Foundation (J.H.Lafleur scholarship) and Réseau de recherche en santé buccodentaire et osseuse (RSBO) for financial support.

I would also like to express my deepest gratitude to the following IRCM companions: Monica Pata, Marissa Rashkovan, Jennifer Alvarez, Marine Barbelanne, Almira Kurbegovic, Michael Lehoux,, Olivier Côté, Brandon Vaz, Chris Law, Eric Massicotte, and Julie Lord, for the countless hours we have spent together filled with supportive gestures and in many ways by teaching, listening, being helpful, and for the multiple fun memories.

To my amazing and long-time friends, Amélie, Audrey, Josée, Mikelsie, Sophia, Mike, Marc, Mélissa, Marie-France, José, and the Laurentides, all of you have contributed a lot to my well-being, personal growth and happiness throughout these years. Thank you so much for EVERYTHING!!

The last but not the least, my wonderful Mom and Dad, Clarissa, Diane, and Éric, who have nurtured this experience with their unconditional love, sacrifices, exemplar hard-working and continuous encouragements that have led me to this life stage despite the geographical distance.

TABLE OF CONTENTS

LIST OF FIGURES

APPENDIX 2: SUPPLEMENTARY MATERIAL

LIST OF TABLES

ABBREVIATIONS

ARO: Autosomal Recessive Osteopetrosis
BAC: Bacterial Artificial Chromosome
BM: Bone marrow
CD2: Cluster of differentiation 2
cKO: Conditional Knock-Out
CLP: Common Lymphoid Progenitor
CMJ: Cortico-medullary junction
cTECs: Cortical thymus epithelial cells
CXCL-12: Chemokine (C-X-C Motif) Ligand 12)
DEGs: Differentially Expressed Genes
DP: Double positive $CD4^{+}CD8^{+}$
DN: Double Negative $CD4^{-}CD8^{-}$
E: Embryonic day
ETPs: Early Thymic progenitors
FACS: Fluorescence Activating Cell Sorting
gl/gl: Grey-lethal mutation
***gl/gl*TR:**gl/gl transgenic mice
H&E: Hematoxylin and Eosin
HSC: Hematopoietic Stem Cells
LSK: $Lineage^{-}Sca1^{+}Kit^{-}$
MCSF: Macrophage Colony Stimulating Factor
mTECs: Medullary thymus epithelial cells
NCCs: Neural crest cells
NFATc1: Nuclear factor of activated T cells cytoplasmic
Ostm1: Osteopetrosis associated transmembrane protein 1
OB: Osteoblast
OC: Osteoclast
P: Post-natal day
qPCR: Real time Polymerase Chain Reaction
Rac1: Rac GTPase 1
RNA: Ribonucleic acid
RANK: Receptor activator of nuclear factor-κb
RANKL: Receptor activator of nuclear factor-κb ligand
RA: Rheumatoid arthritis
RNA Seq: RNA sequencing
SDF-1: Stroma derived factor 1
SP: Single positive $CD4^{+}$or $CD8^{+}$
S1P: Sphingosine -1- phosphate
S1pr1: Sphingosine -1- phosphate receptor 1
TECs: Thymus epithelial cells
TSPs: Thymus seeding progenitors
WT or +/+: Wild-type

PREFACE & CONTRIBUTION OF AUTHORS

ARTICLE 1. **OSTEOPTROTIC GREY-LETHAL MUTATION DISRUPTS THYMUS-AUTONOMOUS T CELL DIFFERENTIATION**

Marie Mutabaruka, Monica Pata, Nathalie Labrecque and Jean Vacher

J.V designed the initial research project. M.M executed the experimental research, collected and interpreted data with general assistance from J.V. and M.P. In addition, N.L. contributed to experimental design and data interpretation for immunology experiments. M.M, N.L and J.V designed the experimental strategy. M.M wrote the manuscript which was reviewed by J.V and N.L.and approved by all authors. This research paper is in preparation to be submitted to Journal of Experimental Medicine.

ARTICLE 2. **CHARACTERIZATION OF THE B CELL POPULATION DEFECT IN *gl/gl* OSTEOPETROTIC MICE**

Marie Mutabaruka, Eva Lee, Monica Pata, and Jean Vacher

J.V designed the initial research project. M.M executed the experimental research, collected and interpreted data with general assistance from J.V. and M.P. Also, E.L have executed analysis and prepared figures for the condition knock-out experiments. In addition, M.M and J.V designed the experimental strategy. M.M wrote the manuscript which was reviewed by J.V. and approved by all authors. This research paper is in preparation.

Technical contributions:

Animal breedings & weanings, genotyping and tissue dissections

Tissue homogenization and cell counting

Flow cytometry staining protocols design and execution

Flow cytometry data analysis, interpretation and presentation

DNA, mRNA and protein isolation or quantification

Semi-quantitative and real-time PCR

Western and Southern blots

Cell-culture using the OP9-DL4 co-culture assay

Microscopy image acquisition

Cloning of Cathepsin K-*Ostm1* transgene construct to generate Ctsk-*Ostm1 gl/gl* transgenic mice

My thesis work presents original contributions to knowledge including:

- Establishment of the *Ostm1* expression profile in all different cell subpopulations during the T cell development with significant expression in ETP/DN1$^{c\text{-}Kit\ hi}$ and DP populations.
- Illustration of the time-dependent defect of T cell differentiation of the osteopetrotic *gl/gl* mice appearing 15 days after birth.
- Description of the DN1-DN2 differentiation arrest leading the drastic loss of DP cells in the *gl/gl* thymi.
- Visualization of the time-dependent defect in thymic structure and architecture of *gl/gl* mice.
- Generation and characterization of the transgenic CD2-*Ostm1 gl/gl* transgenic animal model.
- Observation of the cell-intrinsic function of the osteopetrotic *Ostm1* gene in T cell differentiation independent of the osteoclast activity.
- RNA sequencing of *gl/gl* DN1 population revealing important changes in cell migration genes *Rac1* and *S1pr1* in the absence of *Ostm1* gene.
- Generation of the transgenic animal models CD19-*Ostm1 gl/gl* and the conditional knock-out *Ostm1*^{loxlox} Mb1-Cre^{+} animals.
- Identification of an early B cell loss in *gl/gl* animals from 8 days after birth.
- Proofs of an indirect role of the osteopetrotic *Ostm1* gene in the B cell physiology, possibly related to bone marrow homeostasis.
- Characterization of the T and B cell distribution of the Ctsk-*Ostm1 gl/gl* transgenic animal model.
- Indication of the importance of osteoclast activity in the homeostasis of T and B cell development in Ctsk-*Ostm1 gl/gl* animals.

During my doctoral studies, I have been awarded the Network for Oral and Bone Health Research (RSBO) doctoral scholarship (1st place) and the Jean H Lafleur doctoral scholarship (IRCM). Moreover, the significance of the research content of our first article has been distinguished in national and international scientific meetings with 9 presentation awards.

CHAPTER 1: REVIEW OF LITERATURE

1.1 BONE HOMEOSTASIS

Two hundred and six bones constitute the human skeleton. This material not only occupies 12-20 % of the human body weight, but also serves as the primary source of mineral stock such as ions and calcium. It also plays an important protective function for vital organs such as lungs, heart, liver and the brain. In addition, bone houses the marrow content (Tagliaferri, Wittrant et al. 2015). To accomplish these functions, the skeleton transfers forces from one body part to another with the help of cartilage, muscles, ligaments and tendons which relay loads between bones (Benjamin, Toumi et al. 2006, Tagliaferri, Wittrant et al. 2015). Globally, the mechanical features of bone allow compromise for the strength to absorb impact and the stiffness needed for the flexibility and the adaptability of the skeleton (Burstein, Zika et al. 1975, Cole and van der Meulen 2011).

The self-adaptive property of bone known as bone modeling or remodeling are required to reshape its structure, composition and functions for adjusting to micro-environmental and physiological changes (Seeman 2009). There is enhanced bone formation resulting from high concentration of sex hormones during late puberty (Falahati-Nini, Riggs et al. 2000, Teti 2011). This phenomenon called bone modeling, leads to uncoupled bone formation and bone resorption. In comparison, bone remodeling relies on the cooperation between osteoblasts (bone-forming cells) and osteoclasts (bone-resorbing cells) to maintain bone mass (Seeman 2009, Teti 2011). A balanced osteoblast-osteoclast coupling produces a healthy bone composite containing hydroxyapatite, collagen, small proteoglycan molecules, water, growth factors and non-collagenous proteins. Bone composition also varies with age, sex, species, the type of bone, and disease sensitivity (Lemaire, Tobin et al. 2004). Therefore, the tight control of osteoclast and osteoblast cell number and function is the crucial guardian of balanced bone remodeling, a process that is solicited throughout life during growth, bone micro-damage repairs and fracture healing (Lemaire, Tobin et al. 2004).

1.1.1 Osteoclasts in bone homeostasis

Osteoclasts (OC) originate from hematopoietic ancestors and directly derive from the monocyte/macrophage lineage progenitor cells. The fusion of mononuclear progenitor generates the mature tartrate-resistant-acid-phosphatase (TRAP) positive multi-nucleated osteoclast. Osteoclast differentiation is initiated by M-CSF (macrophage colony stimulating factor) controlling survival and proliferation of osteoclast progenitors as well as inducing RANK (receptor of RANKL) expression on these progenitor cells (Boyle, Simonet et al. 2003).

RANKL is produced and secreted by committed pre-osteoblasts before binding its corresponding receptor on the surface of osteoclast progenitors (Suda, Takahashi et al. 1999). These cells also express and secrete osteoprotegerin (OPG), a soluble decoy molecule that prevents the binding of RANKL to RANK receptor (Burgess, Qian et al. 1999, Lemaire, Tobin et al. 2004). The multiple PTH (parathyroid hormone) receptors on the osteoblast lineage stimulate RANKL expression while inhibiting OPG production, upon activation by PTH (Teitelbaum 2000, Lemaire, Tobin et al. 2004). The Wnt (Wingless related integration site)/β-catenin signaling pathway is important in osteoblast development and commitment and osteocytes also controls OPG stimulation (Baron and Kneissel 2013). The interplay between bone morphogenic proteins (BMPs) and Wnt/β-catenin favor osteoclastogenesis, as BMPs induce both sclerostin and DKK1 (Dickkopf Wnt signaling pathway inhibitor 1) secretion by late osteoblasts/osteocytes to inhibit the Wnt pathway. BMP2 also stimulates Wnt3a expression which in turn enhances osteoclastogenesis via BMP4 (Baron and Kneissel 2013). Additionally, the migration of osteoclast precursors from bone to blood is facilitated by S1P (sphingosine-1- phosphate) via its action on the receptor S1PR1 whereas the chemo-repulsion from bone to blood depends on the receptor S1PR2 (Ishii, Kikuta et al. 2010). S1P is mainly produced by blood cells and osteoclast-derived S1P is involved in osteoblast migration and recruitment (Lotinun, Kiviranta et al. 2013).

Once RANKL binds its receptor RANK, there is recruitment of TRAF-6 (TNF receptor-associated factor 6) and subsequent activation of the downstream signalling molecules including NFk-B, JNK, P38 and ERK. In addition, transcription factors such as MITF (Microphtalmia-Associated-Transcription Factor), c-Fos and NFATC1 (Nuclear factor of activated T cells cytoplasmic) are responsible for the differentiation process (Matsumoto, Kogawa et al. 2004, Kim and Kim 2014).

With the cooperation of MITF and c-Fos, NFATC1 is the key driver of multiple genes specific to osteoclasts such as TRAP, cathepsin K, calcitonic receptor and OSCAR (Lacey, Timms et al. 1998). Positive NFATC1 expression and activity are established with acetylation and ubiquitination while its inhibition is dependent on GSK3β (Kim, Kim et al. 2010, Jang, Shin et al. 2011). To potentiate NFATC1 function, the RANK/RANKL axis induces calcium oscillations through IP3/IP3R. Calcium then leads to calcineurin dependent dephosphorylation of NFATC1 and its translocation from the cytosol to the nucleus where it is transcriptionally active (Lacey, Timms et al. 1998, Ferron, Boudiffa et al. 2011). This calcium dependent NFATC1 induction is also supported by the RANK costimulatory signal provided by OSCAR (Osteoclast-associated receptor), ITAM harboring adapter, FcRgamma and DAP12 (DNAX-Activation Protein 12) (Nakashima and Takayanagi 2011). Furthermore, NFATC1 is down-regulated by M-CSF during the late stage of osteoclastogenesis via ubiquitin-mediated degradation in the cytosol with the contribution of Cbl (Casitas B-lineage lymphoma) and Src kinase proteins (Kim, Kim et al. 2010). Negative regulators of osteoclastogenesis such as Bcl6 (B cell lymphoma 6) normally bind cathepsin K and NFATC1 promoters in the absence of RANKL. Bcl6 is also negatively controlled by Blimp1(Miyamoto 2011). Additionally, the RANKL/NFATC1-dependent molecules DC-STAMP (dendritic cell specific transmembrane protein), CD9 and ATP6v0d2 (ATPase H^+ Transporting V0 Subunit D2) partner with RANKL independent molecules CD44, TRAM2 (Translocation-associate membrane protein 2) and CD47 mediating the cell-cell fusion of osteoclast progenitors (Xing, Xiu et al. 2012, Zhang, Dou et al. 2014).

Overall, inappropriate regulation of the mentioned key molecules can either alter the stability of osteoclast progenitors or fusion of mononuclear progenitors. This results in an abnormal number of mature osteoclasts and disrupts bone resorption leading to imbalanced bone remodeling.

1.1.1.1 Osteoclast morphology and resorptive activity

Mature osteoclasts are similar to epithelial cells in respect to their ability to polarize and form unique plasma membrane domains (Baron 1989, Szewczyk, Fuller et al. 2013). These membrane domains include the sealing membrane which covers the cytoplasmic area forming the sealing zone (**Figure 1.1a**). This membrane domain in contact with the future resorbed pit comprises an irregularly shaped membrane expansion called ruffled border, which is enriched in adhesion subdomains called podosomes (Domon, Yamazaki et al. 2002, Cappariello, Maurizi et al. 2014).

Actin filaments, actin binding proteins and adapter proteins compose podosomes that cluster in a single podosome belt in the peripheral area (**Figure 1.1b**) (Saltel, Chabadel et al. 2008, Schachtner, Calaminus et al. 2013). Moreover, they gather in a unique complex of one or more 'actin rings' that serves as an anchor to the bone area to be digested, in collaboration with integrin receptors (Gay and Weber 2000, Del Fattore, Teti et al. 2008). This structure also acts as an important cell signalling zone allowing calcium mobilization and recruitment and activation of other required proteins.

In addition, the basolateral membrane in proximity to the vascular compartment presents the 'fusion area' where lysosomal vesicles carrying ions and the lysosomal enzymatic cocktail for matrix resorption merge with the ruffled border (**Figure 1.1c**) (Cappariello, Maurizi et al. 2014). This same membrane domain manages the recycling of bone degradation products, cell membranes and lysosomal enzymes as well as vesicular trafficking. This transcytosis trajectory is driven through a secretory domain with the help of other partners such as GTP-binding molecules, microtubules and PLEHKM1 (Pleckstrin homology domain-containing family M member 1) (Hirvonen, Fagerlund et al. 2013, Cappariello, Maurizi et al. 2014).

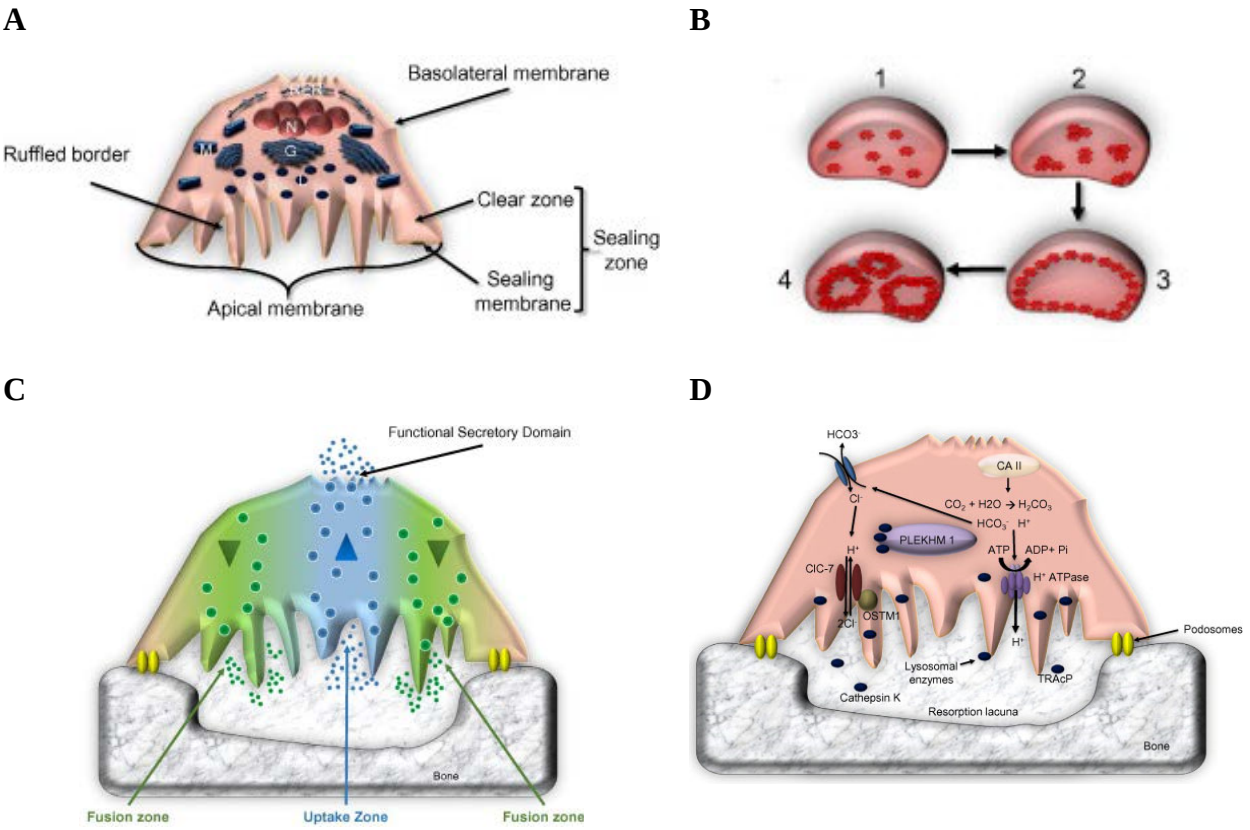

Figure 1.1. Membrane domains and bone resorption activity of osteoclasts.

A) Summary showing the structure and localization of the multiple membrane microdomains of osteoclasts comprising ruffled border, apical membrane, sealing zone and basolateral membrane. B) Dynamic of peripheral localization of podosomes: A single podosome at the initial phase of OC attachment (1); clusters of podosomes to enhance cell-adhesion (2) before forming a podosome belt in fully attached OCs (3) and actins rings (4) during bone resorption. C) The multiple cell trafficking functions of OC involve fusion and uptake zones as well as the functional secretory domain. D) Interaction of ion channels in the resorption lacuna to support bone resorption. Figure is adapted from (Cappariello, Maurizi et al. 2014).

The fast turnover and quick modulation of all these membrane domains dictate the tight and dynamic attachment of osteoclasts to the bone in order to digest the matrix component (Blair, Kahn et al. 1986, Silver, Murrills et al. 1988). During bone resorption, the sealing zone tightly and efficiently isolates the resorption lacuna underneath the ruffled border that features low pH and increased calcium concentration (Silver, Murrills et al. 1988). In addition, bone resorption is initiated by acidification to degrade the bone hydroxyapatite mineral followed by collagen breakdown by cathepsin K (Zaidi, Troen et al. 2001).

The acidification process is supported by ion exchangers including the V-H^+ATPase pump, the chloride ion channel-7 (ClC7) with its subunit OSTM1 (osteopetrosis associated membrane protein 1), all located on the ruffled border (**Figure 1.1d**) (Cappariello, Maurizi et al. 2014). In contrast, the dynamic membrane of the osteoclast lineage is also required for the fusion of osteoclast progenitors. The fusion process includes recruitment and alignment of adhesion molecules to the membrane followed by an interaction of these adhesion molecules leading to actin rearrangement and intracellular signal transduction (Zhou and Platt 2011). Moreover, inhibition of the RANK/RANKL-dependent fusion molecule DC-STAMP leads to osteoclasts with fewer nuclei and a smaller bone resorbed pit, suggesting that osteoclast fusion is also involved in bone resorption (Yagi, Miyamoto et al. 2005, Oursler 2010).

Importantly, bone matrix removed during bone resorption must be quickly replaced by newly recruited osteoblasts during the reversal phase, to balance bone mass throughout a lifetime (Delaisse 2014).

1.1.1.2 Osteoclasts and bone formation

In the basic multicellular unit (BMU), the coupling between osteoclasts and osteoblasts is turned on by growth factors released from the resorbed bone matrix including; transforming growth factor-β (TFG-β), insulin growth factor (IGF), platelet derived growth factor (PDGF) and bone morphogenic protein-2 (BMP-2)(Parfitt 1994, Hughes, Collyer et al. 1995, Tang, Wu et al. 2009, Xian, Wu et al. 2012, Sims and Martin 2015). These growth factors ensure recruitment, migration, survival, commitment and differentiation of pluripotent MSC (mesenchymal stem cells) progenitors (Oreffo, Cooper et al. 2005). These progenitors form the envelope surrounding the red-bone marrow and are found in close proximity to osteoclasts.

In parallel, osteoclasts secrete PDGF-BB which functions as a chemoattractant for pre-osteoblasts (Sanchez-Fernandez, Gallois et al. 2008). The subsequent recruitment, commitment and differentiation of activated osteoblasts is supported by other osteoclast-derived molecules such as Wnt10b, BMP-6, Cthrc1 (collagen triple-helix repeat containing1), C3a (complement component 3a) and S1P (Sphingosine-1-Phosphate) (Hughes, Collyer et al. 1995, Ikeda and Takeshita 2014).

Osteoclasts have been hypothesized to interact directly with immature and mature osteoblasts via membrane-bound factors including Ephrin B2 or Semaphorin 4D, which control positive and negative regulation of osteoblast activity, respectively (Zhao, Irie et al. 2006, Negishi-Koga, Shinohara et al. 2011). Most of these coupling factors can also derive from other cell types including T cells, macrophages and endothelial cells (Sims, Quinn et al.). Moreover, the lining cells residing on the bone surface are also considered as intermediate messengers during the reversal phase separating bone resorption from bone formation. In fact, these quiescent bone cells have retracted to give access to osteoclasts. Following mechanical and hormonal stimulation, bone lining cells can mature into osteoblasts (Tran Van, Vignery et al. 1982, Delaisse 2014). In the absence of other cells, pre-osteoblasts also respond to the abnormal topography of the resorbed pit through the induction of filopodia formation and cytoskeletal changes facilitating cell adhesion and subsequent differentiation (Dalby, McCloy et al. 2006).

Finally, embedded mature osteoblasts in bone matrix are termed osteocytes. The osteocytes produce pro-osteoclastogenesis factors such as M-CSF and RANKL (Mulcahy, Taylor et al. 2011). Mature osteocytes express both Dentin matrix acidic phosphoprotein-1 (DMP-1) and Matrix extracellular phosphoglycoprotein (MEPE), two important factors for bone mineralization and bone resorption (Kogianni and Noble 2007, Alford, Kozloff et al. 2015). In parallel, they are sensitive to osteoclast-derived molecules, including CT-1 (Cardiotrophin-1) ,which once combined with low mechanical loading ensure that sufficient bone is formed (Walker, McGregor et al. 2010, Sims and Martin 2015). To stimulate bone formation, recruitment and survival of MSC progenitors is ensured by TGF-β derived from osteoclasts (Mundy, Boyce et al. 1995). Furthermore, the transcription factor Runx2 (runt-related transcription factor 2) guides their commitment to the osteoblastic lineage (Choi, Lee et al. 2002, Zhao, Zhao et al. 2005).

Runx2 drives the synthesis of proliferation and differentiation genes including: ALP (alkaline phosphate), Col I (collagen type I), Bsp (bone sialoprotein) and Bglap (osteocalcin) with its downstream target, Osterix (Titorencu, Pruna et al. 2014). Mature osteoblasts organize in clusters at the bone surface, actively produce an organic matrix content of collagen type I as well as non-collagenous proteins (Giachelli and Steitz 2000, Titorencu, Pruna et al. 2014). As previously mentioned, mature osteoblasts positively or negatively influence osteoclastogenesis in conjunction with secretion of RANKL and its binding inhibitor, OPG in response to the dynamic skeletal changes (Burgess, Qian et al. 1999).

1.2 BONE HOMEOSTASIS AND HEMATOPOIESIS

In mammals, all cellular blood components derive from HSCs (hematopoietic stem cells) during hematopoiesis which is located in specialized niches in the bone marrow (Zhang, Niu et al. 2003). These marrow niches for HSCs control cell fate by regulating quiescence, proliferation, migration and differentiation. Hematopoiesis involves a multi-cellular complex including HSCs, MSCs (mesenchymal stem cells), CAR (CXCL-12-abundant reticular) cells, osteoblasts, osteoclasts and multiple other cell types (Blin-Wakkach, Rouleau et al. 2014). HSC niches localize near the endosteum, a connective tissue inside the medullary cavity of long bones. This region is also rich in sinusoidal vessels and corresponds to the initial point of osteoclast bone resorption activity (Zhang, Niu et al. 2003, Calvi 2006). This physical proximity advocates for the importance of bone signals in HSCs homeostasis.

1.2.1 Establishment and regulation of hematopoiesis in bone marrow

Prior to bone marrow formation, murine fetal hematopoiesis begins at E9.5-E10 (embryonic day) in the aorta-gonad-meso-nephros region (**Figure 1.2.**) and transits to the fetal liver at E12.5 to E17.5 and the spleen at E13.5 (Medvinsky, Samoylina et al. 1993, Blin-Wakkach, Rouleau et al. 2014). The fetal mobilization of HSCs to the bone marrow at E15.5 is associated with endochondral ossification (**Figure 1.2.**), a process that allows the patterning of the marrow cavity by chondrocytes (Olsen, Reginato et al. 2000, Kronenberg 2003). The signals emanating from chondrocytes induce mesenchymal condensation, differentiation of perichondrial cells in osteoblasts and formation of the required blood vessels by recruiting angiogenic factors (Olsen, Reginato et al. 2000).

Absence of bone resorption activity in an osteopetrotic context results in few or absent HSC niches and bone marrow failure in mice (Dougall, Glaccum et al. 1999) and humans (Nicholls, Bredius et al. 2005). The relocation of hematopoiesis to the spleen and liver of osteopetrotic mice and patients illustrates the interdependence between osteoclast activity and post-natal hematopoiesis (Blin-Wakkach, Rouleau et al. 2014).

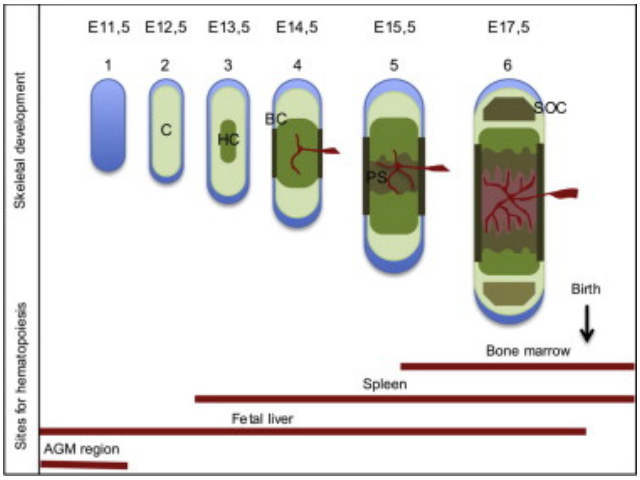

Figure 1.2. Embryonic bone development and early establishment of hematopoiesis. This figure shows the beginning of early hematopoiesis in the AGM (aorta-gonad-meso-nephros) region before its progressive shift to the bone marrow following endochondral ossification steps represented by number 1-6. C: cartilage; HC: hypertrophic cartilage; SOC: Secondary ossification center; PS: Primary spongiosa; BC: Bone collar. Figure is adapted from (Blin-Wakkach, Rouleau et al. 2014) **.**

1.2.1.1 HSC recruitment and maintenance

Bone resorbing activity and bone remodeling are responsible for maintenance of the marrow space serving as the HSC supporting micro environment (Blin-Wakkach, Rouleau et al. 2014). Inactive osteoclasts have been shown to induce fibrosis interfering with hematopoietic niche formation (Teti 2012). In contrast, restoration of osteoclast activity translates to improved bone structure and enhanced HSC homing (Mansour, Wakkach et al. 2012).

Furthermore, calcium derived from resorbed bone matrix accumulates on the endosteum bone to recruit and retain HSC-expressing calcium sensing receptors, crucial cells in post-natal hematopoiesis (Omatsu, Sugiyama et al. 2010). Other osteoclast-derived molecules including MMP9 (Matrix Metallopeptidase 9) and cathepsin K cleave SDF-1 (Stroma derived factor 1) or CXCL-12 (Chemokine (C-X-C Motif) Ligand 12) produced by osteoblasts to facilitate HSC anchorage to the niche (**Figure 1.3**) (Teti 2012). Therefore, absence of osteoclast activity can affect key molecules in HSC homing such as SDF-1 (CXCL-12), Jag-1 and KL1, which are produced by mesenchymal cells (Kimura, Ding et al. 2011, Blin-Wakkach, Rouleau et al. 2014). Additionally, delayed osteoclast (OC) migration and motility in *Cbl*$^{-/-}$ mice lead to an abnormal vasculature in the bone marrow, which blocks subsequent HSC colonization (Chiusaroli, Sanjay et al. 2003).

As previously described, regulation of bone formation through MSC commitment and subsequent mature osteoblast and osteoclast coupling have an indirect effect on the HSC niche (Mansour, Abou-Ezzi et al. 2012). In fact, most important growth factors (e.g. TGF-β) in bone homeostasis also modulate HSC proliferation and survival (Tang, Wu et al. 2009). Once in the marrow niche, HSC are maintained by SDF1 (CXCL-12), Jagged-1, TGF-β, and osteopontin, which explains their limited presence in the bloodstream (Lapid, Glait-Santar et al. 2008, Blin-Wakkach, Rouleau et al. 2014). The correlation between the high number of HSCs and osteoblasts suggests a regulation of HSC maintenance and proliferation by bone formation (Calvi, Adams et al. 2003, Zhang, Niu et al. 2003). All these observations illustrate the close relationship of bone and hematopoiesis.

1.2.1.2 HSC mobilization and fate

The dynamic interaction between HSCs and bone niches coordinates their quiescent, proliferative and differentiation state (Blin-Wakkach, Rouleau et al. 2014). Furthermore, the circadian oscillations impact on bone remodeling and osteoclast activity have been shown to maintain low HSC mobilization (Mendez-Ferrer, Lucas et al. 2008). The HSC migration from bone-marrow is controlled by SDF-1 (CXCL-12) expression which is dependent on the β-adrenergic pathway (Lapid, Glait-Santar et al. 2008, Scadden 2008).

Additionally, adrenergic receptor expression on osteoclasts and osteoblasts is stimulated by stress signals deriving from the nervous system. RANKL secretion from osteoblast is therefore potentiated in response to adrenergic agonists, as well as subsequent high OCs number, bone resorption and HSCs mobilization (Takeuchi, Tsuboi et al. 2001, Elefteriou, Ahn et al. 2005, Li, Zhai et al. 2013).

Consequently, active osteoclast-derived MMP9, cathepsin K and G participate in HSC egress by cleavage of the adhesion molecules VCAM-1 (vascular cell adhesion protein 1) and SDF-1 (**Figure 1.3.**) (Lévesque, Hendy et al. 2003). Massive egress of HSC can be promoted by various signals from bone, immune and nervous system in response to infections, bleeding or other stress stimuli (Lapid, Glait-Santar et al. 2008). This emergency hematopoiesis is generally under control of cytokines, adhesion molecules and growth factor regimens including CD44, VCAM-1, Flt3- ligand and G-SCF (granulocytes colony stimulating factor) (Mendelson and Frenette 2014).

Human and murine hematopoiesis are comparable but distinguished by specific cell-surface markers (Lensch and Daley 2004, Weissman and Shizuru 2008). In mice, HSCs are divided into HSC-LTs (long term hematopoietic stem cells) or HSC-STs (short- term hematopoietic stem cells) based on their ability to repopulate irradiated mice (Morrison, Wandycz et al. 1997). HSC-LTs are rare (1: 10000) compared to the higher frequency of HSC-STs (1:2000) and this rarity explains the difficulty and the lower success rate of bone marrow transplantation (Morrison, Uchida et al. 1995, Wagner, Barker et al. 2002). HSC-LTs undergo self-renewal and multi-lineage differentiation into lymphoid and myeloid progenitors giving rise to all mature blood cells (Dunn 1971, Ho, Medcalf et al. 2015). These cells are heterogenic in lineage restriction and differentiation potential (Ho, Medcalf et al. 2015)

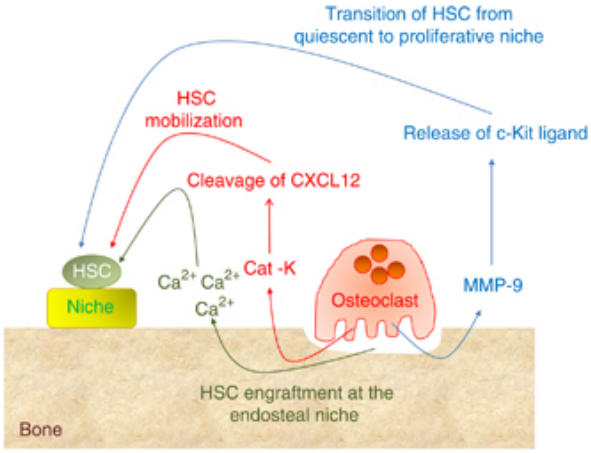

Figure 1.3. Crosstalk between bone resorption by osteoclasts and HSCs maintenance and mobilization.

Osteoclast-derived-secreted molecules such as MMP-9, cathepsin K and calcium facilitate respectively the release of c-Kit ligand and cleavage of anchorage molecule CXCL-12, then participating in HSC mobilization and niche maintenance. Figure is adapted from (Teti 2012).

1.2.1.3 HSC differentiation into lymphoid lineages

The multipotent HSC-LTs generate MPPs (multipotent progenitors)(Weissman 2000). Furthermore, LMPPs (lymphoid primed multipotent progenitors) derive from MPPs (**Figure 1.4**) and are characterized by an increased expression of FLT3 (Adolfsson, Mansson et al. 2005). Transcription factors Ikaros, E2A and PU-1 are crucial players in the primed lymphoid fate of HSCs (Yokota, Sudo et al. 2013, Miyazaki, Miyazaki et al. 2014). LMPPs can either differentiate into GMPs (granulocytes-macrophage progenitor cells) or CLPs (common lymphoid progenitors) (Kondo, Weissman et al. 1997, Wada, Masuda et al. 2008). GMPs possess the ability to generate macrophages or granulocytes while CLPs engender pDC (plasmacytoid dendritic cells), NK (natural killer), ILC (innate lymphoid cell), B and T cell lineages (Lai and Kondo 2006, Pronk, Rossi et al. 2007). CLPs also express the early lymphoid related marker IL-7Rα (IL7 receptor alpha chain)(Kondo, Weissman et al. 1997). In parallel, these cells upregulate the lymphoid related genes IgH and Tcrb while downregulating other genes specific to HSCs and myeloid cells. Satb1 (special AT-rich-sequence binding protein 1) is another crucial mediator of the lymphopoietic potential of HSCs that coordinate the spatial and temporal expression of genes involved in early lymphoid differentiation including IgH from embryonic and aged HSCs (Yokota, Sudo et al. 2013) (**Figure 1.4**).

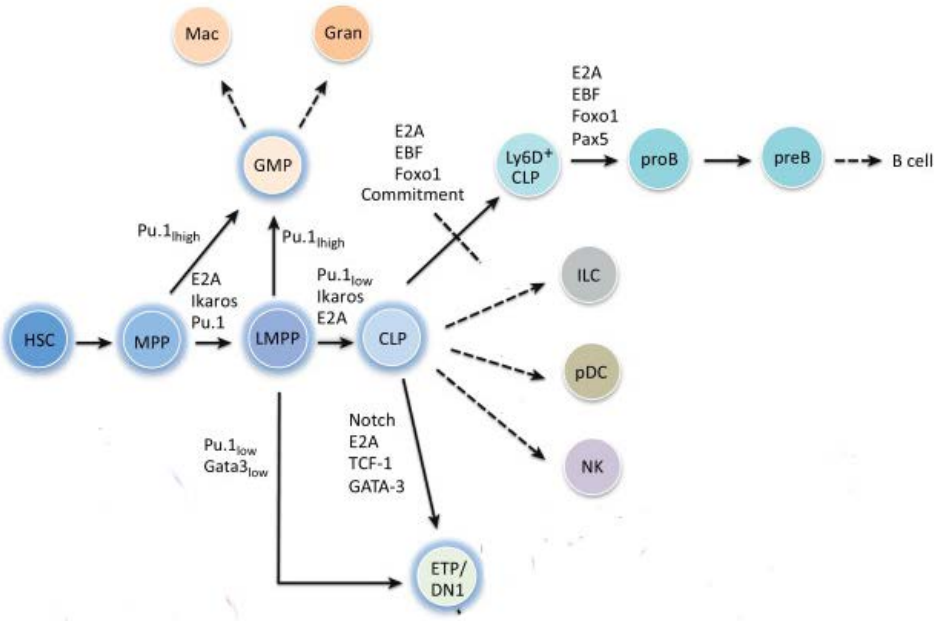

Figure 1.4. Pluripotent differentiation potential of HSCs into lymphoid and myeloid lineages.

This scheme summarizes the pluripotent fate of HSCs in various hematopoietic cell lineages that is under control of a transcriptional network including Gata3, PU-1, Ikaros, Ebf, Notch and E2A. HSC: Hematopoietic Stem Cell; MPP: Multipotent progenitor; LMPP: Lymphoid primed multipotent progenitor; GMP: Granulocytes-macrophage progenitor; CLP: Common lymphoid progenitor; ETP: Early thymic progenitor; pDC: plasmacytoid dendritic cells; ILC: innate lymphoid cell; NK: Natural killer; Mac: Macrophage; Gran: Granulocyte. Figure is adapted from (Miyazaki, Miyazaki et al. 2014).

CLPs are partitioned into a LYD6^{-} (lymphocyte antigen 6 complex, locus D) and LY6D^{+} fraction. LY6D^{+} cells differentiate into pre-pro-B and subsequently into committed pro-B cells (**Figure 1.4.**). They are therefore in favour of differentiation into the B cell lineage (Inlay, Bhattacharya et al. 2009, Mansson, Zandi et al. 2010). Commitment to the B cell lineage from LY6D^{+} CLPs is determined by the transcription network such as key regulators E2A, Foxo (forkhead box O1), Ebf (early B cell factor), Runx1 (Runt-related transcription factor 1) and Pax5 (paired box 5) (Seo, Ikawa et al. 2012, Miyazaki, Miyazaki et al. 2014).

CLPs also possess the ability to give rise to T cell lineage via the intermediate ETP (early thymic cell progenitors) (Bell and Bhandoola 2008, Wada, Masuda et al. 2008). The T lymphoid cell fate of CLPs is controlled by the transcription network including Notch, E2A, TCF-1 (T cell factor 1), Gata-3 (Gata-binding protein 3). In addition, low concentration of PU-1 and Gata-3 drive ETP differentiation from LMPPs (Miyazaki, Miyazaki et al. 2014) (See **Figure 1.4.**).

The physical proximity of immune cell progenitors to the bone marrow component, their common hematopoietic origin as bone resorbing osteoclasts, as well as HSC niche regulation by OC, strongly suggests the existence of cellular communication linking bone and immune system.

1.3 OSTEOIMMUNOLOGY: Crosstalk between bone and lymphoid lineages

Investigation into autoimmune RA (rheumatoid arthritis) has identified modulators derived from immune cells leading to excessive bone destruction (Choi, Arron et al. 2009). These findings led to the birth of osteoimmunology, a discipline that analyzes common molecules in the interplay between the skeletal and immune systems (Takayanagi 2007, Choi, Arron et al. 2009). So far, bone remodeling processes have been shown to occur independently of the immune cells. However, excessive bone destruction in RA patients implicates an enhanced osteoclast activity. The RA osteoimmunologic phenotype is illustrated by an increased RANKL expression from synovial fibroblasts in the inflamed joint and its induction by proinflammatory cytokines deriving from T cells (Choi, Arron et al. 2009). Also, in the RA synovium, activated $CD4^+$ T cells secrete RANKL. The most permissive T cell population for bone resorption is Th-17 T cell subset that expresses Foxp3 in response to IL-6 from synovial fibroblasts. To do so, Th-17 T cells demonstrate high expression of RANKL and induce high RANKL levels in synovial fibroblasts (Guerrini and Takayanagi 2014, Komatsu, Okamoto et al. 2014). Furthermore, pro-inflammatory cytokines that derive from T cells include TNF (tumor necrosis factor), IL-6 (Interleukin 6), IL-1β (Interleukin 1β and IL-17 (Interleukin -17) (Lam, Takeshita et al. 2000, Romas, Gillespie et al. 2002, Sato, Suematsu et al. 2006). TNF is connected to osteoclast formation through TNFRSF1A (tumor necrosis factor receptor superfamily, member 1A) and IL-1β is associated with RANK expression on osteoclast progenitors (Lam, Takeshita et al. 2000, Wei, Kitaura et al. 2005).

RANKL was first cloned in activated T cells. Its expression was detected in B and T cells upon activation (Anderson, Maraskovsky et al. 1997, Wong, Josien et al. 1997). As previously discussed, the RANK-RANKL axis is the main driver of osteoclastogenesis, and is therefore crucial for bone homeostasis through osteoclast and osteoblast coupling. Additionally, the RANK-RANKL axis modulates LTo (mesenchymal lymphoid tissue organizer cells) and LTi (lymphoid tissue inducing cells) responsible for tissue growth and organization of lymph node (Mueller and Hess 2012). Development and maintenance of embryonic and post-natal medullary epithelial cells in the thymus also depend on RANKL expression (Akiyama, Shimo et al. 2008, Akiyama, Shinzawa et al. 2013). Moreover, the reduced B cell number and the defective B cell development seen in *Rank* $^{-/-}$and *Rankl* $^{-/-}$ osteopetrotic mice, respectively, illustrate the intrinsic role of the RANK-RANKL axis in the B populations (Dougall, Glaccum et al. 1999, Kong, Yoshida et al. 1999, Manilay and Zouali 2014). Overall, these observations display the promiscuous function of RANKL in the skeletal and immune systems.

In summary, these studies support the existence of both direct and indirect crosstalk between bone cells and T and B cell lineages.

1.3.1 From bone homeostasis to primitive T cell lineage precursors

Contradictory studies have shown the heterogeneity of CLPs with subsets showing a dominant myeloid fate compared to their lymphoid developmental program. Therefore, myeloid differentiation cues must be shut down as a prerequisite for lymphoid lineage priming and commitment (Kondo 2010). Considering the myeloid origin of bone–resorbing osteoclasts, the early segregation between myeloid and lymphoid precursors may be a key in bone and immune conditions. Furthermore, the maintenance of differentiation activity in the myeloid lineage of fetal liver CLPs suggests that their restricted developmental scheme is acquired in the bone marrow (Mebius, Miyamoto et al. 2001). This fetal versus adult difference is hypothesized to result from the microenvironment content, especially the heterogeneous bone marrow environment including stroma, mesenchymal and other non-hematopoietic cells (Kondo 2010). CLPs are identified by their expression of IL-7 receptor subunits, IL-7Rα or common γ chain (γ_c)(Sims, Quinn et al.). However, unchanged CLPs number within *IL-7* $^{-/-}$ mice indicates that the IL-7 pathway may not be crucial for hematopoietic progenitor commitment in lymphoid lineages (Kikuchi, Lai et al. 2005).

Nevertheless, IL-7Rα remains a key indicator of early lymphoid progenitors in bone marrow and blood (Igarashi, Gregory et al. 2002, Krueger and von Boehmer 2007). A traffic control mechanism has been hypothesized to facilitate the lymphoid restricted fate of CLPs by bringing them into contact with lymphopoietic permissive environment (Svensson, Marsal et al. 2008). Additionally, LMPPs are localized to the inner marrow region whereas the myeloid progenitors are in proximity to the endosteum region (Lai, Watanabe et al. 2009). This physical distribution suggests an indirect relationship between primitive lymphoid precursors and bone cells, probably via the regulation of HSC niches as previously discussed in section 1.2.

1.3.1.1 Thymus seeding progenitors (TSPs) from bone marrow

The rarity of bone marrow progenitors in the blood corresponds to 1 in 100,000 nucleated cells; their rapid clearance from blood makes them very difficult to monitor and study (Wright, Wagers et al. 2001). The primitive thymus progenitors from the bone marrow are negative for lineage markers such as Ter119, Dlx5, CD3e, NK1.1, B220, TCRδγ, CD11, Gr-1, CD4 and CD8. However, they do display similar surface markers with LSKs including Sca-1 and cytokine receptor Kit (c-Kit). Thymus progenitors also include HSCs that are LSK $Flt3^-$(Adolfsson, Borge et al. 2001). The low frequencies of HSCs and LMPPs have been previously confirmed in the blood stream (Zlotoff and Bhandoola 2011, Zepponi, Michaels Lopez et al. 2015). TSPs reside among LMPPs and $FLT3^-$CLPs that are $CCR7^+CCR9^+$ as well as in the CLP-2 fraction. CTPs (circulating T progenitors) are another TSP characterized by $Lin^-Thy\text{-}1^+CD25^-$ initially identified in fetal and confirmed in adult mice (Bhandoola, von Boehmer et al. 2007). Moreover, the majority of primitive T cells are ETPs (early thymic progenitors) or DN1 Kit^{hi} cells that maintain a myeloid potential and a limited B cell potential. ETPs also possess a higher efficiency in $CD4^+CD8^+$ DP cell production (Bhandoola, von Boehmer et al. 2007). Importantly, these T lineage progenitors have to mobilize out of the bone marrow through the circulation to reach the T cell commitment and development center known as thymus.

1.3.1.1.1 Regulation of TSP mobilization and settling

Studies using intravenous transfer of LMPPs and CLPs have generated DP cells after three weeks but the same experiment have failed to generate DP cells from HSCs. Interestingly, intrathymic transfer of all three cell populations have been able to give rise to DP cells, suggesting the existence of selective external factors for thymus entry (Schwarz and Bhandoola 2006). First, the chemokine SDF-1α (CXCL12) and its receptor CXCR4 (Chemokine C-X-C Motif Receptor 4) guide the survival, proliferation and migration of BM progenitors (Lapidot and Petit 2002, Lee, Gotoh et al. 2002, Broxmeyer, Cooper et al. 2005). CXCR4 is responsible for homing and retention to the bone marrow with its ligand SDF-1α derived from osteoblasts and endothelial cells (Lapidot and Petit 2002, Ceradini, Kulkarni et al. 2004). The SDF-1α gradient indicates mobilization status as an increased SDF-1α concentration in the blood leads to enhanced migration of bone marrow progenitors to the blood stream (Hattori, Heissig et al. 2001). Also, the stimulation of rapid progenitor mobilization can be induced in the presence of CXCL8 (CXCL2 ligand IL-8) with or without G-CSF (granulocyte-colony stimulating factor) treatment (Pelus, Bian et al. 2004). Moreover, CD44 expression is enhanced in hematopoietic precursors to mediate cell rolling in the blood stream (Lewinsohn, Nagler et al. 1990, von Andrian and Mempel 2003).

Parabiosis experiments have established the importance of P-selectin (platelet selectin) and PSGL-1 (P-selectin glycoprotein ligand -1) in TCP migration to the thymus (Gossens, Naus et al. 2009). PSGL-1 is also found on LSKs and CLPs (Rossi, Corbel et al. 2005). N-terminal carbohydrate modification of PSGL-1 by glycotransferases is required for PSGL-1 binding to P-selectin. Therefore, interplay of PGSL-1 with endothelial P-selectin guides TSPs, exposing them to chemokine gradients and allowing their interaction with ICAM-1 (endothelial intercellular adhesion molecule-1) and VCAM-1 (vascular cell adhesion molecule-1) for a stable anchorage to thymic endothelium via integrins (Scimone, Aifantis et al. 2006).

Furthermore, high expression of chemokine receptors CCR7 (C-C chemokine receptor type 7) and CCR9 (C-C chemokine receptor type 9) on CLPs, CLP-2 and LMPPs reinforce these precursor cells arrest by modifying integrin stability (Bhandoola, von Boehmer et al. 2007, Zlotoff and Bhandoola 2011). This function is mediated through CCR25 (C-C chemokine receptor type 25) and CCL21 (C-C chemokine ligand 21) expression in thymic stroma (Misslitz, Pabst et al. 2004, Gossens, Naus et al. 2009).

The importance of these receptors has been demonstrated by a 100-fold decrease of ETPs within CCR7/CCR9 double knock-out (DKO) mice in comparison to wild-type animals (Krueger, Willenzon et al. 2010, Zlotoff, Sambandam et al. 2010). Finally, integrin dimers including $\alpha_4\beta_1$ (VLA-4), $\alpha_L\beta_2$ and glycan polysialic acid allow access to the thymus (Scimone, Aifantis et al. 2006, Drake, Stock et al. 2009).

1.3.1.1.2 TSPs and thymus receptivity

The thymus requires a dynamic progenitor input divided into responsive and refractory periods (Foss, Donskoy et al. 2001, Donskoy, Foss et al. 2003). The thymus gate keeper molecules control TSP entry based on the available stromal niche. For example, the level of S1P in plasma is hypothesized to signal peripheral lymphopenia and lower thymic stromal niche occupancy, impacting on P-selectin expression (Gossens, Naus et al. 2009). Once full of ETPs, thymic niches initiate refractory signals by diminishing the gate keeper molecules P-selectin and CCL25 (C-C chemokine ligand 25) for 2 weeks, which is the required time for ETP maturation and relocalization to another thymic compartment (Petrie and Zuniga-Pflucker 2007). Gated TSP input is observed in the first 4 months of post-natal life in mouse model (**Figure 1.5)**. The thymic gate is open for 1 week to fill niches followed by gate closure for 2-3 weeks (Foss, Donskoy et al. 2001). IL-7 signaling indirectly controls gate closure through integrin-mediated adhesion of TSPs (Ariel, Hershkoviz et al. 1997, Kitazawa, Muegge et al. 1997). Parabiosis and radiolabeled experiments have demonstrated a cyclical accumulation of TSPs for 3-5 days, followed by their release into the circulation preceding thymus gate opening. Therefore, TSPs generation and release from bone-marrow are coordinated with thymus load within fetal and adult mice (Donskoy, Foss et al. 2003) (**Figure 1.5)**.

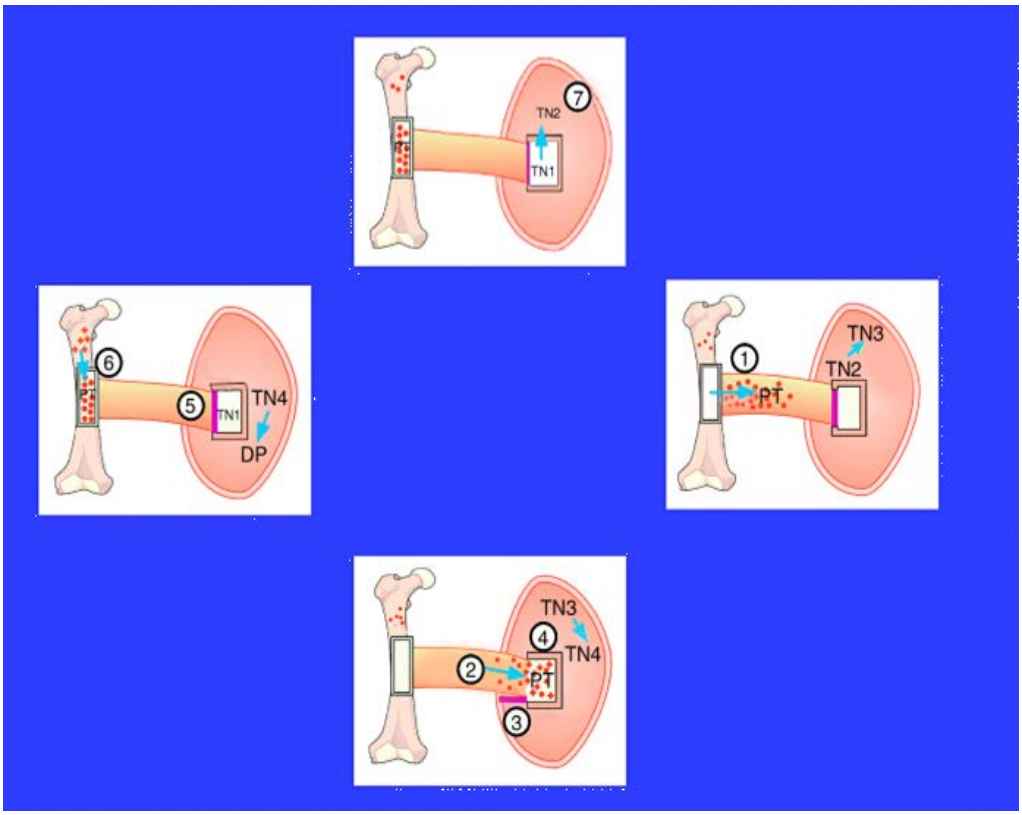

Figure 1.5. The cycling thymus periodicity.

This diagram shows: 1) TSP mobilization from BM into the blood stream. 2) TSP migration to thymus 3) thymus gate opening 4) stromal niche occupancy 5) subsequent gate closure 6) TSP regeneration in BM and 7) resulting sequential T cell developmental program from triple negative TN1 to TN4. Figure is adapted from (Goldschneider 2006)

1.3.1.1.3 Thymus organogenesis and structure

The thymus is a bi-lobed organ that is located behind the sternum and at the top of the heart, in the central area of the thoracic cavity. In the early 1960s, the thymus was identified as the site for T cell differentiation (Miller 1961). Initiation of thymus organogenesis requires NCC (neural crest cells) migration forming the primary stomal component from pharyngeal endoderm and ectoderm in association with the thymus epithelium (Janeway, Travers et al. 1999, Epstein, Li et al. 2000). However, recent studies have confirmed a common origin of all thymus epithelial cells from a single endodermal ancestor (Bennett, Farley et al. 2002, Gill, Malin et al. 2002). NCCs are ectodermal cells that migrate into the pharyngeal region where they constitute the thymus mesenchymal capsule and associate with the vasculature (Foster, Sheridan et al. 2008).

Additionally, interaction of NCCs with thymus epithelial cells (TEC) is essential for thymus organogenesis (Jenkinson, Jenkinson et al. 2003). In fact, NCCs determine positioning of organ borders and separation from pharynx. The initial size of the TEC pool dictates thymus size (Jenkinson, Jenkinson et al. 2003, Jenkinson, Bacon et al. 2008). Moreover, NCC mesenchyme produces EGF (epidermal growth factor), TGF-α (Transforming growth factor α) and IGF (insulin growth factor) to support TEC proliferation and differentiation (Shinohara and Honjo 1997). This cellular interaction then mediates thymus-parathyroid organ separation at E12.5-13, which is followed by a coordinated migration of thymus lobes above the heart (Gordon and Manley 2011). The first migration of TSPs happens before TEC differentiation and other thymic events at E11.5 in mice. However, this early TSPs immigration is not required during thymus organogenesis events at least until E13.5(Gordon and Manley 2011).

The earliest thymus marker in mice is Foxn1 (folkhead family transcription factor) and its expression depends on BMP signaling. Additionally, Bmp4, Fgf8, Shh and Wnt5b are involved in initial patterning of the thymus. Bmp4 promotes thymus fate whereas Shh favours parathyroid development. The Eyes absent (Eya) – Homeobox (Hox) - Sine oculis homeobox (Six) transcription network controls the early phase of thymus formation (Gordon and Manley 2011). The thymus is mainly subdivided into two compartments, the cortex and the medulla which are surrounded by a mesenchymal capsule (**Figure 1.6A and B**). Each compartment is comprised of cortico or medullary epithelial, mesenchymal, endothelial and dendritic cells (**Figure 1.6C**). Both structures serve as supporting micro-environments for developing T cells. Their 3D architecture facilitates TSP entry at the cortico-medullary junction (CMJ) as well as the maintenance of a stereotypical migration route for TSPs (van Ewijk, Wang et al. 1999). Therefore, these progenitors are exposed to key differentiation molecules from surrounding cells in order to produce a diverse repertoire of functional T cell populations (**Figure 1.6C**)(Gordon and Manley 2011).

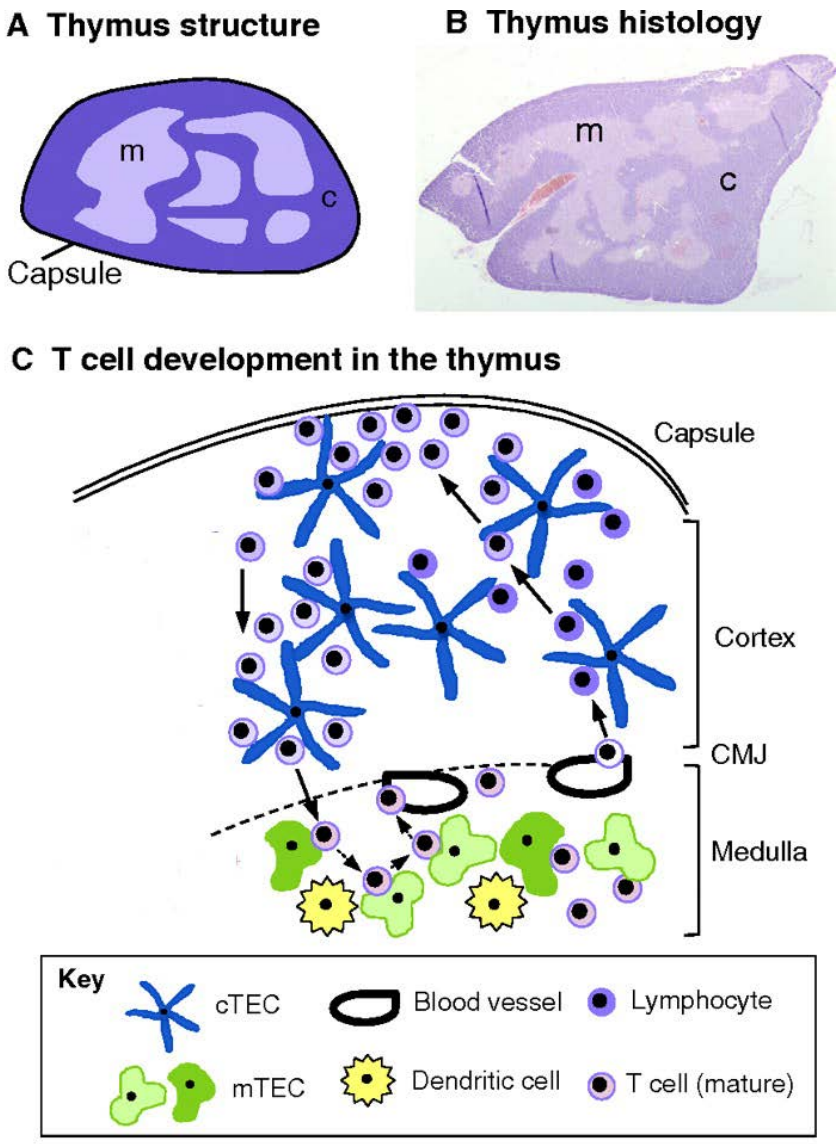

Figure 1.6. The thymus structure.

Illustration depicting: **A**) Schematic representation of the thymus compartments medulla (m) and cortex (c). **B**) Thymus section stained by Hematoxyl & Eosin and displaying the thymus architecture. **C)** Cellular distribution and interactions for thymus-dependent differentiation of immature into mature T cells that involve cTEC and mTEC (medullary and cortical epithelial cells) as well as dendritic cells within the thymus. Illustration adapted from (Gordon and Manley 2011) doi: 10.1242/dev.059998.

1.3.1.2 Intrathymic T cell development

Following TSP (thymus seeding progenitors) recruitment via blood vessels at the cortico-medullary junction (CMJ), T cell development is turned on to guide these multipotent progenitors to T lineage commitment with multiple rounds of proliferation, selection checkpoints and differentiation stages while migrating to the subcapsular zone (Yui and Rothenberg 2014). ETPs are the most multipotent thymic progenitors with preservation of myeloid lineage, natural killer, dendritic cell and B cell potential. They express similar molecules as the bone marrow-derived TSPs, LMPPs and CLPs. Also, these cells are suggested to derive directly from lympho-myeloid-restricted TSPs compared to HSCs in the bone marrow (Rothenberg and Scripture-Adams 2008). These primitive progenitors lack expression of co-receptors CD4 and CD8, and therefore, are called DN (double-negative) populations. The sequential differentiation program starts from the early DN1 to DN4 stages, followed by the $CD4^+CD8^+$ double-positive (DP) transition and finally the maturation into single-positive (SP) $CD4^+$ or $CD8^+$ (**Figure 1.7**)

1.3.1.2.1 DN1 to DN4 transition

Murine DN1s are characterized by surface markers ($Lin^-CD44^+CD25^-$). Surface expression of c-Kit and CD24 distinguishes five DN1 populations: DN1a ($c\text{-}Kit^{hi}CD24^-$), DN1b ($c\text{-}Kit^{hi}CD24^{low}$), DN1c ($c\text{-}Kit^{hi}CD24^+$), DN1d ($c\text{-}Kit^-CD24^+$) and DN1e ($c\text{-}Kit^-CD24^-$)(Porritt, Rumfelt et al. 2004). DN1a and DN1b populations are comparable to ETPs. Once in the thymic cortex, they proliferate extensively and sustain their uncommitted identity as shown by their low or undetectable levels of T lineage specific genes. ETPs that progress to the DN2 stage ($Lin^-CD44^+CD25^+c\text{-}Kit^+$) generally show a significant increase in genes associated with T cells, yet still retains an important uncommitted subpopulation (Rothenberg and Scripture-Adams 2008, Yui and Rothenberg 2014). In fact, the DN2 fraction contains DN2a (Kit^{++}) and DN2b (Kit^+) subpopulations, the latter having lost NK, macrophage, granulocytes and DC potentials (**Figure 1.7**). The fetal lymphoid progenitors that populate the thymus at E12.5 give rise to DN2 at approximately E14.5, whereas, it takes 10 days to reach the post-natal DN2 stage (Porritt, Gordon et al. 2003, Lu, Tayu et al. 2005). Furthermore, DN2b cells shift to the DN3 stage ($Lin^-CD44^{low}CD25^+c\text{-}Kit^{low}$) at which time maximal gene activation of T cell identity and rearrangements of TCRβ, TCRγ and TCRδ genes occur (Yui and Rothenberg 2014).

Gene rearrangement allows pre-TCR assembly comprising CD3, rearranged TCR-β and invariant pre-TCRα in DN3 cells or the surface expression of TCRγδ complex. These TCR complexes permit β-selection or γδ-selection (**Figure 1.7**) (Rothenberg and Scripture-Adams 2008, Teague, Tan et al. 2010). The DN3 population is comprised of DN3a ($Lin^-CD44^-CD25^+CD28^{-/low}$), DN3b ($Lin^-CD44^-CD25^+CD28^+$) and DN3c ($Lin^-CD44^-CD25^{int}CD28^+$) subpopulations (Teague, Tan et al. 2010). In addition, the development stages from ETPs to DN3 including the β-selection checkpoint correspond to the pro-T cell stage. The pairing of pre-TCRα induces downregulation of CD25 at the DN4 stage ($Lin^-CD44^-CD25^-c\text{-}Kit^-$) (**Figure 1.7**). This developmental stage involves DN4a ($Lin^-CD44^-CD25^-CD28^{int}$), DN4b ($Lin^-CD44^-CD25^-CD28^{hi}$) and DN4c ($Lin^-CD44^-CD25^-CD28^{-/low}$) fractions (Teague, Tan et al. 2010)

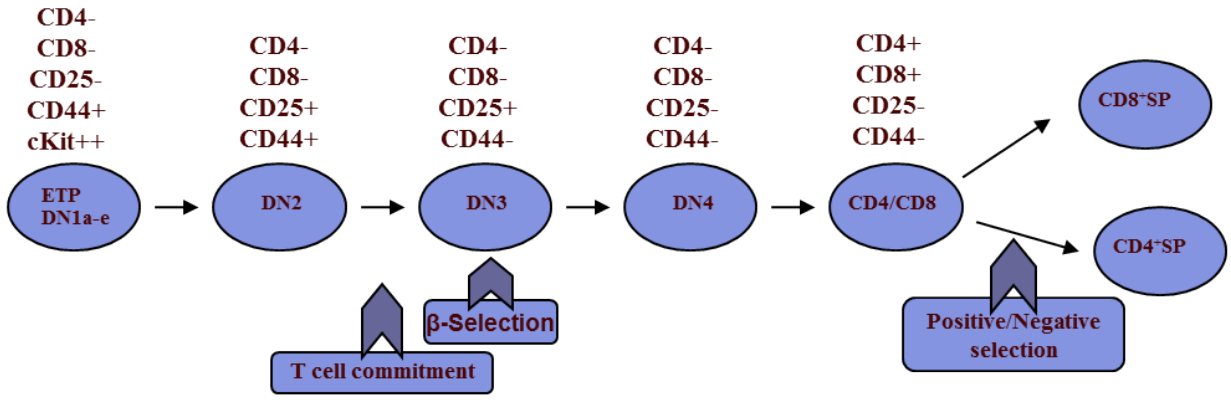

Figure 1.7. Differentiation program of the T cell lineage.

In the cortex, ETP or DN1a and DN1b cells progress through DN2 stages. Developing T cells commit to T lineage at the DN2b stage before shifting to DN3 stages. The β-selection checkpoint ensures further differentiation into DN4 and $CD4^+CD8^+$ DP subsets. Finally, DP cells mature into single positive (SP) $CD4^+$ or $CD8^+$ cells. These cells are positively or negatively selected within the medulla before migrating into peripheral lymphoid tissues. Illustration is adapted from (Yui and Rothenberg 2014)

1.3.1.2.2 DN4 to double-positive (DP) and single-positive (SP) $CD4^+$/$CD8^+$ cells

DN4a ($Lin^-CD44^-CD25^-CD28^{int}$) subpopulation represents the most efficient DP precursor. Moreover, DN4a also has bimodal expression of CD69. This marker is usually associated with positive selection of DP cells and semi-mature SP cells (Yamashita, Nagata et al. 1993). Therefore, DP precursor cells are DN4a ($CD69^-$). In addition, there is an intermediate population between the DN4a and DP stage termed ISP (intermediate single positive $CD4^-CD8^+$). ISP thymocytes mark the transition to Notch-independent T cell survival and proliferation (Xiong, Armato et al. 2011).

Additionally, up-regulation of both CD4 and CD8 co-receptor expression, expansion and rearrangement of the TCRα locus are involved in the DN4a to DP transition stage (**Figure 1.7**) (Teague, Tan et al. 2010, Yui and Rothenberg 2014). DP thymocytes are also characterized by a complete αβT cell receptor (TCR). The fetal lymphoid progenitors take a total of 4 days to produce DPs compared to post-natal DP cells that require approximately 2 weeks (Porritt, Gordon et al. 2003, Lu, Tayu et al. 2005). Both CD4 and CD8 co-receptors potentiate downstream TCR signaling allowing positive or negative selection of DP cells based on their ability to interact with thymic selective ligands. Also, DP cells are unresponsive to the IL-7 pathway due to the overexpression of *SOCS1* (suppressor of cytokine signaling 1). Therefore, the binding of CD8 or CD4 co-receptor to MHC-class I or class II restricted TCRs dictate DP survival (Chong, Cornish et al. 2003, Yu, Park et al. 2006).

In the cortico-medullary junction, DP cells undergo a lineage and functional choice to either become single positive (SP) $CD4^+$ or $CD8^+$. The commitment process follows a stochastic model starting with TCR ligation by MHC on DP (Singer, Adoro et al. 2008, Ellmeier, Haust et al. 2013). This previous step activates positive or negative selection which subsequently down-regulates CD4 or CD8 expression independently of MHC specificity of TCR. The following step is a quality control mechanism monitoring TCR match with MHC specificity. MHC signaling in DP switches off CD8 expression, but not CD4, independent of exposure to MHC class I or II. The resulting $CD4^+CD8^{low}$ population is a key intermediate with the potential to develop into $CD4^+$ or $CD8^+$ SP (Penit 1987). To do this, the $CD4^+CD8^{low}$ population signals via their MHC Class II restricted TCR to mature into $CD4^+$SP.

However, these cells can no longer signal through their MHC Class I restricted TCR in the absence of CD8 co-receptor (Lundberg, Heath et al. 1995, Suzuki, Punt et al. 1995, Ellmeier, Haust et al. 2013). In consequence, they are sensitive to IL-7 and IL-15 which are both critical for $CD8^+$SP production (McCaughtry, Etzensperger et al. 2012). Overall, this stochastic model results into peripheral $CD4^+$ helper T cells and $CD8^+$ cytotoxic T cells.

1.3.1.3 Control of T cell differentiation program

Sequential T cell development progression is coordinated by 1) complex intracellular transcriptional regulation 2) efficient interaction between developing T cells and the epithelial environment, 3) proper thymus migration and egress and 4) the assessment of quality control during selection checkpoints.

1.3.1.3.1 Transcriptional network

The initial differentiation phase (ETPs-DN2a) is a TCR independent stage. It involves engagement of cell-surface Notch 1 on precursor cells (**Figure 1.8**) (Lu, Tayu et al. 2005). In fact, Notch 1 binds its ligands DLL4 (delta-like ligand 4) on thymic epithelial cells triggering the release of intracellular Notch1 and its subsequent binding to RBPJ (recombining protein suppressor of hairless) (Love and Bhandoola 2011, Radtke, MacDonald et al. 2013). Moreover, this interaction recruits the co-activator complex for Notch target gene stimulation. The Notch 1 signalling pathway guides and retains early T cells (ETPs-DN2a) in the specific thymic environment that inhibits alternative lineage choices in favour of the T cell pathway. This Notch-dependent phase is divided into pre-commitment (phase 1) and the T-cell identity (phase2) phases. Both steps are differentiated by participant transcription genes throughout the developmental sequence (Radtke, MacDonald et al. 2013, Yui and Rothenberg 2014).

During phase 1, an exclusive contact between CLPs, LMPPs or ETPs with the thymic environment blocks the non-T cell lineage choices. The engraftment of T cell progenitors is most likely associated to transcription factors Gata-2, Hoxa9 (Homeobox A9) and Meis1 (Meis Homeobox 1). In ETPs, these genes collaborate with Flt3 (FMS-like tyrosine 3) and Gata-3 to shut down the B cell potential. Until now, this inhibitory mechanism is not directly linked to Notch1 (Huang, Sitwala et al. 2012, Garcia-Ojeda, Klein Wolterink et al. 2013, Gwin, Shapiro et al. 2013).

Furthermore, the myeloid and dendritic cells potentials from ETPs to DN2a stages are excluded by downstream activation of Hes 1 by Notch, subsequent repression of C/EBPα and PU-1 transcriptional activity (Carotta, Wu et al. 2010, De Obaldia, Bell et al. 2013).

Several Phase 1 transcription factors are inherited from primitive progenitors. In fact, the "stemness" proto-oncogenes Lmo2, Meis and N-Myc are involved in proliferation, survival and self-renewal of ETPs and DN2a (Riddell, Gazit et al. 2014). These subpopulations are also characterized by the gene expression of Sp1 (encoding PU-1), Bcl11A (B-cell CLL/Lymphoma 11A), Gfi1b (growth factor-independent protein 1B), Erg (Ets-related genes) and Lyl1 (lymphoblastic leukemia 1) (Yui and Rothenberg 2014). In terms of mechanism, Bcl11a controls proliferation of lymphoid progenitors in the fetal liver and bone marrow (Yu, Wang et al. 2012). Lyl1 null mice have demonstrated multiple functions in ETP maintenance, ETP-DN2 transition and c-Kit-dependent ETPs survival (Lecuyer, Herblot et al. 2002, Phelan, Saba et al. 2013). In addition, Lyl1 with the protein TAL-1 forms dimers with E2A and HEB to control Gfi1b expression and the subsequent Notch1 response (Phelan, Saba et al. 2013, Yui and Rothenberg 2014). The majority of these genes are either largely decreased or suppressed at DN2a-DN2b transition except for Lyl1, which is suppressed at DN3a stage, and Erg/N-Myc silenced at the β-selection checkpoint (Yui, Feng et al. 2010, Yui and Rothenberg 2014)(**Figure 1.8**).

In addition, Notch induction in ETPs results in increased Gata-3 and Tcf7 encoding Tcf-1 which are both pro T lineage commitment genes. These genes also collaborate with pre-thymic genes such as Myb, Runx1, Ikaros and E2A to maintain cell survival and proliferative expansion (Hosoya, Kuroha et al. 2009, Germar, Dose et al. 2011, Yui and Rothenberg 2014). For example, the Notch-RBPJ complex is an enhancer at the Tcf-1 promoter starting at ETP stage and fully active at DN2-DN3 transition. Consequently, Tcf-1 activates Gata-3 and represses E2A inhibitor. Tcf-1 is also important in post-natal T cell precursor cells (Germar, Dose et al. 2011, Xu, Carr et al. 2013). In parallel, Gata3 plays a significant dose-dependent role for cell survival, growth, specification and commitment in this early differentiation phase 1. Gata-3 excludes the B cell potential of ETP and potentiates Bcl11b expression at the DN2a-DN2b transition. It also inhibits PU-1 while activating Ets gene in DN2b cells and guiding DN3 cells through β-selection (Yui and Rothenberg 2014) (**Figure 1.8**).

During the T cell identity phase, the stable expression of Tcf-1 and Gata3 indicates transition to DN2b stage. This stage is characterized by low proliferation rate, silencing of c-Kit expression and fully Notch-dependent cell survival. In DN2b cells, Bcl11b represses c-Kit (Yui, Feng et al. 2010, Yui and Rothenberg 2014). Increased expression of Ets1 and Ets2 genes explains their desensitization to IL7R signalling. Also, E proteins and Notch enhance Rag1, Rag2, Ptcra and CD3e genes, all necessary for Tcr rearrangement. Additionally, slower cell proliferation correlates with intensified Tcr gene recombination by Rag genes. Therefore, DN2b status marks the end of possible alternative fate (Wojciechowski, Lai et al. 2007, David-Fung, Butler et al. 2009). In fact, the myeloid potential of DN2b cells is terminated with PU-1 silencing by Runx1, Tcf-1 and Gata-3. Their NK (Natural killer) and ILC2 (innate lymphoid cells type 2) differentiation choices are neutralized by Bcl11b (B-cell lymphoma-Leukemia 11b) and Id2 (Inhibitor of DNA binding 2) repression. Moreover, Bcl11b is involved in silencing other phase1 genes such as Lyl1 and Bcl11A to ensure T commitment (Yui, Feng et al. 2010, Wong, Walker et al. 2012, Yui and Rothenberg 2014) (**Figure 1.8**).

DN3a cell survival relies on variable expression of the transcription network involving Runx1-CBFβ, Notch, Gata-3, Gfi, Bcl11b, Myb and Ets1. In DN3a subset, Cd3 gene expression is controlled by E proteins, Gata-3 and Tcf-1 genes. Rag genes are regulated by E proteins, Gata-3 and Hes 1. Also, Notch and E proteins induce Ptcra gene. (Zhang, Mortazavi et al. 2012, Yui and Rothenberg 2014). Additionally, Ikaros and E2A drive proliferation and differentiation. To do this, E2A modulates cell cycle via Cdkn1A expression and provides survival support through upregulation of Pik3ip1 (inhibitory phosphoinositide 3-kinase-interacting protein 1) and Dapk1 (growth-suppressive death-associated kinase 1) (Winandy, Wu et al. 1999, Engel and Murre 2004, Xu, Carr et al. 2013). Moreover, Ikaros contributes significantly to β-selection by suppressing Notch target genes following induction of a pre-TCR signal (Germar, Dose et al. 2011, Yui and Rothenberg 2014).

Therefore, Notch target genes and IL-7R are completely silenced in the DN3b population and the quiescent state is disrupted (Taghon, Yui et al. 2006). These cells rapidly proliferate and are highly responsive to CXCR4 (Janas, Varano et al. 2010, Tussiwand, Engdahl et al. 2011). Extensive proliferation diversifies the TCR repertoire pool and favours selection of T committed cells. The β-selection transcription hallmark is essentially the dramatic downregulation of Notch target genes resulting from an absence of intracellular Notch signaling (Yui and Rothenberg 2014).

In addition, β-selection induces stable gene activation of RORγt, Pouf6FI and Aiolos which promotes DN4 proliferation. Also, transient gene activation of Egr2 and Id3 inhibits RORγt expression. Id3 represses temporary E protein expression which is restored at a later time point. DN4-ISP to DP transition involves expression of co-receptor CD4 or CD8. Wnt mediator β-catenin with Tcf-1 and Lef1 modulate gene expression of CD4, CD8 and CD2 genes to create the DP phenotype (Xu, Sharma et al. 2009, Yui and Rothenberg 2014). The upstream enhancer E4P drives CD4 expression in DP thymocytes but not in mature SP $CD4^+$. In contrast, Runx1 regulates DN4 to DP transition by inhibiting CD4 expression in DN cells . Moreover, RORγt expression is specific to DP cell viability via induction of Bcl2l1 with the collaboration of Myb (Xi, Schwartz et al. 2006).

As previously mentioned, the intermediate $CD4^+CD8^{low}$ subpopulation is the precursor of $CD4^+$ and $CD8^+$ single positive cells (Cummins and Thompson 1997). During SP $CD8^+$ differentiation, Runx3 is increased by Ets1 to inhibit CD4 expression. Runx3 also induces multiple $CD8^+$T specific genes including cytotoxic enzyme perforin and granzyme B, IFN-γ (interferon-gamma) and the transcription factor Eomesodermin (Foss, Donskoy et al. 2001). Additionally, Irf1 (IFN regulatory factor 1) is another transcription factor that induces $CD8^+$ lineage differentiation by either direct stimulation of CD8 expression or an indirect promotion of MHC-I (MHC class I) in thymic epithelial cells (Shortman and Wu 1996, Prockop and Petrie 2004). In addition, IL-7 signaling pathway promotes CD8 lineage choice via ThPOK silencing and Runx3 induction (Penit 1987, Singer, Adoro et al. 2008).

Furthermore, ThPOK inhibits SP $CD8^+$ restricted genes dependent on Runx3 gene. It therefore drives commitment towards SP $CD4^+$ (Jotereau and Le Douarin 1982). In addition, the positive regulator MAZR of ThPOK restricts CD8α expression by binding CD8a gene enhancer (Bhandoola, Sambandam et al. 2003). Gata-3 is another ThPOK upstream gene that is required for CD4 lineage specification. Moreover, the high expression level of Myb is determinant for $CD4^+$ differentiation and maintenance (Penit 1988, Merchant 2010).

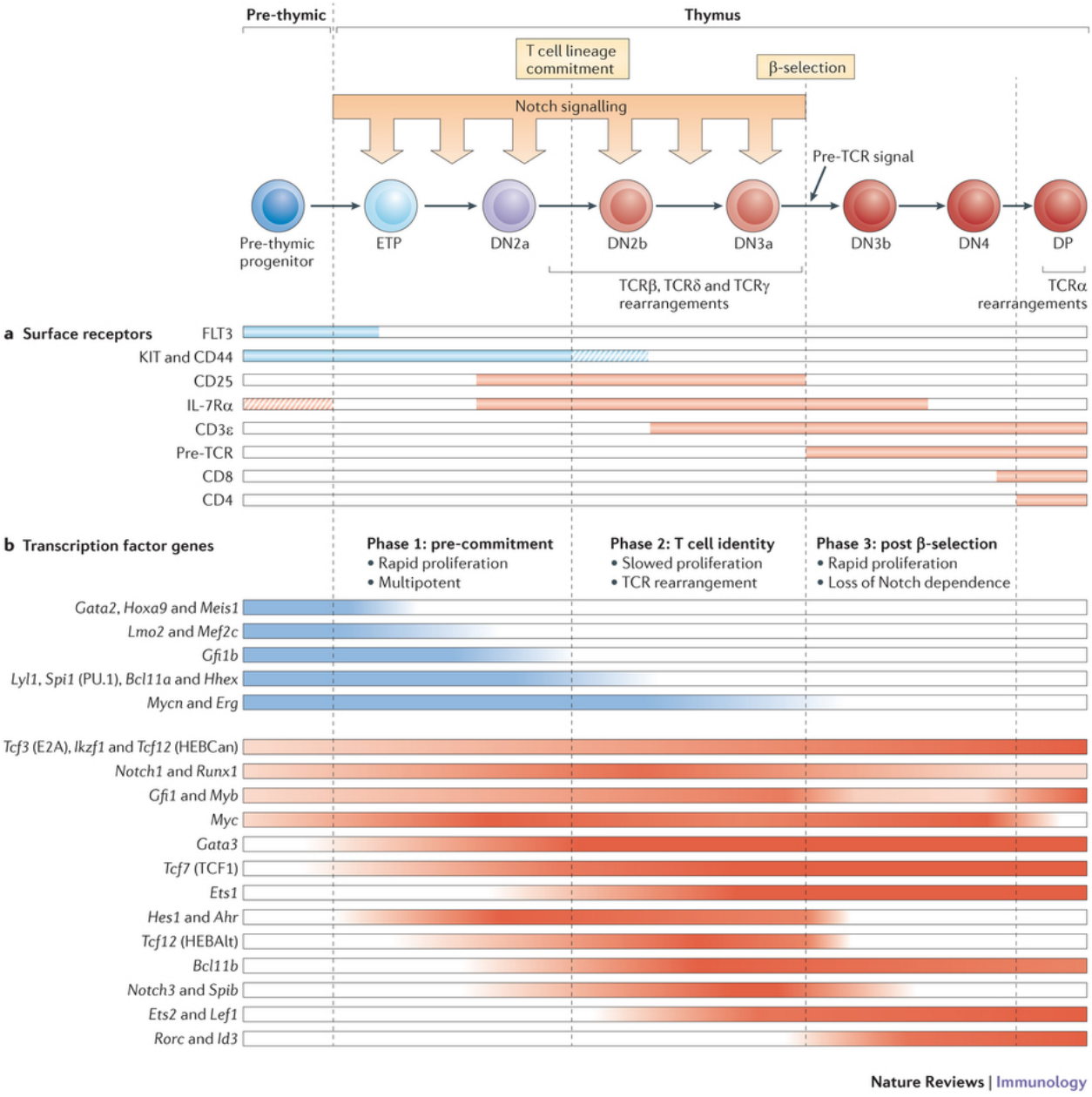

Figure 1.8. Summary of transcriptional network in T cell development.

A) Visual representation of specific surface markers and corresponding differentiation stages.

B) Distribution of crucial transcription factors in correlation with T cell developmental sequence. Important genes from phase 1 to β-selection are shown in blue and the T cell identity genes are in red. Dashed lines indicate each phase interval. Color intensity correlates with expression level. Figure is adapted from (Yui and Rothenberg 2014)

1.3.1.3.2 Lympho-thymic environment crosstalk

Lympho-thymus environment interaction represents intercellular contact between developing T cells and the thymus epithelial cells (TECs), mesenchymal cells and other thymus resident cells such as dendritic cells and macrophages (Manley, Richie et al. 2011). The 3D conformation of this epithelial environment relies mainly on lympho-stroma contact. This lympho-stroma crosstalk involves signals derived from developing T cells and signaling molecules primarily from stromal epithelial cells and the mesenchymal component. Together, these molecules support T lineage commitment, differentiation, survival and selection to produce a diverse T cell repertoire (Manley 2000, Lind, Prockop et al. 2001). Consequently, the exclusive stroma organization dictates thymus cell number and size with maximum size and cortical thickness attained at approximately 4 weeks (Manley, Richie et al. 2011).

Thymus epithelial cells (TECs) are comprised of cortical TECs (cTECs) and medullary TECs (mTECs) which express cytokeratin 8 ($K8^+$) and cytokeratin 5 ($K5^+$), respectively. Both cell types derive from an intermediate common precursor that is a double-positive $K5^+K8^+$ epithelial subset (Anderson, Jenkinson et al. 2006, Anderson and Takahama 2012). The DN1-DN2 developmental stages serve as a crucial step during the establishment of cTECs. In fact, a higher proportion of double-positive $K5^+K8^+$ TECs are found at the cortico-medullary junction (CMJ) in consequence of T differentiation blockage at or prior to DN2 stage, illustrating the necessity of differentiating T subsets into TECs plasticity. However, T differentiation blockage at DN3 or later does not affect cortical epithelial thymus organization and differentiation (Hollander, Wang et al. 1995, Klug, Carter et al. 1998, van Ewijk, Hollander et al. 2000). The loss of DN4-DP subpopulations severely impairs mTECs development and expansion, suggesting a link between positive and negative selection molecules and the homeostasis of thymus medulla (Surh, Ernst et al. 1992, Shores, Van Ewijk et al. 1994, Anderson and Takahama 2012). Also, mature SP $CD4^+$ or $CD8^+$ produce ligands to activate mTECs receptors including RANK, CD40 and LTβR (lymphotoxin-β-receptor). These interactions are involved in Aire-expressing mTECs development and global thymus medulla maintenance (Rossi, Kim et al. 2007, Manley, Richie et al. 2011).

Growth factors (e.g. Fgf10) from thymic mesenchyme are involved in early thymus stromal development. In collaboration with epithelial cells, mesenchymal fibroblasts also regulate T cell differentiation by organizing an extracellular matrix scaffold presenting growth factors and cytokines such as IL-7 to immature T cells (Revest, Suniara et al. 2001, Dazzi, Ramasamy et al. 2006). In contrast, dendritic cells are efficient antigen presenting cells in the medulla. They participate in negative selection by presenting tissue-restricted self-antigens to eliminate auto-reactive developing T cells. Moreover, macrophages are disposing of T cells that fail negative or positive selection and undergo apoptosis (Gallegos and Bevan 2004, Koble and Kyewski 2009, Manley, Richie et al. 2011).

Furthermore, cell-autonomous and dose-dependent epithelial functions in T cell development have been shown in Foxn1-deficient mice (Blackburn, Augustine et al. 1996, Bleul, Corbeaux et al. 2006). In fact, highly purified cTECs provide Notch ligands to support and maintain T cell differentiation. Therefore, expression of these Notch ligands overlaps with fetal T cell colonization at approximately E12 (Harman, Jenkinson et al. 2003). Specifically, ligation of Notch 1 to the ligand Dll4 (Delta-like 4) is involved in initiating T cell commitment and intrathymic T cell differentiation (Ciofani and Zuniga-Pflucker 2007, Hozumi, Mailhos et al. 2008, Koch, Fiorini et al. 2008, Mohtashami, Shah et al. 2013).

In addition, survival and expansion of ETPs and DN2/3 depend on both c-Kit and the cytokine receptor IL-7Rα which modulate the pro-survival signal from Bcl-2 along with other cytokines (Kang and Der 2004, Massa, Balciunaite et al. 2006). The high levels of c-Kit and IL-7/IL-7Rα promote competition between proliferation and differentiation resulting in progression arrest from the DN2 to DN3 stage. Also, IL7-Rα expression in early T precursors such as CLPs allows for their interaction with the T permissive micro-environment. To support these functions, the thymic stroma provides stem cell factor (SCF) as the c-Kit ligand and IL-7 cytokine (Ciofani and Zuniga-Pflucker 2007).

Finally, TECs produce Wnt proteins that bind to Frizzled receptors (Fz) expressed on DN cells providing signals for early T cell differentiation, adhesion and proliferation (Staal, Weerkamp et al. 2004, Weerkamp, Baert et al. 2006). In addition, sonic and indian hedgehog (SHh and IHh) as well as Bmp signaling pathways are other lympho-stroma molecules inducing ETPs-DN3 survival, expansion and progression(Ciofani and Zuniga-Pflucker 2007).

1.3.1.3.3 Intra-thymus migration & egress

The developmental progress of DN cells coincides with their migration from cortico-medullary junction (CMJ) towards the sub-capsular zone (SCZ). Also, this exclusive intrathymic migration dictates the localization and motility of developing T cells towards the appropriate thymus niche (Ciofani and Zuniga-Pflucker 2007, Love and Bhandoola 2011). The organized trajectory of the early DN population is influenced by its expression of CCR9, CCR7 and CXCR4 chemokines. The global chemokine interaction results in integrin activation and expression; for example, VCAM-1 expression on cTECs which is essential for T cell migration (Plotkin, Prockop et al. 2003, Benz, Heinzel et al. 2004, Misslitz, Pabst et al. 2004).

CXCR4 is hypothesized to drive away DN1 from the medulla via CXCL-12 (SDF-1) ligand (Plotkin, Prockop et al. 2003). At the DN2 and DN3 stages, exposure to CCL25 (CCR9 ligand) and CXCL-12 produced by cTECs or fibroblasts prolongs chemokine signaling to accelerate DN motility from mid-cortex to SCZ. However, the significant expression of CCL19 and CCL21 (CCR7 ligands) in the medulla indicates a deferred role for CCR7 (Bunting, Comerford et al. 2011, Love and Bhandoola 2011). Additionally, CCR9 is crucial for DN2 and DN3 localization in the SCZ prior to β-selection. DN3 cells migrate back to the cortex after β-selection as they progress to DP stage. This is promoted by the collaboration between the CXCR4/CXCL-12 axis and pre-TCR providing both migration and survival signals (Benz, Heinzel et al. 2004, Trampont, Tosello-Trampont et al. 2010).

DP cells show high response to CXCL-12 and CCL25. However, their positive-selection results in decreased CXCR4 expression and induction of CCR7, CCR4 and CCR9. Therefore, they become sensitive to medullary chemokine ligands including CCL17, CCL19, CCL21 and CCL22 (Bunting, Comerford et al. 2011). Consequently, CCR7 is required for relocation of SP $CD8^+$ and $CD4^+$ cells to the medulla (Ueno, Saito et al. 2004, Nitta, Nitta et al. 2009). In addition, ephrins, neuropilins and semaphorins are negative regulators of the chemokine dependent migration (e.g. CXCL-12) of developing T cells (Mendes-da-Cruz, Stimamiglio et al. 2012).

Mature SP $CD4^+$ or $CD8^+$ express CCR7 and are highly responsive to CCL19. This interaction facilitates their export by exposing them to endothelial cells (Petrie 2003). Moreover, it increases their response to a S1P gradient, a GPCR highly expressed in pericytes at the CMJ and in the circulation. The plasma S1P binds S1P receptor 1 (S1pr1) on mature T cells. In contrast, S1pr1 expression is downregulated by induction of c-type lectin CD69, illustrating the importance of transient CD69 expression for mature SP cell egress (Feng, Woodside et al. 2002, Rivera, Proia et al. 2008, Zachariah and Cyster 2010). For this purpose, mature SP populations reside in the thymus medulla for 4-5 days and transition from a semi-mature $CD69^{hi}CD62L^{low}CD24^{hi}$ stage to the mature $CD69^{low}CD62L^{hi}CD24^{low}$phenotype. Thus, TCR signaling promotes cell egress via CCR7, CD62L and S1pr1 expression. Also, CD62L is associated with transmigration in peripheral lymphoid tissues, but not with mature SP cell egress (Love and Bhandoola 2011).

1.3.1.3.4 Selection checkpoints in T cell development

TCR assembly at the surface of developing T cells is responsible for generating the vast T cell repertoire. In addition, the expression status of TCR or TCR fractions dictates life versus death decisions of developing T cells, following specific selection checkpoints. The αβ T cell populations express TCR that is composed of α and β chains as opposed to the γδ T lineage. The unique TCRβ chain rearrangement generates a single type of TCRβ protein at the cell surface at DN3a stage (von Boehmer 2005). This is a determining factor for β-selection checkpoint and T differentiation progress independent of TCRα chain. In addition, the unique expression of TCRβ limits the diversity of TCRβ chains that are present on a single T cell. TCRβ chain is also linked to pTα (encoded by Ptcra gene) and CD3 to form pre-TCR. Therefore, pre-TCR synergizes with Notch signaling to stimulate DN3 progress beyond the β-selection checkpoint to DP stage (Michie and Zuniga-Pflucker 2002, Ciofani, Schmitt et al. 2004, von Boehmer 2005).

Positive and negative selection relies on equilibrium between antigen presentation via MHC and antigen receptor rearrangement on the surface of developing DP and SP cells (Starr, Jameson et al. 2003). Protein/DNA complexes including recombinase activating genes (RAGs) orchestrate multiple DNA breakage and rejoining events during locus rearrangements, generating multiple productive TCR gene α.This process allows for development of the adaptive immune system.

In consequence, pairing of rearranged α and β chains form MHC restricted TCR, signaling the end of V(D)J recombination (Starr, Jameson et al. 2003, Schatz and Swanson 2011).

TCR affinity is evaluated during positive selection of DP cells. In the outer cortex, these cells are exposed to specific TCR ligands triggering positive selection. This involves combinatorial recognition of exclusive peptides presented on MHC by cTECs (Starr, Jameson et al. 2003, Klein, Kyewski et al. 2014). TCR affinity for positive selection ligands is lower than negative selection ligands. Moreover, rare self-peptides with low affinity are capable of inducing positive selection to increase individual antigen specificity. Overall, positive selection promotes predictable identification of self-antigens by T cell, which in turn facilitates an efficient response to pathogens. Subsequent TCR signalling results in maturation and relocation of positively selected $CD4^+$ or $CD8^+$ to the medulla. Moreover, failure to undergo positive selection leads to death of a large portion of DP cells (Stefanova, Dorfman et al. 2002, Starr, Jameson et al. 2003, Klein, Kyewski et al. 2014). Positively–selected $CD4^+CD8^+$cells are characterized by TCRβ and CD69 expression and divided as $TCR\beta^{low}CD69^+$ or $TCR\beta^{int}CD69^+$ subsets (Van De Wiele, Marino et al. 2004).

Negative selection also affects cortical cell to a lesser extent. This negative selection relies on the interaction between DP, SP $CD4^+$ and SP $CD8^+$ with antigen presenting cells (APCs) such as DCs (dendritic cells). In the medulla, T cell tolerance is induced by mTECs expressing tissue-restricted antigens (TRAs) in collaboration with resident and migratory DC subpopulations (Daley, Hu et al. 2013, Stritesky, Xing et al. 2013, Klein, Kyewski et al. 2014). For example, direct presentation of TRAs by mTECs triggers negative selection of SP $CD8^+$ and promotes SP $CD8^+$ T cell tolerance. Also, the medulla provides a confined environment facilitating intercellular antigen transfer between mTECs and other APCs. In parallel, resident DCs present self-antigens that are captured from the thymus environment. In contrast, migratory DCs display blood-borne self-antigens and transport them from the thymus to the periphery (Klein, Kyewski et al. 2014).

1.3.2 Bone homeostasis and B cell lineage

As mentioned in sections 1.1 and 1.2, bone homeostasis is carried out by osteoblast and osteoclast coupling. This indirectly supports lymphopoiesis including B lineage development through HSC niche maintenance (see section 1.2). In parallel, osteoblasts produce CXCL-12 and IL-7 with the help of parathyroid hormone (PTH). Both molecules induce B cell commitment and participate in B cell development (Calvi, Adams et al. 2003, Zhu, Garrett et al. 2007). Moreover, mature B cells indirectly modulate bone resorption by producing OPG and RANKL that regulate osteoclast differentiation. Interestingly, as opposed to RANKL deficiency, OPG deficiency stimulates B cell development suggesting a bi-lateral function for OPG and RANKL in bone and B cells (Kong, Yoshida et al. 1999, Yun, Tallquist et al. 2001, Horowitz, Fretz et al. 2010). Furthermore, osteopetrotic mice models with inactive osteoclasts display a significant B cell loss, suggesting a potential crosstalk between osteoclast activity and the B-cell differentiation (Mansour, Anginot et al. 2011). Moreover, osteoclast progenitors affect other bone marrow hematopoietic cells by producing cytokines in presence of RANKL (Xing, Schwarz et al. 2005). Finally, B cell commitment controls bone resorption rate via the specific inhibition of CCL3 by the transcription factor Pax5 in B cell precursors and limits the differentiation of early B cell precursors into osteoclast (Delogu, Schebesta et al. 2006).

1.3.2.1 Bone marrow-dependent B cell differentiation

Early B cell differentiation takes place in the bone marrow cavity, where B lineage progenitors develop from hematopoietic precursors. The successful progress of the differentiation sequence allows migration to the spleen and the lymph node for further maturation. Early stage of B cell lineage differentiation involves lymphoid precursors LMPPs/ELPs that differentiate into CLPs $LY6D^{+}$ (Inlay, Bhattacharya et al. 2009, Miyazaki, Miyazaki et al. 2014). This late population generates the precursor of B lineage termed the pre-pro-B cells or fraction A. This precursor expresses B cell-lineage marker B220 (CD45R) but not the surface immunoglobulin. Subsequent differentiation of fraction A is distinguished by the expression of various cell surface markers resulting in five B cell subsets called fraction B, C, D, E and F (**Figure 1.9**)(Nagasawa 2006, Hardy, Kincade et al. 2007).

The surface markers are grouped as follows: fraction A ($B220^{+}$ $CD19^{-}$ $c\text{-}kit^{+}CD43^{+}IgM^{-}IgD^{-}$) is the pre-pro B subset; fraction B ($B220^{+}$ $CD19^{+}c\text{-}Kit^{-}CD43^{+}IgM^{-}IgD^{-}$) is the pro-B subset; fraction C ($B220^{+}$ $CD19^{+}c\text{-}Kit^{-}CD43^{+}IgM^{+}IgD^{-}$) is the early/large(pre)-B population; fraction D ($B220^{+}CD19^{+}c\text{-}Kit^{-}CD43^{-}IgM^{-}IgD^{-}$) is the late/small large (pre)-B; fraction E ($B220^{+}$ $CD19^{+}$ $c\text{-}Kit^{-}CD43^{-}IgM^{+}IgD^{-}$) is the immature/newly formed B population and fraction F ($B220^{+}CD19^{+}c\text{-}Kit^{-}CD43^{-}IgM^{low/hi}IgD^{hi}$) is the mature/follicular B-cell (**Figure 1.9**) (Hardy, Kincade et al. 2007).

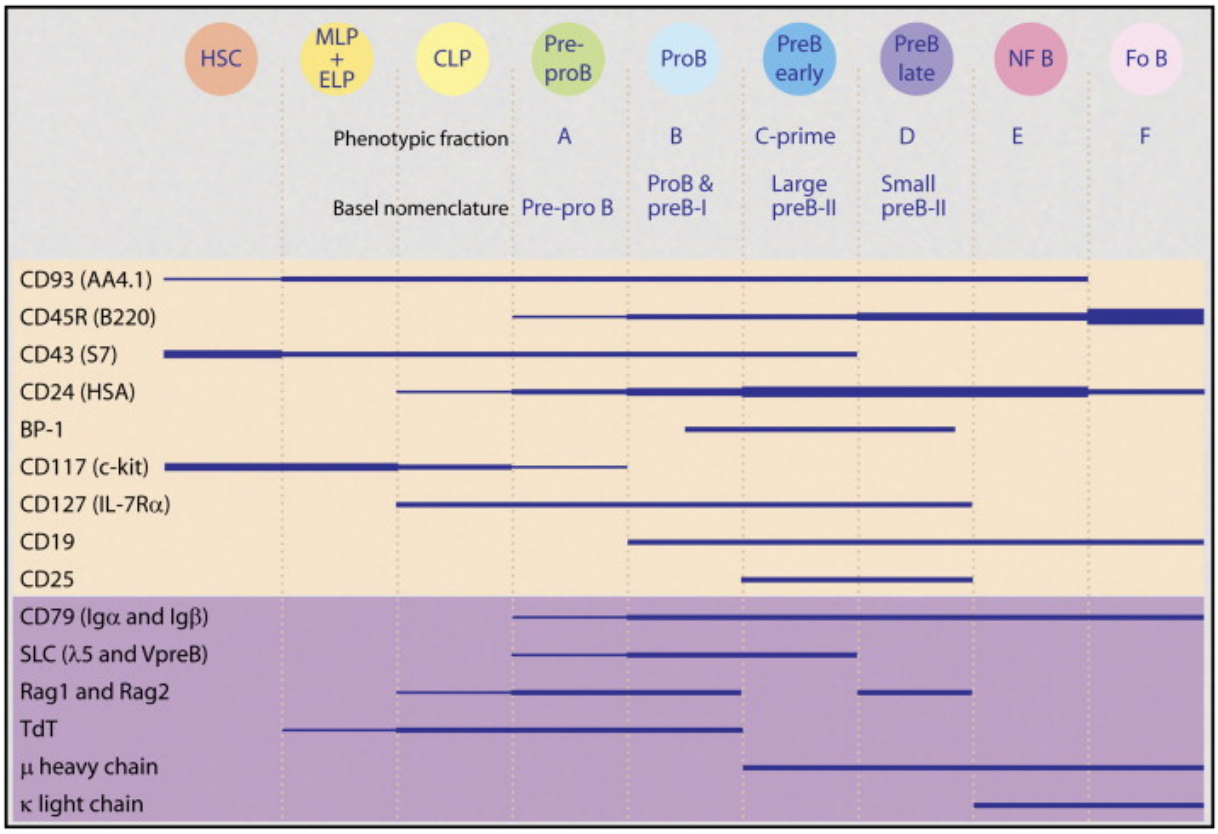

Figure 1.9. Schematic representation of early B lineage differentiation.

Surface marker expression and the corresponding differentiation stage characterized by CLPs, pre-pro B, pro-B, pre B, immature and mature B populations. HSC: Hematopoietic stem cell; MLP: Multipotent lymphoid progenitors; ELP: Early lymphoid progenitors; CLP: Common lymphoid progenitors; NF B: Non-follicular B cells and Fo B: Follicular B cells. Figure adapted from (Hardy, Kincade et al. 2007)

Pro-B cells rearrange immunoglobulin heavy-chain (IgH) gene through successive V(D)J recombination to become (pre)-B cells which are identified by their expression of μM chain (transmembrane version of μ IgH). This μM chain is the initial determinant check-point during B cell development. Successful selection leads to the successive expansion and rearrangement of immunoglobulin light-chain (IgL) gene. In the immature B subset, surface expression of IgM corresponds to the second check-point. This promotes negative selection allowing tolerance mechanisms to delete or edit autoreactive cells (Hardy and Hayakawa 2001, Shapiro-Shelef and Calame 2005). Therefore, naive B cells that bypass this selection checkpoint can exit the marrow for further maturation in peripheral lymphoid tissues. BCR signaling and the low number of peripheral follicular B cells are hypothesized to drive immature B cell emigration from the bone marrow (Pillai and Cariappa 2009).

1.3.2.1.1 Transcriptional regulation

Transcriptional regulators PU-1, Ikaros, E2A/E47, Ebf1 and Pax5 are crucial during early B cell development in mice. Ebf1 and Pax5 act in B lineage specific progenitors (Ramirez, Lukin et al. 2010). In addition, downstream signaling by the IL-7 pathway is required for Foxo1 activation and its subsequent functions at distinctive stages in B cell differentiation (Dengler, Baracho et al. 2008, Szydlowski, Jablonska et al. 2014). The transcription factor cMyb acts upstream Ebf1 to regulate pro-B cells survival and differentiation. Moreover, Runx1 deficiency in B cell progenitors results in inhibition of early B cell differentiation. Also, this developmental defect correlates with reduced expression of E2A, Ebf1 and Pax5, indicating a role for Runx1 in B development (Ramirez, Lukin et al. 2010, Yokota, Sudo et al. 2013).

The low concentration of PU-1 promotes B-cell fate through remodeling of Pax5 enhancer. Ikaros contributes to B cell identity by promoting lymphoid choice from CLPs and by inhibiting NK cell fate. In addition, absence of Ikaros abrogates B cell commitment even in the presence of Ebf1 and Pax5. Ikaros also collaborates with Ebf1 and E2A to ease chromatin accessibility which is required for V(D)J recombination (Thompson, Cobb et al. 2007, Papathanasiou, Attema et al. 2009, Ramirez, Lukin et al. 2010).

E2A protein initiates Ebf1 and Pax5 expression in pro-B cells turning on the B cell commitment program and guiding cell maturation in germinal centers. Ebf1 expression contributes to B cell specific gene priming prior to their later expression and is required beyond the pre-pro stage. Moreover, Ebf1 and Pax5 repress certain genes, inducing other lineages (Ramirez, Lukin et al. 2010, Yokota, Sudo et al. 2013). Overall, combination of multiple transcription factors including E2A, Ebf1, Pax5, Runx1 and Ets proteins activates Mb-1 gene that encodes Igα, a component of pre- and mature B cell receptor (BCR) (Sigvardsson, Clark et al. 2002, Maier, Ostraat et al. 2004). In addition, expression of the BCR co-receptor CD19 is driven via enhancer remodeling by E2A and promoter binding by Ebf1 and Pax5 (Ramirez, Lukin et al. 2010).

1.3.2.1.2 Bone marrow microenvironment

During B cell lineage differentiation processes, the marrow environment provides crucial factors for cell growth, survival and proliferation. Multiple supporting molecules deriving from surrounding cells include CXCL-12/CXCR4, Flt-3/Flt3-ligand, RANK/RANKL and SCF/c-Kit axis (Nagasawa 2006). The stroma cells, osteoblasts and reticular cells produce CXCL-12 to stimulate anchorage and growth of pre-pro B cells in the developmental niche (Egawa, Kawabata et al. 2001, Horowitz, Fretz et al. 2010). The Flt3/Flt3 ligand axis also establishes the number of pre-pro-B and pro-B fractions through regulation of the CLP population. In addition, the SCF/c-Kit axis signals the niche location to developing pro-B cells and pre-B cells. It also maintains B cell precursor number and pro-B cell proliferation synergistically with IL-7 cytokine derived from stroma cells (Waskow, Paul et al. 2002, Driessen, Johnston et al. 2003, Nagasawa 2006). Also, IL-7 derived from bone marrow mesenchyme participates in early B lineage development by acting on the expansion of CLPs and pre-pro-B cells. Moreover, the RANK/RANKL axis is essential for the pro-B to pre-B transition stage as well as during expansion of pre-B cells (Guerrini and Takayanagi 2014).

To facilitate these molecular interactions, developing pre-pro-B cells are in close proximity to CXCL-12^{hi} reticular cells which surround bone marrow sinuses. In contrast, pro-B cells are located farther from CXCL-12^{hi} cells but remain close to IL-7- expressing stroma cells. Additionally, pre-B cells are not found near either the CXCL-12^{hi} cells or IL-7- expressing cells, indicating their independence from the marrow environment (Tokoyoda, Egawa et al. 2004, Nagasawa 2006).

1.4 OSTEOPETROSIS: Example of an osteoimmunology disease

The imbalanced osteoclast-osteoblast coupling is caused by abnormal bone cell number or activity. This phenotype impacts the overall bone homeostasis and the dependent marrow content including the lymphoid lineages. Consequently, this results in medical conditions such as osteopetrosis. This genetic disorder has diverse forms based on the model of inheritance, the type of genetic mutations and the severity. The most frequently diagnosed form of osteopetrosis is the mild form termed adult autosomal dominant type II or Albert-Schönberg disease. The most severe and lethal form is autosomal recessive osteopetrosis (ARO) affecting infants (Coudert, de Vernejoul et al. 2015).

1.4.1 Pathophysiology of ARO

The incidence of ARO is between 1:200000 and 1:300000 in children. This condition begins in utero and appears after birth. It is characterized by multiple symptoms. Abnormal bone remodeling in ARO patients leads to growth delay, deformed cranial bone, fragile bones and compromised teeth growth. In general, this abnormal remodeling originates from inactive osteoclasts and is illustrated by higher bone density visualized by X-ray. Consequently, ARO patients also display important hematologic abnormalities, bone marrow failure, extra medullary hematopoietic or hepatosplenomegaly. Immunoglobulin levels range from normal to low and impairment in peripheral B cell maturation has been reported in some patients (Guerrini, Sobacchi et al. 2008, Pangrazio, Cassani et al. 2012). In addition, ARO patients can sometimes be identified by macrocephaly with frontal bossing and concomitant neurological issues as well as cranial nerve entrapment leading to visual impairment and hearing loss.

Until now, the curative regimen includes hematopoietic cell transplantation or interferon-gamma and calcitriol treatment to slow down hematological progression (Mazzolari, Forino et al. 2009, Essabar, Meskini et al. 2014, Orchard, Fasth et al. 2015). Overall, HSC transplantation can cure osteopetrosis if administered in *utero* or early in life of ARO patients without neurological phenotype (Sobacchi, Schulz et al. 2013). Otherwise, these treatments only increase long-term survival. As a result, the absence of treatment and significant bone marrow graft failure explain premature death of ARO patients within a decade. This high death rate is mostly related to susceptibility to infections, anemia and hemorrhages (Blin-Wakkach, Wakkach et al. 2004, Orchard, Fasth et al. 2015).

1.4.2 ARO-dependent gene mutations

Three major spontaneous mutations are associated with the recessive form of osteopetrosis. They have been established in osteopetrotic mice models and confirmed in ARO patients. In general, these osteopetrotic patients and mice models have normal or higher osteoclast number that fail to resorb the bone matrix (Sobacchi, Frattini et al. 2001, Blin-Wakkach, Wakkach et al. 2004).

The mutation of *TCRG1* (T cell immune regulator 1) gene is the most frequent, occuring in 50% of ARO patients. *TCRG1* encodes the alpha 3 subunit of the vacuolar proton pump (V-ATPase). This pump is located at the ruffled border of active osteoclasts, where it regulates proton transport to the resorption lacunae and concomitant acidification (Sobacchi, Frattini et al. 2001). The second important mutation affects 10% of ARO patients and targets the *CLCN7* gene encoding for Chloride Channel 7. This channel is responsible for maintaining electro-neutrality during the acidification process of bone resorption (Kornak, Kasper et al. 2001). Moreover, 5% of ARO patients have mutations of *OSTM1* (Osteopetrosis-associated transmembrane protein 1), a gene coding for the β-subunit of *CLCN7* and participating in its transport to the ruffled border of osteoclasts. Mutation in *OSTM1* and *CLCN7* genes can also be responsible for severe neurodegeneration in ARO patients (Chalhoub, Benachenhou et al. 2003, Kasper, Planells-Cases et al. 2005, Lange, Wartosch et al. 2006, Pangrazio, Poliani et al. 2006).

1.4.3 Osteopetrotic Grey-lethal mouse

In the last decade, the Grey-lethal (*gl/gl*) mouse has been established as one of the most relevant osteopetrotic mouse models for study of infantile autosomal recessive osteopetrosis. The *gl/gl* mice were discovered in 1935 by Grüneberg (Gruneberg 1935). However, the spontaneous *Ostm1* gene mutation and the gene responsible for the *gl/gl* phenotype were only characterized almost 70 years later. In general, these mice are identified by their smaller size, grey-coat color, absence of tooth eruption, a higher bone density, anemia and a high number of inactive osteoclasts (**Figure 1.10**). The *gl/gl* phenotype recapitulates the main human symptoms of ARO patients (Chalhoub, Benachenhou et al. 2003).

The *Ostm1* gene is 25 Kb containing six exons and five introns. The ubiquitous expression of the *Ostm1* gene has been detected as early as E 12.5. Also, the unique *Ostm1* transcript of 3kb is found in various tissues including fetal liver, bone, brain, thymus and spleen. Furthermore, this gene encodes a protein of 338 amino acids or 38 kDa. OSTM1 protein features a signal peptide and a type I transmembrane domain in its C-terminal domain (**Figure 1.10**). Furthermore, the murine and human OSTM1 proteins display 83% homology (Chalhoub, Benachenhou et al. 2003). Additionally, 10 N-glycosylation sites have been identified in its luminal domain (Lange, Wartosch et al. 2006). This results in OSTM1 proteins of ~ 60 kDa and 80 kDa. In parallel, the cellular localization of OSTM1 in the endoplasmic reticulum (ER), golgi apparatus and lysosomes suggests a function associated with intracellular trafficking and organelle dispersion. This late function could also result from the multiple interactors of OSTM1 via its C-terminal domain (Pandruvada, Beauregard et al. 2015)(Pandruvada, Beauregard et al. 2015)(Pandruvada, Beauregard et al. 2015).

The *gl/gl* mutation affects the *Ostm1* locus and corresponds to a 7.5 Kb deletion including the promotor region, the first exon and a portion of the first intron. This spontaneous deletion is associated with a repetitive motif LINE-1 and generates a null phenotype that lacks *Ostm1* transcript and protein expression. The first human OSTM1 mutation has been described in a patient homozygous for the mutation that is characterized by a G to A transition at the donor splice site of intron 5.

This leads to exon 5 skipping and absence of the (type I) transmembrane domain of the truncated protein. This human *OSTM1* mutation causes premature death at approximately 31 days-old and is associated with severe ARO (Chalhoub, Benachenhou et al. 2003, Quarello, Forni et al. 2004, Maranda, Chabot et al. 2008). Until now, two nonsense, one frame-shift and one splice site mutations as well as micro deletions are identified in ARO patients. All these mutations perturb OSTM1 function and cause a lethal osteopetrotic phenotype (Mazzolari, Forino et al. 2009, Ott, Fischer et al. 2013).

Analysis of the *gl/gl* bone phenotype reveals 20% increase in osteoclasts number with defective activity to resorb the bone matrix. Despite their ability to attach the bone surface, the functional defect of *gl/gl* osteoclasts is illustrated by an underdeveloped ruffled border and actin rings that are responsible for ion transport during bone resorption. Defective *gl/gl* osteoclasts impact on the remodelling of trabecular bone leading to 3-fold increase in bone density. Moreover, the *gl/gl* bone marrow cavity is drastically reduced and filled by bone (Rajapurohitam, Chalhoub et al. 2001).

Furthermore, the grey-coat color of *gl/gl* mice is explained by an abnormal distribution and clumping of the yellow pigment (pheomelanin) in the murine hair and detectable only on an agouti background (GRÜNEBERG 1936). *Ostm1* gene is hypothesized to regulate the trafficking of this yellow pigment (unpublished data from Vacher Lab). *gl/gl* mice can also develop severe neuronal and retinal photoreceptor degeneration independently of hematopoietic defects. Investigation of both pathologies revealed a novel *Ostm1* function in the regulation of an autophagic pathway and the related inflammatory response (Heraud, Griffiths et al. 2014).

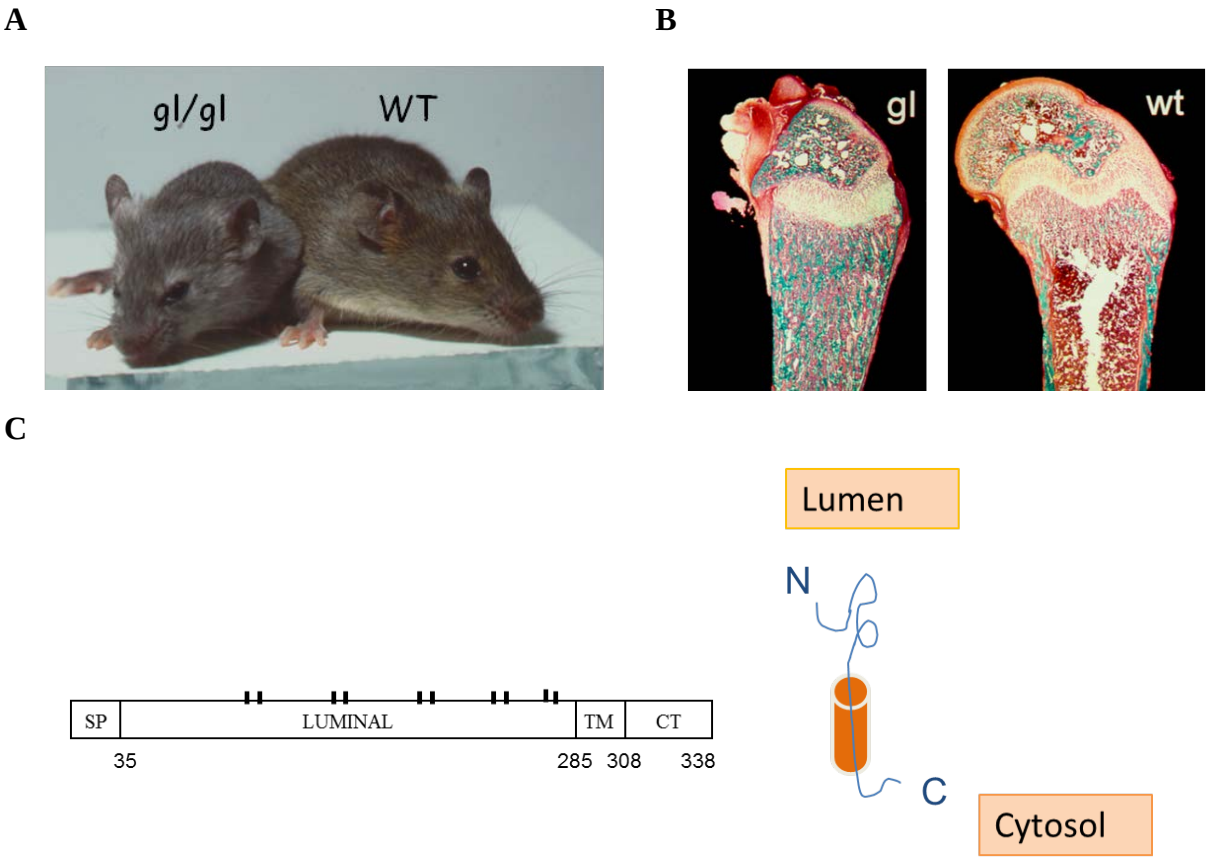

Figure 1.10. Characteristics of the osteopetrotic Grey-lethal mice.

A) *gl/gl* mouse displays grey coat color compared to agouti control. **B**) Femur histologic sections show a severe reduction of bone marrow in *gl/gl* mice. **C**) Schematic representation of the OSTM1 protein structure including SP (signal peptide), Luminal domain containing 10 glycosylation sites, TM (Transmembrane domain) and CT (C-terminal) domain. Figure is adapted from unpublished data from Vacher lab and (Rajapurohitam, Chalhoub et al. 2001, Pandruvada, Beauregard et al. 2015).

1.5 HYPOTHESIS AND RESEARCH GOAL

One major hematopoietic phenotype of *gl/gl* mice is linked to deregulation of the lymphoid lineages including a decreased B lymphoid population and an altered T cell differentiation and maturation. These lymphoid defects of *gl/gl* mice are consistent with the higher susceptibility to infections that has been depicted in ARO patients.

The transgenesis strategies to rescue all osteopetrosis associated phenotypes have been previously tested in our laboratory. For example, PU-1-*Ostm1-gl/gl* transgenic animals have demonstrated the rescue of osteopetrotic and hematopoietic B and T cells defects. Based on these results, we have hypothesized that *Ostm1* gene may be required in additional hematopoietic lineages and/or in a crosstalk mechanism between other hematopoietic cells for osteoclast activation.

Therefore, my research goal is to determine the role of *Ostm1* gene in T and B lymphoid phenotypes in the *gl* osteopetrotic context and to investigate the potential crosstalk between inactive osteoclasts and the lymphoid phenotype of the osteopetrotic *gl/gl* mice.

To do so, the first part of my project details the *gl/gl* thymus phenotype, the subsequent T cell differentiation defects based on the *Ostm1* gene expression profile. Also, the specific Ostm1 gene overexpression of T cell lineage in *gl/gl* mice is used to understand the Ostm1 contribution at a cellular level independent of the other osteopetrotic hallmarks (Chapter 2)

To understand the role of *Ostm1* in B lineage, chapter 3 describes the B lymphoid defects of *gl/gl* mice. It also discusses analysis of the transgenic *gl/gl* mice with the *Ostm1* overexpression targeted to B cell lineage and the mice with B cell specific deletion of *Ostm1* gene by using the cre-lox system.

CHAPTER 2: THE THYMUS PHENOTYPE OF *gl/gl* OSTEOPETROSIS

2.1. PREFACE

Our previous analysis of the *gl/gl* animals demonstrated a broader defect in hematopoietic lineages aside from osteoclasts. In fact, the transgenesis strategy using the PU-1 promoter allowed us to restore *Ostm1* gene expression both in myeloid and lymphoid lineages of *gl/gl* mice. This study revealed an abnormal T lineage distribution in the *gl/gl* thymus. Moreover, the T cell rescue of PU-1-*Ostm1 gl/gl* transgenic mice demonstrated the requirement of the *Ostm1* gene for normal T cell distribution in the thymus (**Figure 2.1**). However, the cause of defective T cell distribution in *gl/gl* mice needs to be determined. For this purpose, I dissected the *gl/gl* thymus phenotype throughout T cell developmental (objective 1).

Furthermore, this previous work could not exclude the myeloid contribution in the T cell rescue of PU-1-*Ostm1 gl/gl* transgenic mice, since the PU-1 promoter targets both myeloid and lymphoid lineages. In addition, the rescued bone-marrow of these transgenic mice has raised the possibility of a potential indirect function for *Ostm1* gene in T lineage development either by restoring osteoclast activity or by regulating the T cells precursor niche. Thus, the direct versus indirect contribution of the *Ostm1* gene in the T lineage phenotype of *gl/gl* animals remains unclear (Objective 2). For this purpose, we mainly restored *Ostm1* expression in the T lineage by using a mouse in which the CD2 promoter activates expression of *Ostm1* to generate CD2-*Ostm1-gl/gl* transgenic mice. I then characterized the osteopetrotic and lymphoid phenotypes of the CD2-*Ostm1-gl/gl* transgenic mice. Finally, I investigated the molecular differences at the transcriptional level that could explain the T cell developmental defect in the absence of the *Ostm1* gene.

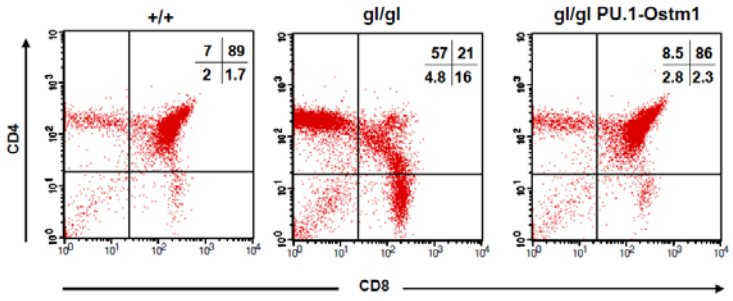

Figure 2.1. The rescued T cell distribution in *gl/gl* PU-1-*Ostm1* mice.
Surface expression of CD4 and CD8 markers and the corresponding T cell distribution within the thymus and in comparison to wild-type and *gl/gl* animals (Pata, Heraud et al. 2008).

2.2. ARTICLE 1

Osteopetrotic grey-lethal mutation disrupts thymus-autonomous T cell development

Marie Mutabaruka[1,3], Monica Pata[1], Nathalie Labrecque [2,4], Jean Vacher [1,2,3]

[1] Institut de Recherches Cliniques de Montréal, Montréal, Québec H2W 1R7, Canada
[2] Département de Médecine, Université de Montréal, Montréal, Québec H3T 3J7, Canada
[3] Division of Experimental Medicine, McGill University, Montréal, Québec H3A 1A3, Canada
[4]Centre de Recherche Hôpital Maisoneuve-Rosemont, Montréal, Québec H1T 2M4, Canada

*In preparation to be submitted to Journal of Experimental Medicine

Competing financial interests

The authors declare no competing financial interests.

Corresponding author

Correspondence should be addressed to Jean Vacher: jean.vacher@ircm.qc.ca

2.2.1. ABSTRACT

Mutations affecting the *Ostm1* gene are responsible for the most severe form of autosomal recessive osteopetrosis, both in humans and in grey-lethal (*gl/gl*) mice. This osteopetrotic phenotype is associated with increased inactive osteoclasts, obliteration of marrow space, and major lymphopoietic defects leading to increased susceptibility to infections and premature death in mice at three weeks of age. The altered distribution of the double and single positive $CD4^+$ and $CD8^+$ T cells in *gl/gl* mice suggests an unknown role for the *Ostm1* gene in T-cell differentiation. Until now, it was unclear whether this depletion of DP ($CD4^+CD8^+$) thymocytes in *gl/gl* mice resulted from an impaired bone marrow input or from a cell-intrinsic deregulation. Our study reports a progressive deficit from ETPs to DP T-cells in *gl/gl* thymi. Subsequent *ex vivo* co-culture assays of *gl/gl* ETPs cells revealed faster differentiation that could be related to *Rac1* overexpression. Interestingly, the T cell specific restoration of *Ostm1* expression was able to normalize *Rac1* level and the thymic distribution of T cell populations. However, these transgenic mice maintained an osteopetrotic bone marrow. Together, these findings provide the first evidence of an early cell-autonomous role for *Ostm1* gene in thymus-dependent T cells homeostasis independently of the myeloid osteoclast lineage.

2.2.2. INTRODUCTION

Osteoimmunology highlights the molecular interplay between the bone and the immune systems (Arron and Choi 2000, Takayanagi 2005, Lorenzo, Horowitz et al. 2008). Newly-differentiated mature T cells display an increased expression of *RANKL* (receptor activator of nuclear factor-κb ligand) (Lacey, Timms et al. 1998) which is known to control osteoclast (OC) differentiation upstream of the NFATc1 (nuclear factor of activated T cells cytoplasmic) transcription factor (Danks and Takayanagi 2013). Additionally, T lymphocytes help to maintain bone homeostasis by secreting the pro-inflammatory IL-17 (Interleukin 17) which induces high RANKL secretion from mesenchymal cells to initiate osteoclastogenesis (Lacey, Timms et al. 1998, Danks and Takayanagi 2013). An indirect crosstalk between bone homeostasis and lymphoid lineages was also revealed via the capacity of mature bone resorbing osteoclasts (OC) to modulate the hematopoietic stem cell (HSC) niche residing in the marrow and the concomitant LSK ($Lineage^{-}Sca1^{+}Kit^{-}$) cells containing the lymphoid progenitor pool (Kollet, Dar et al. 2006, Mansour, Abou-Ezzi et al. 2012, Mansour, Wakkach et al. 2012, Blin-Wakkach, Rouleau et al. 2014). Consequently, an undermined synchronicity of hematopoietic lineages can result in immunodeficiency and subsequent vulnerability to infections depicted in osteopetrotic patients (Blin-Wakkach, Bernard et al. 2004, Guerrini, Sobacchi et al. 2008, Essabar, Meskini et al. 2014).

The *grey-lethal* (*gl/gl*) osteopetrotic mice are characterized by a spontaneous null mutation in the *Ostm1* (Osteopetrosis associated transmembrane protein 1) gene. This mutation leads to ineffective OC resorption, obliteration of bone marrow (BM) space, anemia, deregulation of hematopoietic lineages, and premature death linked to the most severe form of ARO (autosomal recessive Osteopetrosis) (Rajapurohitam, Chalhoub et al. 2001, Chalhoub, Benachenhou et al. 2003, Maranda, Chabot et al. 2008). The clinical relevance was confirmed in *OSTM1* patients who display similar bone and hematopoietic defects, leading to a high susceptibility to infection and premature death under 10 years of age (Quarello, Forni et al. 2004, Lange, Wartosch et al. 2006, Pangrazio, Poliani et al. 2006, Maranda, Chabot et al. 2008). Only an early bone marrow transplantation with effective engraftment can alleviate osteopetrotic features in ARO patients and extend their lifespan (Coccia, Krivit et al. 1980, Gerritsen, Vossen et al. 1994, Villa, Guerrini et al. 2009, Sobacchi, Schulz et al. 2013).

The complete rescue of the OC defect as well as the hematopoietic B and T cells deficit in PU-1-*Ostm1-gl/gl* transgenic mice supported a hematopoietic crosstalk for production of active OC (Pata, Heraud et al. 2008). More specifically, restoration of the T-lymphoid distribution of immature double positive (DP: $CD4^+CD8^+$) and mature single positive (SP) $CD4^+$ or $CD8^+$ populations in PU-1-*Ostm1-gl/gl* transgenic mice suggested a role for the *Ostm1* gene in the T cell differentiation program or the restoration of the BM niche (Pata, Heraud et al. 2008).

Mobilization of early thymic cell progenitors (ETPs: $Lineage^-Sca1^+CD44^+c\text{-}Kit^{hi}$) from the BM through the bloodstream is essential to initiate the T cell differentiation program (Yokota, Huang et al. 2006, Cyster 2009, Gossens, Naus et al. 2009, Zuniga-Pflucker 2009, Shah and Zuniga-Pflucker 2014). In the thymus, T cell development progresses from double-negative (DN: $CD4^-CD8^-$) to double positive (DP: $CD4^+CD8^+$) stages that give rise to mature and functional single positive (SP $CD4^+$ or $CD8^+$) cells. DN populations consist of four immature subsets including DN1 ($CD44^+CD25^-$), DN2 ($CD44^+CD25^+$), and DN3 ($CD44^-CD25^+$), which, following TCR beta gene rearrangement, become DN4 ($CD44^-CD25^-$).

Proper T cell development relies on the integrity of the three-dimensional architecture of thymic epithelial cells combined with production of chemokines and specific signals such as Notch that are essential for survival, proliferation, and intrathymic homing and migration of $ETPs/DN1ckit^{hi}$ cells (Misslitz, Pabst et al. 2004, Bleul, Corbeaux et al. 2006, Mohtashami and Zuniga-Pflucker 2006, Takahama 2006, Yokota, Huang et al. 2006, Petrie and Zuniga-Pflucker 2007, Gossens, Naus et al. 2009). $ETPs/DN1ckit^{hi}$ migrate from the cortico-medullary junction to the sub-capsular region where they differentiate into DN2/DN3 cells, and then become DP in the outer cortex before maturing into SP $CD4^+$ or $CD8^+$cells in the medulla (Misslitz, Pabst et al. 2004, Bleul, Corbeaux et al. 2006, Mohtashami and Zuniga-Pflucker 2006, Takahama 2006, Yokota, Huang et al. 2006, Petrie and Zuniga-Pflucker 2007, Gossens, Naus et al. 2009). Furthermore, cellular lifespan combined with an early T cell progenitor input from the BM determine thymocyte turnover.

When BM contribution is compromised, thymus-autonomous differentiation maintain productivity of existing early T lymphocytes that have gained an extended lifespan in the absence of new competitors for stromal niches. In conjunction with the maintained homeostatic proliferation of peripheral T cells, this prevents depletion of T cell populations to sustain a long-term immune response (Tan, Ernst et al. 2002, Martins, Ruggiero et al. 2012, Peaudecerf, Lemos et al. 2012, de Barros, Vicente et al. 2013).

To investigate the exclusive role of the *Ostm1* gene in T cell lineage, the expression of this gene was confirmed from DN1 to mature SP T cells, supporting a role of *Ostm1* within T lineage homeostasis of *gl/gl*. Our current study revealed the time-dependent thymus degeneration resulting from combined events initiated at the ETP/DN1 stage and associated with the loss of *Ostm1*. Second, specific restoration of *Ostm1* in T cells of *gl/gl* mice under the control of the CD2 (Cluster of differentiation 2) promoter within *gl/gl*TR (CD2-*Ostm1 gl/gl* transgenic mice) distinguished the BM function from the cell-intrinsic function of *Ostm1* in thymic homeostasis (Lang, Wotton et al. 1988, Lang, Mamalaki et al. 1991, Monostori, Lang et al. 1991, de Boer, Williams et al. 2003). All *gl/gl*TR showed a rescue in the T cell distribution from early thymocytes to mature cells while in the *gl/gl* stromal environment. However, *gl/gl*TR mice maintained an underdeveloped osteopetrotic BM and die prematurely, suggesting a T cell-autonomous role for *Ostm1* during thymocyte differentiation. Furthermore, RNA-seq experiments revealed a different transcriptome signature of early T cell population (DN1: Lineage$^-$CD44$^+$CD25$^-$) isolated from control, *gl/gl* and *gl/gl*TR thymi. Overexpression of *S1pr1* and *Rac1* coincide with the enhanced *gl/gl* DN1 cells migration *in vitro*. Furthermore, this altered transcriptome of *gl/gl*DN1 migration was normalized within CD2-*Ostm1gl/gl* DN1.

In summary, this study provides the first evidence of the time-dependent effect of *Ostm1* in potentiating thymus-autonomous T cell development by regulating intrathymic migration of early T population via *Rac1/S1pr1* independent of BM input.

2.2.3. MATERIALS AND METHODS

Mice

The mouse strain GL/Le dl^J +/+gl was obtained from The Jackson Laboratory (Bar Harbor, ME) and maintained by heterozygous brother × sister mating for ~200 generations. Homozygous *gl/gl* mice were used for analysis with +/+ littermates as controls. All experiments on animals were approved by the institutional animal care committee and Canadian Council on Animal Care.

Generation and analysis of transgenic animals

CD2-*Ostm1* transgenic animals (129sv/C3H): The CD2-*Ostm1* construction was produced using the *Ostm1* cDNA (1.055 kb) with a V5 tag linked to the CD2 promoter (1.8 kb, XhoI/XbaI) upstream, poly(A) signal (0.8 kb) and hCD2Locus control region (LCR) sequence (6Kb) downstream. Linearized transgene (ECoRI/SmaI) was injected into fertilized oocytes from F2 (C3H×C57BL/6). Transgenic mice were identified by PCR primers targeting transgenic CD2-Ostm1 and endogenous Ostm1. PCR amplification conditions were 94 °C, 5 min, followed by 30 cycles of 94 °C for 30secs, 65°C for 30secs, and 72 °C for 10 min. Transgene integrity and copy number were determined by Southern blot using a radioactive probe targeting exon1 of *Ostm1* gene. Transgenic lines were crossed with heterozygous gl/+ mice to generate *gl/gl* CD2-*Ostm1* transgenic progenies at F2.

Expression Analysis

Total RNA from enriched early T-lineage progenitor (ETPs), mature and immature thymocytes populations, and tissues including bone marrow, brain, kidney, thymus, liver, and spleen was isolated with Trizol or MagMax total RNA isolation kit (Life technologies) protocols from CD2-Ostm1 transgene expression was quantified by using 1µg of total RNA by semi-quantitative PCR. Experimental conditions were 94 °C for 5 min, followed by 30 cycles of 94 °C for 0.5 min, 65°C for 0.5 min, and 72 °C for 0.5 min. CD2-*Ostm1* transgene and *Ostm1* expression were determined and normalized to S16 gene by real-time quantitative PCR using 50ng to 1µg of DNase (Invitrogen)-treated total RNA. All reactions were performed in triplicate using a Syber Green Master Mix (Life technologies).

PCR conditions were 94 °C, 15 min, followed by 45 cycles of 94 °C for 0.5 min, 55 °C for 0.5 min, and 72 °C for 0.5 min by MX4000 Multiplex quantitative PCR analyzer or 50 °C for 2 min; 95 °C for 10 min followed by 45 cycles of 95 °C for 15 sec, 60 °C for 30 sec with Viia 7 Real-time PCR system (life technologies).

RNA extraction of 50ng to 300ng from sorted cells was used for cDNA synthesis using qScript cDNA supermix protocol (Quanta biosciences). Quantification of gene expression including endogenous *Ostm1*, CD2-*Ostm1* transgene, endogenous *CD2*, *Rac1*, *S1pr1*, *Spns2*, *Sphk1*, *Sphk2*, *Sgpp1*, *Sgpp2*, *Sgpl1 and S16* was performed at 50 °C, 2 min, 95 °C for 10 min followed by 45 cycles of 95 °C for 15 sec, 60 °C for 30 sec by Viia 7 Real-time PCR system (life technologies).

Flow cytometry and cell sorting

Fluorescence-Activated Cell Sorting (FACS) Analysis: Flow cytometry analysis was carried out on a single cell suspension from spleen and thymus in phosphate-buffered saline with 1% heat-inactivated fetal bovine serum. Nucleated cells (1.5×10^6) were stained with antibodies from eBioscience: phycoerythrin-conjugated anti-CD4, anti-B220, anti-CD19, anti-TCR-β or Streptavidin; fluorescein isothiocyanate-conjugated anti-CD8, anti-CD44, anti-Ly6-G, anti-CD62L, anti-Lys-51 or Streptavidin; APC conjugated anti-cKit, anti-CD44, anti-CD45; Pe-Cy7 conjugated anti-CD25, anti-Sca-1 and anti-MHCII. Data acquisition and analysis were respectively done with CellQuest and FlowJo softwares on a BD FACS Calibur four-color flow cytometer and BD LSR cytometer.

Cell sorting: ETPs, DN1 to DN4 populations were sorted using Moflo cytometer, followed by RNA extraction using MagMax Total RNA isolation kit protocol (Life technologies).

Bone cellular analysis

Ex Vivo OC Differentiation- Spleen derived OC-like cells were differentiated from spleen-derived macrophage progenitor cell *in vitro* for 6 days in α-minimal essential medium (AMEM) supplemented with 10% fetal bovine serum, 10 ng/ml macrophage-colony-stimulating factor (M-CSF), and 50 ng/ml receptor activator of NF-κB ligand (RANKL). OC morphology and nuclei number were assessed using an Axiopholt 12 (Zelda) microscope with 10x, 20X and 40x magnifications.

Western Blot

Proteins were isolated from hematopoietic tissues (spleen and thymus), kidney, liver and brain in RIPA buffer containing proteinase inhibitors cocktail: PMSF, β-Glycerophosphate, Sodium vanadate and proteinase inhibitor cocktail. Tissue protein extract was quantified by Bradford assay on ELISA reader (Roche). V5-*Ostm1* transgene protein expression was detected following an overnight incubation with a primary antibody anti-V5-HRP (Invitrogen) in Tris-buffered saline, 0.1% tween 20 (TTBST 1X) and Bovine serum albumin (BSA) 3%. Following incubation with stripping solution at 55^{o}C for 30 minutes, PVDF membrane was incubated with the primary antibody β-actin from Sigma for 1-2hrs, washed 3 times in TTBST 1X followed by a second incubation with anti-mouse IgG HRP for 1hr. Protein detection and quantification were determined via BioRad Image lab software.

Histological and X-ray Analysis

Thymus and spleen samples from mice of P8, P15 and P21 were fixed in 10% phosphate-buffered formalin and embedded in paraffin. Sections were stained with hematoxylin and eosin (H&E) and anti-Ki67. Tissue sections were mounted, and analyzed using an Axiopholt microscope (Zelda) at 10 X, 20 X and 40 X magnifications. Bone density from P14 and P21 mice were evaluated by X-Ray scan using Faxitron MX20 (18 Kv, 10 s).

***In vitro* transwell migration assay**

Thymus from *gl/gl, gl/gl*TR and control mice at P19 were isolated and homogenized in RPMI1640 + 0.5% BSA under sterile conditions. Total cells were rested for 2 hours at 37°C and 5% CO_2. Cell input of 2 x 10^6 cells in 100µl of migration medium in the upper chamber and 600µl of RPMI1640 + 0.5% BSA with or without 100ng/µl of SDF-1α (Peprotech) in the bottom chamber of a 24-well transwell plate (Corning, 5.0µm, cat #3421). Migrated DN1 percentage was assessed after 2 or 18 hours incubation at 37°C and 5% CO_2. Percentage of migrated DN1 (Lin^- $CD44^+$ $CD25^-$) cells in the lower chamber was normalized to the DN1 percentage in the separate input well.

RNA sequencing

RNA of sorted DN1 cells from 2 to 3 different litters of 19 days-old: wild-type (2), *gl/gl*TR (2) and *gl/gl* (3) animals was extracted and pooled. Total RNA was isolated using MagMax total RNA isolation kit (Life technologies). RNA integrity and quality were assessed by Bionanalyzer RNA pico chips (Agilent). Ribosomal RNA depletion was performed using kit Epicentre. Generation of transcriptome libraries from 4 to 25ng of total RNA using TruSeq stranded Kit including RNA fragmentation followed by cDNA and double strand cDNA synthesis, cDNA fragmentation, end repair of fragmented cDNA, adapter oligonucleotide ligation and 15 cycles of PCR enrichment using Illumina protocol and reagents. Quality control was validated by using Nanodrop. Size and concentration control were determined by HSdna chip and quantification by quantitative PCR. Samples were pooled and amplified in cDNA clusters using cBot (Illumina). Paired-end sequencing (PE50) was performed on HiSeq 2000. Raw data are accessible through: GEO number: GSE72184.

Computational analysis

The raw data reads were zipped in FASTQ format. Gene expression analysis was executed following current protocol (Trapnell, Roberts et al. 2012, Trapnell, Roberts et al. 2014). Big wag files were generated from BAM files to facilitate UCSC browser alignment. Differential gene expression was evaluated using Cuffdiff 2.2.1 (http://cufflinks.cbcb.umd.edu/manual.html#cuffdiff). Analyzed data were processed and presented by using CummeRbund 2.6.1 (http://compbio.mit.edu/cummeRbund/) with R 3.1.0. Biological pathway changes corresponding to differentially expressed genes were determined by using Ingenuity Pathway Analysis (IPA) 2014(Qiagen:http://www.ingenuity.com/products/ipa http://www.ingenuity.com/wp-content/uploads/2014/06/Citation-Guidelines.pdf); and Database for Annotation, Visualization and Integrated Discovery (DAVID): https://david.ncifcrf.gov/. All referred webpages above describe how to install computational programs and tools for RNA Sequencing analysis.

OP9-DL4 co-culture assays

OP9 stromal cells expressing DL4 were plated at 2.0×10^4cells/well and co-cultured with sorted *gl/gl*ETPs and control ETP cells (~ 500 to 750 cells). The cells were incubated in Opti-α-modified Eagle medium (OPTIMEM) supplemented with 50 µM of 2-mercaptoethanol (Sigma); 2 ng/mL of IL-7; 10 ng/mL Fms-like tyrosine kinase 3 ligand and 20 ng/mL of Stem Cell Factor (PeproTech) and 20 % charcoal-stripped fetal bovine serum (Sigma). Cell differentiation from DN1 to DP stage was assessed using Fluorescence-Activating Cell sorting after 5, 8, 15 and 20 days in culture.

Statistical Analysis

Values are expressed as mean ± SEM. Statistical analysis was performed using Graphpad Prism software (San diego, CA). Unpaired two-sample Student's t test was used for statistical analysis with $p \geq 0.05$ considered significant.

2.2.4. RESULTS

***gl/gl* thymi exhibit abnormal architecture and cellularity**

To investigate the potential consequence of the loss of *Ostm1* in T lineage homeostasis, thymus architecture and T lymphoid populations were characterized in *gl/gl* mice. Thymus sections from *gl/gl* mice showed a time-dependent structural disorganization when compared to age-matched controls (**Fig 2.2A**). At post-natal (P) day 15 and 21, *gl/gl* mice exhibited an unclear cortico-medullary demarcation and the thymi cortices from these mice were hypocellular (**Fig 2.2A**). Additionally, **Table 1.1** summarizes other *gl/gl* thymus features at P21. This includes severe reduction of animal body weight and the diminished thymus/body weight ratio indicating an independent reduction of thymus size. Concordant with these data, total *gl/gl* thymus cellularity was approximately 100-fold lower. The number of immature DP ($CD4^+/CD8^+$) population is drastically reduced and there is 2 fold less mature SP $CD4^+$ or $CD8^+$ populations.

To define the timeframe of this thymic phenotype, T cell distribution was monitored within *gl/gl* and control thymi harvested from mice at P3, P8, P15 and P21. *gl/gl* thymic cellularity and T lineage distribution at P3 and P8 showed no significant difference when compared to controls (**Fig 2.2B**). However, by P15, total thymic cellularity was 100-fold reduced within *gl/gl* thymi and reached a maximum depletion at P21 **(Fig 2.2B**). These data suggest age-dependent thymus cell depletion and disorganized thymic architecture starting at P15 within *gl/gl* animals.

Therefore, to explore gene relevance in T cell populations, quantitative *Ostm1* gene expression was established within sorted early cell (DN1-DN4) and mature T cell (SP $CD4^+$ or $CD8^+$) subsets. A significant fold-change in DN1c-Kit^{++} and DP populations supports the functional relevance of *Ostm1* in these T cell subsets (**Fig 2.2C**). Interestingly, the severe depletion from 85% to 18% of the DP population occurs at P15 and reaches 11.5% of DP population at P21 in *gl/gl* thymus compared to control (**Fig.2.2D**).

Collectively, these findings suggest that in absence of *Ostm1*, a time-dependent deficit of DP population and subsequent degenerative changes occur within the thymus.

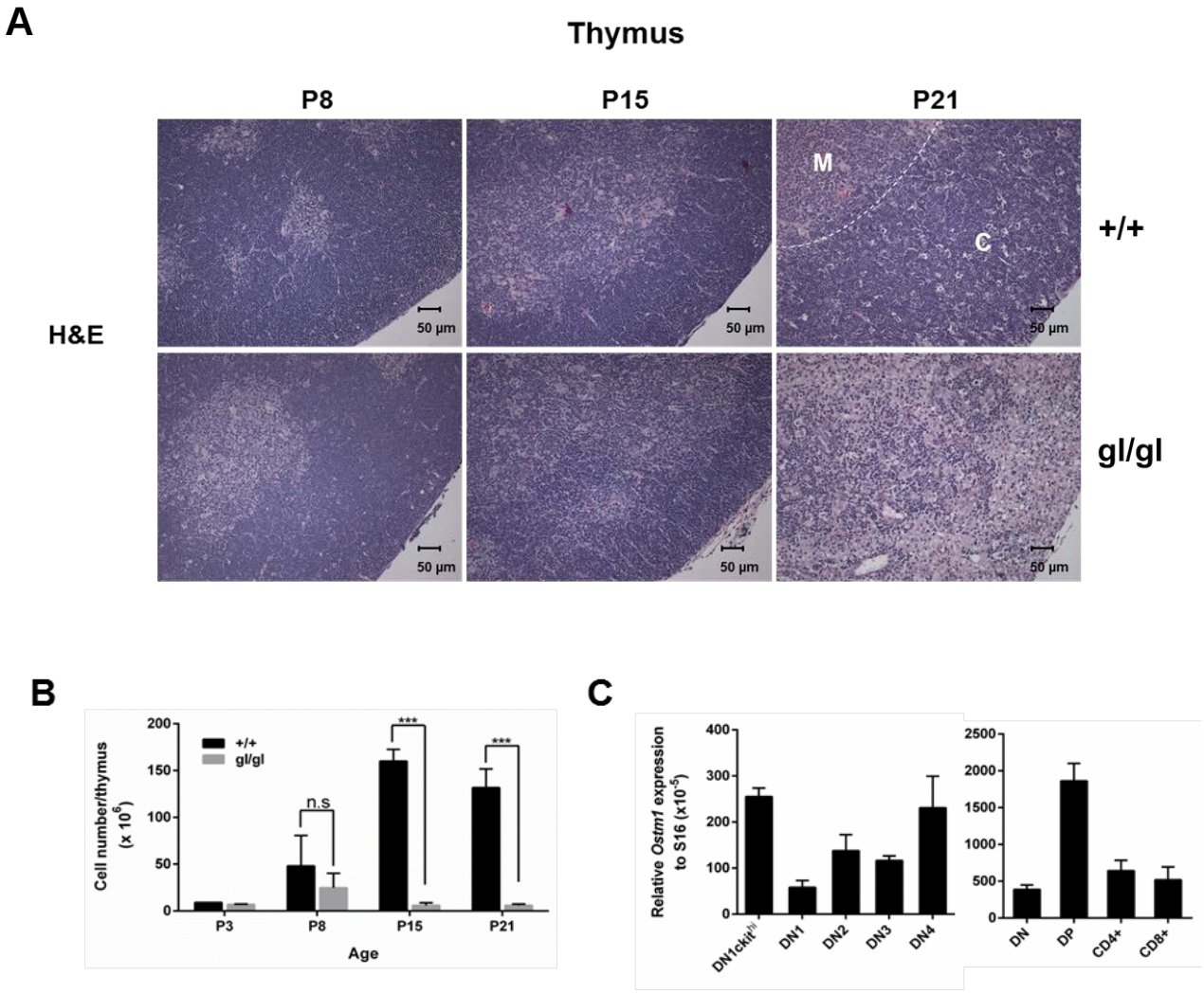

Figure 2.2. *gl/gl* thymi exhibit abnormal architecture and cellularity.

(A) Histology sections showing tissue integrity of control (+/+) and *gl/gl* thymi dissected from mice of 8, 15 and 21 days-old (n=2) by Hematoxylin and Eosin (H&E) staining and magnification at 20X. (**B**) Total cellularity (n=3) within *gl/gl* and control thymi from 3, 8, 15 and 21 days-old mice, data as mean of cell number x 10^6 ± SEM with ***p<0.001. (**C**) Quantitative *Ostm1* gene expression of sorted T cell populations (n=4) from DN1cKit^{hi} to DN4 (left panel) and from DP to mature SP CD4$^+$ or CD8$^+$ (right panel) populations isolated from +/+ thymus of 21 days-old mice. Figures (**A**-**B**) represent data from age-matched mice.

Table 1.1. Thymic lymphoid cellularity of grey-lethal (*gl/gl*) mice

mice	n	Body weight (gr)	Cell number/ Thymus (x 10^6)	Thymus/body weight (%)	$CD4^-CD8^-$	$CD4^+CD8^+$	$CD4^+$	$CD8^+$
+/+	5	15.8 ± 3.4	149.1 ± 65.3	0.509 ± 0.062	3.5 ± 1.0	111.6 ± 3.9	8.3 ± 0.8	3.5 ± 0.5
gl/gl	5	4.6 ± 0.9***	12.8 ± 2.5 ***	0.235 ± 0.091***	1.0 ± 0.4*	1.2 ± 0.8***	4.2 ± 1.3*	1.5 ± 0.5*

Data are expressed as means of cell number x 10^6 ± SEM *p<0.05; ***p<0.001

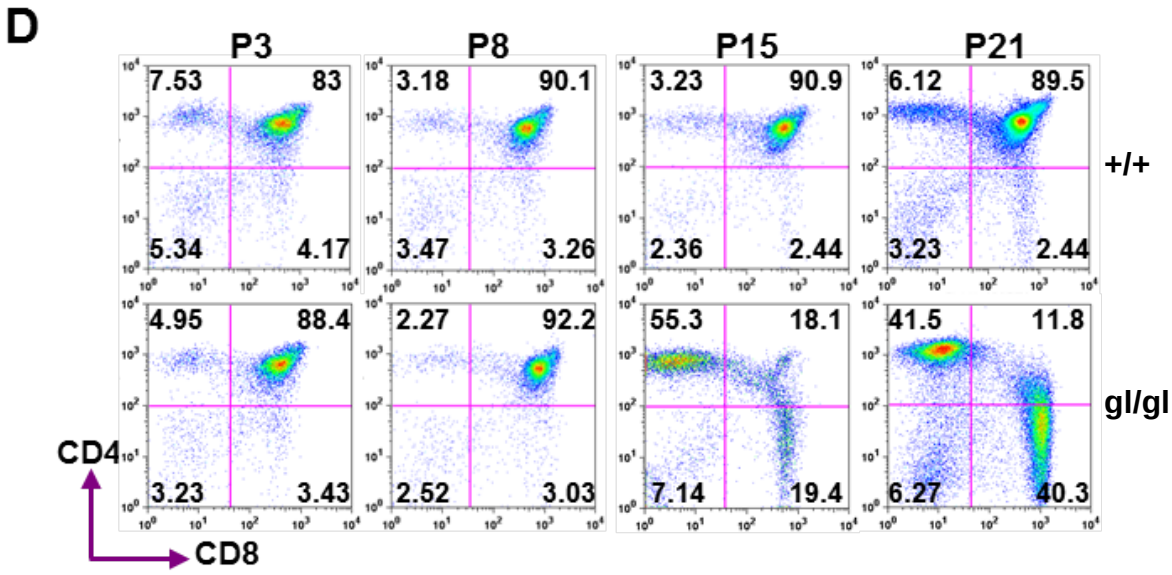

Figure 2.2. *gl/gl* thymi exhibit abnormal architecture and cellularity (continued)

(**D**) Time-course analysis of (DP: $CD4^+CD8^+$) cells distribution in 3, 8, 15 and 21 days-old control and *gl/gl* thymus.

Loss of *Ostm1* leads to defective T cell development

In the thymus, the DP cell pool is modulated by three factors: ETP input from BM, the subsequent differentiation of ETPs into the right proportion of DN1-DN4 populations, and the differentiation kinetic of DP cells into mature SP $CD4^+$ or $CD8^+$ cells (Bhandoola, Sambandam et al. 2003, Prockop and Petrie 2004, Petrie and Zuniga-Pflucker 2007). Therefore, to examine the impact of *Ostm1* depletion on thymocyte homeostasis, the deficit of DP cells was dissected within *gl/gl* thymus based on this T cell developmental scheme at the culminant age point P21.

For this purpose, we first confirmed that the majority of *gl/gl* DP cells were TCR-β^{int} or $CD69^+$(**Fig 2.3A**), indicating that the reduced DP population in *gl/gl* thymus express the αβ TCR and could produce mature SP cells (Bhandoola, Cibotti et al. 1999). Interestingly, the TCR-β and CD69 expression of mature SP $CD4^+$ or SP $CD8^+$ within the *gl/gl* thymus was similar to control, implying that there are newly-developed mature T cells within *gl/gl* thymus (**Fig 2.3A**). Moreover, we noticed a small TCR-β^{hi} subset within *gl/gl* DP and SP $CD8^+$cells, as well as $CD69^{hi}$ subset within the *gl/gl* DP (**Fig 2.3A**) which could also indicate a slight increase in negative selection of the *gl/gl* thymus (Van De Wiele, Marino et al. 2004).

Mature SP $CD4^+$ or $CD8^+$ cells from the positively-selected DP population have previously been shown to migrate into peripheral lymphoid tissues to mediate immune response (Weinreich and Hogquist 2008). Despite the 2.5 fold reduction of splenic cellularity in *gl/gl* mice, newly-differentiated mature SP $CD4^+$ or $CD8^+$ cells were normally distributed in the *gl/gl* spleen (**Fig 2.3B**) and lymph node (**Appendix 1.1**). Furthermore, the frequency of naïve T cells ($CD62L^+CD44^+$) across mature SP $CD4^+$ or $CD8^+$ fractions within the *gl/gl* spleen are slightly increased compared to control (**Fig 2.3B**).

Collectively, these observations suggest that the earliest *gl/gl* thymocytes prior to P15 have a normal distribution and differentiation compared to wild-type thymocytes. The *gl/gl* thymocytes also maintained the ability to colonize peripheral lymphoid tissue such as the spleen and lymph nodes at P21 (**Appendix 1.1**). Our findings illustrate the time-dependent defective T cell differentiation of *gl/gl* mice.

Furthermore, the normal distribution and egress of mature $CD4^+$ or $CD8^+$ SP suggest that DP depletion in the *gl/gl* thymus may result from earlier T cell developmental defects. To address this, we first determined by flow cytometry the percentage of ETPs in the thymus at P21. The ratio of the number of ETPs to the total cell number was 3 times lower within *gl/gl* thymus when compared to the control, suggesting that the disturbance of T cell development in *gl/gl* mice occurs due to previous T cell developmental defects prior to the DP stage (**Fig 2.3C)**. Thus, these findings led us to monitor early T cell differentiation of the DN1 to DN4 populations within the *gl/gl* thymus at P8, P15 and P21. Surprisingly, an important differentiation block at the DN1 to DN2 transition is observed in the *gl/gl* thymus, and coincides with the presence of intermediary subset ($CD44^{int}CD25^{int}$) in the *gl/gl* thymus at P15 and P21 (**Fig 2.3D**).

To validate causality between this aberrant T cell differentiation pattern and *Ostm1* gene mutation, ETPs (500–1500) from *gl/gl* and control mice were co-cultured *in vitro* on an OP9 BM-derived stroma layer expressing the Notch-ligand, DL4. The ETPs were monitored during 5, 8, 15 and 20 days for their differentiation potential into DN1-DN4 subsets and DP thymocytes. This *in vitro* experiment demonstrates a rapid decrease of the DN2-DN3 subsets and subsequent increase of the DN4 fraction (**Fig 2.3E**, top panel) and DP subsets (**Fig 2.3E**, bottom panel) at day 15 of culture of *gl/gl* ETPs. By day 20, both control and *gl/gl* ETPs reached a similar percentage of DP population (**Fig 2.3E**). This suggests an accelerated differentiation of *gl/gl* ETPs when compared to the control. Surprisingly, this co-culture assay exhibits the maintenance of the *gl/gl* T cell development *in vitro* with an increased effectiveness; which also suggest either a normal Notch1 responsiveness or a Notch-independent differentiation of *gl/gl* ETPs.

Taken together, the early *gl/gl* differentiation block at the DN1-DN2 stage *in vivo* from P15 combined with an intensified *gl/gl* ETP differentiation *in vitro* suggest an *Ostm1* function in the time-dependent exhaustion of the T cell differentiation programme.

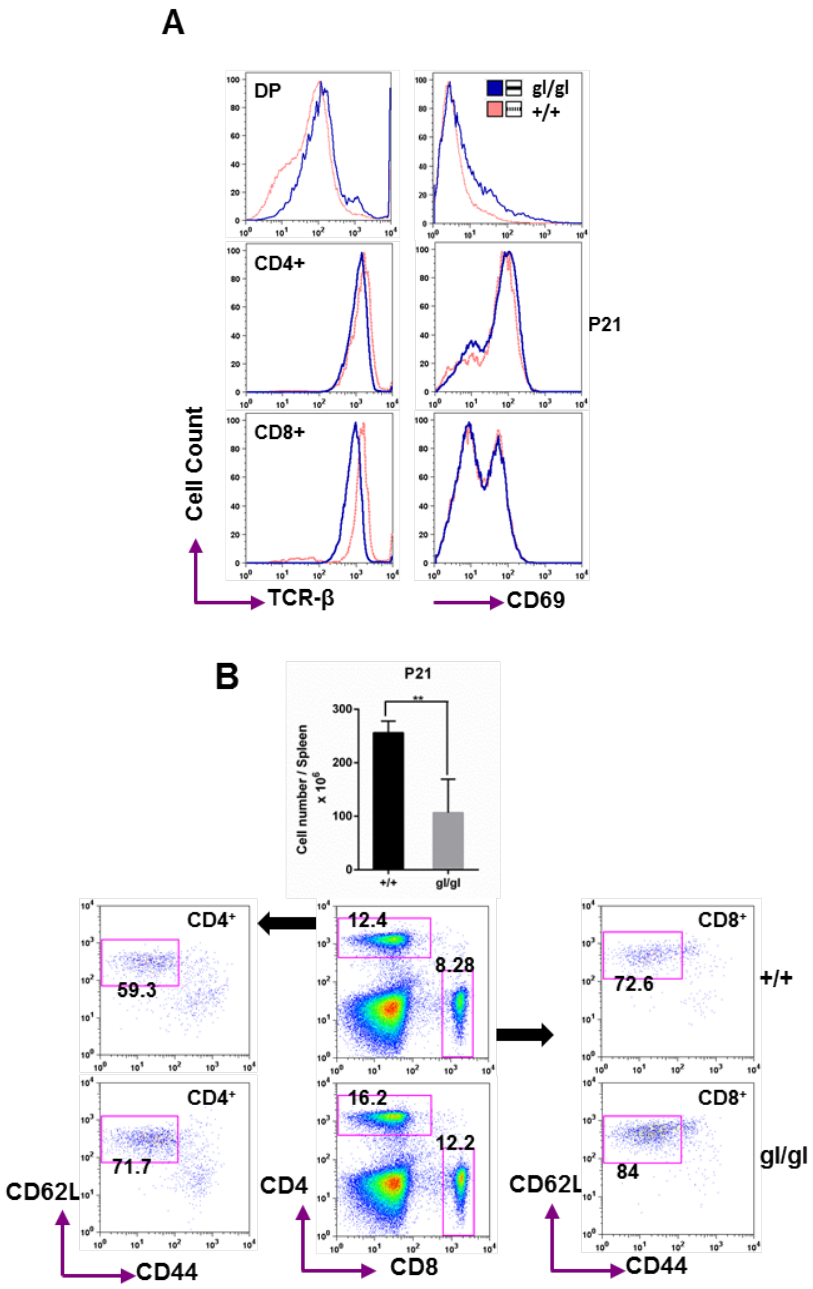

Figure 2.3. Loss of *Ostm1* leads to defective T cell development

(**A**) Flow cytometry profiles (n= 3) showing TCR-β and CD69 expression level of DP and SP $CD4^+$ or $CD8^+$ populations within *gl/gl* or +/+ thymi at P21. (**B**) Total cell number per spleen (n=4) with **p<0.001 and flow cytometry profiles (n=3) representing distribution of peripheral mature SP $CD4^+$ or $CD8^+$ and corresponding naïve T cells fractions ($CD62L^+CD44^+$) within +/+ and *gl/gl* spleen at P21

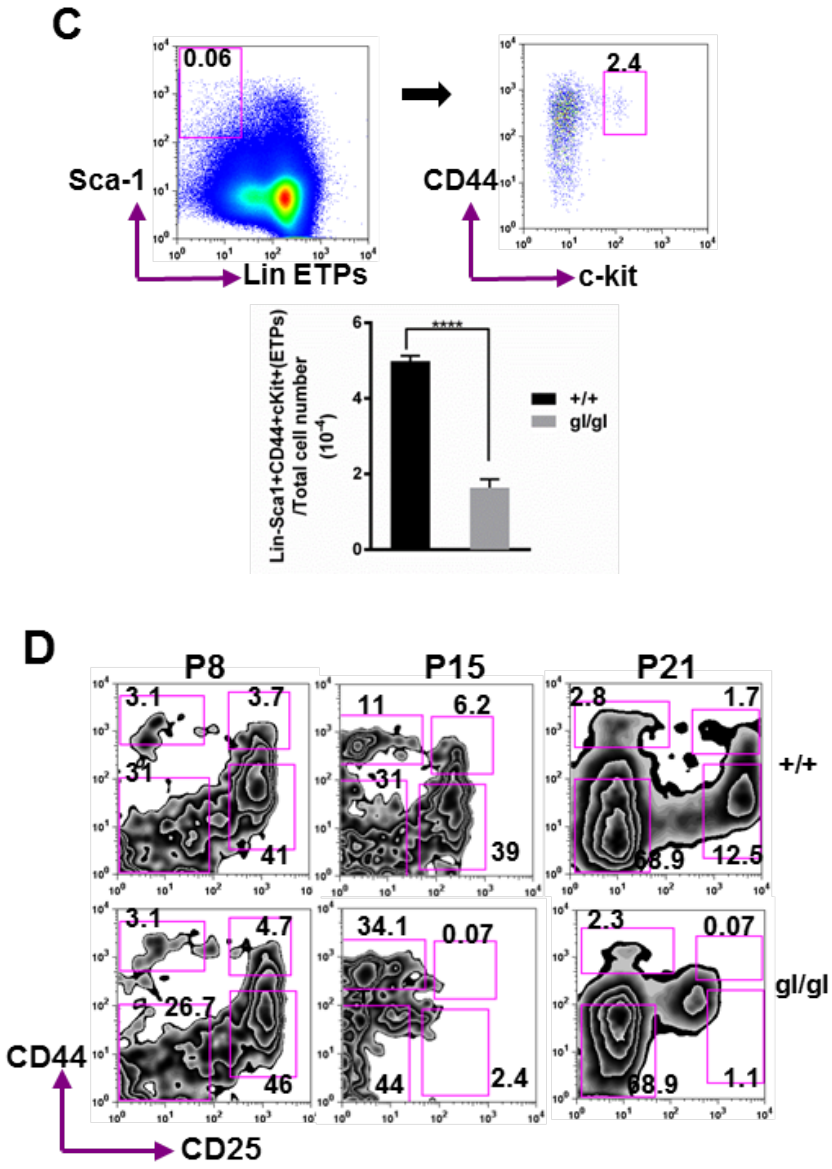

Figure 2.3. Loss of *Ostm1* leads to defective T cell development (continued)

(**C**) Flow cytometry analysis, gating strategies for ETPs ($Lin^{-}Sca1^{+}cKit^{+}CD44^{+}$) population and representation of ETPs number/total thymocytes ratio (n=6) within gl/gl and +/+ thymi with ****p<0.0001 at P21. (**D**) Time-course analysis of early T cell distribution (n=6) including ($DN1:CD44^{+}CD25$), ($DN2:CD44^{+}CD25^{+}$), ($DN3:CD44^{-}CD25^{+}$) and ($DN4:CD44^{-}CD25^{-}$) populations within aged-matched *gl/gl* and +/+ mice of 8, 15 and 21 days-old.

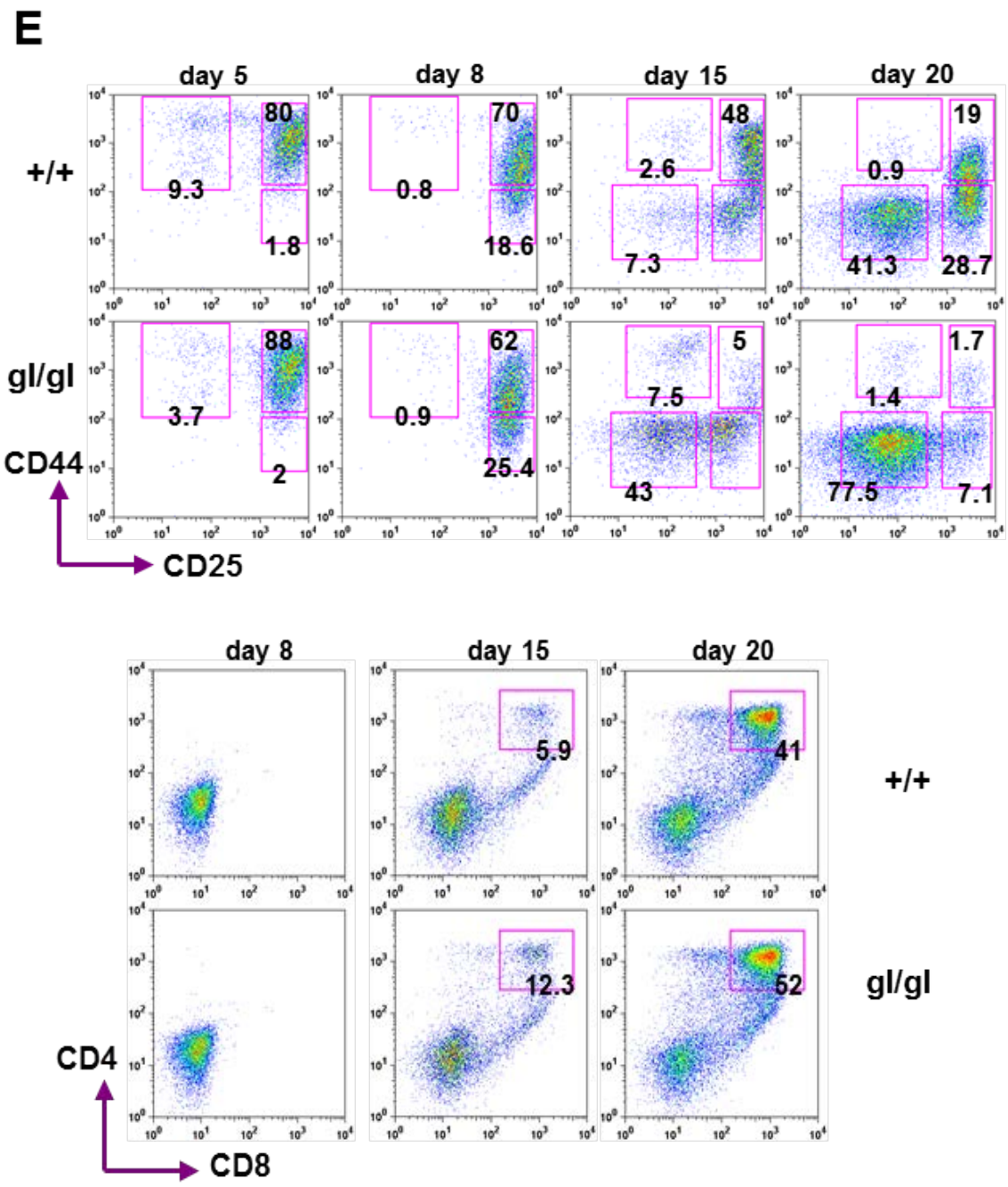

Figure 2.3. Loss of *Ostm1* leads to defective T cell development (continued)

(**E**) Differentiation potential of both control and *gl/gl* ETPs ($Lin^{-}Sca1^{+}cKit^{hi}CD44^{+}$) into DN1 to DN4 (top panel) and DP subsets (bottom panel) following 5, 8, 15 and 20 days *in vitro* co-culture assay (n=3) on OP9-DL4 stroma cells.

Restoration of *Ostm1* expression in the T lineage rescues thymic differentiation

To examine the functional relevance of *Ostm1* exclusive to the process of T cell differentiation and maturation without its involvement in extrinsic contributors such as thymic stromal organization or BM development, *Ostm1* expression was re-established in the T lineage of the *gl/gl* mice under the control of the human CD2 promoter (Lang, Wotton et al. 1988, de Boer, Williams et al. 2003).

The transgene construct included the first intron of the human CD2 gene, followed by cDNA sequence of the murine *Ostm1* gene fused to V5 tag and CD2 locus control region at the 5' end (**Fig 2.4A**). Southern blot analysis was used to validate CD2-*Ostm1* transgene integrity and copy number. Therefore, two transgenic animal lines, 777 and 805, were established with 13 and 5 transgene copies–respectively (**Appendix 1.3A**). The quantitative CD2-*Ostm1* transgene expression was observed in hematopoietic tissues, including the thymus, spleen, and bone marrow of both CD2-*Ostm1* transgenic lines. In addition, relative expression of the CD2-*Ostm1* transgene correlated with transgene copy number, with a higher fold-change in Line 777 compared to Line 805 (**Fig 2.4A**). Consistently, immunoblotting showed significant transgene protein expression in similar hematopoietic tissues including thymus, spleen and bone marrow of both transgenic lines (**Fig 2.4B**).

Next, thymus integrity of CD2-*Ostm1* transgenic animals was analyzed. Improved tissue architecture was observed in thymus sections (**Appendix 1.5**). Flow cytometry profiles confirmed unchanged DN1-DN4 and $CD4^+CD8^+$ distribution in the CD2-*Ostm1*+/+ thymus, as well as the distribution of mature SP $CD4^+$ or $CD8^+$ in the thymus and spleen within both CD2-*Ostm1* transgenic lines compared to control at P21 (**Fig 2.4C**). In parallel, cell sorting combined with quantitative PCR pointed-out the correlation between endogenous *Ostm1* gene and CD2-Ostm1 transgene expression within T cell populations, with an increased expression of both genes in $DN1ckit^{hi}$, DN4 (left panel) and DP populations (right panel) (**Fig 2.4D**). Therefore, the specific expression of the CD2-*Ostm1* transgene in the T lineage does not alter normal T cell development. This allows CD2-*Ostm1* +/+ transgenic animals to be crossed with gl/+ to generate CD2-*Ostm1 gl/gl* transgenic progeny at F2 to study the role of *Ostm1* expression in T cells.

To illustrate the cell-intrinsic role of *Ostm1*, T cell lineage differentiation was analyzed within the thymi of +/+, CD2-*Ostm1* +/+ (+/+TR), *gl/gl* and CD2-*Ostm1 gl/gl* (*gl/gl*TR) mice. *gl/gl*TR thymi exhibit a partial rescue in total cell number (**Fig 2.4E**) with a two-fold increase when compared to *gl/gl* thymi, but remain significantly diminished when compared to control thymi at P21. Interestingly, the ETP/total cell number ratio in both transgenic lines is enhanced 2-fold compared to +/+ thymus and increases 4-fold in comparison to *gl/gl* ETPs/total cell ratio at P21 (**Fig 2.4F**). In line with this observation, the subsequent differentiation block at the DN1 to DN2 transition stage depicted in *gl/gl* animals is also rescued within *gl/gl*TR thymus at P21 (**Fig.3G**). Importantly, distribution of DP cells within *gl/gl*TR is comparable to the control or +/+ TR and significantly higher than the *gl/gl* DP fraction (**Fig 2.4G**).

To verify the BM cavity implication following a potential crosstalk between the rescued T cell lineage and osteoclast activation, osteopetrosis was evaluated in CD2-*Ostm1 gl/gl* animals. An *in vitro* differentiation assay generated oversized osteoclasts from *gl/gl* and *gl/gl*TR spleen which were previously shown to be inactive (Rajapurohitam, Chalhoub et al. 2001), as opposed to osteoclasts generated from control and +/+TR spleen with normal morphology (**Fig 2.4H**). X-Ray radiographs display bone accumulation within marrow cavity of the *gl/gl*TR femur at P21, resulting both in higher bone density and smaller femur bone length when compared to the control and +/+TR femur **(Fig. 2.4I)**. However, these parameters do not differ when compared to the *gl/gl* femur (**Fig. 2.4I**). Interestingly, the lower frequency of common lymphoid progenitors (CLPs) is maintained in *gl/gl*TR BM and is comparable to *gl/gl* mice (**Fig 2.4J**), supporting the maintenance of an underdeveloped bone marrow and an osteopetrotic phenotype within *gl/gl*TR mice.

Together, these results indicate age-dependent and cell-intrinsic contribution of the *Ostm1* gene in early T cell differentiation events independently of marrow input.

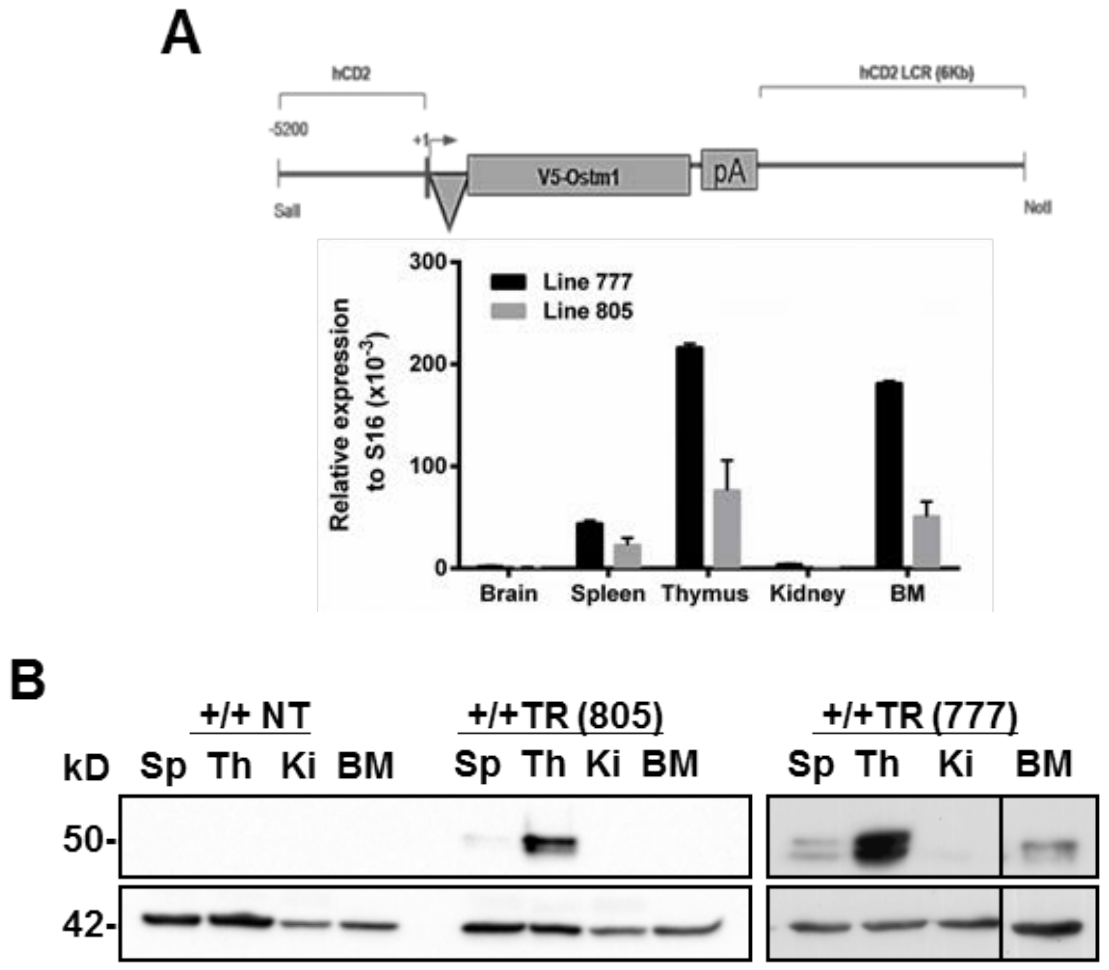

Figure 2.4. Restoration of *Ostm1* expression in the T cell lineage rescues thymic differentiation.

(**A**) Construct of CD2-*Ostm1* transgene containing the locus control region (LCR) sequence at the 3'end and the V5 tag fused to *Ostm1* cDNA sequence under the control of human Cluster of differentiation 2 (CD2) regulatory sequences at the 5'end. (**B**) Tissue specific expression of the CD2-*Ostm1* transgene (n=3) in +/+TR 777 and 805. Immunoblotting of transgenic protein expression (n=4) within hematopoietic tissues isolated from +/+ versus +/+TR805 and +/+TR777 animals

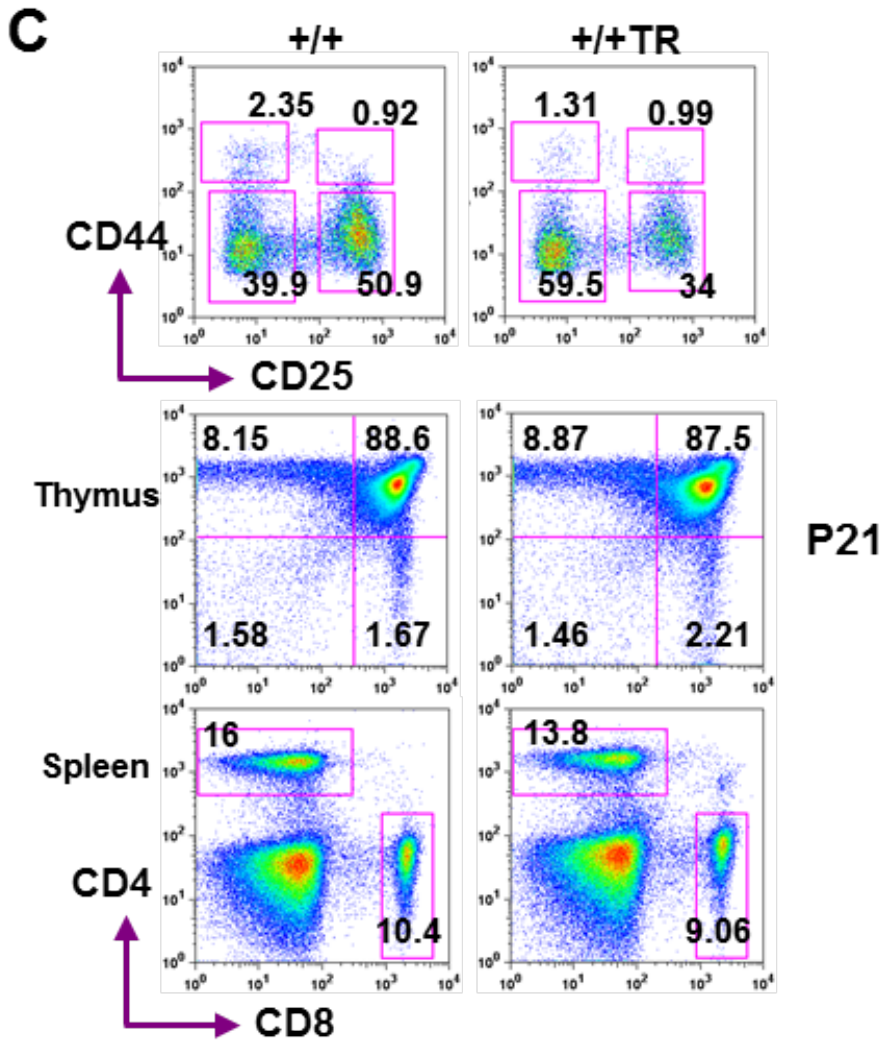

Figure 2.4. Restoration of *Ostm1* expression in the T cell lineage rescues thymic differentiation (Continued)

(**C**) Distribution profiles (n=6) of immature DN1-DN4 and DP, mature SP $CD4^+$ or $CD8^+$ populations in the thymus as well as mature SP $CD4^+$ and $CD8^+$ in the spleen of +/+TR mice at P21.

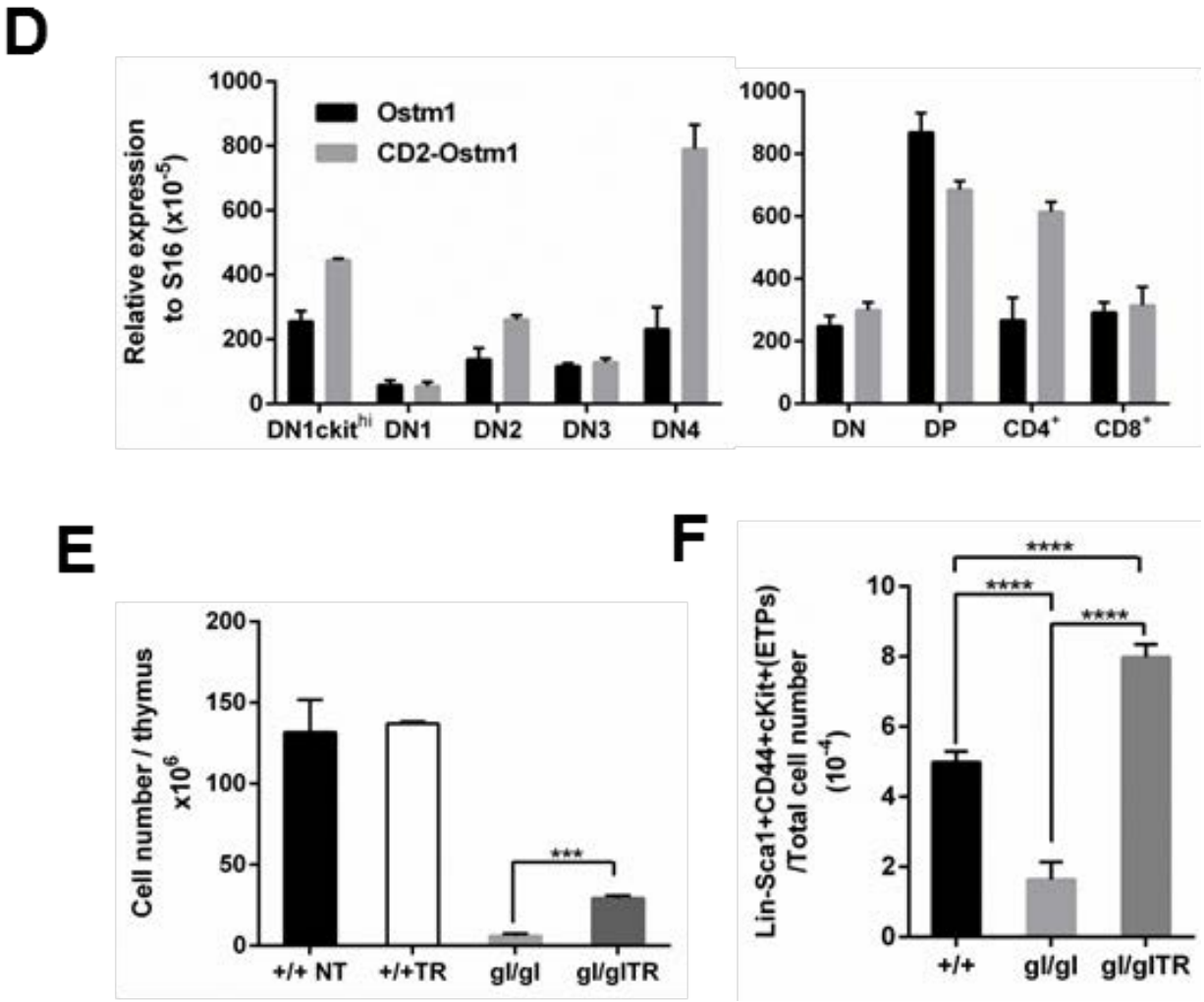

Figure 2.4. Restoration of *Ostm1* expression in the T cell lineage rescues thymic differentiation (Continued)

(**D**) Quantitative expression of the *Ostm1* gene and CD2-*Ostm1* transgene (n=3) from enriched DN1ckit^{hi} to DN4 (left panel) and from DP to SP CD4^{+} or CD8^{+} (right panel) populations of +/+TR thymus at P21. (**E**) Total cell number per thymus in five age-matched +/+, +/+TR, *gl/gl* and *gl/gl*TR animals with ***p<0.001 at P21. (**F**) ETPs (Lin^{-}Sca1^{+}cKit^{+}CD44^{+}) number/total cells ratio (n=4) within +/+, +/+TR, *gl/gl* and *gl/gl*TR thymi with ****p<0.0001 at P21

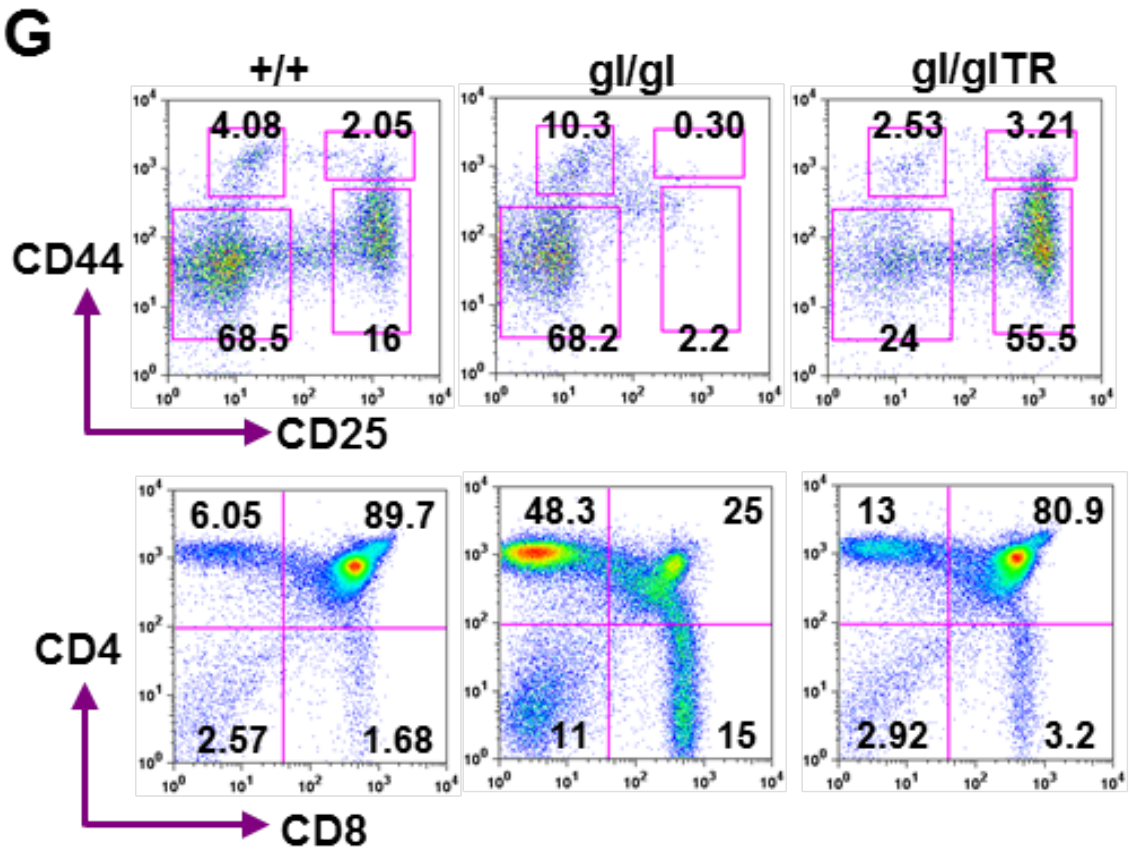

Figure 2.4. Restoration of *Ostm1* expression in the T cell lineage rescues thymic differentiation (Continued)

(**G**) Differentiation from DN1 to DN4 stage (n=6) and from DP to mature SP $CD4^+$ or $CD8^+$ (n= 10) within +/+, *gl/gl* and *gl/gl*TR thymi

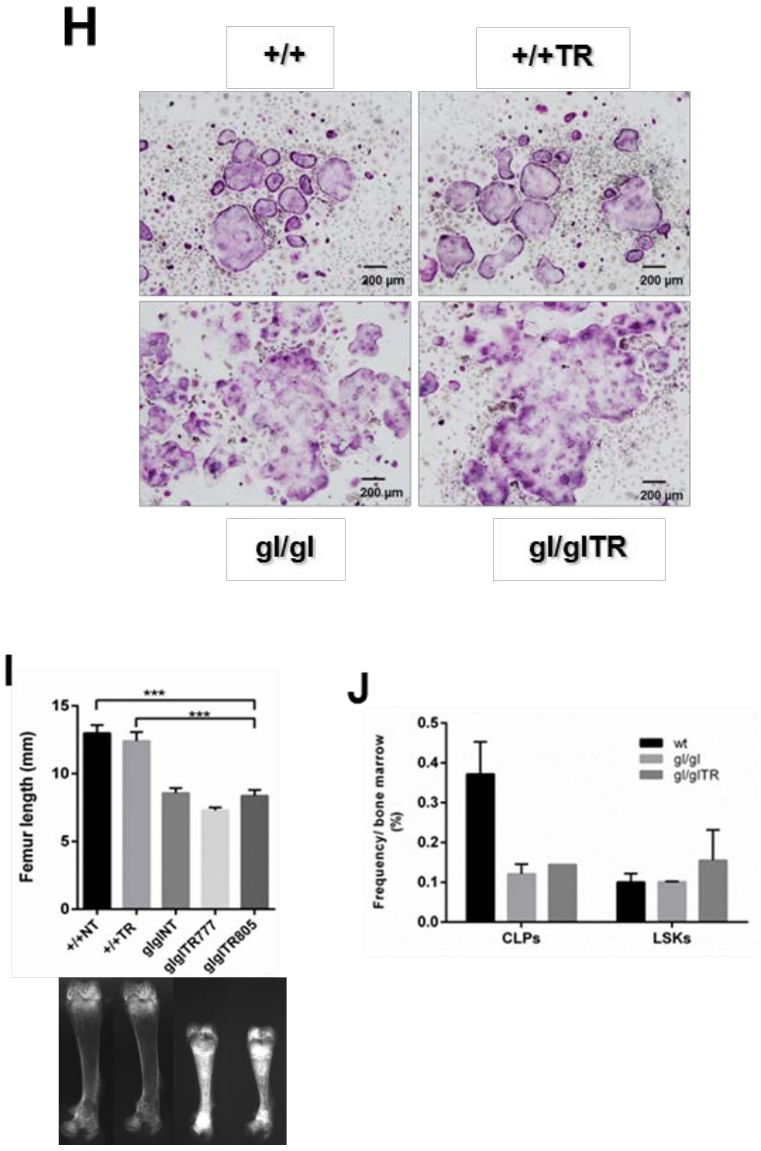

Figure 2.4. Restoration of *Ostm1* expression in the T cell lineage rescues thymic differentiation (Continued).

(**H**) Osteoclasts differentiated *in vitro* from splenic progenitors of +/+, +/+TR, *gl/gl* and *gl/gl*TR mice in presence of M-CSF and RANKL (20X). (**I**) Bone length (mm) and illustration of bone density (n=3) of dissected femur from control, +/+TR, *gl/gl* and *gl/gl*TR mice. (**J**) Frequency of common lymphoid progenitors (CLPs) and (LSKs: Lin^{-} $Sca1^{+}$ C-kit^{hi}) within bone-marrow cavity of +/+, *gl/gl* and *gl/gl*TR animals.

Altered transcriptome profile of *gl/gl* DN1 thymocyte population

To further determine the early role of *Ostm1* during thymopoiesis, the transcriptome was examined within the early DN1 population. RNA was sequenced from enriched DN1 (Lin^- $CD44^+CD25^-$) populations from *gl/gl*, *gl/gl*TR and control thymi. Besides, alignment of over 10 transcripts to a single mapped gene is the minimal threshold to define a DEG (differentially-expressed gene) as opposed to false-positive or background.

A majority of transcripts were similarly distributed across both, *gl/gl*TR DN1 and controlDN1 samples. However, an important number of outlier transcripts were found across the *gl/gl* DN1 transcriptome. There was a consistent distribution pattern of most DEGs from *gl/gl* DN1 sample when compared to control DN1 and *gl/gl*TR DN1 transcripts as identified by red arrows (**Fig 2.5A**). Furthermore, 146 DEGs were identified between *gl/gl* DN1 and control DN1 samples, 205 DEGs differentiated *gl/gl* DN1 and *gl/gl*TR DN1, and only 17 DEGs varied between *gl/gl*TR DN1 and controlDN1 samples (**Fig 2.5B**). DEGs within the *gl/gl* DN1sample were divided in down-regulated (**Fig 2.5C**) and up-regulated group genes (**Fig 2.5D**) when compared to *gl/gl*TR DN1 or control DN1 and presented in heat-maps. Therefore, this analysis identified the comparable gene expression signature between *gl/gl*TR DN1 and wt DN1 as opposed to *gl/gl* DN1 sample.

To examine the biological functions associated with the altered transcriptome within *gl/gl* DN1 transcripts, DEGs were scrutinized with bioinformatics tools including Database for Annotation, Visualization and Integrated Discovery (DAVID), Ingenuity Pathway analysis (IPA) and Gene Set Enrichment Analysis (GSEA). Based on their importance in T cell biology, significant variations in 11 biological functions and 5 signaling pathways were revealed as significantly deregulated in *gl/gl* DN1when compared to control DN1 ($10^{-9} < p < 10^{-4}$; **Fig 2.5E**). These biological processes include cell-to-cell interactions, cell migration, immune cell trafficking, and hematological system development, all of which are important for the T cell differentiation program.

As previously described, the stereotypical migration of immature T cells covers several microns in the thymus to promote interaction with cortical thymus epithelial cells. This cell crosstalk requires both signaling chemokines for specific differentiation stages and thymocytes-derived molecules that maintain the thymus micro-environment (Witt and Robey 2004). Therefore, cell migration of *gl/gl* DN1 was further dissected at the transcriptome level by using GSEA. DEGs related to migration were ranked from most to least up-regulated or down-regulated genes (Kollet, Dar et al. 2006). GSEA reveals that cell migration genes within *gl/gl* DN1sample are mostly grouped in the portion of up-regulated genes ($p < 0.01$) and a normalized enrichment score (NES) of 1.42 when compared to control DN1, whereas a significant p-value <0.0001 and NES of 1.77 are observed when *gl/gl* are compared to *gl/gl*TR DN1 (**Fig 2.5F**).

Together, these observations indicate a significant up-regulation of T cell migration genes in sorted *gl/gl* DN1 cells which was corrected in *gl/gl*TR DN1 population when compared to control DN1.

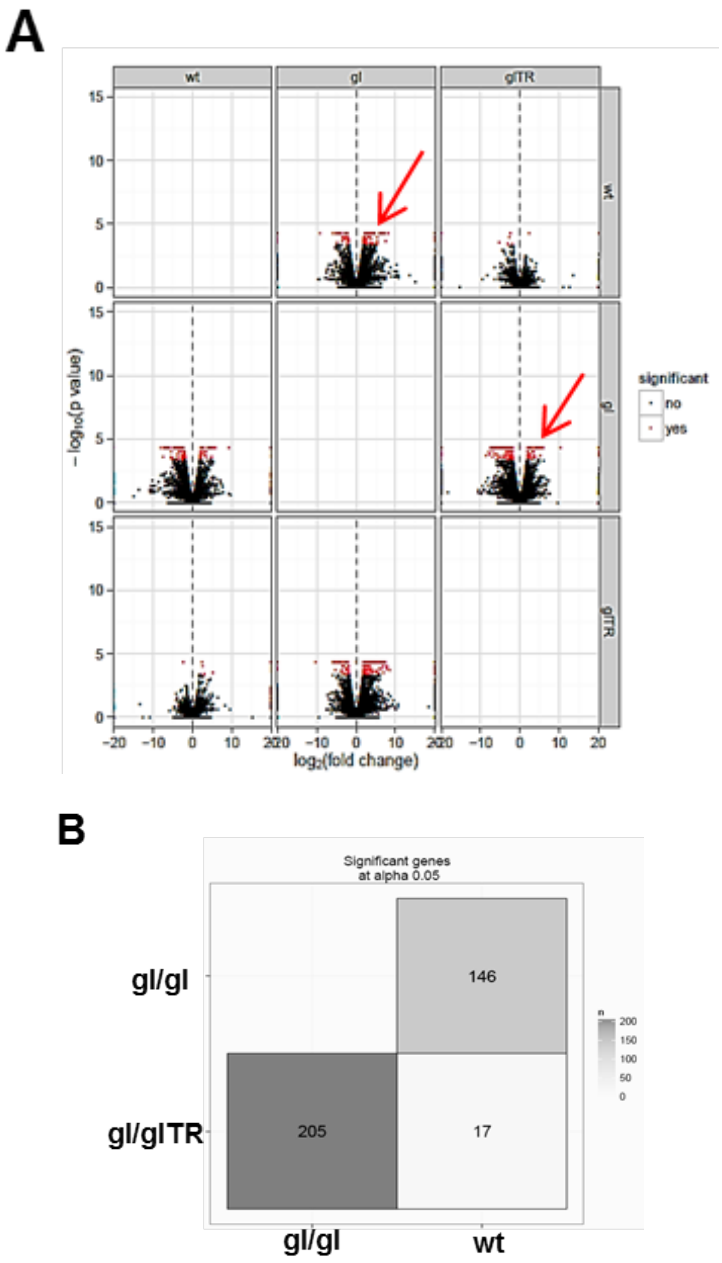

Figure 2.5. Altered transcriptome profile of *gl/gl* DN1 thymocyte population

(**A**) CummeRbund volcano plot shows individual distribution of transcript within cell extract from sorted (DN1: Lineage^{-}CD44^{+}CD25^{-}) cells of control, *gl/gl* and CD2-*Ostm1 gl/gl*TR animals, transcripts were grouped and ranked according to the distribution similarities or differences. (**B**) Sig matrix representation of the differentially expressed genes number within sorted *gl/gl* DN1 in comparison to wt DN1 or *gl/gl*TR DN1.

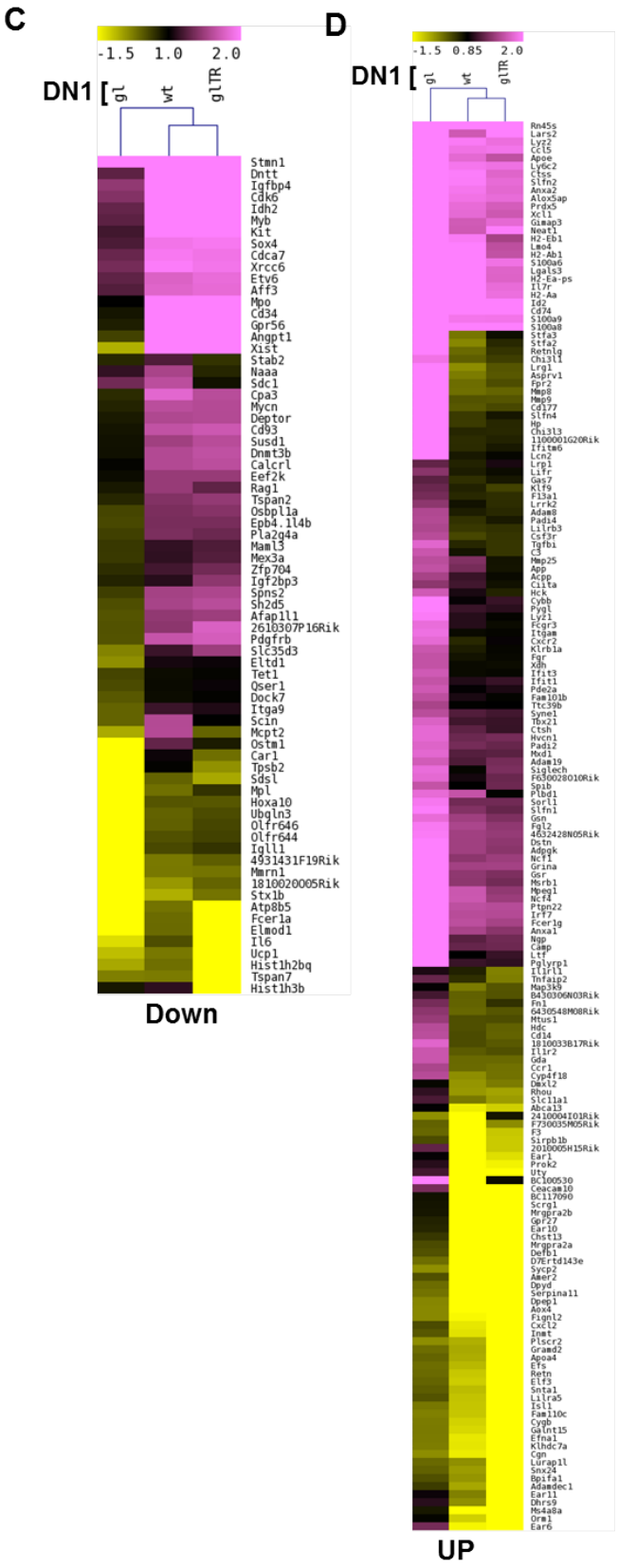

Figure 2.5. Altered transcriptome profile of the *gl/gl* DN1 thymocyte population (Continued)

(**D**) Heat map representation of all down-regulated genes across *gl/gl* DN1 transcripts when compared to wt DN1 and *gl/gl*TR DN1 (**C**). Heat map representation of all up-regulated genes across *gl/gl* DN1 transcripts when compared to controlDN1 and *gl/gl*TR DN1

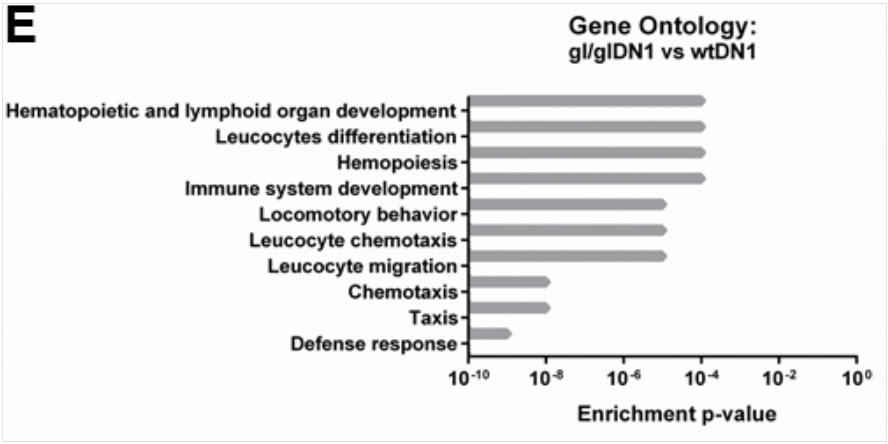

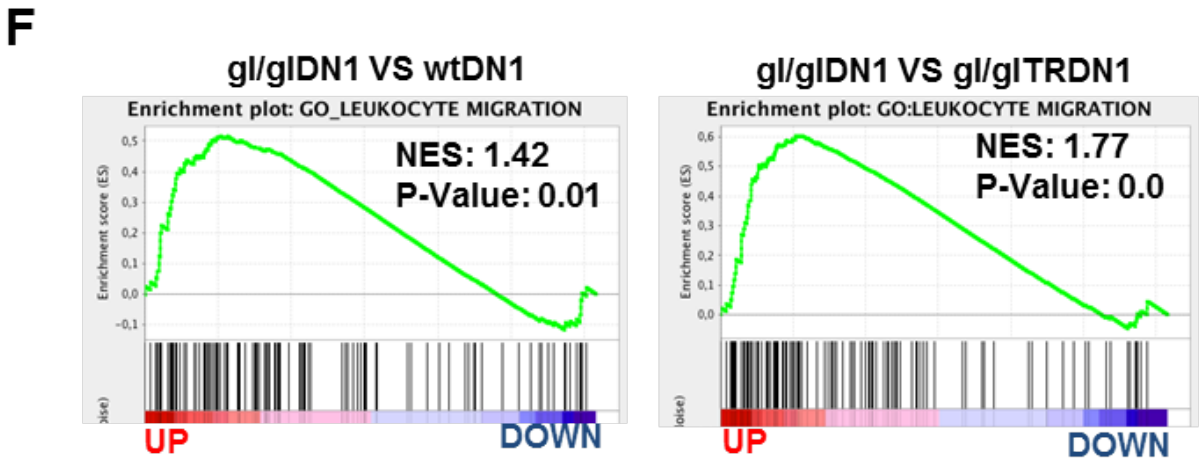

Figure 2.5. Altered transcriptome profile of *gl/gl* DN1 thymocyte population (Continued)

(**E**) Summary of Goterms and corresponding biological functions connected to differentially expressed genes across *gl/gl* DN1 transcripts compared to control DN1 transcripts with a significant p-value ranging from 10^{-9} to 10^{-4}. (**F**) GSEA ranking of the migration gene set from top to bottom extreme of up-regulated or down-regulated genes within *gl/gl* DN1 sample when compared to control DN1 or *gl/gl*TR DN1 samples with the corresponding enrichment p-value and normalized enrichment score (NES). The statistical unit NES illustrates the degree of overrepresentation at the top or bottom extreme of the entire ranked list of migration genes.

Impaired migration of DN1 T cells in *gl/gl* mice

Abnormal levels of transcripts associated with cell migration within *gl/gl*DN1sample compared to control DN1 and *gl/gl*TR DN1 is summarized at the individual gene level in heat map representation (**Fig 2.6A**). Three genes important for the S1P (Sphingosine-1-phosphate) pathway, known to be crucial in immune cell migration (Dorsam, Graeler et al. 2003), were displayed at the top of the DEGs in *gl/gl* DN1 when compared to either control DN1 or *gl/gl*TRDN1. Interestingly, both RNA-sequencing and qPCR revealed a significant up-regulation of quantitative *Rac1* (Rac GTPase 1) and *S1pr1* (Sphingosine-1-phosphate receptor 1) (**Fig 2.6B**). However, other important S1P pathway players including *Sphk1* (Sphingosine kinase 2), *Sgpp2* (Sphingosine-1- phosphate phosphatase 2), and *Sgpl1* (Sphingosine-1-Phosphasate Lyase) remain unchanged at the mRNA level within the *gl/gl* DN1 sample when compared to control and *gl/gl*TRDN1 cells (**Fig 2.6B**), suggesting no modulation in S1P production or break-down.

Over the course of 2 hours, *in vitro* transwell migration assays confirmed a 30-33% accelerated migration of *gl/gl* DN1 cells in comparison to the undetectable migration of control DN1 and *gl/gl*TR DN1 cells in the presence of CXCL-12 (SDF-1α) (**Fig 2.6C**). This enhanced migration of *gl/gl* DN1 overlaps with the overexpression of *Rac1*. Importantly, *Rac* 1 gene expression and migration speed were normalized in *gl/gl*TR DN1 population (**Fig 2.6B and 2.6C**), suggesting that normalizing the intrathymic DN1 trafficking could sustain a longer T cell differentiation.

Overall, the *Ostm1* null mutation stimulates important cell migration genes including *Rac1* expression, which have been shown to correlate with down regulation of CD25 (de Barros, Vicente et al. 2013).This could result in accelerated T cell differentiation and the subsequent progressive exhaustion. Consequently, our study reports a novel function for *Ostm1* in the maintenance of long-term T lymphocytes differentiation by stabilising early T cell trafficking through normalized *Rac1* expression level, and therefore prolonging intrathymic ETPs life span and number despite a compromised BM input (**Fig 2.6D)**.

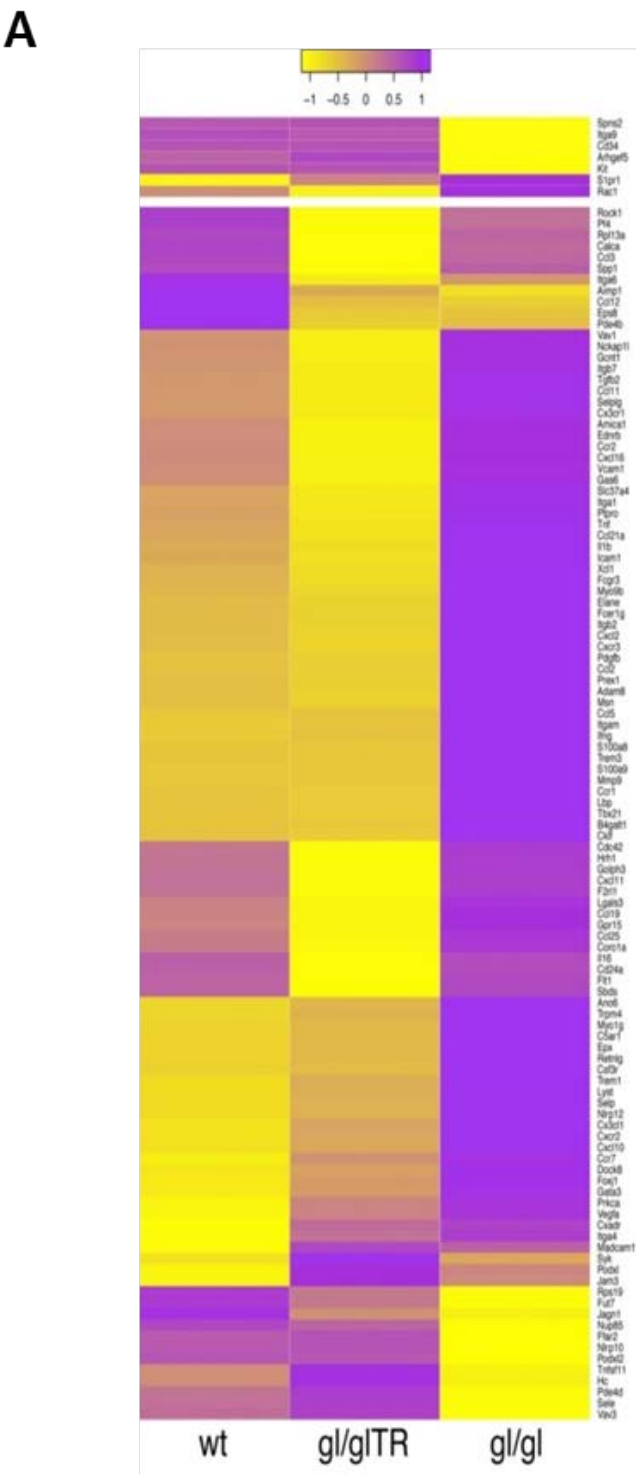

Figure 2.6. Impaired migration of DN1 T cells in *gl/gl* mice.

(**A**) Heat map representation of individual migration genes identified at the top of differentially expressed genes in *gl/gl* DN1 compared to control DN1 and *gl/gl*TR DN1.

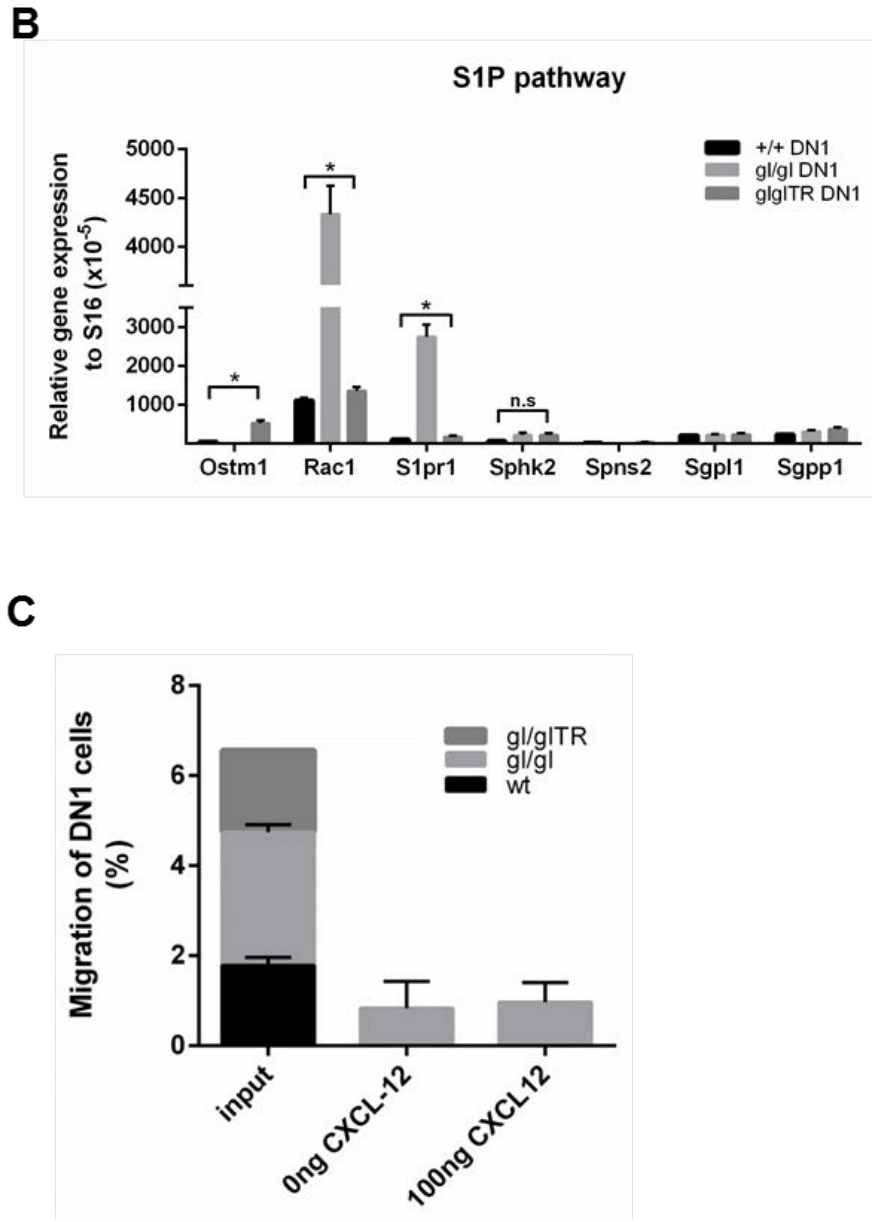

Figure 2.6. Impaired migration of DN1 T cells in *gl/gl* mice (Continued).

(**B**) Quantitative expression of *Ostm1*, *Rac1*, *S1pr1*, *Sphk1*, *Sgpl1*, *Sgpp2* and *Spns2* genes within *gl/gl* DN1 compared to control DN1 and *gl/gl*TRDN1. (**C**) Percentage of migrated DN1 cells out of the thymus input ($2x10^6$ cells) from control, *gl/gl*, and *gl/gl*TR animals, with or without 100 ng/µl of CXCL-12 after 2 or 18 hours.

D

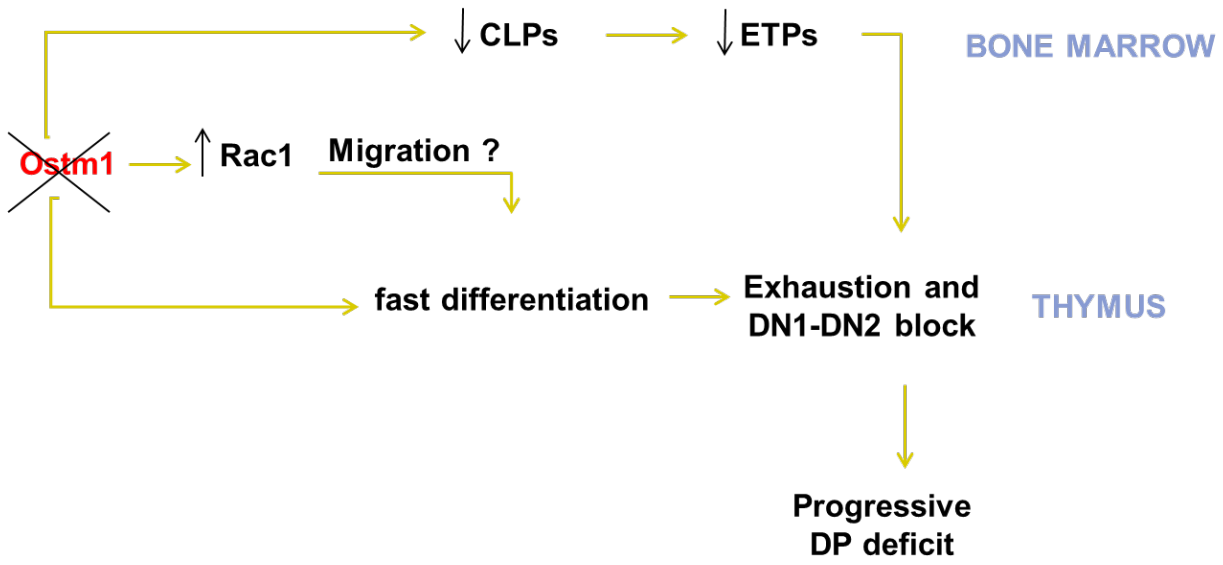

Figure 2.6. Impaired migration of DN1 T cells in *gl/gl* mice (Continued).

(**D**) Proposed model for *Ostm1* gene function in T cell differentiation. Absence of *Ostm1* could enhance *gl/gl* DN1 cells migration by stimulating intrinsic *Rac1* expression probably via S1pr1. Consequently, this stimulation of intrathymic migration of DN1 cells could lead to faster differentiation kinetics. This late phenotype combined with lower ETP cell ratio from the compromised *gl/gl* BM could then result into the progressive exhaustion of T cell differentiation with a time-dependent block at the DN1-DN2 transition as well as the subsequent dramatic loss of DP cells. Therefore, declining thymus cellularity results in *gl/gl* thymus atrophy.

2.2.5. DISCUSSION & CONCLUSION

The previous rescue of T cell defects in PU-*Ostm1gl/gl* transgenic mice suggested a functional relevance of the *Ostm1* gene in the T cell lineage, but could not distinguish it from the contribution of the BM component. Our study presents novel data expanding the knowledge about *Ostm1* gene function and demonstrating its role in the T lineage differentiation. The absence of *Ostm1* led to the time-dependent depletion of the DP population, with a severe decline in total thymic cellularity of *gl/gl* mice from P15. This time-dependent phenotype of DP *gl/gl* thymocytes correlated with the similar TCR-β and CD69 expression of *gl/gl* DP. Combined with the normal distribution of naive SP $CD4^+$ or $CD8^+$ in the *gl/gl* spleen or lymph nodes, both phenotypes illustrate a normal development of αβ T cells prior to P15. Additionally, the drastic reduction in DP population correlated with the time-dependent disorganized thymus architecture and tissue atrophy of *gl/gl* mice.

This *gl/gl* DP deficit could result from combined events beginning with the lower number of ETPs seeding the thymus that could be attributed to either a compromised BM input or a cell-intrinsic defect. Further investigation revealed the *gl/gl* ETP differentiation arrest at the DN1-DN2 transition *in vivo* from P15. In parallel, these *gl/gl* ETPs displayed an accelerated differentiation into DN1-DN4 and DP subsets *in vitro* co-culture system on OP9-DL4, suggesting an indirect role of *Ostm1* in the early defect of *gl/gl* T cell differentiation. Additionally, the *gl/gl* DN1 thymocytes population overexpressed the migration genes *S1pr1* and *Rac1* compared to control DN1that could be connected to the fast-paced differentiation *in vitro*. Interestingly, T cell specific restoration of *Ostm1* in CD2-*Ostm1gl/gl* transgenic animals rescued T cell differentiation from DN1 to DP. Also, the enhanced distribution of migration genes was normalized in *gl/gl*TR DN1 cells. Furthermore, CD2-*Ostm1gl/gl* transgenic animals showed a partial rescue in total thymus cellularity and preserved osteopetrotic features such as shorter femurs, under-developed BM cavity and premature death around 3 weeks. Collectively, these new findings were in favor of the cell- intrinsic role of *Ostm1* in T cell differentiation for regulating migration of early DN1 cells possibly via *Rac1* and *S1pr1*.

The time-dependent T cell phenotype of *gl/gl* at P15 coincided with discontinued differentiation of the first wave of thymic precursors recruited to the fetal thymus at E.13 and lasting for two weeks (Jotereau, Heuze et al. 1987). Also, the fast differentiation of *gl/gl* ETPs *in vitro* recapitulates the behavior of the first generation of T cells that usually proliferate extensively before TCR-β rearrangement (Ikawa, Masuda et al. 2004) and exhibit a faster rate of differentiation or migration in order to establish peripheral T cells as soon possible during early fetal thymopoiesis (Jotereau, Heuze et al. 1987). In addition, the decline of *gl/gl* T cell populations is exacerbated approximately at the recruitment time of the second wave of thymus progenitors from the BM. This recruitment step normally occurs around 18-25 days after birth and is characterized by complete independence from the neonatal immune system versus the maternal immune system (Cummins and Thompson 1997). Therefore, this time-dependent behavior of *gl/gl* thymocytes could be associated with inefficient thymus periodicity of *gl/gl* mice.

In general, the positive regulation of the thymus receptivity to colonisation of pro-thymocytes depends on available thymic niches that designate responsive or refractory periods, during which mobilization of T cell progenitor from the BM is turned on or off (Jotereau and Le Douarin 1982, Foss, Donskoy et al. 2001). For this reason, the underdeveloped BM environment of *gl/gl* mice could desynchronize thymus receptivity resulting in a post-natal T cell phenotype and sabotaging independence of the neonatal immune system. In that case, reduced input of thymic seeding progenitors from a compromised BM would alleviate the competition between new arrivals and old T cells for stomal niches resulting in an extended lifespan of developing T cells (Martins, Ruggiero et al. 2012). In the present study, a compromised BM was observed in *gl/gl* animals at P0, P10 and P15 (unpublished observations) and lead to lower frequency of post-natal CLPs. This could have disrupted recruitment of new pro-thymocytes and prolonged the cell-intrinsic life of fetal DN1 cells in the *gl/gl* thymus until exhaustion and progressive disruption of T cell differentiation culminating at P15. Importantly, the rescue of *gl/gl* T cell distribution in CD2-*Ostm1 gl/gl* transgenic mice despite the maintenance of a compromised BM environment and lower CLP percentage suggests the prevalence of intrathymic *Ostm1* function in sustaining early T cell development.

The DP pool usually correlates with the fraction of DN cells in competition for the thymic stromal niche without being constrained by thymus size (Prockop and Petrie 2004). On this basis, the altered thymic parameters of *gl/gl* animals and the thymus phenotype are independent of the smaller body weight or organ size. Furthermore, reduced *gl/gl* DP cells could result from lower ETPs ratio, cells that were previously identified as the most efficient progenitor of DP in the thymus (Godfrey, Zlotnik et al. 1992, Porritt, Rumfelt et al. 2004) and their disrupted differentiation could lead to abnormal distribution in the DN1-DN4 populations. Other studies supported the critical impact of DN cells number on the total thymus cellularity, reconciling the overlap between the drastic *gl/gl* thymus hypocellularity and the altered DN1-DN4 distribution at P15. In conjunction with this, the ambiguous cortico-medullary junction (CMJ) in the *gl/gl* thymus correlates with the smaller ratio of *gl/gl* ETP population to total thymocytes, as previous regeneration experiments identified CMJ as the preferred location of first cycling DN1 cells before moving to the outer cortex to differentiate into DP cells (Kyewski 1987, Penit 1987, Penit 1988). Interestingly, the obstructed CMJ, the ratio of *gl/gl* ETPs to total thymocytes and the distribution of DN1-DN4 cells were efficiently restored in CD2-*Ostm1* transgenic thymus suggesting the contribution of *Ostm1* in ETPs cell maintenance and differentiation.

In contrast, the inhibited differentiation of *gl/gl* ETPs at the DN1-DN2 stages could be explained by an interrupted Notch-dependent crosstalk from developing thymocytes towards thymus epithelial cell progenitors or vice-versa resulting in underdeveloped and disorganized three-dimensional architecture of the thymic environment (Anderson, Jenkinson et al. 2006). However, the maintained *gl/gl* ETP differentiation *in vitro* on BM-derived OP9-DL4 cells indicated normal Notch responsiveness in early *gl/gl* T cells. In parallel, restoration of *Ostm1* in the T lineage boosted the *gl/gl* ETP ratio in CD2-*Ostm1 gl/gl* transgenic thymus and prolonged their subsequent differentiation beyond P15. Therefore, defective differentiation of *gl/gl* ETPs could be exacerbated by the lower ETPs frequency resulting from the perturbed post-natal input from the abnormal *gl/gl* BM. In addition, the limited number of CLPs and/or a cell-intrinsic defect could shorten ETPs life span leading to their progressive exhaustion and an interrupted T cell differentiation within *gl/gl* mice after birth.

The conserved spatio-temporal migration of ETPs cells across thymus environment is usually controlled by adhesion molecules, chemokines and molecules gradients from the CMJ towards the outer cortex and this restricted migratory pattern is essential for normal T cell development (Petrie and Zuniga-Pflucker 2007). Intriguingly, RNA sequencing established a significant up-regulation of cell migration genes in sorted *gl/gl* DN1 compared to control DN1. Specifically, up-regulation of quantitative Rac GTPase 1 (*Rac1*) and Sphingosine-1-phosphate receptor 1 (*S1pr1*) was confirmed by qPCR. The contribution of *Rac1* in T cell development was previously shown within Rac1 transgenic mouse in which sustained *Rac1* expression under CD2 promoter induced an accelerated β-selection in pre-T cell as well as the reduction of CD25 precipitating the DN3 to DN4 transition (de Barros, Vicente et al. 2013). On this basis, we can speculate that an enhanced DN1 cells migration is probably related to *Rac1* overexpression combined with the down-regulation of CD25 and the limited ETP ratio, which could induce the progressive DN1-DN2 transition blockage. Moreover, *Rac1* overexpression was shown to precipitate the β-selection checkpoint and to mitigate the positive and negative selection of DPs which could potentiate the T cell differentiation program in the *gl/gl* thymus. Overall, the limited ETP input with the subsequent fast-paced differentiation pattern may progressively exhaust the neo-natal T cell development program. Our interesting transcriptome observations are promising although the molecular mechanism between *Ostm1*, *S1pr1* and *Rac1* remains to be fully investigated.

Furthermore, the present study cannot totally rule out the important role of the compromised BM cavity in the *gl/gl* thymus phenotype, and this interaction needs to be fully characterized. Nevertheless, the restored expression of *Ostm1* from ETPs to mature SP $CD4^+$ and $CD8^+$ populations under the CD2 promoter in all CD2-*Ostm1 gl/gl* transgenic thymi (de Boer, Williams et al. 2003) equilibrates *Rac1* and *S1pr1* expression level, ETP percentage and the distribution of DN1-DN4 and DP cells. It partially recovers total thymus cell number and improves thymus architecture. Importantly, the rescued *gl/gl* T cell phenotype with preservation of defective bone resorbing osteoclasts, underdeveloped BM cavity and lower CLPs in the BM as well as maintenance of other osteopetrotic hallmarks in all CD2-*Ostm1 gl/gl* transgenic animals revealed a thymus-intrinsic *gl/gl* phenotype. Collectively, these observations are in favor of the cell-autonomous *Ostm1* function in thymocytes differentiation independent of osteoclasts lineage inactivity.

In conclusion, our findings distinguished a thymus-intrinsic phenotype from the osteopetrotic phenotype of *gl/gl* mice. This study also details the sequential time-dependent deficit of thymocytes that usually precedes the death of the osteopetrotic *gl/gl* animal (Wiktor-Jedrzejczak, Grzybowski et al. 1983, Jotereau, Heuze et al. 1987). Our results strongly support a progressive exhaustion of the T cell differentiation program in the absence of the *Ostm1* gene resulting from lower ETP percentage combined with an enhanced trafficking in correlation with *Rac1* overexpression and the concomitant faster differentiation of early DN1.

2.2.6. APPENDIX 1

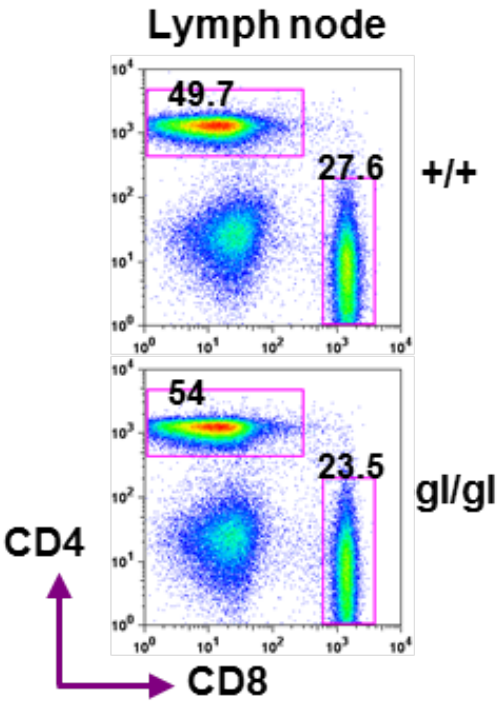

Appendix 1.1. Distribution of mature single-positive $CD4^+$ or $CD8^+$ in peripheral lymphoid tissue

Flow cytometry plots representing the percentage of mature T cells in the lymph node harvested from +/+ and *gl/gl* animals at P21 (n = 4) show similar distribution.

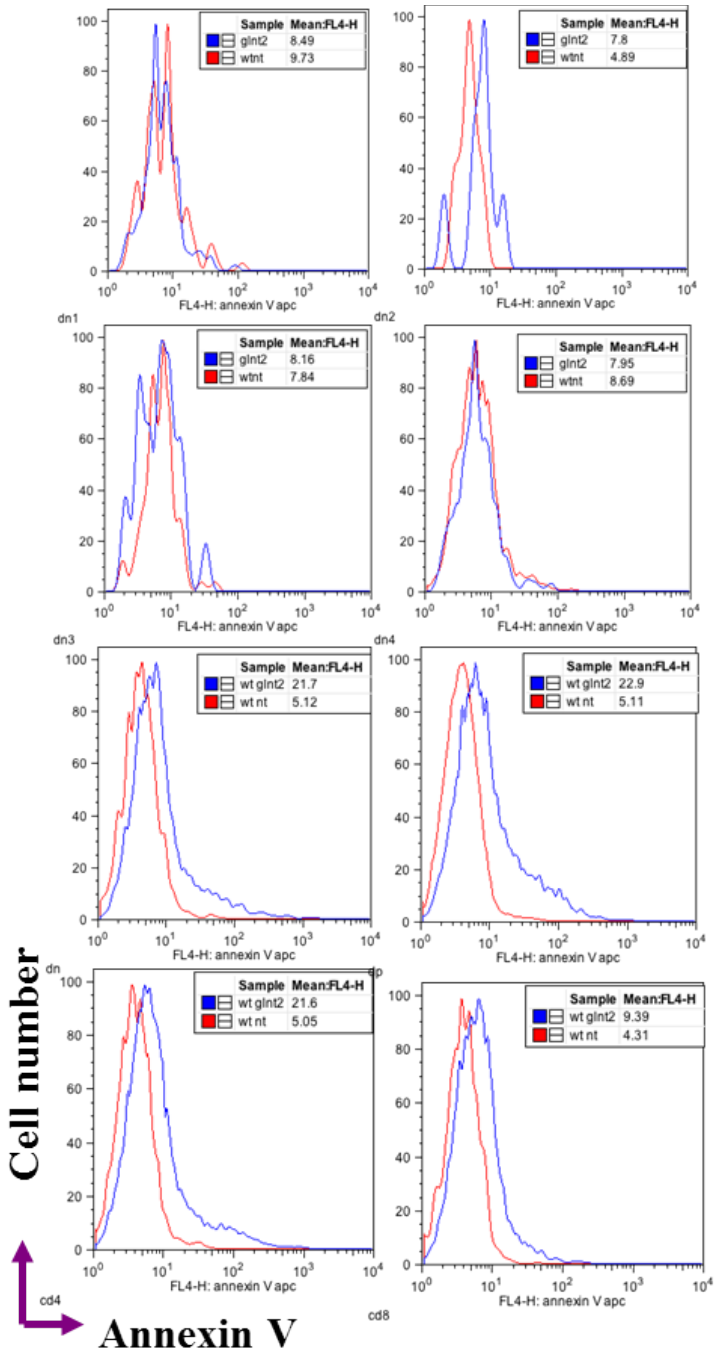

Appendix 1.2. Apoptosis quantification with Annexin V positive T cells in *gl/gl* thymus.

Flow cytometry plot representing the distribution of DN1-DN4, DP and SP CD4$^+$or CD8$^+$ cells expressing Annexin V on the Y axis as well as the intensity of expression on the X axis. Surface expression of Annexin V was used to identify apoptotic cells within +/+ (red) and *gl/gl* (blue) thymus at P21 (n = 2).

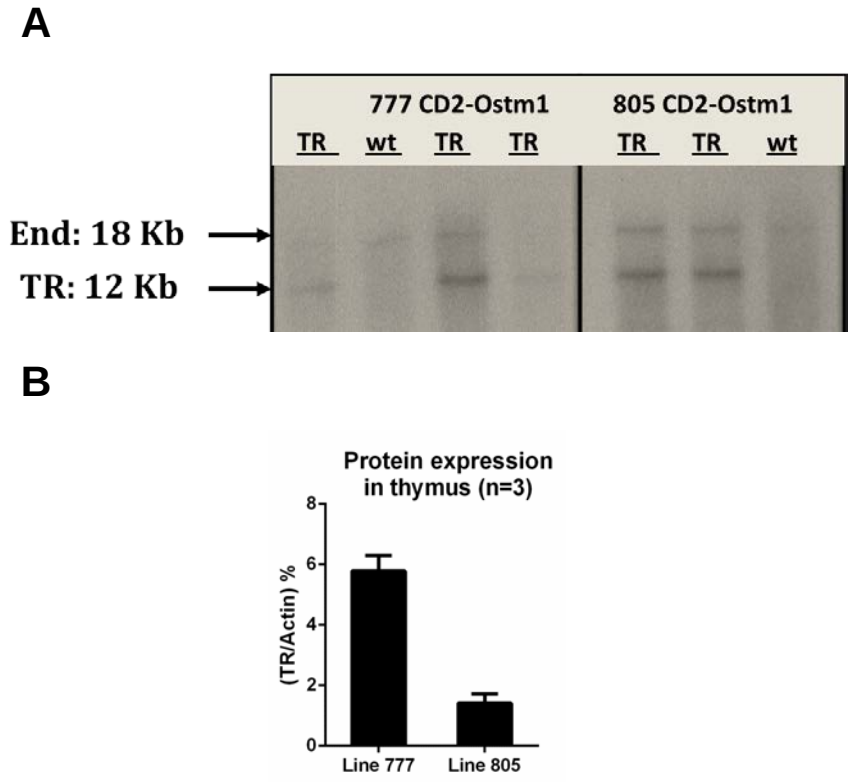

Appendix 1.3. **Characterization of +/+ CD2-Ostm1 transgenic founder.**

A) Southern blot analysis showing the copy number of CD2-*Ostm1* transgene expression (777: 13 copies; 805 : 5copies) (n =2). **B**) Protein quantification of CD2-*Ostm1* transgene in both CD2-*Ostm1* transgenic lines 777 and 805. **C**) Quantitative expression of endogenous *Ostm1* gene within tissues from +/+ mice in comparison to CD2-Ostm1 transgenic animals (n =3).

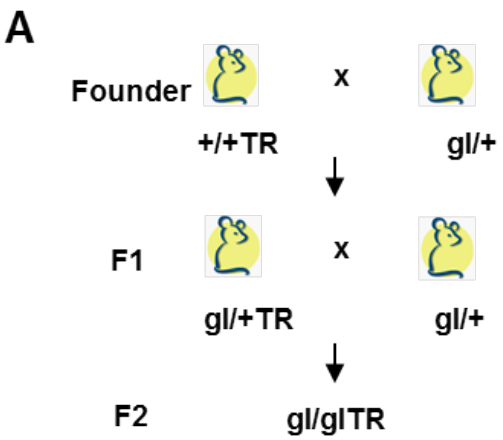

B

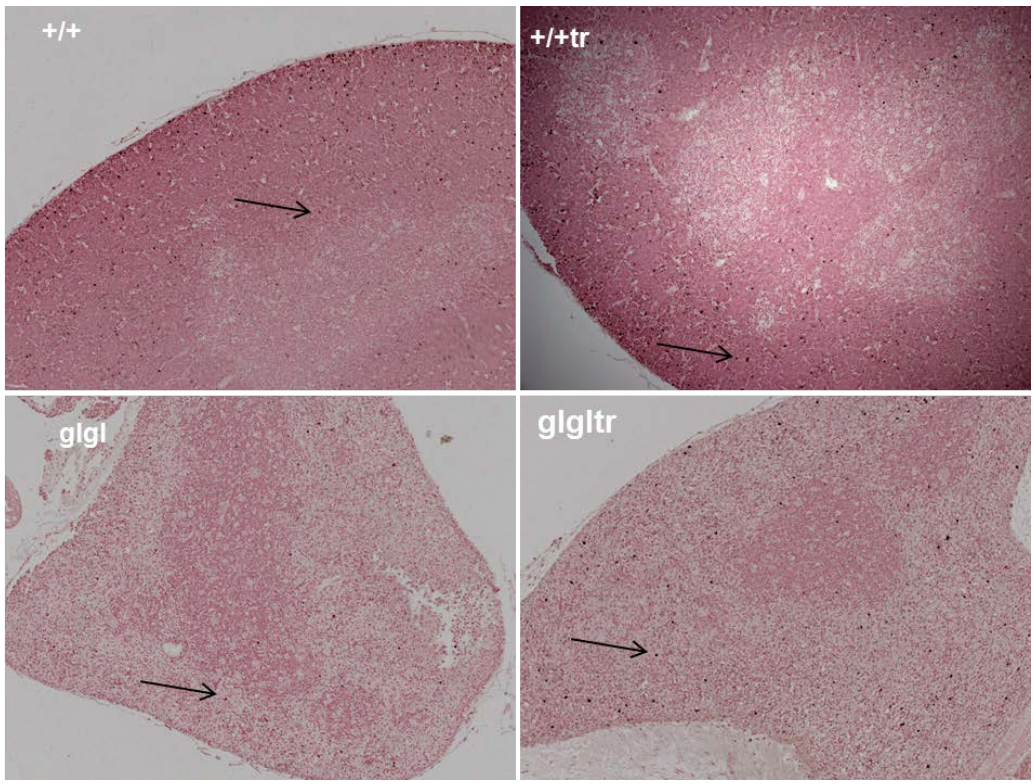

Appendix 1.4. Generation and phenotyping of the CD2-*Ostm1-gl/gl* transgenic progenies. **A**) Schematic representation of the breeding strategy to establish *gl/gl* CD2-*Ostm1* mice. **B**) Histology sections stained with Ki-67 antibody and visualized at 10X to monitor proliferative cells in medulla and cortex as indicated by black arrow within +/+, +/+ TR, *gl/gl*, and *gl/g*l TR mice at P21.

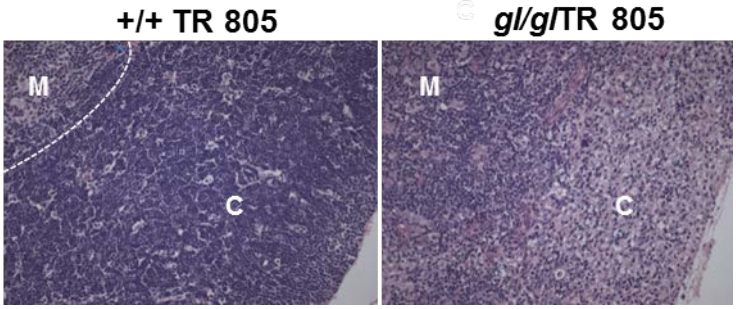

Appendix 1.5. H&E staining of *gl/gl* and *gl/gl*TR thymi

Histology sections stained with H& E and visualized at 20X comparing thymus architecture and structure from +/+TR and *gl/gl* TR777 animals at P21.

A

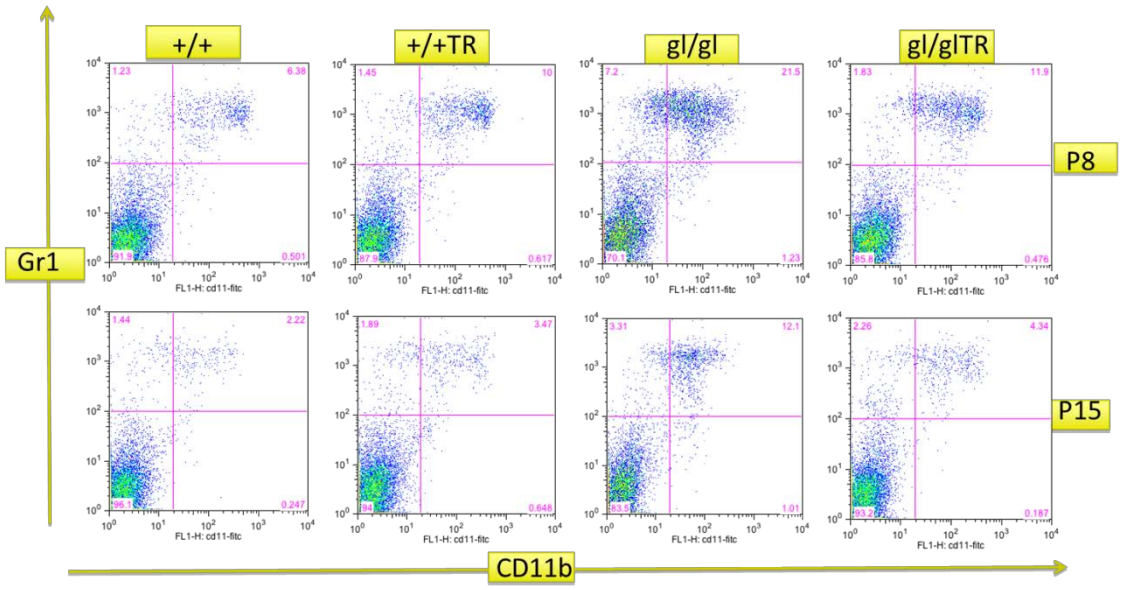

B

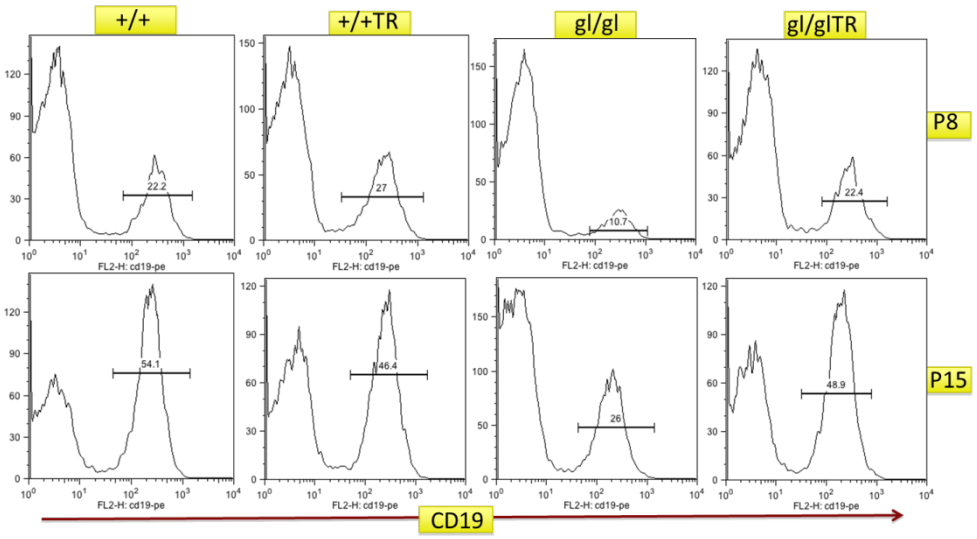

Appendix 1.6. Distribution of CD11b/Gr-1 and B cells in CD2-*Ostm1* transgenic spleen

A) Percentage of macrophage-granulocytes targeted with surface markers CD11b and Gr-1 by flow cytometry analysis of +/+, +/+TR,*gl/gl* and *gl/gl*TR spleen at P8 and P15. **B**) Percentage of B cells targeted by surface expression of CD19 by flow cytometry analysis of +/+, +/+TR, *gl/gl* and *gl/gl*TR spleen.

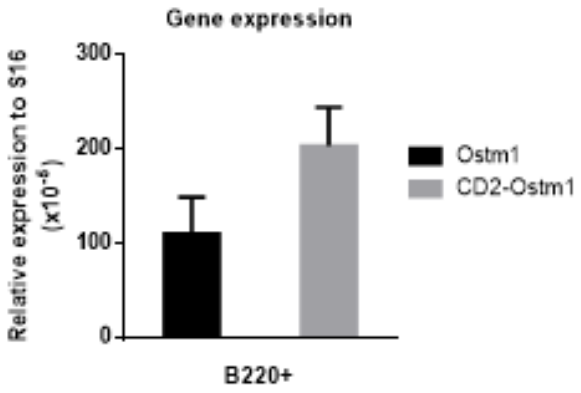

Appendix 1.7. Endogenous and transgene *Ostm1* expression in B cells at P21

Quantitative PCR expression of endogenous *Ostm1* and CD2-*Ostm1* transgene in sorted B220 positive B cells harvested from +/+ CD2-*Ostm1* spleen of 3 weeks-old mice.

Table 1.2. IPA comparative biological analysis between DN1 wt and *gl/gl* cells detected by RNA seq

Summary of Analysis - wt_gl - pValue<.01

Top Diseases and Bio Functions

Diseases and Disorders

Name	p-value	# Molecules
Immunological Disease	3,26E-52 - 1,13E-06	174
Connective Tissue Disorders	1,82E-34 - 7,19E-08	112
Inflammatory Disease	1,82E-34 - 1,13E-06	153
Skeletal and Muscular Disorders	1,82E-34 - 2,27E-07	139
Inflammatory Response	1,19E-32 - 1,12E-06	177

Molecular and Cellular Functions

Name	p-value	# Molecules
Cell Death and Survival	5,40E-34 - 1,13E-06	227
Cellular Movement	4,99E-33 - 8,51E-07	171
Cell-To-Cell Signaling and Interaction	1,19E-32 - 1,12E-06	159
Cellular Growth and Proliferation	1,23E-30 - 7,89E-07	236
Cellular Development	5,14E-27 - 9,63E-07	227

Physiological System Development and Function

Name	p-value	# Molecules
Hematological System Development and Function	1,19E-32 - 9,85E-07	189
Immune Cell Trafficking	1,19E-32 - 8,52E-07	140
Tissue Morphology	1,32E-26 - 4,26E-07	110
Tissue Development	4,03E-20 - 9,85E-07	144
Organismal Survival	1,58E-19 - 1,03E-06	110

Table 1.3. IPA comparative biological analysis between DN1 sorted *gl/gl* and *gl/gl*TR cell populations detected by RNA seq

Summary of Analysis - gl_glTR - pValue<.01

Top Diseases and Bio Functions

Diseases and Disorders

Name	p-value	# Molecules
Immunological Disease	1,69E-61 - 1,87E-07	210
Inflammatory Response	3,66E-40 - 3,67E-07	210
Connective Tissue Disorders	3,74E-39 - 3,27E-08	131
Inflammatory Disease	3,74E-39 - 4,30E-07	175
Skeletal and Muscular Disorders	3,74E-39 - 5,29E-08	128

Molecular and Cellular Functions

Name	p-value	# Molecules
Cell-To-Cell Signaling and Interaction	6,12E-42 - 5,14E-07	191
Cellular Movement	7,70E-42 - 5,19E-07	205
Cell Death and Survival	4,27E-41 - 4,83E-07	269
Cellular Growth and Proliferation	6,81E-34 - 3,19E-07	265
Cellular Development	2,01E-32 - 5,31E-07	270

Physiological System Development and Function

Name	p-value	# Molecules
Immune Cell Trafficking	7,70E-42 - 5,19E-07	168
Hematological System Development and Function	3,66E-40 - 5,31E-07	224
Tissue Morphology	1,79E-29 - 5,16E-07	129
Tissue Development	2,11E-24 - 5,14E-07	198
Organismal Survival	1,31E-23 - 6,13E-08	136

Table 1.4. DAVID comparative analyses of biological pathways between DN1 wt and *gl/gl* DN1 cell populations detected by RNA seq

Table II. BIOLOGICAL CHANGES WITHIN WT DN1 vs gl/gl DN1				
Term	**Fold enrichment**	**P-value**	**Cellular function**	**# of genes**
GO:0006952	5.820977633	2.73E-09	Defense response	19
GO:0042330	12.59197479	8.55E-08	Taxis	10
GO:0006935	12.59197479	8.55E-08	Chemotaxis	10
GO:0050900	19.15151515	1.36E-05	Leukocyte migration	6
GO:0030595	25.41713431	3.93E-05	Leukocyte chemotaxis	5
GO:0007626	5.742783483	5.60E-05	Locomotory behavior	10
GO:0002520	4.652627975	2.75E-04	Immune system development	10
GO:0030097	4.921405288	4.56E-04	Hemopoiesis	9
GO:0002521	6.765969555	5.61E-04	Leukocyte differentiation	7
GO:0048534	4.395988353	9.54E-04	Hemopoietic or lymphoid organ development	9
GO:0002244	22.87542088	0.083227443	Hemopoietic progenitor cell differentiation	2

Table III. PATHWAY CHANGES WITHIN WT DN1 vs gl/gl DN1				
Term	**Fold enrichment**	**P-value**	**Pathway**	**# of genes**
mmu04640	8.720364742	5.10E-04	Hematopoietic cell lineage	6
mmu04060	4.50313917	6.11E-04	Cytokine-cytokine receptor interaction	9
mmu04062	4.024783727	0.014533405	Chemokine signaling pathway	6
mmu04670	4.103701055	0.069354906	Leukocyte transendothelial migration	4
mmu04810	2.813020884	0.094623602	Regulation of actin cytoskeleton	4

Table 1.5. DAVID comparative analyses of biological pathways between DN1*gl/gl* and *gl/gl* TRDN1 cell populations detected by RNA seq

Table IV. BIOLOGICAL CHANGES WITHIN gl/gl DN1 vs gl/glTR DN1				
Term	**Fold enrichment**	**P-value**	**Cellular function**	**# of genes**
GO:0006952	5.632780612	3.50E-12	Defense response	26
GO:0042330	10.68519004	1.41E-08	Taxis	12
GO:0006935	10.68519004	1.41E-08	Chemotaxis	12
GO:0006955	4.327388535	6.53E-08	Immune response	21
GO:0050900	15.8	4.59E-06	Leukocyte migration	7
GO:0007626	5.279258816	6.18E-06	Locomotory behavior	13
GO:0030595	21.56825397	7.02E-06	Leukocyte chemotaxis	6
GO:0002521	4.784507042	0.003376867	Leukocyte differentiation	7
GO:0030097	3.480136596	0.004277503	Hemopoiesis	9
GO:0048534	3.108591764	0.00828943	Hemopoietic or lymphoid organ development	9
GO:0002520	2.961065375	0.010920286	Immune system development	9
GO:0030217	5.108270677	0.042885669	T cell differentiation	4
GO:0002320	24.26428571	0.078985664	Lymphoid progenitor cell differentiation	2
Term	**Fold enrichment**	**P-value**	**Pathway**	**# of genes**
mmu04640	9.758503401	5.54E-07	Hematopoietic cell lineage	10
mmu04060	3.359484778	0.002382651	Cytokine-cytokine receptor interaction	10
mmu04612	5.404709576	0.004542811	Antigen processing and presentation	6
mmu04514	3.193692022	0.037063036	Cell adhesion molecules (CAMs)	6
mmu04670	3.444177671	0.054254604	Leukocyte transendothelial migration	5

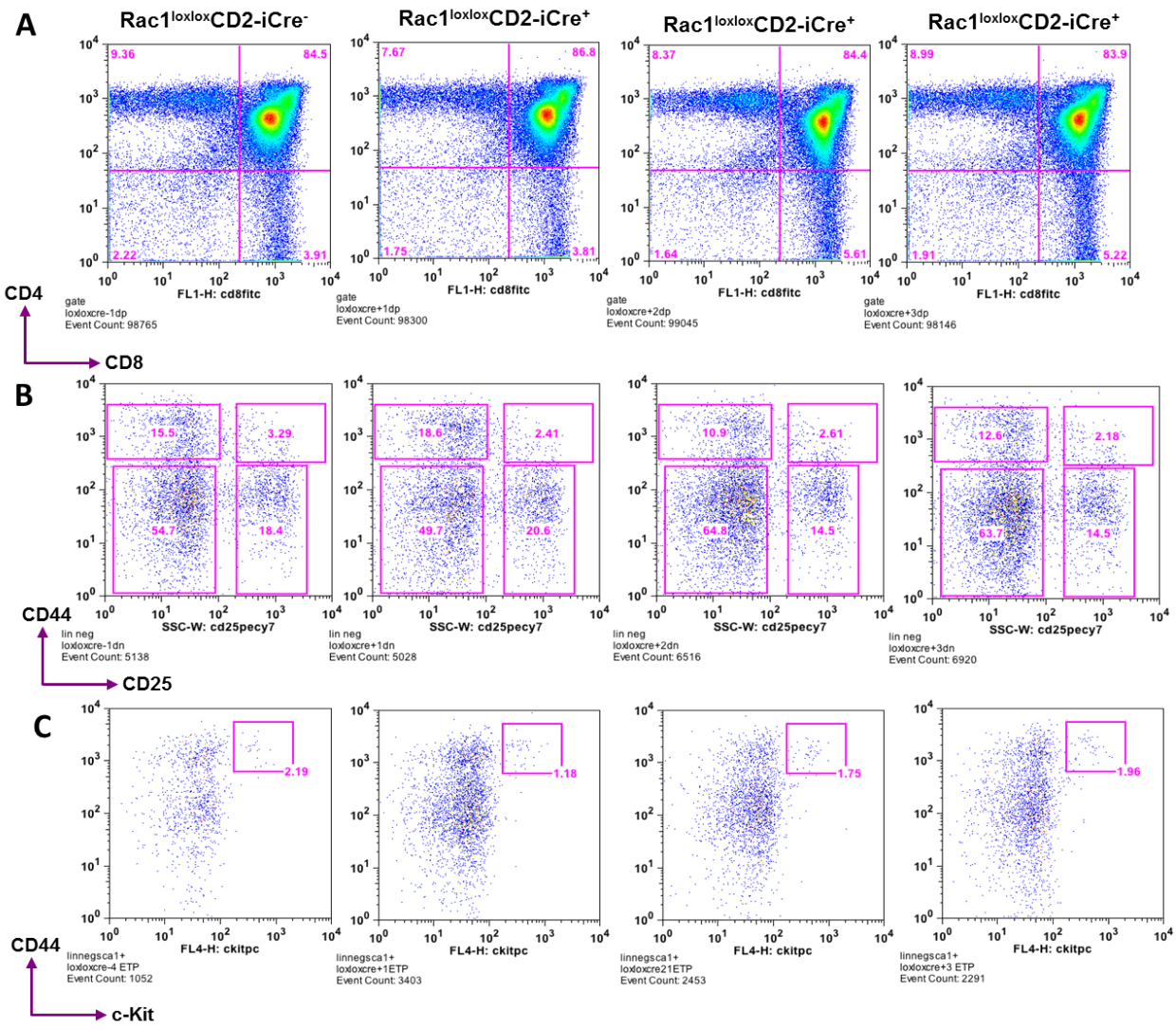

Appendix 1.8. The thymic lymphoid phenotype of *Rac1* $^{lox/lox}$CD2-iCre^{+}mice in comparison to *Rac1* $^{lox/lox}$CD2-iCre^{-} animals at P21.

The CD2 promotor have been used to target specific *Rac1* deletion from early to mature T cell population in the generated conditional *Rac1* $^{lox/lox}$CD2-iCre^{+} animals. The distribution of the **(A)** CD4/CD8, **(B)** DN1-DN4 and **(C)** ETPs population remains unchanged in three independent *Rac1* $^{lox/lox}$CD2-iCre^{+} thymi compared to *Rac1* $^{lox/lox}$CD2-iCre^{-} thymus

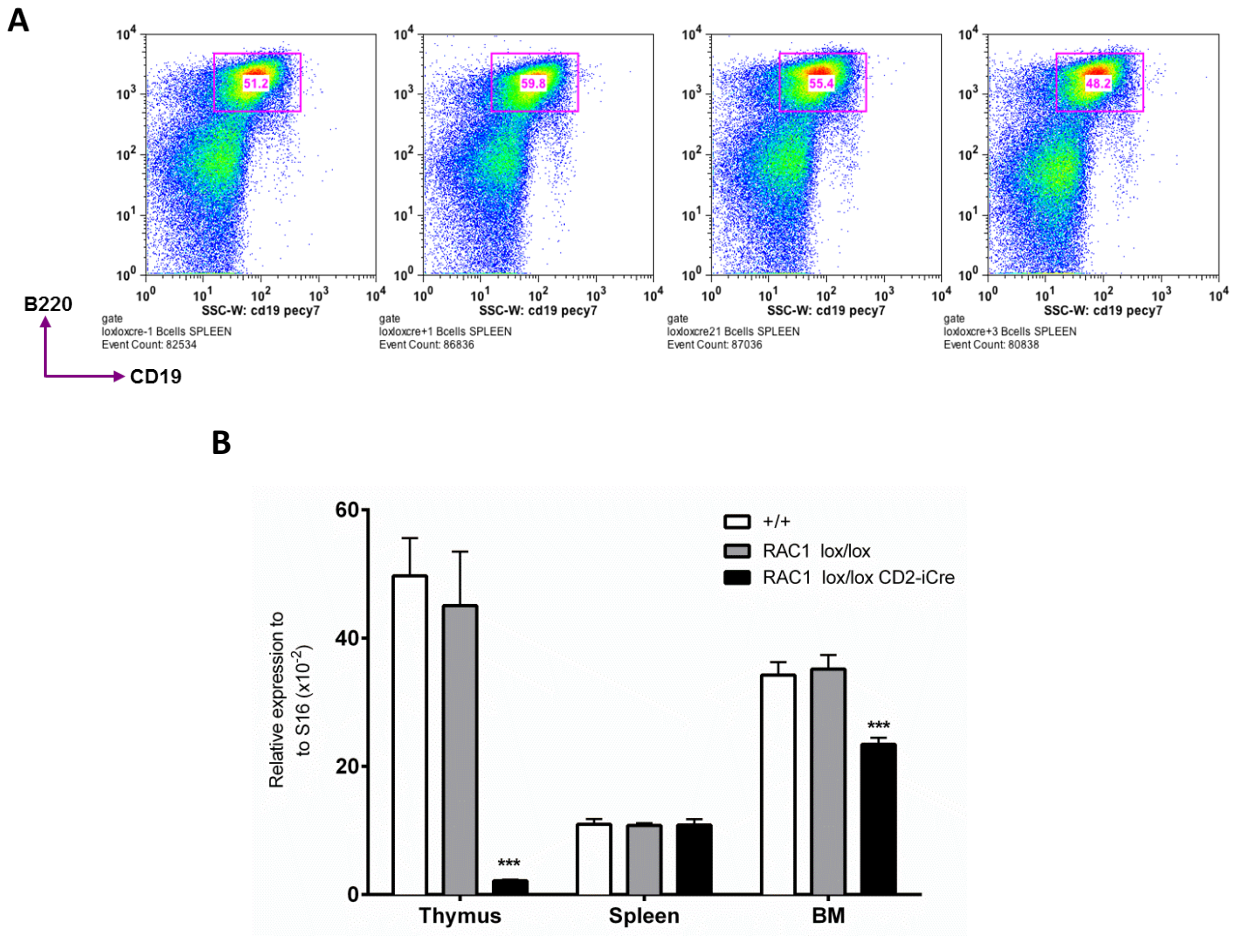

Appendix 1.9. Characterization of splenic lymphoid distribution and gene expression profile of *Rac1*$^{lox/lox}$CD2-iCre^{+} mice compared to *Rac1*$^{lox/lox}$CD2-iCre^{-} animals.

(A) Flow cytometry graphs representing splenic B cell populations of *Rac1*$^{lox/lox}$CD2-iCre^{+}mice compared to *Rac1*$^{lox/lox}$CD2-iCre^{-} animals at P21. **(B)** Quantitative PCR expression of endogenous *Rac1* in lymphoid tissues of three independent Rac1$^{lox/lox}$CD2-iCre^{+} animals compared to *Rac1*$^{lox/lox}$CD2-iCre^{-} and +/+ mice at P21**.**

2.2.7. ACKNOWLEDGEMENTS

We thank members of Dr. Tarik Moroy laboratory for helpful discussions and technical assistance especially Marissa Rashkovan and Dr Charles Vadnais for technical help and critical reading of the manuscript. We also thank Dr. Vibhuti Davé for CD2 plasmid, Dr. J.C Zuñiga-Pflucker for supplying OP9-DL4 stroma cell line, Dr. Marie Trudel for *Rac1*$^{lox/lox}$ animals as well as Eric Massicotte and Julie Lord (Flow cytometry core facility at IRCM) for the tremendous technical assistance. This work was supported by Canadian Institutes of Health Research grant to Dr. Jean Vacher

2.2.8. REFERENCES

Akiyama, T., et al. (2012). "RANKL-RANK interaction in immune regulatory systems." World J Orthop **3**(9): 142-150.

Anderson, G., et al. (2006). "Establishment and functioning of intrathymic microenvironments." Immunol Rev **209**: 10-27.

Arron, J. R. and Y. Choi (2000). "Bone versus immune system." Nature **408**(6812): 535-536.

Belyaev, N. N., et al. (2012). "Global transcriptional analysis of primitive thymocytes reveals accelerated dynamics of T cell specification in fetal stages." Immunogenetics **64**(8): 591-604.

Bhandoola, A., et al. (1999). "Positive Selection as a Developmental Progression Initiated by αβTCR Signals that Fix TCR Specificity prior to Lineage Commitment." Immunity **10**(3): 301-311.

Bhandoola, A., et al. (2003). "Early T Lineage Progenitors: New Insights, but Old Questions Remain." The Journal of Immunology **171**(11): 5653-5658.

Bleul, C. C., et al. (2006). "Formation of a functional thymus initiated by a postnatal epithelial progenitor cell." Nature **441**(7096): 992-996.

Blin-Wakkach, C., et al. (2004). "[Osteopetrosis, from mouse to man]." Med Sci (Paris) **20**(1): 61-67.

Blin-Wakkach, C., et al. (2014). "Roles of osteoclasts in the control of medullary hematopoietic niches." Arch Biochem Biophys.

Chalhoub, N., et al. (2003). "Grey-lethal mutation induces severe malignant autosomal recessive osteopetrosis in mouse and human." Nat Med **9**(4): 399-406.
Coccia, P. F., et al. (1980). "Successful bone-marrow transplantation for infantile malignant osteopetrosis." N Engl J Med **302**(13): 701-708.

Cummins, A. G. and F. M. Thompson (1997). "Postnatal changes in mucosal immune response: a physiological perspective of breast feeding and weaning." Immunol Cell Biol **75**(5): 419-429.

Cyster, J. G. (2009). "Settling the thymus: immigration requirements." J Exp Med **206**(4): 731-734.

de Barros, S. C., et al. (2013). "Intrathymic progenitor cell transplantation across histocompatibility barriers results in the persistence of early thymic progenitors and T-cell differentiation." Blood **121**(11): 2144-2153.

de Boer, J., et al. (2003). "Transgenic mice with hematopoietic and lymphoid specific expression of Cre." Eur J Immunol **33**(2): 314-325.

Dorsam, G., et al. (2003). "Transduction of multiple effects of sphingosine 1-phosphate (S1P) on T cell functions by the S1P1 G protein-coupled receptor." J Immunol **171**(7): 3500-3507.

Essabar, L., et al. (2014). "Malignant infantile osteopetrosis: case report with review of literature." Pan Afr Med J **17**: 63.

Foss, D. L., et al. (2001). "The importation of hematogenous precursors by the thymus is a gated phenomenon in normal adult mice." J Exp Med **193**(3): 365-374.

Gerritsen, E. J., et al. (1994). "Bone marrow transplantation for autosomal recessive osteopetrosis. A report from the Working Party on Inborn Errors of the European Bone Marrow Transplantation Group." J Pediatr **125**(6 Pt 1): 896-902.

Godfrey, D. I., et al. (1992). "Phenotypic and functional characterization of c-kit expression during intrathymic T cell development." J Immunol **149**(7): 2281-2285.
Gomez, M., et al. (2000). "Control of pre-T cell proliferation and differentiation by the GTPase Rac-I." Nat Immunol **1**(4): 348-352.

Gossens, K., et al. (2009). "Thymic progenitor homing and lymphocyte homeostasis are linked via S1P-controlled expression of thymic P-selectin/CCL25." J Exp Med **206**(4): 761-778.

Ikawa, T., et al. (2004). "Identification of the earliest prethymic T-cell progenitors in murine fetal blood." Blood **103**(2): 530-537.

Jotereau, F. V. and N. M. Le Douarin (1982). "Demonstration of a cyclic renewal of the lymphocyte precursor cells in the quail thymus during embryonic and perinatal life." J Immunol **129**(5): 1869-1877.

Kyewski, B. A. (1987). "Seeding of thymic microenvironments defined by distinct thymocyte-stromal cell interactions is developmentally controlled." J Exp Med **166**(2): 520-538.

Lang, G., et al. (1991). "Deletion analysis of the human CD2 gene locus control region in transgenic mice." Nucleic Acids Res **19**(21): 5851-5856.

Lang, G., et al. (1988). "The structure of the human CD2 gene and its expression in transgenic mice." EMBO J **7**(6): 1675-1682.

Lange, P. F., et al. (2006). "ClC-7 requires Ostm1 as a beta-subunit to support bone resorption and lysosomal function." Nature **440**(7081): 220-223.

Lorenzo, J., et al. (2008). "Osteoimmunology: interactions of the bone and immune system." Endocr Rev **29**(4): 403-440.

Mansour, A., et al. (2012). "Osteoclasts promote the formation of hematopoietic stem cell niches in the bone marrow." J Exp Med **209**(3): 537-549.

Mansour, A., et al. (2012). "Role of osteoclasts in the hematopoietic stem cell niche formation." Cell Cycle **11**(11): 2045-2046.

Maranda, B., et al. (2008). "Clinical and cellular manifestations of OSTM1-related infantile osteopetrosis." J Bone Miner Res **23**(2): 296-300.

Martins, V. C., et al. (2012). "Thymus-autonomous T cell development in the absence of progenitor import." J Exp Med **209**(8): 1409-1417.

Misslitz, A., et al. (2004). "Thymic T cell development and progenitor localization depend on CCR7." J Exp Med **200**(4): 481-491.

Mohtashami, M. and J. C. Zuniga-Pflucker (2006). "Three-dimensional architecture of the thymus is required to maintain delta-like expression necessary for inducing T cell development." J Immunol **176**(2): 730-734.

Monostori, E., et al. (1991). "Human CD2 is functional in CD2 transgenic mice." Immunology **74**(3): 369-372.

Pangrazio, A., et al. (2006). "Mutations in OSTM1 (grey lethal) define a particularly severe form of autosomal recessive osteopetrosis with neural involvement." J Bone Miner Res **21**(7): 1098-1105.

Pata, M., et al. (2008). "OSTM1 bone defect reveals an intercellular hematopoietic crosstalk." J Biol Chem **283**(45): 30522-30530.

Peaudecerf, L., et al. (2012). "Thymocytes may persist and differentiate without any input from bone marrow progenitors." J Exp Med **209**(8): 1401-1408.
Penit, C. (1987). "In vivo proliferation and differentiation of prothymocytes in the thymus." Immunol Res **6**(4): 271-278.

Penit, C. (1988). "Localization and phenotype of cycling and post-cycling murine thymocytes studied by simultaneous detection of bromodeoxyuridine and surface antigens." J Histochem Cytochem **36**(5): 473-478.

Petrie, H. T. and J. C. Zuniga-Pflucker (2007). "Zoned out: functional mapping of stromal signaling microenvironments in the thymus." Annu Rev Immunol **25**: 649-679.

Porritt, H. E., et al. (2004). "Heterogeneity among DN1 prothymocytes reveals multiple progenitors with different capacities to generate T cell and non-T cell lineages." Immunity **20**(6): 735-745.

Prockop, S. E. and H. T. Petrie (2004). "Regulation of thymus size by competition for stromal niches among early T cell progenitors." J Immunol **173**(3): 1604-1611.

Quarello, P., et al. (2004). "Severe malignant osteopetrosis caused by a GL gene mutation." J Bone Miner Res **19**(7): 1194-1199.

Rajapurohitam, V., et al. (2001). "The mouse osteopetrotic grey-lethal mutation induces a defect in osteoclast maturation/function." Bone **28**(5): 513-523.

Sato, Y., et al. (2009). "Rac GTPases are involved in development, survival and homeostasis of T cells." Immunol Lett **124**(1): 27-34.

Shah, D. K. and J. C. Zuniga-Pflucker (2014). "An overview of the intrathymic intricacies of T cell development." J Immunol **192**(9): 4017-4023.

Shultz, L. D. (1991). "Immunological mutants of the mouse." American journal of anatomy **191**(3): 303-311.
Sobacchi, C., et al. (2013). "Osteopetrosis: genetics, treatment and new insights into osteoclast function." Nat Rev Endocrinol **9**(9): 522-536.

Subramanian, A., et al. (2005). "Gene set enrichment analysis: a knowledge-based approach for interpreting genome-wide expression profiles." Proc Natl Acad Sci U S A **102**(43): 15545-15550.

Takahama, Y. (2006). "Journey through the thymus: stromal guides for T-cell development and selection." Nat Rev Immunol **6**(2): 127-135.

Takayanagi, H. (2005). "Osteoimmunological insight into bone damage in rheumatoid arthritis." Mod Rheumatol **15**(4): 225-231.

Takayanagi, H., et al. (2002). "Induction and activation of the transcription factor NFATc1 (NFAT2) integrate RANKL signaling in terminal differentiation of osteoclasts." Dev Cell **3**(6): 889-901.

Tan, J. T., et al. (2002). "Interleukin (IL)-15 and IL-7 jointly regulate homeostatic proliferation of memory phenotype CD8+ cells but are not required for memory phenotype CD4+ cells." J Exp Med **195**(12): 1523-1532.

Trapnell, C., et al. (2012). "Differential gene and transcript expression analysis of RNA-seq experiments with TopHat and Cufflinks." Nat Protoc **7**(3): 562-578.

Trapnell, C., et al. (2014). "Corrigendum: Differential gene and transcript expression analysis of RNA-seq experiments with TopHat and Cufflinks." Nat Protoc **9**(10): 2513.

Villa, A., et al. (2009). "Infantile malignant, autosomal recessive osteopetrosis: the rich and the poor." Calcif Tissue Int **84**(1): 1-12.

Weinreich, M. A. and K. A. Hogquist (2008). "Thymic emigration: when and how T cells leave home." Journal of immunology (Baltimore, Md. : 1950) **181**(4): 2265-2270.

Wiktor-Jedrzejczak, W., et al. (1983). "Osteopetrosis associated with premature thymic involution in grey-lethal mice. In vitro studies of thymic microenvironment." Clin Exp Immunol **52**(3): 465-471.

Witt, C. M. and E. A. Robey (2004). "The ins and outs of CCR7 in the thymus." J Exp Med **200**(4): 405-409.

Yokota, T., et al. (2006). "Tracing the first waves of lymphopoiesis in mice." Development **133**(10): 2041-2051.

Zuniga-Pflucker, J. C. (2009). "The original intrathymic progenitor from which T cells originate." J Immunol **183**(1): 3-4.

CHAPTER 3: ANALYSIS OF THE B CELL POPULATION DEFECT IN *gl/gl* OSTEOPETROTIC MICE

3.1. PREFACE

Our previous transgenesis strategy using PU-1 promoter has allowed us to restore *Ostm1* gene expression both in myeloid, B and T lymphoid lineages of *gl/gl* mice. This study has also illustrated a significant B cell defect induced by the *gl/gl* mutation. Furthermore, the normalized B cell distribution within PU-1-*Ostm1 gl/gl* transgenic 737 and 761 lines supports an unknown intrinsic Ostm1 function in the B lineage homeostasis (**Table 1.6)**.

To connect *Ostm1* gene mutation with the disrupted B cell distribution of *gl/gl* mice, I have measured endogenous *Ostm1* expression and dissected the *gl/gl* B cell defect based on the B cell developmental sequence. To investigate further the B cell intrinsic function of *Ostm1* independent of the osteoclast lineage, our laboratory have restored Ostm1 expression in B cells of *gl/gl* animals under the control of CD19 promoter by generating the CD19-*Ostm1 gl/gl* transgenic progenies. In parallel, we have conditionally deleted the *Ostm1* gene in the B cells in the presence of Cre expression under the control of Mb-1 promoter by generating the conditional knock-out (cKO) *Ostm1*$^{lox/lox}$ Mb1-Cre^{+} animals. Overall, I have assessed endogenous *Ostm1* and CD19-Ostm1 expression in CD19-*Ostm1-gl/gl* mice, as well as the Cre expression and subsequent *Ostm1* deletion in cKO animals. Additionally, I initiated the study of B cell differentiation in both transgenic and cKO animals.

Table 1.6. B lymphoid cellularity of grey-lethal (*gl/gl*) in spleen and BM

Mice	n	Spleen			Bone Marrow		
		Myeloid lineage		B-lymphoid lineage	Myeloid lineage		B-lymphoid lineage
		CD11b^{+}	CD11b^{+}Ly6-G^{+}	B220^{+}	CD11b^{+}	CD11b^{+}Ly6-G^{+}	B220^{+}
+/+ NT	6	11.5±1.6	5.2±2.0	61.9±17.2	11.8±3.1	21.1±6.4	50.1±9.3
+/+ TR	4	9.4±4.9	4.3±1.6	55.1±14.2	9.7±3.1	21.5±7.3	51.4±5.7
gl/gl NT	5	15.6±2.0**	10.2±4.7**	39.9±8.9 *	NA	NA	NA
gl/gl TR 737	5	8.7±1.2	4.0±1.2	59.2±6.3	10.0±1.7	26.7±4.5	47.2±2.7
gl/gl TR 761	3	11.3±1.5	4.2±1.4	55.6±7.8	14.9±2.9	28.2±1.8	41.0±6.9

(Pata, Heraud et al. 2008)

3.2. ARTICLE 2

Characterization of the defective B cell population in *gl/gl* osteopetrotic mice

Marie Mutabaruka[1,3], Eva Lee[1,4], Monica Pata[1], and Jean Vacher [1,2,3]

[1] Institut de Recherches Cliniques de Montréal, Montréal, Québec H2W 1R7, Canada
[2] Département de Médecine, Université de Montréal, Montréal, Québec H3T 3J7, Canada
[3] Division of Experimental Medicine, McGill University, Montréal, Québec H3A 1A3, Canada
[4]Department of Biochemistry, McMaster University, Hamilton, Ontario L8S 4L8, Canada

*Manuscript in preparation

Competing financial interests

The authors declare no competing financial interests.

Corresponding author

Correspondence should be addressed to Jean Vacher: jean.vacher@ircm.qc.ca

3.2.1. ABSTRACT

The total B cell defect and developmental arrest are frequent hallmarks which could be associated with susceptibility to infections reported in osteopetrotic mouse models and patients. Previous investigations have shown that several osteopetrotic gene mutations are indirectly involved in B cell physiology by regulating homeostasis of the bone marrow component, the site of post-natal early B cell development. Additionally, the bone marrow-dependent-B cell physiology relies on the balance between cell-intrinsic mechanisms and the support of the marrow environment. Our *gl/gl* osteopetrotic model also recapitulates the B cell defect, but the connection between *Ostm1* gene mutation and this defective B cell lineage remains unclear. To address this question, our study demonstrates an early B cell deficit from approximately 8 days of age and blockage at the early B differentiation stage in *gl/gl* progenies of 21 days-old compared to age-matched control animals. Moreover, this early B cell phenotype resulted in reduced mature B cell population in the *gl/gl* spleen. Intriguingly, total B cell deficit and the developmental blockage are maintained in all CD19-*Ostm1 gl/gl* transgenic mice, in which *Ostm1* expression is specifically restored in the B cell lineage from pro-B to mature B stages. Moreover, the Mb1-Cre-mediated knockout of the *Ostm1* gene in pre-pro B cells within *Ostm1* $^{lox/lox}$ Mb1-Cre^{+} animals did not induce any significant osteopetrotic B cell phenotype in the spleen and BM. Collectively, our observations support an indirect function of the *Ostm1* gene in the defective B cell physiology depicted in osteopetrotic *gl/gl* mice, possibly via modulation of osteoclast activity and bone marrow space.

3.2.2. INTRODUCTION

Osteopetrotic human patients and murine models display a severe B cell phenotype which is characterized by diminished peripheral B cells. This phenotype also translates to reduced serum Ig levels, hypoglubulinemia and abnormal antibody responses to antigens (Dougall, Glaccum et al. 1999, Kong, Yoshida et al. 1999, Guerrini, Sobacchi et al. 2008). However, other studies have demonstrated an indirect link between osteopetrotic gene mutations such as *RANK* and *RANKL* with the osteopetrotic-associated B cell phenotype. In addition, these studies have shown that the lack of a bone marrow (BM) cavity resulting from inactive osteoclasts and the higher bone density in osteopetrotic models is an obvious explanation for this B cell defect, since the BM micro-environment is the initial location for early B cell development (Mansour, Anginot et al. 2011, Perlot and Penninger 2012).

In the BM, early B cell differentiation is regulated by the gene rearrangements and drastic changes in transcriptional gene expression to produce a functional B cell receptor on the surface of developing B cells. The differentiation sequence involves five subsets beginning with the pre-pro-B cells ($B220^{+}CD19^{-}c\text{-}Kit^{+}CD43^{+}IgM^{-}IgD^{-}$) and followed by pro-B subset ($B220^{+}CD19^{+}CD43^{+}IgM^{-}IgD^{-}$);the early/large(pre)-B population ($B220^{+}$ $CD19^{+}CD43^{+}IgM^{+}IgD^{-}$); the late/small large (pre)-B ($B220^{+}CD19^{+}CD43^{-}IgM^{-}IgD^{-}$) and the immature/newly formed B population ($B220^{+}$ $CD19^{+}CD43^{-}IgM^{+}IgD^{-}$) which migrate to the spleen to differentiate into mature/follicular B-cell ($B220^{+}CD19^{+}CD43^{-}IgM^{low/hi}IgD^{hi}$) (Hardy and Hayakawa 2001, Hardy, Kincade et al. 2007).

Our *gl/gl* mouse contains the osteopetrotic *Ostm1* gene mutation and recapitulates most phenotypes associated with osteopetrosis including inactive osteoclasts, toothless, short life span, the T and B cell defect and an obliterated BM cavity (Rajapurohitam, Chalhoub et al. 2001, Chalhoub, Benachenhou et al. 2003, Pata, Heraud et al. 2008). Interestingly, specific restoration of *Ostm1* gene expression in the B cell lineage, under the control of the PU-1 promoter, has rescued the abnormal B cell number and the BM cavity of PU-1-*Ostm1-gl/gl* transgenic progenies. This study illustrates the importance of *Ostm1* gene function in the B cell population but its direct or indirect connection remains to be clarified (Pata, Heraud et al. 2008).

To address this question, *Ostm1* gene expression was established from the pre-B to mature splenic B cell population of *gl/gl* animals under control of the murine CD19 promoter in CD19-*Ostm1-gl/gl* transgenic progenies (Rickert, Roes et al. 1997). Importantly, the total B cell deficit and an early B cell differentiation blockage are demonstrated in the *gl/gl* spleen and exacerbated in CD19-*Ostm1-gl/gl* transgenic animals when compared to +/+ progenies. Together, these findings support either an indirect *Ostm1* role in B cell physiology and/or an off-target effect of the CD19-*Ostm1* transgene.

Furthermore, *Ostm1* gene expression is detected from pre-pro to mature B differentiation stages and this expression pattern coincides with an early B developmental arrest resulting in the depletion of peripheral mature B cells in *gl/gl* spleen. To investigate its B cell-intrinsic function, *Ostm1* gene expression is abolished in early B cell populations with the mb1-Cre-mediated deletion from the pre-pro-B cell subset of *Ostm1*^{loxlox}Mb1-Cre^{+} mice (Hobeika, Thiemann et al. 2006). Despite an efficient deletion of endogenous *Ostm1* gene in hematopoietic tissues containing at least 50% of B cells, there is no detectable B cell deficit or B cell developmental defect in conditional knock-out *Ostm1*^{loxlox}Mb1-Cre^{+} animals.

Collectively, these findings indicate that the osteopetrotic *Ostm1* mutation plays an indirect function in the B cell physiology, possibly through the disrupted osteoclast activity.

3.2.3. MATERIALS AND METHODS

Mice

The mouse strain GL/Le dl^J +/+gl was obtained from The Jackson Laboratory (Bar Harbor, ME) and maintained by heterozygous brother × sister mating for ~200 generations. Homozygous gl/gl mice were used for analysis with +/+ littermates as controls. All experiments on animal were approved by the institutional animal care committee and Canadian Committee for Animal Protection.

Generation and analysis of transgenic and conditional Knock-Out animals

The transgene construct is included in the CD19 BAC RP23-335K9 (152kb), obtained from the Children's Hospital Oakland Research Institute (CHORI). The coding sequence of CD19 has been replaced at the ATG by a cassette including a V5 tagged *Ostm1* cDNA (1.1kb) in frame with an IRES-iEGFP-polyA.

CD19-*Ostm1* transgenic animals (129sv/C3H): Linearized non-circular BAC was injected into fertilized oocytes from F2 (C3H×C57BL/6). Transgenic mice were identified by PCR primers targeting transgenic CD19-*Ostm1* and endogenous *Ostm1*. PCR amplification conditions were 94 °C, 5 min, followed by 30 cycles of 94 °C for 30secs, 65°C for 30secs, and 72 °C for 10 min. Transgene integrity and copy number were determined by Southern blot using a radioactive probe targeting exon1 of *Ostm1* gene. Transgenic lines were crossed with heterozygous gl/+ mice to generate *gl/gl* BAC CD19-*Ostm1* transgenic progenies at F2.

***Ostm1*^{loxlox}Mb-1 Cre$^+$ conditional knock-Out animals:** Mb-1 Cre^+ transgenic mice were obtained from Dr Tarik Moroy (IRCM). *Ostm1*$^{lox/lox}$ mice were previously generated in the Vacher lab and contain floxed exon 5 coding sequence for the transmembrane domain of OSTM1 protein. Following crossing, *Ostm1*$^{lox/lox}$ Mb-1 Cre^+ progenies were identified by PCR primers lox/+ and Mb1-Cre. PCR amplification conditions were 94 °C, 5 min, followed by 30 cycles of 94 °C for 30secs, 65°C for 30secs, and 72 °C for 10 min. Deletion of the exon5 of *Ostm1* in these conditional KO results in truncated and inactive OSTM1 protein in B cell lineage.

Expression Analysis

Total RNA from was isolated with Trizol or MagMax total RNA isolation kit (Life technologies) protocols from enriched pre-pro B cells, pro-B, immature B and mature B populations, and tissues including bone marrow, brain, kidney, thymus, liver, and spleen. CD19-*Ostm1* transgene expression was quantified by using 1µg of total RNA by semi-quantitative PCR. Experimental conditions were 94 °C for 5 min, followed by 30 cycles of 94 °C for 0.5 min, 65°C for 0.5 min, and 72 °C for 0.5 min. CD19-*Ostm1* transgene and *Ostm1* expression were determined and normalized to S16 gene by real-time quantitative PCR using 50ng to 1µg of DNase (Invitrogen)-treated total RNA. All reactions were performed in triplicate in a Syber Green Master Mix (Life technologies). PCR conditions were 94 °C, 15 min, followed by 45 cycles of 94 °C for 0.5 min, 55 °C for 0.5 min, and 72 °C for 0.5 min by MX4000 Multiplex quantitative PCR analyzer or 50 °C for 2 min; 95 °C for 10 min followed by 45 cycles of 95 °C for 15 sec, 60 °C for 30 sec with Viia 7 Real-time PCR system (life technologies).

RNA was extracted followed by RNA extraction using MagMax Total RNA isolation kit protocol (Life technologies) from sorted B cell populations. 50ng to 300ng of RNA were used for cDNA synthesis using qScript cDNA supermix protocol (Quanta biosciences). Quantification of gene expression including endogenous *Ostm1*, CD19-*Ostm1* transgene and S16 was performed at 50 °C, 2 min, 95 °C for 10 min followed by 45 cycles of 95 °C for 15 sec, 60 °C for 30 sec by Viia 7 Real-time PCR system (life technologies).

Flow cytometry and cell sorting

FACS Analysis: Flow cytometry analysis was carried out on spleen and thymus single cell suspension in phosphate-buffered saline with 1% heat-inactivated fetal bovine serum. Nucleated cells (1.5×10^6) were stained with antibodies from eBioscience: phycoerythrin-conjugated anti-B220, anti-CD19, or Streptavidin; fluorescein isothiocyanate-conjugated anti-IgM or anti-streptavidin; APC conjugated anti-c-Kit, anti-CD43; Pe-Cy7 conjugated anti-IgD. Data acquisition and analysis were respectively done with CellQuest and FlowJo softwares on a BD FACS Calibur four-color flow cytometer and BD LSR cytometer.

Cell sorting: pre-pro B, pro-B, immature and mature B populations were sorted using Moflo sorter.

Western Blot

Proteins were isolated from hematopoietic tissues (spleen and thymus), kidney, liver and brain in RIPA buffer containing proteinase inhibitors cocktail: PMSF, β-Glycerophosphate, Sodium vanadate and proteinase inhibitor cocktail. Tissue protein extract was quantified by Bradford assay on ELISA reader (Roche). V5-*Ostm1* transgene protein expression was detected following an overnight incubation with a primary antibody anti-V5-HRP (Invitrogen) in Tris-buffered saline, 0.1% tween 20 (TTBST 1X) and Bovine serum albumin (BSA) 3%. Following incubation with stripping solution at 55^{o}C for 30 minutes, PVDF membrane was incubated with the primary antibody β-actin from Sigma for 1-2hrs, washed 3 times in TTBST 1X followed by a second incubation with anti-mouse IgG HRP for 1hr. Protein detection and quantification were determined via BioRad Image lab software.

Southern Blot

Genomic DNA is isolated from tail of different CD19-*Ostm1* +/+ transgenic mice. Restriction enzyme EcoR1 is used to digest the DNA followed by DNA migration and transfer on nylon membrane. The membrane is then hybridized with a radiolabeled probe targeting exon1 of *Ostm1*. The resulting bands are analyzed using Image Quant software (Molecular Dynamics) and the expected bands for the CD19-*Ostm1* transgene are quantified for total pixels along with the expected endogenous *Ostm1* bands. The EcoRI digestion results in specific bands associated with the CD19-*Ostm1* transgene (6.5Kb) and the endogenous *Ostm1* (14.5Kb). A ratio of the transgene to the endogenous is used to determine the number of copies in each transgenic line.

Statistical Analysis

Values are expressed as mean ± SEM. Statistical analysis was performed using Graphpad Prism software (San diego, CA). Unpaired two-sample Student's t test was used for statistical analysis with $p \geq 0.05$ considered significant.

3.2.4. RESULTS

The early B cell deficit of the osteopetrotic *gl/gl* mice

The B cell deficit of *gl/gl* was studied in comparison to +/+ animals by monitoring $CD19^+$ B cells within *gl/gl* and control spleens harvested from mice at P8 and P15. This analysis revealed a 50% reduction of the B cell population from the age of P8 to P15. Overall, this observation supports an early B cell phenotype of the *gl/gl* mice that starts approximately from 8 days of age (**Fig 3.1**).

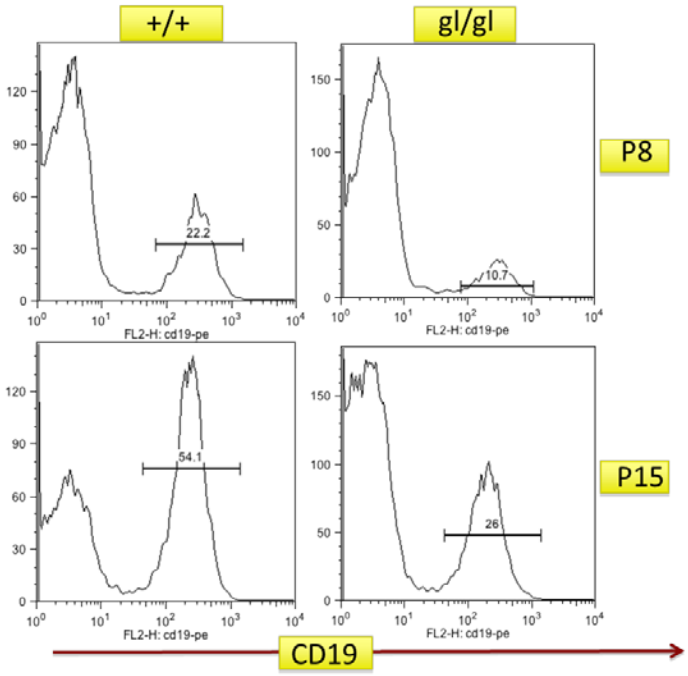

Figure 3.1. The early B cell deficit of the osteopetrotic *gl/gl* mice

Flow cytometry histogram comparing the distribution of B cell population characterized by CD19 surface expression within +/+ and *gl/gl* spleen from animals of 8 and 15 days-old.

Generation of the B cell-specific *Ostm1* transgenic mice

To examine if *Ostm1* impacts B cell homeostasis without extrinsic contribution from osteoclast activity or the BM component, *Ostm1* expression was re-established in the B lineage under the control of the CD19 promoter. CD19 is one of the most reliable surface biomarkers for B cells and it is expressed from pre-B cells until terminal differentiation to plasma cells (Rickert, Roes et al. 1997).

The transgene construct included CD19 regulatory sequences upstream the coding cassette including a V5 tagged *Ostm1* cDNA (1.1kb) in frame with an IRES-iEGFP-polyA and CD19 coding sequences (**Fig 3.2A**). Southern blot analysis validated CD19-*Ostm1* transgene integrity and copy number. Therefore, two transgenic animal lines, BAC 921 and 636 were established with 1.3 and 36 transgene copies, respectively (**Fig 3.2B and data not shown**). The quantitative CD19-*Ostm1* transgene expression was mainly detected in the spleen, BM, and liver of BAC 921 transgenic line (**Fig 3.2C**). In addition, endogenous *Ostm1* expression in BAC 921 transgenic tissues was comparable to the level of control tissues (**Fig 3.2D**). Consistently, immunoblotting displayed significant transgene protein expression in similar tissues including spleen and BM of BAC 921 transgenic lines by using V5 antibody (**Fig 3.2E**). Overall, these experiments demonstrated specific and significant expression of CD19-*Ostm1* transgene in hematopoietic cells contained in the spleen and BM.

Cell-sorting allows enrichment of B cell subsets in correlation with the B cell differentiation sequence. Thus, quantitative expression of B cell populations from +/+ and CD19-*Ostm1* +/+ transgenic spleens revealed a significant increase of endogenous Ostm1 gene when compared to CD19-*Ostm1* transgene expression in the sorted pre-pro B ($B220^+ckit^+$), pro-B ($B220^+CD43^+$), preB/immature ($B220^+IgM^+$) and mature B ($B220^+IgD^+$) (**Fig 3.2F**). Together, these data showed CD19-*Ostm1* transgene expression in the B cell lineage of transgenic mice. On this basis, +/+ CD19-*Ostm1* transgene were crossed with gl/+ progenies to generate CD19-*Ostm1-gl/gl* transgenic animals at F2 in which *Ostm1* gene expression was restored in the B cell lineage (**Fig 3.2G**).

A

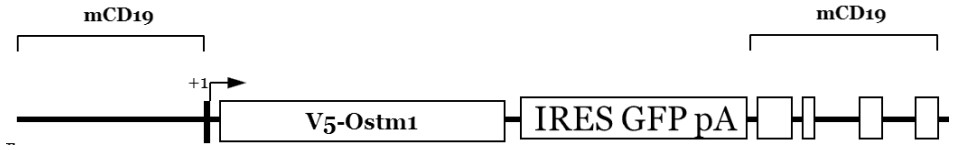

B

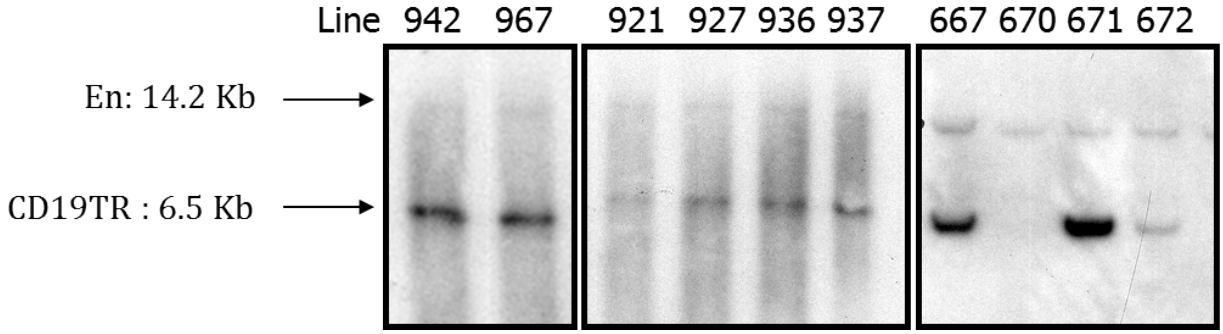

Figure 3.2. Generation of the B cell specific *Ostm1* transgenic mice

A) Construct of BAC CD19-*Ostm1* transgene consisting of the Cluster of differentiation 19 (CD19) regulatory sequences flanking the V5 and GFP tags fused to *Ostm1* cDNA sequence directly under the control of mouse CD19 regulatory sequence at the N-terminus. **B)** Multiple CD19-*Ostm1* transgenic lines were obtained with variable transgene copy numbers as determined by Southern blot. Only CD19-*Ostm1* transgenic (+/+TR) BAC 921 with 1.3 transgene copy number survived and could reproduce.

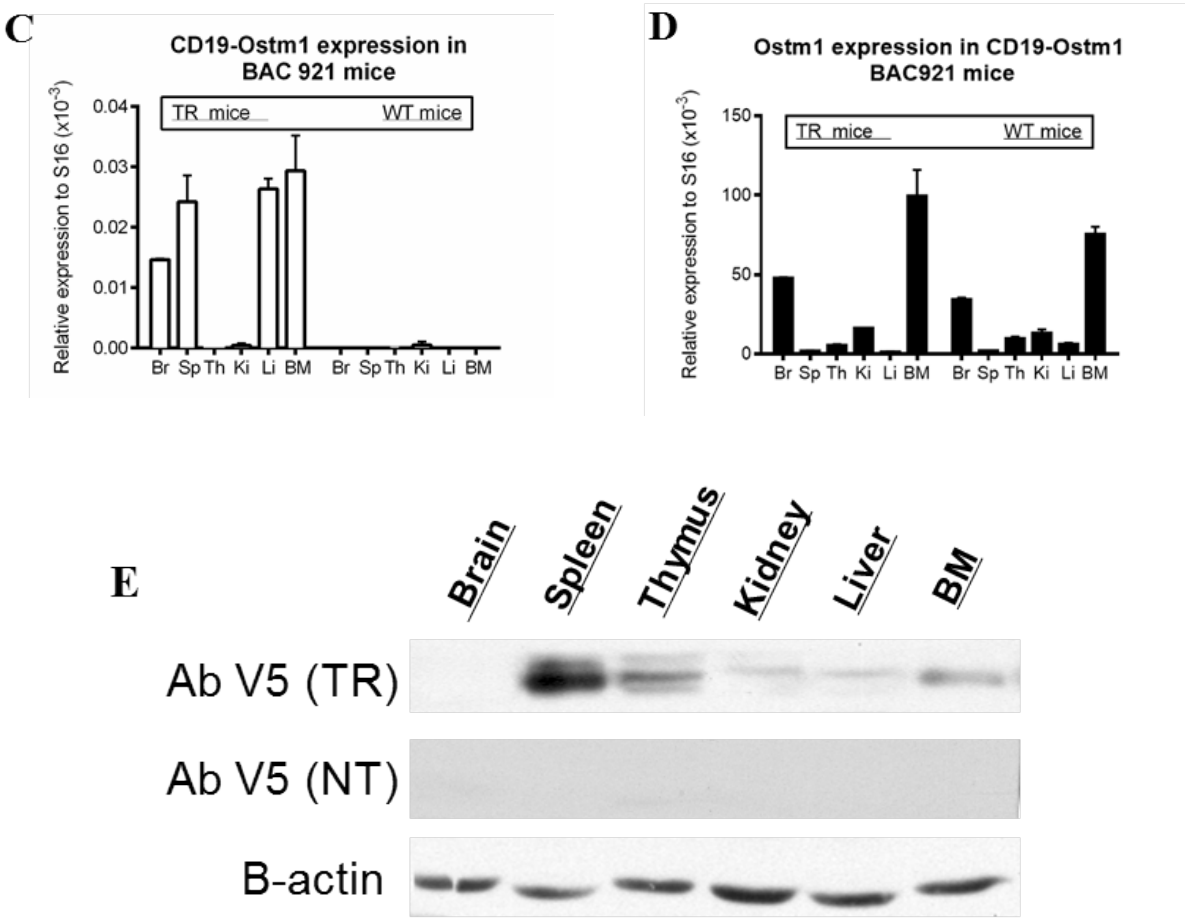

Figure 3.2. Generation of the B cell specific *Ostm1* transgenic mice (Continued)

C) Quantitative expression of CD19-*Ostm1* transgene in tissues of +/+ NT and +/+ BAC921 transgenic animals at P21. **D**) Quantitative expression of endogenous *Ostm1* gene in tissues of +/+ NT and +/+ BAC921 transgenic animals at P21.**E**) Immunoblotting of transgenic protein expression (n=2) within tissues isolated from +/+ NT versus +/+ BAC921 transgenic animals.

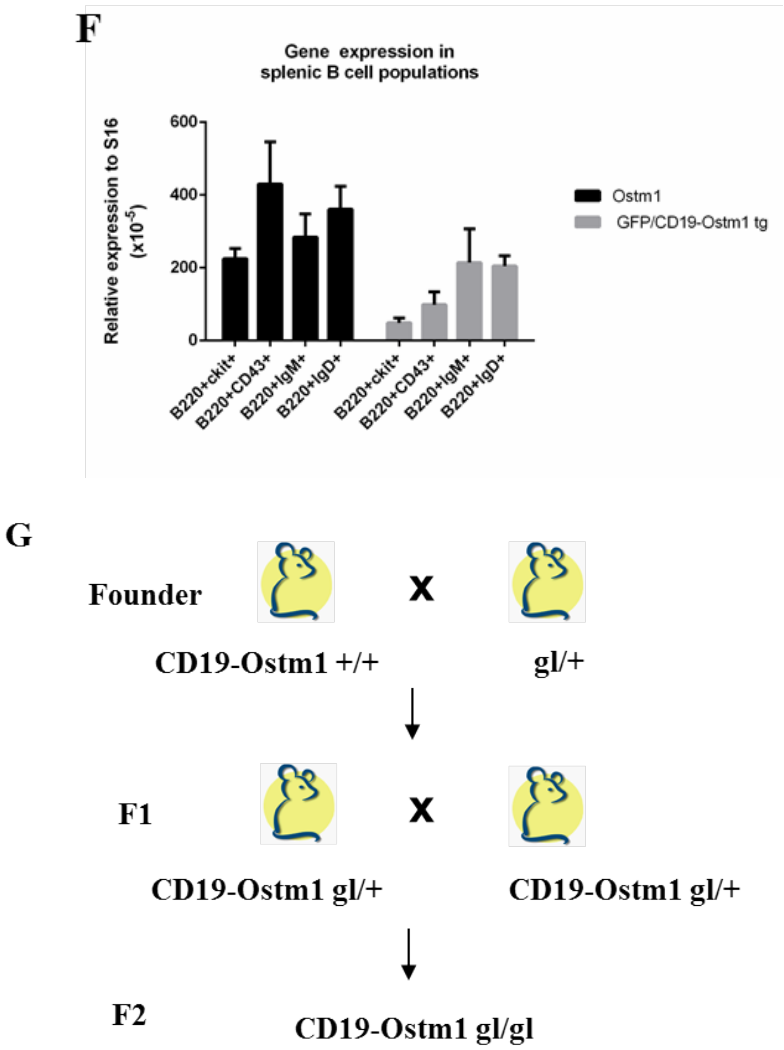

Figure 3.2. Generation of the B cell specific *Ostm1* transgenic mice (Continued)

F) Quantitative expression of the endogenous *Ostm1* gene and CD19-*Ostm1* transgene within enriched B populations harvested from +/+ NT and +/+ BAC921 transgenic spleens at P21 (n=1). **G**) Schematic representation of the crossing strategy to generate *gl/gl* BAC CD19-*Ostm1* transgenic animals at F2.

Exacerbated B cell deficit in *gl/gl* CD19-*Ostm1* transgenic mice

Initial characterization of *gl/gl* CD19-*Ostm1* transgenic mice revealed comparable osteopetrotic manifestations to parental *gl/gl* mice, including smaller size, decreased body weight, compromised BM and other hallmarks such as absent tooth eruption and premature death around three weeks (data not shown).

Importantly, the flow cytometry analysis of total B cell populations illustrated the maintenance of the significant defect in CD19-*Ostm1 gl/gl* animals at P21. In fact, 27.9% of CD19 positive cells were observed in the CD19-*Ostm1 gl/gl* spleen compared to 77% in the control spleen and 45% in the *gl/gl* spleen **(Fig 3.3A**). These data strongly suggest that either an inefficient expression or an intrinsic deleterious effect of the CD19-*Ostm1* transgene which have a negative impact on B cell homeostasis.

To verify the CD19-*Ostm1* transgene expression, we made use of the GFP sequence fused to the *Ostm1* coding sequence that is contained within the transgene construct. Consequently, GFP expression is relative to CD19-*Ostm1* transgene expression and can be detected by flow cytometry. Therefore, flow cytometry histogram showed an exclusive and significant expression of GFP in the CD19-positive population of CD19-*Ostm1gl/gl* transgenic animals compared to control and *gl/gl* animals at P21 **(Fig 3.3B**). Together, these data support an efficient translation of the CD19-*Ostm1* transgene in B cells.

Based on the B cell developmental sequence, this analysis shows a significant depletion of pre-B cells ($CD19^+CD43^+$), immature B cells ($CD19^+IgM^+$) and mature B cells ($CD19^+IgD^+$) along with accumulated pre-pro B cells ($CD19^-CD43^+$) within *gl/gl* spleen in comparison to +/+ spleen. This *gl/gl* B cell phenotype is recapitulated and even exacerbated within CD19-*Ostm1 gl/gl* transgenic progenies, illustrating the inefficiency of CD19-*Ostm1* transgene at rescuing the B cell deficit in *gl/gl* mice.

Collectively, these findings demonstrated no rescue of the B cell deficit of *gl* mutation following restoration of *Ostm1* gene expression under the control of the CD19 promoter, suggesting either the non-cell autonomous function of *Ostm1* in B cells or the requirement of using a promoter targeting *Ostm1* gene expression at earlier B cell developmental stages compared to CD19 promoter (e.g Mb-1).

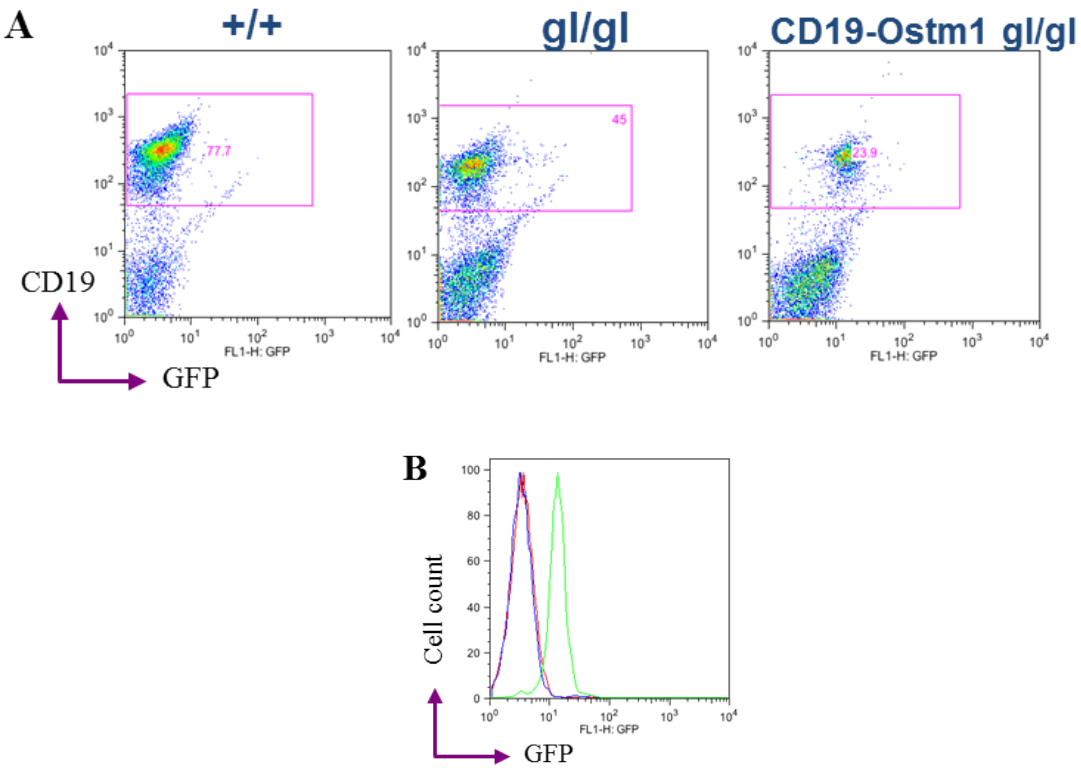

Figure 3.3. Exacerbated B cell deficit in *gl/gl* CD19-*Ostm1* transgenic mice.

A) Flow cytometry profiles (n= 3) showing CD19 and GFP expression level of total B cell population within +/+ or *gl/gl* and CD19-*Ostm1* spleens at P21. **B**) Histogram representing intensity of GFP expression related to CD19-*Ostm1* transgene expression within +/+ (red) and *gl/gl* (blue) and CD19-*Ostm1 gl/gl* (green) animals at P21.

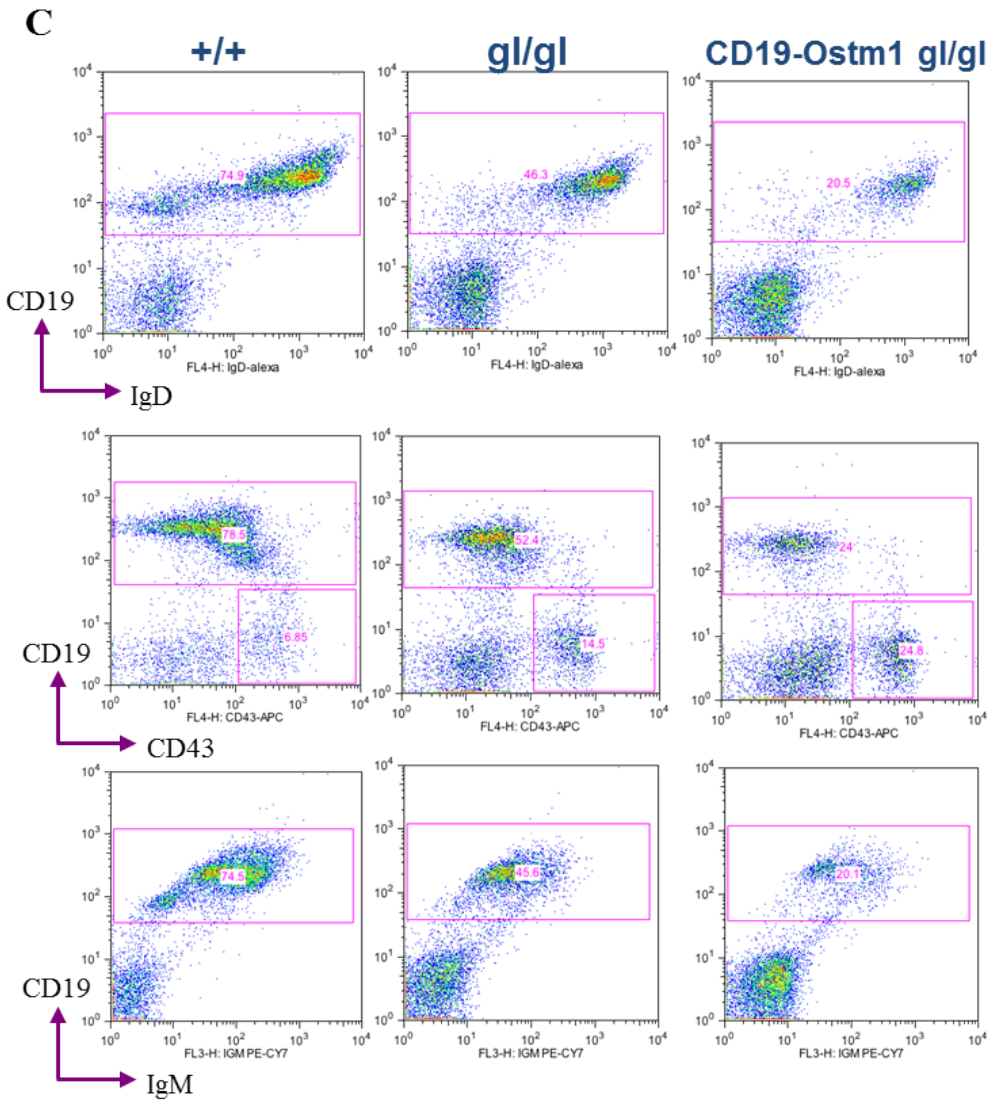

Figure 3.3. Exacerbated B cell deficit in *gl/gl* CD19-*Ostm1* transgenic mice (Continued).

C) Flow cytometry profiles (n=3) dissecting the distribution of the $CD19^{+}IgD^{+}$, $CD19^{+}CD43^{+}$, $CD19^{+}CD43^{-}$ and $CD19^{+}IgM^{+}$ populations during B cell development within +/+ or *gl/gl* and CD19-*Ostm1* spleens at P21.

Generation and Characterization of the B cell specific *Ostm1* cKO animals

Conditional *Ostm1* ablation (cKO) was induced in Mb1-Cre-expressing mice to target the deletion of *Ostm1* exon 5 earlier in the B cell lineage in comparison to the CD19 promoter. This strategy allowed us to study the *Ostm1* cell-intrinsic function independently of the myeloid lineage. The Mb1 gene encodes the Ig-alpha signalling subunit of the B cell antigen receptor and is expressed exclusively in B cells from the early pre-pro-B cell differentiation stage throughout B cell development in the BM and spleen (Hobeika, Thiemann et al. 2006) (**Fig 3.4A**).

To investigate the Mb1-Cre recombination efficiency and tissue specificity, *Ostm1* gene expression was quantified using PCR in hematopoietic tissues spleen and BM as well as in the brain as a positive control from *Ostm1*$^{lox/lox}$ Mb1-Cre^{+} mice and *Ostm1*$^{lox/lox}$ Mb1-Cre^{-} progenies. Two bands were observed in both the spleen and BM from the *Ostm1*$^{lox/lox}$ Mb1-Cre^{+}mice. The upper band represented the endogenous *Ostm1* gene and it was visible in all the samples (**Fig 3.4B**). This was attributed to 40% and 80% of other cell types present in the spleen and BM which were not targeted by Mb1-Cre, respectively. On the other hand, the lower band corresponded to the delta band and suggested that *Ostm1* gene deletion was exclusive to the spleen and BM (**Fig 3.4B**). The absence of the delta band in the brain and the kidney (data not shown) combined with high Mb1-Cre expression detected in the spleen and BM of *Ostm1*$^{lox/lox}$ Mb1-Cre^{+} mice (**Fig 3.4C**), both suggested the specific *Ostm1* deletion into the main tissues housing early and late B cell development such as spleen and BM.

Flow cytometry was used to study the B cell development in the BM and the spleens of *Ostm1*$^{lox/\ lox}$ Mb1-Cre^{+} (cKO) and the *Ostm1*$^{lox/\ lox}$ Mb1-Cre^{-} mice (control). The total B cell population in spleen and BM was unchanged between the control and the cKO based on the expression of B220 (**Fig 3.4D and E**).c-Kit expression characterizes early pro-B cell, while CD43 is expressed from pro-B cell to pre-B cell. Later in the development pathway, IgM is expressed in immature B cell and it is co-expressed with IgD in mature B cells (Hardy, Kincade et al. 2007). On this basis, flow cytometry analysis of the B cell distribution showed no significant differences between the cKO and control mice, suggesting an indirect function of the *Ostm1* gene in B cell development (**Fig 3.4D and E**).

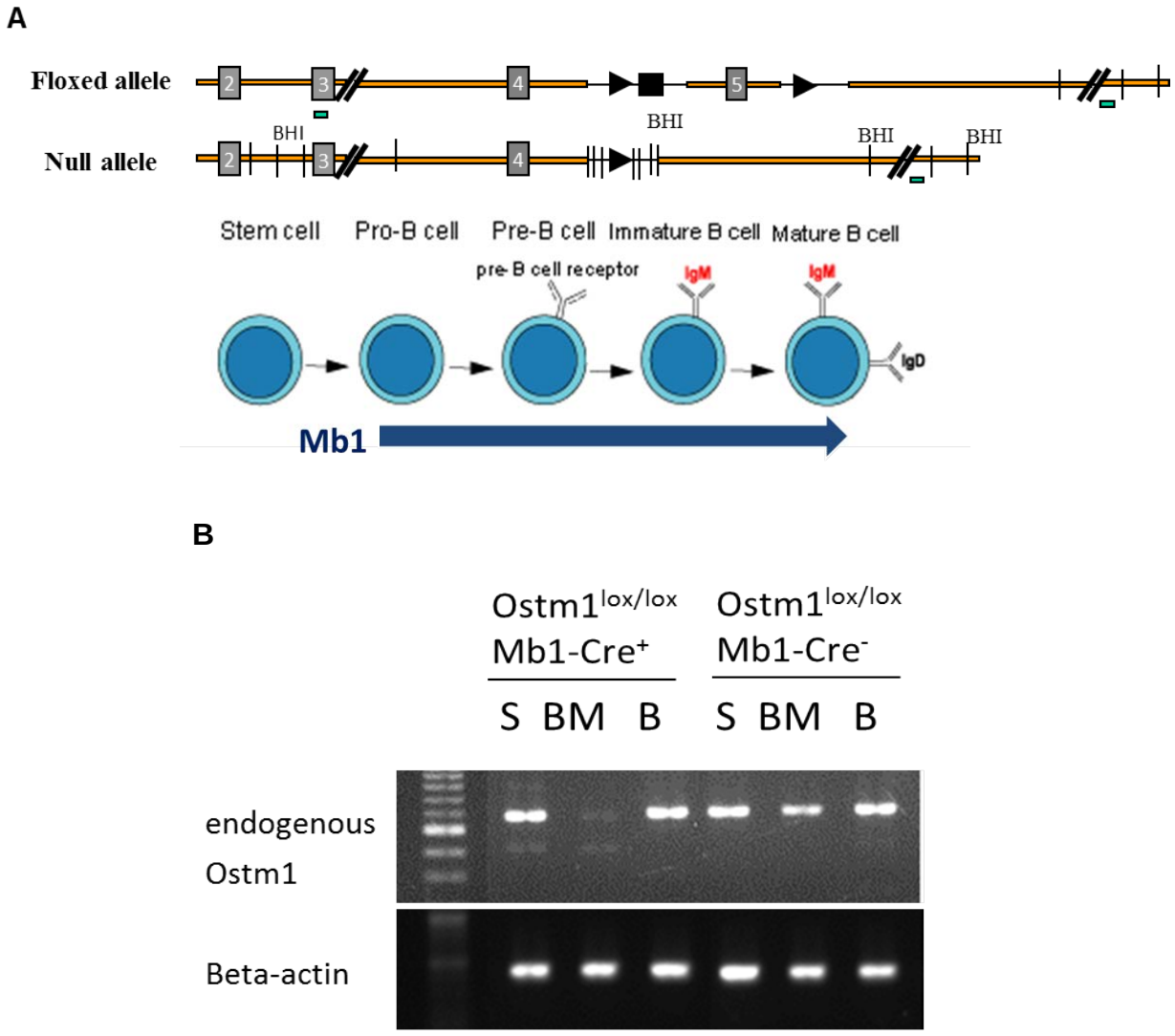

Figure 3.4. Generation and Characterization of the B cell specific *Ostm1* conditional knock out mice.

(A) Schematic representation showing exon 5 of the *Ostm1* gene flanked by flox sequence and the cre expression under control of the Mb1 promoter to induce the specific deletion of *Ostm1* from early populations of the B cell lineage. (**B**) Quantitative expression of endogenous *Ostm1* measured within the BM and the spleen (S) of the *Ostm1*$^{lox/lox}$ Mb1 Cre^{+} and *Ostm1*$^{lox/lox}$ Mb1 Cre^{-} transgenic animals at P21.

C

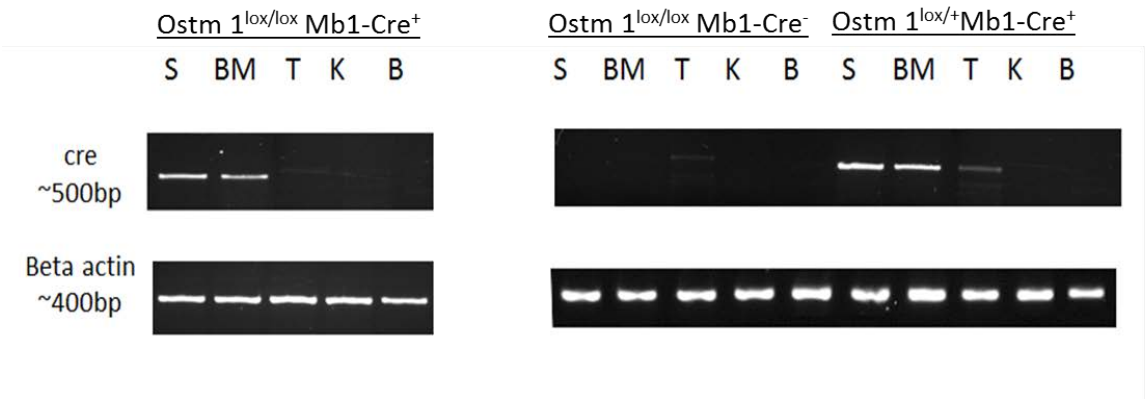

Figure 3.4. Generation and Characterization of the B cell specific Ostm1 conditional knock out mice (Continued).

(**C**) Quantitative Cre expression within the bone marrow (BM), spleen (S), thymus (T), kidney (K) and brain (B) of *Ostm1*$^{lox/lox}$ Mb1-Cre^{+} and *Ostm1*$^{lox/lox}$ Mb1-Cre^{-} transgenic as well as the *Ostm1*$^{lox/+}$ Mb1-Cre^{+} animals at P21

D

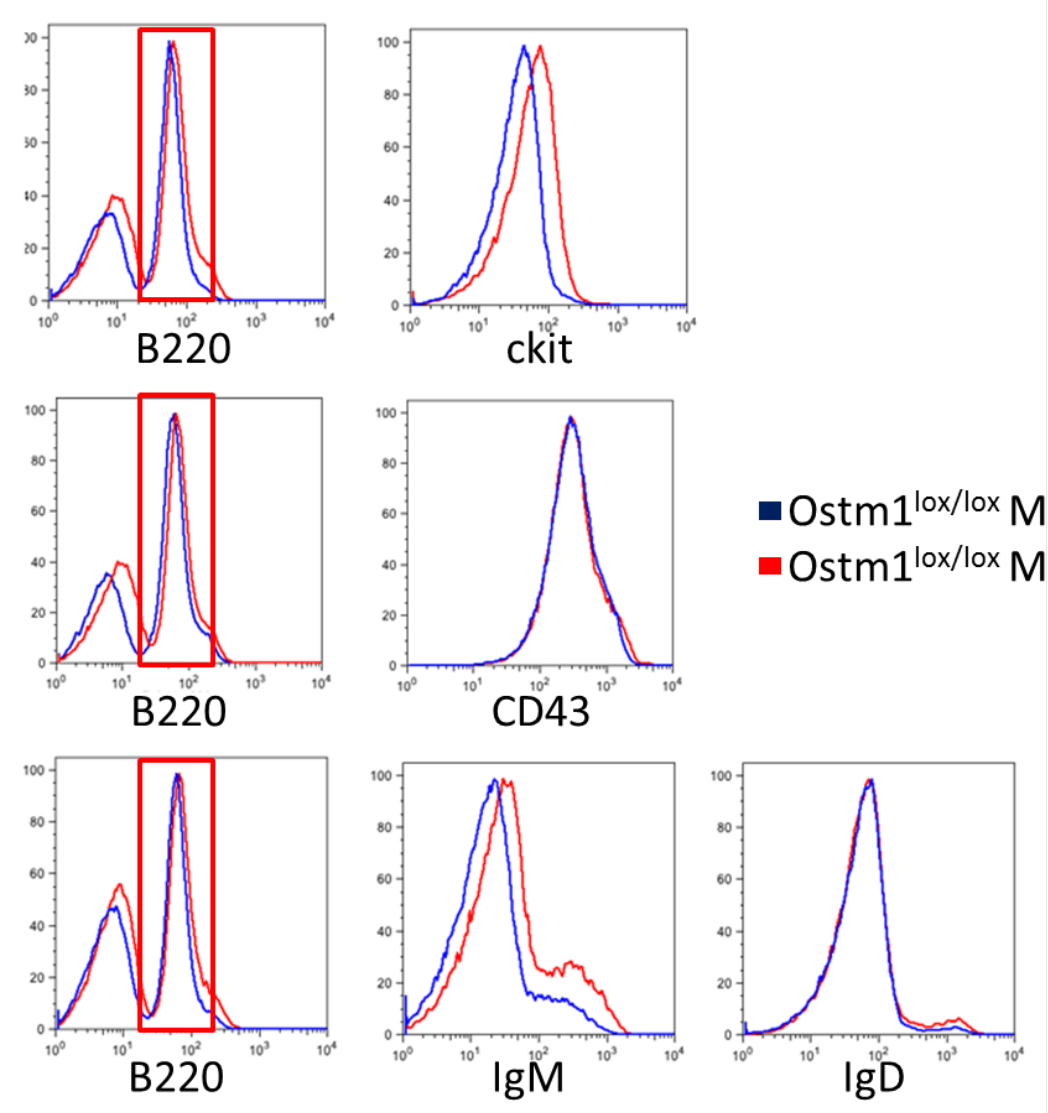

Figure 3.4. Generation and Characterization of the B cell specific *Ostm1* conditional knock out mice (Continued).

(D) Flow cytometry histograms showing the distribution of B220 positive cells and targeting B subpopulations including pre-pro B ($B220^{+}c\text{-}Kit^{+}$), pre-B ($B220^{+}$ $CD43^{+}$), immature B ($B220^{+}$ IgM^{+}) and mature B cells ($B220^{+}$ IgD^{+}) within *Ostm1*$^{lox/lox}$Mb1-Cre^{+} in comparison to *Ostm1*$^{lox/lox}$Mb1-Cre^{-} bone marrow.

E

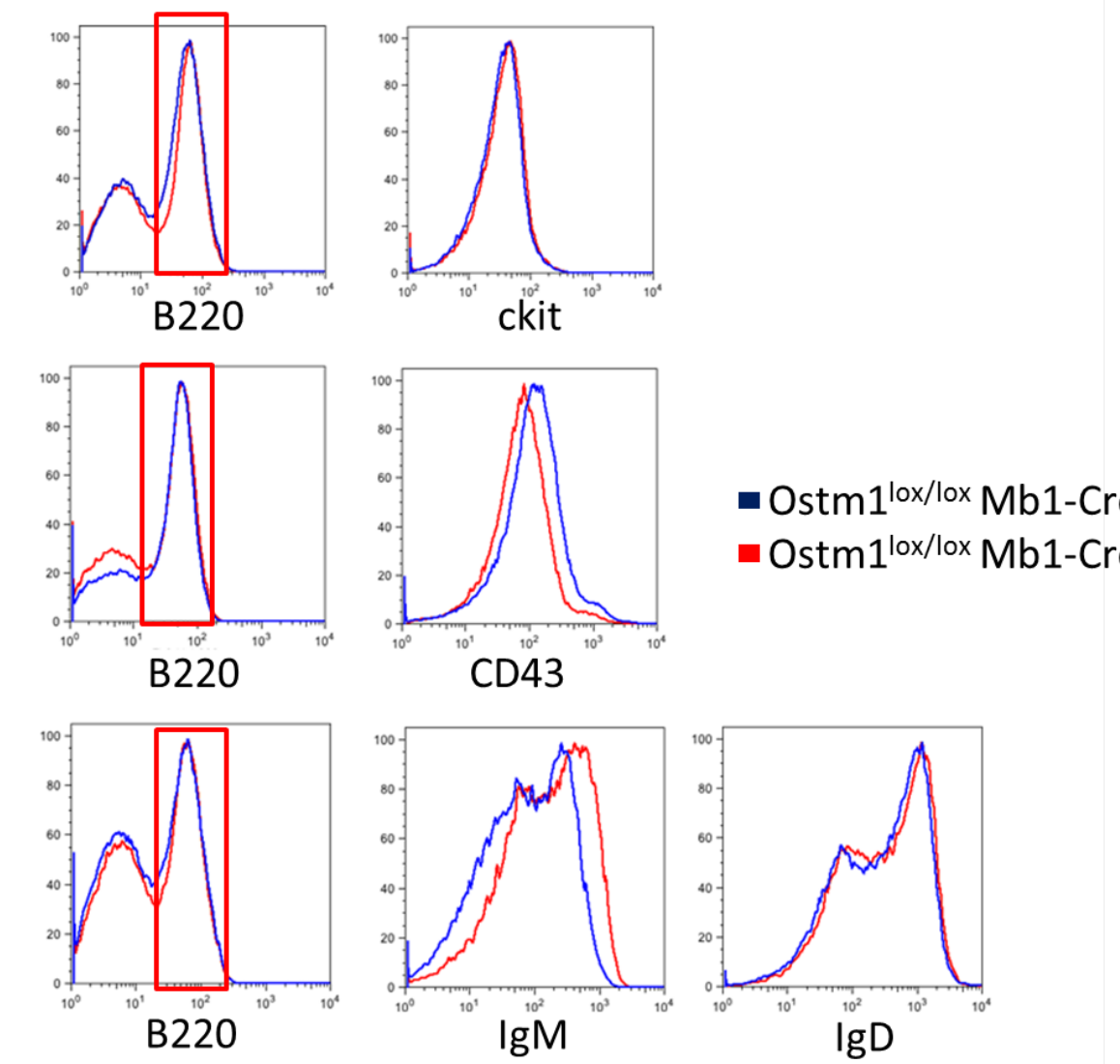

Figure 3.4. Generation and Characterization of the B cell specific conditional *Ostm1* knock out mice (Continued).

(E) Flow cytometry histograms showing the distribution of B220 positive cells and targeting B subpopulations including pre-pro B ($B220^{+}c\text{-}Kit^{+}$), pre-B ($B220^{+}$ $CD43^{+}$), immature B ($B220^{+}$ IgM^{+}) and mature B cells ($B220^{+}$ IgD^{+}) within *Ostm1*$^{lox/lox}$Mb1-Cre^{+} in comparison to *Ostm1*$^{lox/lox}$Mb1-Cre^{-} spleen.

3.2.5. DISCUSSION & CONCLUSION

Cooperation between IL-7 receptors expressed on developing B cells and the BM microenvironment determines proliferation and survival of early B cells. In addition, cell-autonomous mechanisms including gene rearrangements participate in these early homeostatic events by generating a functional pre-BCR. Importantly, a balance between cell-autonomous functions and BM-derived molecules dictates commitment of early B cells and the subsequent differentiation progress (Carsetti 2000). The pronounced B cell depletion resulting from several osteopetrotic genes have mostly been related to the obliterated BM environment (Mansour, Anginot et al. 2011, Perlot and Penninger 2012). Nevertheless, our investigation is the first to connect the *Ostm1* gene mutation and the B cell deficit of osteopetrotic *gl/gl* mice, as well as to support the contribution of BM content.

Our findings revealed that the early B cell phenotype characterizing *gl/gl* mice was detectable at 8 days of age in the spleen. We also have illustrated the differentiation blockage at early B differentiation stage and the subsequent total B cell and peripheral mature B cell deficit in *gl/gl* osteopetrotic mice. Surprisingly, the depletion of B cell population was not corrected following *Ostm1* gene rescue in the B cell lineage under the CD19 promoter, suggesting an indirect *Ostm1* function to sustain B cell development. In addition, the total B cell and peripheral B cell deficit of *gl/gl* mice were undetectable after conditional *Ostm1* ablation in B cells within *Ostm1*$^{lox/lox}$Mb1-cre^{+} spleen and BM, suggesting that *Ostm1* deletion could not impact the B cell development when the BM cavity was intact. Collectively, our results indicated that B cell depletion mainly result from the obliterated *gl/gl* BM space.

The B cell deficit was detected as early as P8 and the 50% decrease is sustained from P8 to P21 in *gl/gl* mice. Besides, B cell development usually shifts from fetal to the BM cavity approximately at E17.5 (Medvinsky, Samoylina et al. 1993, Mansour, Abou-Ezzi et al. 2012, Blin-Wakkach, Rouleau et al. 2014). Therefore, the early defective B population of *gl/gl* could occur after the B cell progenitors mobilize to the compromised *gl/gl* BM. This assumption makes it difficult to ascertain the direct function of *Ostm1* gene in B cell development, since *Ostm1* expression is also required in osteoclast activity which could affect B cell biology.

Bone homeostasis determines formation of the BM cavity during endochondral ossification prior to establishment of the BM content and the recruitment of HSCs, which are the earliest lymphoid cell ancestors. This process is also osteoclast dependent (Olsen, Reginato et al. 2000, Kronenberg 2003, Blin-Wakkach, Rouleau et al. 2014). Moreover, the importance of osteoclast activity in the B cell development was previously shown via the maintenance of the B cell niche, and this could be the missing clue in the B cell deficit of osteopetrotic *gl/gl* mice (Mansour, Anginot et al. 2011, Mansour, Abou-Ezzi et al. 2012, Blin-Wakkach, Rouleau et al. 2014).

Additionally, the exacerbated B cell deficit of CD19-*Ostm1 gl/gl* progenies was consistent with an indirect *Ostm1* function since *Ostm1* expression was B lineage exclusive in these transgenic animal. Nevertheless, the lower expression of the CD19-*Ostm1* transgene compared to the endogenous *Ostm1* in sorted B cell populations of CD19-*Ostm1* BAC 921 progenies could enhance the B cell phenotype in *gl/gl* transgenic mice. CD19 promoter which re-established *Ostm1* from the pro-B cell to mature B stage was not able to rescue the B cell deficit, suggesting that *Ostm1* could be required either in earlier B cell subsets such as pre-pro B. T or the off-target effect of the CD19-*Ostm1* transgene. Together, these observations support the importance of spatial-temporal expression of *Ostm1* gene to assist B cell homeostasis.

To examine the temporal effect in B cell physiology, *Ostm1* gene expression was eliminated from the pre-pro B stage using Mb1-Cre-mediated deletion (Hobeika, Thiemann et al. 2006) , and this resulted in undetectable B cell deficit or defective B cell differentiation in *Ostm1*$^{lox/lox}$Mb1-Cre^{+} animals. This surprising observation could be explained by the normal BM compartment in *Ostm1*$^{lox/lox}$Mb1-Cre^{+} animals despite an efficient depletion of *Ostm1* in early B cells contained in hematopoietic tissues. Collectively, our results consolidated the contribution of the BM in the *gl/gl* B cell phenotype and the non-cell-autonomous role of *Ostm1* in B cell homeostasis.

3.2.7. ACKNOWLEDGEMENTS

We thank members of Dr. Tarik Moroy laboratory for helpful discussions and technical assistance especially Dr. Julie Ross and Marissa Rashkovan for technical help and critical reading of the manuscript. We also thank Dr. Tarik Moroy for supplying Mb1-Cre animals, as well as Eric Massicotte and Julie Lord (Flow cytometry core facility at IRCM) for the tremendous technical assistance. This work was supported by Canadian Institutes of Health Research grant to Dr. Jean Vacher.

3.2.8. REFERENCES

Blin-Wakkach, C., M. Rouleau and A. Wakkach (2014). "Roles of osteoclasts in the control of medullary hematopoietic niches." Arch Biochem Biophys **561**: 29-37.

Carsetti, R. (2000). "The development of B cells in the bone marrow is controlled by the balance between cell-autonomous mechanisms and signals from the microenvironment." J Exp Med **191**(1): 5-8.

Chalhoub, N., N. Benachenhou, V. Rajapurohitam, M. Pata, M. Ferron, A. Frattini, A. Villa and J. Vacher (2003). "Grey-lethal mutation induces severe malignant autosomal recessive osteopetrosis in mouse and human." Nat Med **9**(4): 399-406.

Dougall, W. C., M. Glaccum, K. Charrier, K. Rohrbach, K. Brasel, T. De Smedt, E. Daro, J. Smith, M. E. Tometsko, C. R. Maliszewski, A. Armstrong, V. Shen, S. Bain, D. Cosman, D. Anderson, P. J. Morrissey, J. J. Peschon and J. Schuh (1999). "RANK is essential for osteoclast and lymph node development." Genes Dev **13**(18): 2412-2424.

Guerrini, M. M., C. Sobacchi, B. Cassani, M. Abinun, S. S. Kilic, A. Pangrazio, D. Moratto, E. Mazzolari, J. Clayton-Smith, P. Orchard, F. P. Coxon, M. H. Helfrich, J. C. Crockett, D. Mellis, A. Vellodi, I. Tezcan, L. D. Notarangelo, M. J. Rogers, P. Vezzoni, A. Villa and A. Frattini (2008). "Human Osteoclast-Poor Osteopetrosis with Hypogammaglobulinemia due to TNFRSF11A (RANK) Mutations." The American Journal of Human Genetics **83**(1): 64-76.

Hardy, R. R. and K. Hayakawa (2001). "B cell development pathways." Annu Rev Immunol **19**: 595-621.

Hardy, R. R., P. W. Kincade and K. Dorshkind (2007). "The Protean Nature of Cells in the B Lymphocyte Lineage." Immunity **26**(6): 703-714.

Hobeika, E., S. Thiemann, B. Storch, H. Jumaa, P. J. Nielsen, R. Pelanda and M. Reth (2006). "Testing gene function early in the B cell lineage in mb1-cre mice." Proceedings of the National Academy of Sciences **103**(37): 13789-13794.

Kong, Y. Y., H. Yoshida, I. Sarosi, H. L. Tan, E. Timms, C. Capparelli, S. Morony, A. J. Oliveira-dos-Santos, G. Van, A. Itie, W. Khoo, A. Wakeham, C. R. Dunstan, D. L. Lacey, T. W. Mak, W. J. Boyle and J. M. Penninger (1999). "OPGL is a key regulator of osteoclastogenesis, lymphocyte development and lymph-node organogenesis." Nature **397**(6717): 315-323.

Kronenberg, H. M. (2003). "Developmental regulation of the growth plate." Nature **423**(6937): 332-336.

Mansour, A., G. Abou-Ezzi, E. Sitnicka, S. E. Jacobsen, A. Wakkach and C. Blin-Wakkach (2012). "Osteoclasts promote the formation of hematopoietic stem cell niches in the bone marrow." J Exp Med **209**(3): 537-549.

Mansour, A., A. Anginot, S. J. Mancini, C. Schiff, G. F. Carle, A. Wakkach and C. Blin-Wakkach (2011). "Osteoclast activity modulates B-cell development in the bone marrow." Cell Res **21**(7): 1102-1115.

Medvinsky, A. L., N. L. Samoylina, A. M. Muller and E. A. Dzierzak (1993). "An early pre-liver intraembryonic source of CFU-S in the developing mouse." Nature **364**(6432): 64-67.

Olsen, B. R., A. M. Reginato and W. Wang (2000). "BONE DEVELOPMENT." Annual Review of Cell and Developmental Biology **16**(1): 191-220.

Pata, M., C. Heraud and J. Vacher (2008). "OSTM1 bone defect reveals an intercellular hematopoietic crosstalk." J Biol Chem **283**(45): 30522-30530.

Perlot, T. and J. M. Penninger (2012). "Development and Function of Murine B Cells Lacking RANK." The Journal of Immunology **188**(3): 1201-1205.

Rajapurohitam, V., N. Chalhoub, N. Benachenhou, L. Neff, R. Baron and J. Vacher (2001). "The mouse osteopetrotic grey-lethal mutation induces a defect in osteoclast maturation/function." Bone **28**(5): 513-523.

Rickert, R. C., J. Roes and K. Rajewsky (1997). "B Lymphocyte-Specific, Cre-mediated Mutagenesis in Mice." Nucleic Acids Research **25**(6): 1317-1318.

CHAPTER 4: DISCUSSION & CONCLUSION

4.1. ROLE OF THE *Ostm1* GENE IN LYMPHOID T & B CELLS

Our *in vivo* analyses of the *gl/gl* and CD2-*Ostm1 gl/gl* thymi support a function for the *Ostm1* gene in the T cell differentiation process. Absence of *Ostm1* results in a severe thymus phenotype and perturbs the T cell development sequence. Intriguingly, overexpression of the *Ostm1* gene in the T cell lineage of the *gl/gl* mice rescues most thymus defects but does not improve other osteopetrotic features.

We have shown that the *Ostm1* gene expression profile in the T lineage is pronounced in early DN1 and immature DP populations. Interestingly, *Ostm1* mutation negatively impacts the early stages of T cell differentiation by reducing the distribution of the ETP population, blocking the differentiation at the DN1-DN2 transition and drastically decreasing the DP population. This thymic phenotype of *gl/gl* progeny is also reflected by abnormal thymic structure and size. We have also established that the *gl/gl* thymus phenotype is a time-dependent event beginning at P15 and culminating at P21. Finally, our *in vitro* co-culture of *gl/gl* ETPs with the OP9-DL4 stroma line demonstrates maintained differentiation of the early *gl/gl* T population in the presence of the Notch ligand DL4. This latest observation raises the potential implication of thymus micro-environment in the *gl/gl* T cell phenotype.

Specific overexpression of *Ostm1* driven by the CD2 promoter in early to mature T populations of *gl/gl* animals rescues ETPs distribution, corrects the differentiation pattern of DN1-DN4 transition, and restores the DP pool. However, thymus cellularity is only partially restored and the number of bone marrow (BM)-derived thymus seeding progenitors, such as CLPs, remains low. Additionally, these transgenic mice conserve an obliterated BM cavity, abnormal osteoclasts and die prematurely at around 3 weeks.

Sequencing analysis of the transcriptome in early T cells reveals important variations in *gl/gl*DN1 cells compared to control DN1. Moreover, the most significant differentially expressed genes in *gl/gl* DN1 cells, such as *Rac1*, are associated with cell migration which suggests a role of *Ostm1* in early T cell trafficking. Interestingly, all these transcriptional differences are normalized in *gl/gl* transgenic (*gl/gl*TR) DN1 cells. Overall, this study supports the cell-intrinsic function of the *Ostm1* gene in T cell differentiation.

We also analyzed the B cell defect in *gl/gl* spleen. This data shows an important deficit of total B cells resulting from the *Ostm1* mutation and this defect is detected from P8 until the time of death at P21. Additionally, this osteopetrosis-associated B cell defect translates into significant reduction of peripheral immature and mature B cell populations in the *gl/gl* spleen at P21.

Rescue of *Ostm1* gene expression in the B cell lineage of *gl/gl* mice under the control of the CD19 promoter fails to correct the distribution of total B cells, immature and mature B cell populations; in fact, these defects are exacerbated in CD19-*Ostm1 gl/gl* transgenic spleen. This result can either be explained by the poor efficiency or deleterious effects of the CD19-*Ostm1* transgene or the potential non-cell-autonomous function of *Ostm1* in B cell physiology.

To circumvent the potential weaknesses of the CD19-*Ostm1 gl/g*l transgenic mouse model, we investigated the conditional ablation of *Ostm1* gene in early B cells using the Mb1-Cre system. The resulting conditional knockout animals *Ostm1*^{loxlox} Mb1-Cre^{+} exhibit no apparent B cell phenotype despite a significant reduction of *Ostm1* in hematopoietic tissues containing B cells. Moreover, these conditional mice do not display any other osteopetrotic defects. Collectively, these findings suggest an indirect contribution of the *Ostm1* gene in B cell differentiation, possibly through its impact on the BM-dependent early B cell differentiation (Nagasawa 2006, Mansour, Anginot et al. 2011).

Our proposed model (**Figure 4.1**) suggests that the *Ostm1* mutation induces overexpression of *S1pr1* in the ETPs/DN1 populations, and increases expression of the downstream *Rac1*. This can affect T cell differentiation by increasing cell migration, inhibiting CD25 expression and promoting the rapid ETP differentiation (de Barros, Vicente et al. 2013, Steffen, Ladwein et al. 2013). For example, enhanced migration can compromise ETP expansion at the CMJ (Lind, Prockop et al. 2001, Vasseur, Le Campion et al. 2001). Both compromised expansion and fast-paced differentiation of ETPs can lead to the progressive T cell differentiation blockage at the DN1-DN2 transition and the concomitant drastic deficit of DP populations in the *gl/gl* thymi. Besides, this time-dependent phenotype is pronounced after birth with the inefficient bone marrow input of thymic seeding progenitors including CLP and ETP populations.

Additionally, obliterated bone marrow space and poor CLP population in the absence of the *Ostm1* gene can compromise the B cell differentiation and extramedullary B lymphopoiesis in the spleen. This latest possibility may require the contribution of non-functional osteoclasts (Mansour, Anginot et al. 2011, Miyamoto 2013)

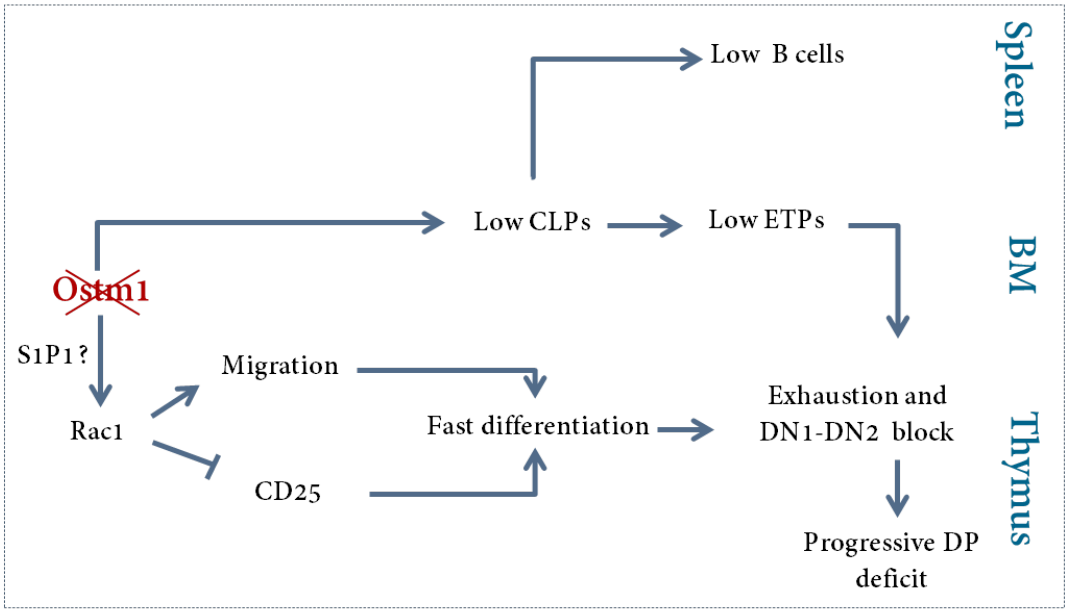

Figure 4.1. Proposed model summarizing potential functions of the *Ostm1* mutation in T cell and B cell differentiation

4.2. IS THE TIME-DEPENDENT T CELL DEFICIT OF *gl/gl* A RESULT OF THE OSTEOPETROTIC BM?

Our study shows lower CLPs numbers in the *gl/gl* BM (**Fig.2.4J**). As mentioned previously, the CLP population derives from a HSC ancestor and is part of the LSK pool (Miyazaki, Miyazaki et al. 2014). However, there was no significant change in the distribution of LSKs in *gl/gl* BM (**Fig.2.4J)**, suggesting that the cell deficit is specific to the lymphoid primed population of CLPs in *gl/gl* BM.

The correlation between HSC number and niche size is regulated by osteoblast number (Zhang, Niu et al. 2003). Osteoblasts have also been shown to induce initial HSC niche formation without affecting the LSK compartment. Consequently, the unchanged number of osteoblasts in *gl/gl* mice (**data not shown**) could reflect the maintained HSC niches in *gl/gl* BM and this is consistent with the normal number of LSKs (Mansour, Abou-Ezzi et al. 2012). In addition, the closed BM cavities resulting from inactive bone-resorbing osteoclasts have been associated with normal HSC mobilization to the periphery in the osteoclast-less osteopetrotic mice, and chemical-mediated osteoclast ablation enhanced HSC mobilization (Miyamoto, Yoshida et al. 2011, Miyamoto 2013). In this scenario, the reduced CLPs number could be due to an altered HSC mobilization and their subsequent less efficient differentiation into CLPs caused by the *gl/gl* osteoclast-rich osteopetrosis (Rajapurohitam, Chalhoub et al. 2001) as well as the reduced space for a CLP niche.

Additionally, the low number of *gl/gl* CLPs could illustrate a compensatory mechanism by developing faster into ETP populations before migrating to the *gl/gl* thymus in order to take over the defective T cell development. In this context, the fast differentiation of *gl/gl* ETP population (**Fig.2.3E)** could be inherited from *gl/gl* CLPs (Zlotoff and Bhandoola 2011, Miyazaki, Miyazaki et al. 2014). Moreover, the thymus periodicity for progenitor colonization has been directly connected to full and empty status of the thymic niches (Foss, Donskoy et al. 2001). Therefore, an accelerated differentiation of *gl/gl* ETPs could result in enhancing emptiness of the thymic niches, thus allowing for the thymic gate-opening and concomitant input from the thymus seeding progenitors, including CLPs and ETPs, in order to replenish thymic niche and sustain long-term T cell differentiation.

This idea is reinforced by our observations in the CD2-*Ostm1 gl/gl* transgenic model, where marrow space and CLPs number reflect similar findings in *gl/gl* mice (**Fig.2.4**) despite their rescued ETP number and T cell differentiation. This observation reveals low CLPs number as a consequence of reduced *gl/gl* marrow space. Additionally, this data could suggest a time-limitation of the CLP compensatory effect for the cell intrinsic defect of *gl/gl* ETPs, possibly due to their limited number. Therefore, these findings could explain the visible T cell depletion in *gl/gl* mice (**Fig.2.2**),at the time point where lymphopoiesis is entirely dependent on BM input at approximately two weeks after birth (Jotereau, Heuze et al. 1987).

A recent study has shown the limited expansion capacity of the first fetal ETP progenitors entering the thymus at E12 as well as their accelerated differentiation to generate fewer DP cells. In contrast, the second wave of ETPs at E16 displayed a high proliferation rate and efficient differentiation to generate a higher number of αβ T cells (Ramond, Berthault et al. 2014). Interestingly, the rapid *in vitro* differentiation of ETPs **(Fig.2.3E)** and the deficit production of DP cells in the *gl/gl* thymi (**Fig.2.2D**) recapitulate hallmarks of first generation fetal progenitors recruited at E12. In this scenario, limited cell cycle progression of the fetal-like *gl/gl* ETPs could induce their time-dependent exhaustion, thus connecting the *Ostm1* gene to the cycling or the recruitment of future generations of ETPs.

Overall, the *gl/gl* time-dependent phenotype becomes more apparent at the shift from fetal to post-natal lymphopoiesis (**Fig.2.2D**). Consequently, the reduced BM space and the shortage of CLP populations to compensate for the fetal-like differentiation of *gl/gl* ETPs into mature T cells are responsible for time-dependent abnormal T cell differentiation within *gl/gl* thymi.

4.3. DOES THE THYMUS ENVIRONMENT CONTRIBUTE TO *gl/gl* T CELL PHENOTYPE?

Time-dependent differentiation arrest of *gl/gl* ETPs at DN1-DN2 transition (**Fig.2.3D**) could either initiate or result from disrupted Notch-dependent crosstalk between developing thymocytes and thymus epithelial cells progenitors, thus leading to an underdeveloped and disorganized three-dimensional architecture of the *gl/gl* thymus structure (**Fig.2.2A**) (Anderson, Jenkinson et al. 2006). Nevertheless, maintained *in vitro gl/gl* ETP differentiation in the presence of BM-derived OP9-DL4 (**Fig.2.3E)** and the similar quantitative expression of Notch1 or Deltex1 (**data not shown**) between *gl/gl* DN1, control DN1 and *gl/gl*TR DN1 suggest either normal Notch responsiveness or Notch-independent differentiation of early *gl/gl* T cells. These observations interrogate the intrathymic communication between developing *gl/gl* T populations and thymus environment *in vivo*.

Previous studies have shown an overlap between differentiation arrest of cortical epithelial progenitors at the immature stage and T cell development block before DN2 stage , as well as, the required interaction between fetal stroma cells and early pro-thymocytes to form the premature thymus cortex (Hollander, Wang et al. 1995, Klug, Carter et al. 1998). From these observations, we can speculate that a hindered lympho-stroma crosstalk *in vivo* could occur following post-natal differentiation arrest at the DN1-DN2 transition in *gl/gl* thymi. However, our findings did not characterize the lympho-stroma crosstalk that could potentially assist the rescue of T cell differentiation within CD2-*Ostm1* transgenic mice.

Multiple features of *gl/gl* thymus including reduced thymus population, disorganized thymus architecture and unclear cortico-medullary junction (CMJ) border (**Fig.2.2A**) resemble thymus involution features, which usually occur in 6 months-old mice (Manley, Richie et al. 2011). The premature thymus involution has been previously reported in *in vitro* studies of osteopetrotic *gl/gl* thymus and has been exhibited by the decelerated involution of all stroma progenitors and subsequent time-dependent increase in mature stroma cell number (Wiktor-Jedrzejczak, Grzybowski et al. 1983).

Moreover, the decreased number of stroma progenitors has been recently connected to rapid differentiation kinetic during the recovery of the declining thymic stroma cell population (Boehm and Swann 2013). Consequently, the boosted *gl/gl* ETP ratio in CD2-*Ostm1* transgenic thymi (**Fig.2.4F**) could reverse the thymic degenerative changes by either providing an appropriate ratio of T cell progenitors per stroma cell to extend lympho-stromal interactions in the thymic niche, or by stimulating the recovery of stroma cell progenitor differentiation, which in turn assists the expansion, maintenance and differentiation of *gl/gl* ETPs (Anderson, Jenkinson et al. 2006). This theory may be supported by the partial improved thymus structure of CD2-*Ostm1 gl/gl* animals (**Appendix 1.5**), which correlated with partial rescue of total thymocytes (**Fig.2.4E**).

Importantly, absence of peripheral inflammation in g*l/gl* animals (**data not shown**) and improved thymus structure of CD2-*Ostm1 gl/gl* transgenic mice despite their premature death strongly suggests that this early thymus involution phenotype is independent of inflammatory signals or the unknown cause of death in *gl/gl* animals.

4.4. HOW COULD *Ostm1* INDUCE RESCUE OF T CELL HOMEOSTASIS?

Restoration of *Ostm1* gene in the T cell lineage within the *gl/gl* thymus environment is able to increase the ratio of ETP populations by 4-fold, to rescue the developmental profile from DN1 to DN4 stages and the subsequent distribution of DP populations (**Fig.2.4**). Moreover, maintenance of osteopetrotic bone marrow, low CLPs and abnormal osteoclasts exhibit the cell-intrinsic function of the *Ostm1* in early T populations

In the thymus, the CMJ region has been established as the main site for proliferative expansion of the blood-borne ETPs/DN1 which is mediated by chemokines and growth factors secreted by the stroma environment (Lind, Prockop et al. 2001). ETPs/DN1 cells enter the CMJ where they undergo rounds of cell division before ceasing to proliferate as they migrate away from the CMJ for further commitment and differentiation steps in the outer cortex (Vasseur, Le Campion et al. 2001, Cai, Landman et al. 2007).

As shown previously, *gl/gl* ETPs has recapitulated the fetal-like phenotype as illustrated by their accelerated differentiation *in vitro* and lower production of the DP population *in vivo* (**Fig.2.2 and Fig.2.3E**). Additionally, time-dependent disruption of *gl/gl* thymus structure with an unclear CMJ demarcation (**Fig.2.2A)** could disrupt proliferative signals for *gl/gl* ETPs. Together, these observations indicate the potential impact on the proliferative state of ETPs/DN1 populations in the absence of *Ostm1* gene, which is consistent with an increase of Ki-67 positive cells in CD2-*Ostm1 gl/gl* transgenic thymus sections (**Appendix 1.4**).

T cell-specific *Ostm1* expression in CD2-*Ostm1* transgenic mice could recover the *gl/gl* T cell intrinsic defect by maintaining the productivity of existing ETPs beyond P15 in CD2-*Ostm1 gl/gl* transgenic thymi. Although, this hypothesis has been difficult to evaluate in a time-dependent fashion due to the premature death of CD2-*Ostm1gl/gl* transgenic mice at around 3 weeks, these animals have showed an exacerbated expansion of ETP population (**Fig.2.4F)** and an improved thymus structure (**Appendix 1.5).** c-Kit and IL7R expression have been implicated in supporting pro-thymocyte expansion and survival (Rodewald, Ogawa et al. 1997). Interestingly, reduction of c-Kit expression has been observed in *gl/gl* DN1 compared to control, while it has been rescued to normal levels in DN1 from CD2-*Ostm1 gl/gl* mice (**Fig.2.6A).** Overall, these observations align with an impact of *Ostm1* in early T cell expansion and/or acquired self-renewal ability in the absence of BM input.

Ostm1 gene could participate in the compensatory mechanism of the discontinued colonization of BM-derived T cell progenitors after birth. To this end, *Ostm1* expression could support a longer survival of existing *gl/gl* ETPs to alleviate the shortage of thymic progenitors resulting from the lower number of CLP and ETP populations. This scenario would be relevant because of: 1) Diminished competition for growth factors and cytokines between few incoming (**Fig.2.4J)** and resident ETPs (**Fig.2.3C)** in the *gl/gl* thymic niches. 2) Rescued c-Kit expression in *gl/gl*TRDN1 (**Fig.2.6A)** that could contribute to increasing their thymic expansion and survival following restoration of *Ostm1* expression. 3) As previously shown, absence of competition between young BM-derived progenitors and old thymus DN T cell residents could promote self-renewal ability and *in situ* ageing of old DN2/DN3 T cells (Martins, Busch et al. 2014). 4) Normalized expression of genes involved in T cell migration such as *Rac1* and *S1pr1* (**Fig.2.6A and B),** could slow down old ETPs at the CMJ, thus prolonging their interaction with proliferative signals in *gl/gl* CD2-*Ostm1* thymi.

Altogether, these hypotheses implicate *Ostm1* gene in prolonged ETP expansion to sustain long-term thymus-autonomous T cell development which have been adequately revealed in the case of progenitor deprivation (Rodewald, Ogawa et al. 1997, Lind, Prockop et al. 2001, Martins, Ruggiero et al. 2012, Peaudecerf, Lemos et al. 2012).

In conclusion, *Ostm1* mediates transcriptional variations of Rho family GTPase including *Rac1* (**Fig.2.6A and B)** which is involved in cytoskeletal organization, microtubules dynamics, and cell polarity of T cells (Phee, Au-Yeung et al. 2014). Consequently, overexpression of *Rac1* in the absence of *Ostm1* could result in dramatic changes in the cytoskeletal structure, interfering with engagement of ETP receptors with chemokines, growth factors and proliferative signals derived from the cortical epithelial environment (Manley, Richie et al. 2011), promoting early exhaustion of T cell differentiation.

Overall, re-establishment of *Ostm1* expression in the T cell lineage of *gl/gl* thymus have increased ETPs expansion by 4-fold with normalized *Rac1* and *S1pr1* expressions, and subsequent rescue of T cell differentiation pattern from DN1 to SP $CD4^{+}$ or $CD8^{+\cdot}$.

4.5. IS B CELL DEFICIT SECONDARY TO THE COMPROMISED BM AND INACTIVE OSTEOCLASTS?

Our study using transgenic mice expressing *Ostm1* exclusively in the B cell lineage under the control of the CD19 promoter has failed to rescue the low B cell number in the spleen of CD19-*Ostm1 gl/gl* animals. Furthermore, conditional deletion of the *Ostm1* gene from the earliest B cell population to mature B cells has been performed under the control of the Mb1-Cre expression system and it did not promote the B cell defect of *gl/gl* animals. The results suggest an indirect function for the *Ostm1* gene in B cell populations (**Chapter 3)**.

BM signaling molecules play an important role in early B cell development to generate peripheral B cell populations found in the spleen (Nagasawa 2006). Therefore, the compromised BM of *gl/gl* could interfere with this early B cell development in many ways resulting in reduced numbers of total B cells in the *gl/gl* spleen. This theory is also consistent with the early detection of total B cell deficit in *gl/gl* spleen from 8 day old mice.

Extramedullary hematopoiesis has been reported in the spleen and liver of osteopetrotic mice to compensate for their reduced BM cavity. The same study has showed an extramedullary myelopoiesis in the spleen and liver whereas B lymphopoiesis has only been detected in the liver of these osteopetrotic animals. In these animals, altered generation of B populations was not related to the lack of growth factors provided by the stoma environment in the BM. Consequently, this previous work suggested that reduced osteopetrotic BM could abrogate the space for HSC niches leading to B cell development arrest (Tagaya, Kunisada et al. 2000). As in other osteopetrotic animals, the *gl/gl* BM volume could then interfere with extramedullary B cell lymphoid by compromising the location of early B cell progenitors in extravascular spaces of the marrow near the bone cortex. Consequently, B lymphopoiesis would also be interrupted as it begins from the peripheral subendosteal area (Tagaya, Kunisada et al. 2000).

Furthermore, extramedullary B lymphopoiesis of *gl/gl* could either be altered by an abnormal retention of early B cell populations in their bone marrow niches. This hypothesis aligns with a report showing the importance of osteoclast activity in mediating the retention of B cell progenitor by affecting the production of BM-derived factors (Mansour, Anginot et al. 2011). Therefore, reduced immature and mature B populations in *gl/gl* spleen could either illustrate an altered retention or the compromised mobilization of early B cell progenitors from BM niches. This also indicates the need to characterize other potential sites for extramedullary B cell development, such as the liver, in *gl/gl* animals.

Surprisingly, the rescued B cell population in the CD2-*Ostm1 gl/gl* transgenic mice has revealed the possibility to recover extramedullary B lymphopoiesis in *gl/gl* spleen while the BM was still compromised. This scenario is possible with the overexpression of the *Ostm1* gene in B cell populations under the control of the CD2 promoter. However, this phenotype would require further investigation by measuring expression of the CD2-*Ostm1* transgene in the CLP population and early B progenitors, as well as the quantification of pre-pro B mobilization from BM to the spleen. These experiments could help to dissociate the CD2-*Ostm1* transgene effect on the BM niche containing CLP/pre-pro B cells from its intrinsic modulation of early B progenitors trafficking to peripheral lymphoid tissues.

Overall, compromised BM volume and inactive osteoclasts of the grey-lethal mice could compromise homeostasis of the B cell progenitor niche resulting in the disruption of extramedullary B cell development in *gl/gl* spleen.

4.6. THE OSTEOIMUNOLOGY LESSON OF THE CTSK -*Ostm1 gl/gl* TRANSGENIC MICE

Our research also investigates the relationship between inactive bone resorption and defective B and T cell homeostasis in *gl/gl* animals. For this purpose, *Ostm1* gene expression is re-established in mature osteoclasts of *gl/gl* mice under the control of the cathepsin K (Ctsk) promoter. The Ctsk-*Ostm1 gl/gl* transgenic mice demonstrate normalized lifespan, osteoclast activity, and bone parameters (Pata. M et al, unpublished data). These mice also show rescued cellularity in the thymus and spleen (**Table 1.7**), as well as normal distribution of B cell and the T cell lineage including ETPs, DN1 to DN4, DP, and SP $CD4^+$ or $CD8^+$ (**Appendix 2.1 and 2.4).** Altogether, these data reveal the contribution of active bone resorption in promoting T and B cell homeostasis.

Our findings are further supported by the undetectable expression of endogenous *Ctsk* and transgene Ctsk-*Ostm1* in sorted $CD3^+$T and $B220^+$B cells (**Appendix 2.2)** Undetectable expression of the endogenous *Ctsk* and Ctsk-*Ostm1* transgene is confirmed in flow cytometry sorted ETP populations of Ctsk-*Ostm1* +/+ transgenic animals, and normal expression of endogenous *Ostm1* gene is demonstrated in the same cell population (**Appendix 2.3).**

Furthermore, conditional ablation of *Ostm1* expression in mature osteoclasts mediated by the Ctsk-Cre has resulted in osteopetrotic phenotype highlighted by premature death, loss of tooth eruption and, inactive osteoclasts in conditional $Ostm1^{lox/lox}$ Ctsk-Cre^+ progenies (Pata M et al, unpublished data). T cells and B cell deficiencies as well as accumulation of macrophage-granulocytes populations are recapitulated in these conditional $Ostm1^{lox/lox}$ Ctsk-Cre^+ animals.

Collectively, these results exhibit the importance of crosstalk between osteoclast activity and homeostasis of B and T cell differentiation. These observations are compatible with BM-dependent thymus colonization of CLPs and ETPs. Consequently, the rescued osteoclast activity in the presence of *Ostm1* has re-established a normal marrow space that could contain normal numbers of CLPs and ETPs and promote subsequent efficient progenitor input within Ctsk-*Ostm1gl/gl* thymus after birth. Therefore, the subsequent competition between young progenitors and old thymus resident DN cells could compensate for the reduced number and fast-paced differentiation of *gl/gl* ETP, by maintaining thymic cell turnover and avoiding *in situ* ageing of DN2/3 cells (Martins, Busch et al. 2014). Surprisingly, *Rac1* expression is diminished in sorted ETPs from Ctsk-*Ostm1*+/+ transgenic mice (**Appendix 2.3),** suggesting that ETP trafficking could also be modulated by osteoclast activity. Moreover, the inverse correlation between osteoclast activity and HSC mobilization into the periphery has been demonstrated previously (Miyamoto, Yoshida et al. 2011). Hence, the rescued osteoclast activity could stabilize HSC mobilization supporting the generation of CLP and ETP populations.

Overall, Ctsk-*Ostm1 gl/gl* transgenic animals support crosstalk between osteoclast activity and early lymphoid cell input to sustain T and B cell differentiation programs within *gl/gl* lymphoid tissues.

4.7. THE GREY-LETHAL MOUSE AS AN ANIMAL MODEL TO SUPPORT OSTEOIMMUNOLOGY STUDIES

The *gl/gl* osteopetrotic mouse model is characterized by inactive bone resorbing osteoclasts causing a higher bone density and an abnormal BM cavity (Rajapurohitam, Chalhoub et al. 2001). These mice also exhibit an altered T cell differentiation and a significant B cell deficit (Pata, Heraud et al. 2008).

The data from our studies allowed for clarification of the T cell intrinsic function of *Ostm1* from its indirect role in B cell physiology. Maintenance of an abnormal osteoclast physiology and a compromised BM in CD2-*Ostm1 gl/gl* transgenic mice (**Fig.2.4H and I)** suggests an insignificant role of normal T and B cell development (**Appendix 1.6 and 1.7)** in the molecular interplay stimulating osteoclast activity and BM homeostasis.

In contrast, the potential molecular interplay from active osteoclasts in promoting T and B cell lineage development and number is strongly supported by Ctsk-*Ostm1 gl/gl* transgenic animals (**Appendix 2)**. These latest findings illustrate the promising potential of using *gl/gl* mice to dissect biological pathways involved in the crosstalk between lymphoid cell homeostasis and osteoclast activity or bone remodeling.

Most studies in osteoimmunology use animal models of rheumatoid arthritis which exhibit enhanced osteoclast activity induced by inflammatory cytokines (Takayanagi 2007, Choi, Arron et al. 2009, Castaneda, Simon et al. 2011). In contrast, the *gl/gl* osteopetrotic mice offer an in vivo model with enhanced osteoclast differentiation producing inactive bone-resorbing osteoclasts. Hence, these mice could represent another mouse model to identify cytokines other than RANKL that can be produced by T and B cell lineages to stimulate osteoclast activity or bone-remodeling. For example, *gl/gl* mice could facilitate the study of other osteoimmunological markers in the absence of severe inflammatory conditions. Additionally, these animals could be useful for characterizing the potential positive feedback between bone resorption efficiency and immune cell activation or responses.

4.8. PERSPECTIVES AND KEY POINTS

Maintained differentiation of the *gl/gl* ETP population *in vitro* co-culture differentiation assay suggest either conserved responsiveness to Notch or *gl/gl* ETP differentiation independent of Notch signaling. Therefore, this result interrogates the potential effect mediated by the *gl/gl* thymus environment in either initiating or potentiating abnormal T cell development of *gl/gl* mice.

Time-dependent disruption of T cell development at DN1-DN2 transition and DP cell loss coincides with the time point for independence of the neo-natal immune system, which mainly relies on BM content. Consequently, the obliterated BM of *gl/gl* could also be involved in this time-dependent T cell phenotype. Thus, it is crucial to distinguish intrinsic versus extrinsic influence of the *Ostm1* gene in the time-dependent aspect of abnormal T cell development in *gl/gl* mice.

Furthermore, the differential expression pattern of migration-associated genes in *gl/gl* DN1cells should be studied at the cellular level by using appropriate functional assays. It would also be of interest to investigate the molecular connection between the *Ostm1*gene and the early T cell migration changes once they are confirmed *in vivo*. The additional data gathered from these experiments could offer more insight into the general function of the *Ostm1* gene.

The exacerbated B cell phenotype of the CD19-*Ostm1 gl/gl* mice suggests the importance of gene expression level and the specificity of B cell differentiation stage regulated by the *Ostm1* mutation. However, further investigation is needed to confirm the efficiency of the CD19-*Ostm1* transgene either by demonstrating CD19-*Ostm1* BAC integrity in all transgenic lines or analyzing other transgenic lines with a higher expression of the CD19-*Ostm1* transgene. Additionally, Mb1-Cre expression and *Ostm1* deletion efficiency should be confirmed *in cellulo* of sorted B subpopulations based on the B cell differentiation sequence.

In conclusion, the comparative study of the aforementioned results in the osteopetrotic *gl/gl* mice and other animal models could reveal data that support identification of molecular pathways that are responsible for crosstalk between bone and immune cells.

4.9. CONCLUSIONS

My thesis work presents analysis of *Ostm1* gene function in the lymphoid B and T cell homeostasis. First, we characterized the time-dependent defect in T cell development resulting in thymus atrophy in *gl/gl* animals. These studies also suggest a contribution of the *Ostm1* gene in T cell development during modulation of ETPs expansion and reduction of *Rac1* expression in ETPs/DN1 populations. These results also illustrate the subsequent role of *Ostm1* in T cell differentiation from early DN1 to mature SP $CD4^+$ or $CD8^+$.Moreover, these data reveal the importance of *Ostm1* expression to prolong long-term thymus-autonomous T cell differentiation in response to the progenitor deprivation resulting from an osteopetrotic *gl/gl* BM. Secondly; we have initiated the characterization of defective B cell differentiation in *gl/gl* mice. Our findings indicate the non-cell-autonomous effect of *Ostm1* expression in the abnormal B cell physiology. Further analyses indicate that restoration of BM volume could efficiently compensate for the *gl/gl* ETP intrinsic defect. These data also suggest an induction of the B cell lineage phenotype in *gl/gl* mice mediated by negative crosstalk between inactive osteoclasts and the B cell niche. Overall, these studies have illustrated the promising potential of the osteopetrotic *gl/gl* mouse model to support research in osteoimmunology.

APPENDIX 2: SUPPLEMENTAL RESULTS

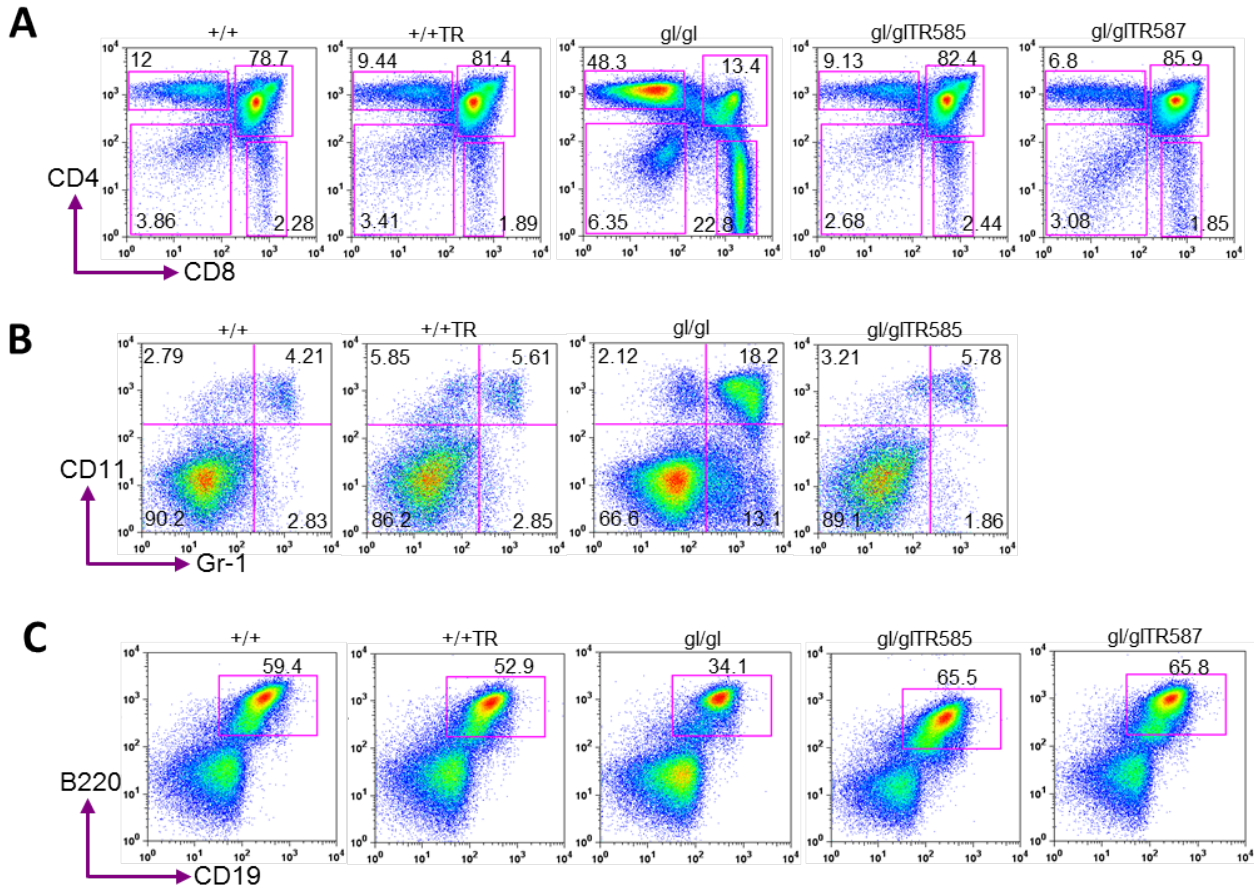

Appendix 2.1. Lymphoid and myeloid phenotype of *gl/gl* Ctsk-*Ostm1* transgenic mice.

The cathepsin K (Ctsk) promotor has been used to target *Ostm1* gene expression in mature and active osteoclasts of transgenic *gl/gl* Ctsk-*Ostm1* animals. **A**) Flow cytometry comparing the distribution of T cell expressing surface markers CD4 and CD8 at P21. **B)** Flow cytometry graphs representing the distribution of macrophage-granulocytes population based on their surface expression of CD11b and Gr-1 at P21. **C)** Distribution of the splenic B cell population identified with surface expression of B220 and CD19 at P21.

Table 1.7. Cellularity of lymphoid tissues in *gl/gl* Ctsk-*Ostm1* transgenic mice

mice	n	Body weight (gr)	BM cell count/ (x 10^6/ Femur)	Cell number/ Thymus (x 10^6)	Thymus/body weight (%)	Cell number/ Spleen (x 10^6)	Spleen/body weight (%)
+/+	1	13.6	12.8	119.5	0.53	109.8	0.67
+/+TR	1	13.0	21.3	102.8	0.54	119	0.7
gl/gl	1	6.6	-	31.2	0.77	42	1.1
gl/glTR	4	10.8 ± 1.1***	14.5 ± 0.5***	113.7 ± 8.0 ***	0.73 ± 0.003***	104.3 ± 15.9*	0.71 ± 0.004***

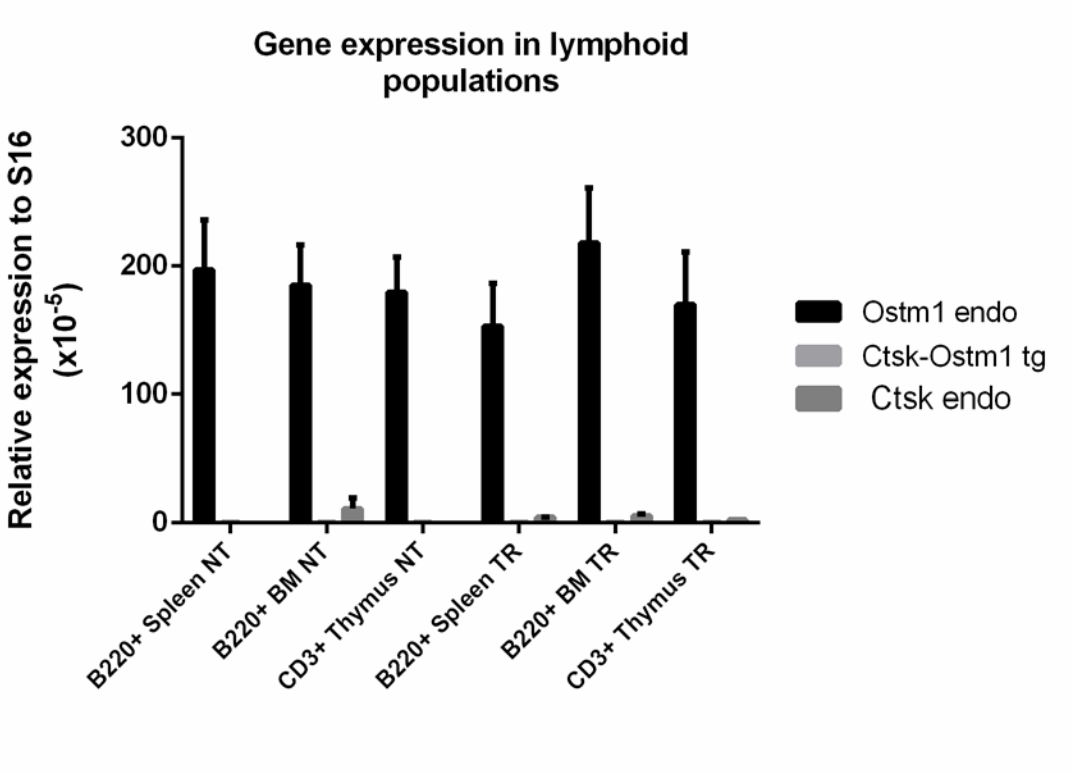

Appendix 2.2. Endogenous *Ostm1, Cathepstin K* and the transgene Ctsk-*Ostm1* expression in lymphoid populations by qPCR.

Quantitative expression of enogenous *Ostm1* and *Cathepstin k* (Ctsk) as well as transgence Ctsk-*Ostm1* in enriched B220 positive B cells from the spleen and enriched CD3 positive T cells from the thymus harvested from +/+ NT and +/+ Ctsk-*Ostm1* TR mice at 3 weeks of age.

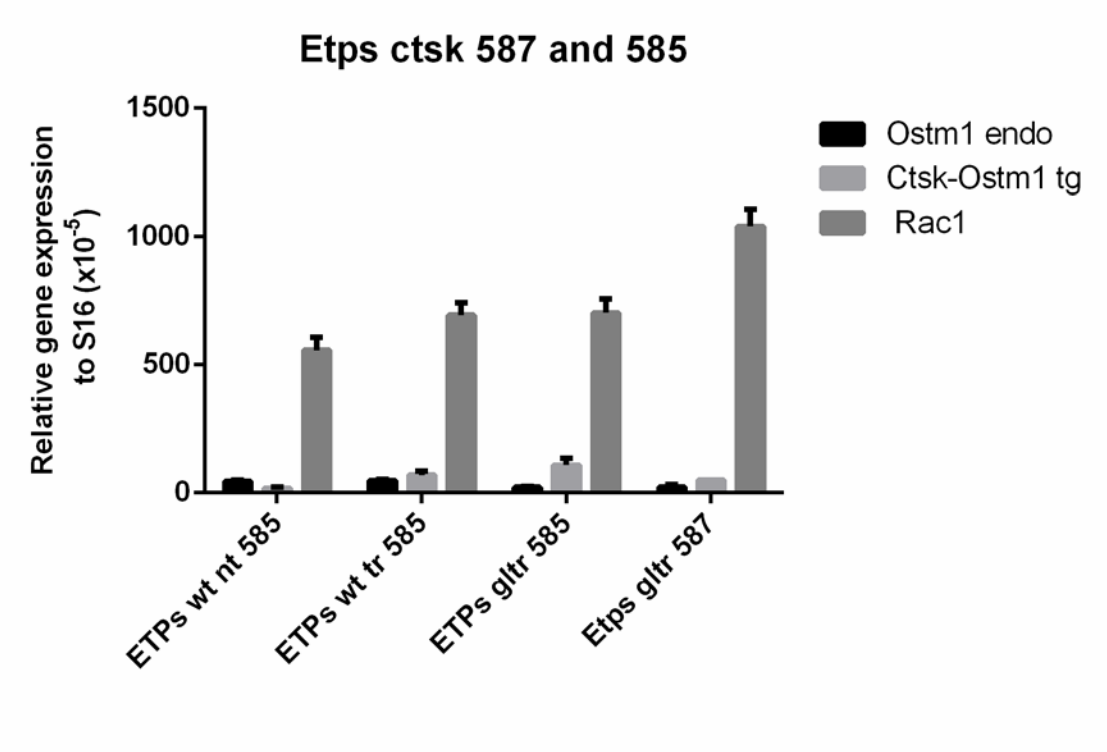

Appendix 2.3. Endogenous *Ostm1*, *Rac1* and the transgene Ctsk-*Ostm1* expression in ETPs populations by qPCR.

Quantitative expression of endogenous *Ostm1* and *Rac1* as well as Ctsk-*Ostm1* transgene in sorted ETPs cells from the thymus harvested from +/+ TR and *gl/gl* Ctsk-*Ostm1* TR mice line 585 and line 587 at 3 weeks of age.

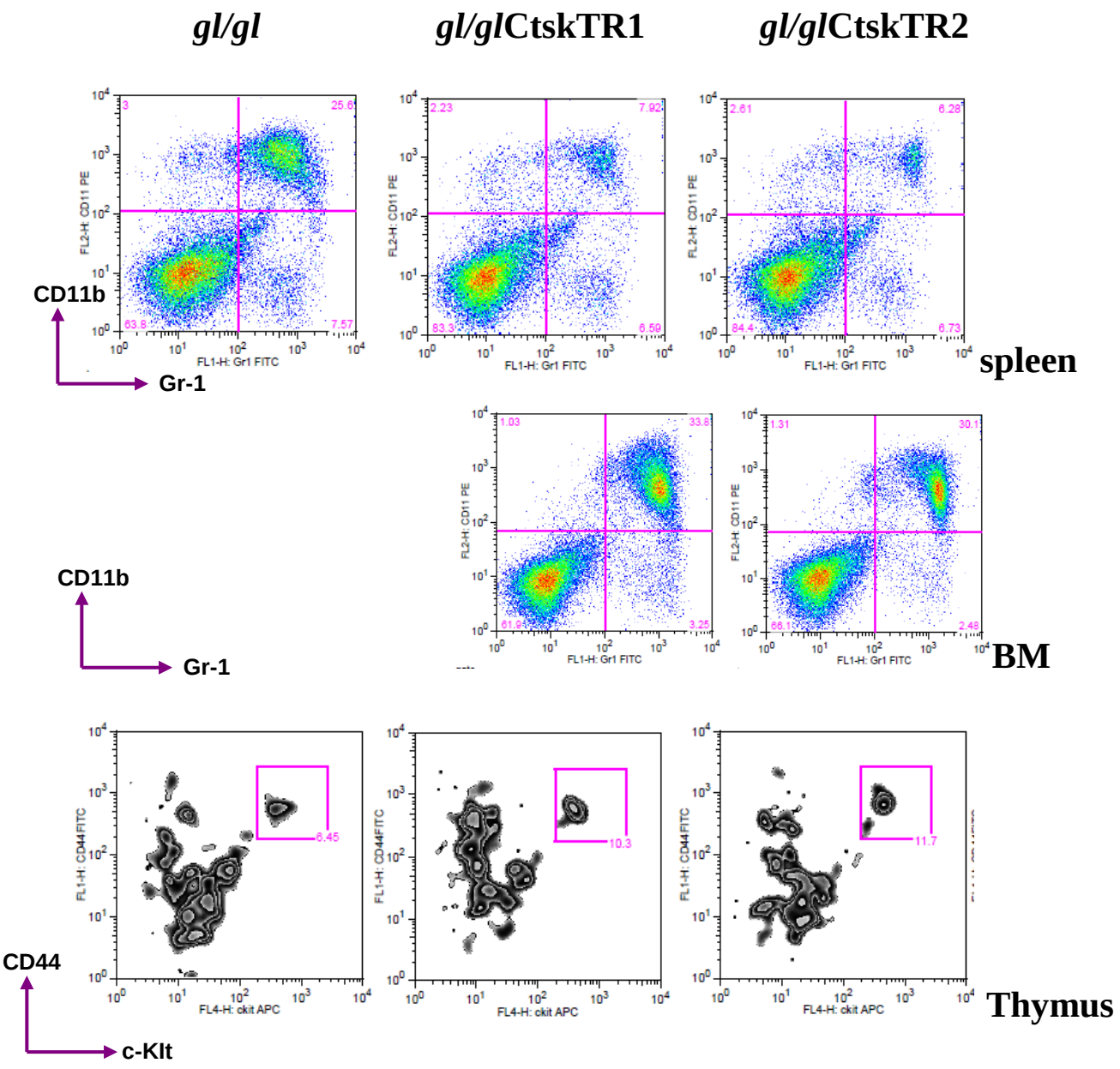

Appendix 2.4. Lymphoid and myeloid phenotype of *gl/gl* Ctsk-*Ostm1* transgenic mice in comparison to *gl/gl* animals at P21.

A) Normalized distribution of the splenic macrophage-granulocytes identified with surface expression of CD11b and Gr-1 in *gl/gl* Ctsk-*Ostm1* transgenic compared to *gl/gl* mice. **B)** Flow cytometry graphs representing the corrected macrophage-granulocytes distribution in the bone marrow of *gl/gl* Ctsk-*Ostm1* transgenic compared to *gl/gl* mice. **C)** Flow cytometry plot showing rescued distribution of ETPs within *gl/gl* Ctsk-*Ostm1* transgenic in comparison to *gl/gl* thymi.

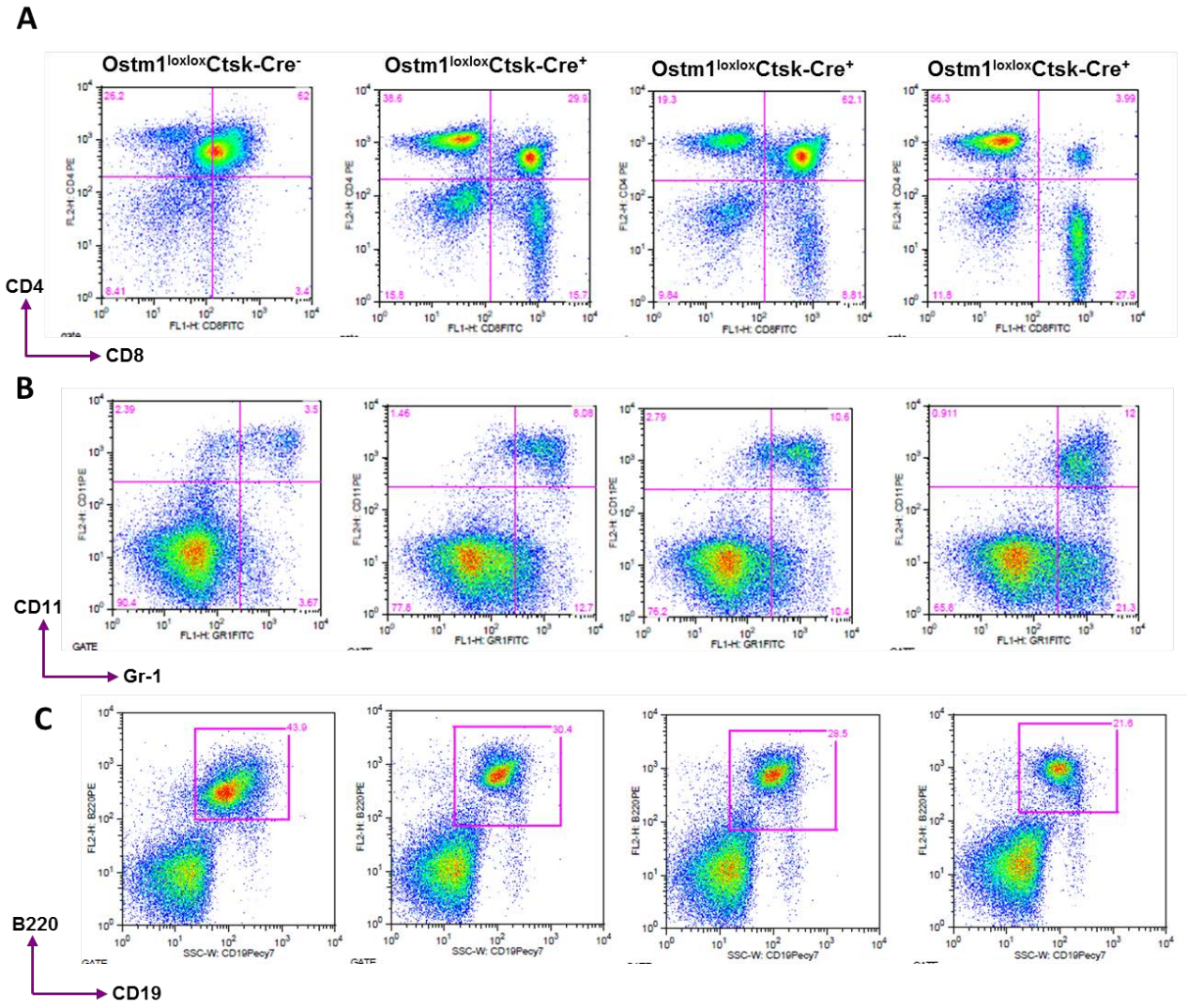

Appendix 2.5. Thymic and splenic lymphoid and myeloid phenotype of three independent conditional knock-out *Ostm1*$^{lox/lox}$ Ctsk-Cre $^{+}$mice.

A) Flow cytometry comparing the distribution of T cell expressing surface markers CD4 and CD8. **B)** Flow cytometry panels representing the macrophage-granulocytes population based on their surface expression of CD11b and Gr-1. **C)**. Distribution of the splenic B cell population identified with surface expression of B220 and CD19.at P21

Table 1.8. List of primers used in quantitative PCR assays

qPCR		
qS16	FOR	GCTACCAGGGCCTTTGAGATG
qS16	REV	AGGACGGATTTGCTGGTGTGG
qOstm1 EX5	FOR	GCTTCCTTCACTCAGAGCAA
qOstm1 EX6	REV	GTGAGAATGCAACTTGTCCGA
qOstm1 E6	FOR	GCCAACATTCAAGAAAATGC
qCD2-gl	REV	CACATCAGGAGGGCAGAAATC
qOstm1 E6	FOR	GCCAACATTCAAGAAAATGC
qCD19-gl	REV	GGAATGCTCGTCAAGAAGACAGG
qiCre	FOR	CCTGGTCTGGACACAGTG
qicre	REV	TTGCCCCTGTTTCACTATCC
qCD2	FOR	TGCGGTCTTGCAAGGGACAGATTT
qCD2	REV	GGACAGACCTTTCTCTGGACAGTT
qCD19	FOR	GGTCCCAGTCCTATGAAGATATGAG
qCD19	REV	CCTCTCCTTCCCATGCTGGTTCTA
qGFP	FOR	GACCCTGAAGTTCATCTGCA
qGFP	REV	CCGTCGTCCTTGAAGAAGA
qRac 1	FOR	CTGAAGTGCGACACCACTGT
qRac 1	REV	CTTGAGTCCTCGCTGTGTGA
qSpns2	FOR	GGATCCGCCATCTTCATCTG
qSpns2	REV	GAGGATGTCTGCAGTGATGG
qSphk2	FOR	TGGGCTGTCCTTCAACCTCATACA
qSphk2	REV	AGTGACAATGCCTTCCCACTCACT
qS1pr1	FOR	GTGTAGACCCAGAGTCCTGCG
qS1pr1	REV	AGCTTTTCCTTGGCTGGAGAG
qSgpp1	FOR	CCTGCTGGAGTTCACTAGTTT
qSgpp1	REV	GTCCACCAATGGGTAGAAGATAA
qSgpl1	FOR	GCTCTGGGATCCAACGATTT
qSgpl1	REV	CGCTTCCGAGTATGTACTAACG
qSgpp2	FOR	CCCTTTCACCCACTGGAATATC
qSgpp2	REV	GGCATTCCGTACTCTGCAATAA
qCtsk	FOR	CCAATACGTGCAGCAGA
qCtsk	REV	TGCATCGATGGACACAGA

Table 1.9. List of primers used in genotyping and RT-PCR assays

Genotyping		
GL + F1	FOR	CCTCTGGAAGACTAATACTTGCTG
GL + R1	REV	GCCTGGAACAGAGCAAAGC
GL + F2	FOR	GCTACATCTGGGTCCTTTCG
GL + R2	REV	CGCTTGCTTTTGTCTGTTACCTTTGTGTTC
V5 AgeI	FOR	GTGTGTACCGGTAAGCCTATCCCTAAC
GL EX5REV1	REV	GGACACCGTGTCGCTGCAGGTGAC
pCD2	FOR	TCCACCAGTCTCACTTCAGGTCCC
pCD19	FOR	TGCTGGGTGACAGGGAGGGG
Cre FRO	FOR	AATGCTTCTGTCCGTTTGC
Cre REV	REV	CGGCAACACCATTTTTTCTG
Gl 5' FOR3 (lox/+)	FOR	AATAGCCAGGGTTGCACAGAGAGT
GL EX5 REV2 (lox/+)	REV	ACGGCCTTGTGCATACAGGTAAGA
GL 3’ REV1	REV	GCATCGGCACATGAACTCTTCACT
CD2 icre	FOR	TGTGGATGCCACCTCTGATGAAGT
CD2 icre	REV	ATGTGGATCAGCATTCTCCCACCA
Mb-1 Cre	FOR	CCCTGTGGATGCCACCTC
Mb-1 Cre	REV	GTCCTGGCATCTGGTCAGAG

RT-PCR		
B-actin	FOR	TGACGATATCGCTGCGCTG
B-actin	REV	ACATGGCCTGGGGTGTTGAAG
Ostm1Ex3	FOR	CCTGCTTTGAGCATAACCTGC
Ostm1Ex6	REV	CTGCAGTCCCAACATTTCGTGAG
GFP	FOR	CCTGAAGTTCATCTGCACCA
GFP	REV	ACTGGGTGCTCAGGTAGTGG

BIBLIOGRAPHY

Adolfsson, J., O. J. Borge, D. Bryder, K. Theilgaard-Monch, I. Astrand-Grundstrom, E. Sitnicka, Y. Sasaki and S. E. Jacobsen (2001). "Upregulation of Flt3 expression within the bone marrow Lin(-)Sca1(+)c-kit(+) stem cell compartment is accompanied by loss of self-renewal capacity." Immunity **15**(4): 659-669.

Adolfsson, J., R. Mansson, N. Buza-Vidas, A. Hultquist, K. Liuba, C. T. Jensen, D. Bryder, L. Yang, O. J. Borge, L. A. Thoren, K. Anderson, E. Sitnicka, Y. Sasaki, M. Sigvardsson and S. E. Jacobsen (2005). "Identification of Flt3+ lympho-myeloid stem cells lacking erythro-megakaryocytic potential a revised road map for adult blood lineage commitment." Cell **121**(2): 295-306.

Akiyama, T., Y. Shimo, H. Yanai, J. Qin, D. Ohshima, Y. Maruyama, Y. Asaumi, J. Kitazawa, H. Takayanagi, J. M. Penninger, M. Matsumoto, T. Nitta, Y. Takahama and J. Inoue (2008). "The tumor necrosis factor family receptors RANK and CD40 cooperatively establish the thymic medullary microenvironment and self-tolerance." Immunity **29**(3): 423-437.

Akiyama, T., M. Shinzawa, J. Qin and N. Akiyama (2013). "Regulations of gene expression in medullary thymic epithelial cells required for preventing the onset of autoimmune diseases." Front Immunol **4**: 249.

Alford, A. I., K. M. Kozloff and K. D. Hankenson (2015). "Extracellular matrix networks in bone remodeling." Int J Biochem Cell Biol **65**: 20-31.

Anderson, D. M., E. Maraskovsky, W. L. Billingsley, W. C. Dougall, M. E. Tometsko, E. R. Roux, M. C. Teepe, R. F. DuBose, D. Cosman and L. Galibert (1997). "A homologue of the TNF receptor and its ligand enhance T-cell growth and dendritic-cell function." Nature **390**(6656): 175-179.

Anderson, G., W. E. Jenkinson, T. Jones, S. M. Parnell, F. A. Kinsella, A. J. White, J. E. Pongrac'z, S. W. Rossi and E. J. Jenkinson (2006). "Establishment and functioning of intrathymic microenvironments." Immunol Rev **209**: 10-27.

Anderson, G. and Y. Takahama (2012). "Thymic epithelial cells: working class heroes for T cell development and repertoire selection." Trends Immunol **33**(6): 256-263.

Ariel, A., R. Hershkoviz, L. Cahalon, D. E. Williams, S. K. Akiyama, K. M. Yamada, C. Chen, R. Alon, T. Lapidot and O. Lider (1997). "Induction of T cell adhesion to extracellular matrix or endothelial cell ligands by soluble or matrix-bound interleukin-7." Eur J Immunol **27**(10): 2562-2570.

Arron, J. R. and Y. Choi (2000). "Bone versus immune system." Nature **408**(6812): 535-536.
Baron, R. (1989). "Polarity and membrane transport in osteoclasts." Connect Tissue Res **20**(1-4): 109-120.

Baron, R. and M. Kneissel (2013). "WNT signaling in bone homeostasis and disease: from human mutations to treatments." Nat Med **19**(2): 179-192.

Bell, J. J. and A. Bhandoola (2008). "The earliest thymic progenitors for T cells possess myeloid lineage potential." Nature **452**(7188): 764-767.

Benjamin, M., H. Toumi, J. R. Ralphs, G. Bydder, T. M. Best and S. Milz (2006). "Where tendons and ligaments meet bone: attachment sites ('entheses') in relation to exercise and/or mechanical load." Journal of Anatomy **208**(4): 471-490.

Bennett, A. R., A. Farley, N. F. Blair, J. Gordon, L. Sharp and C. C. Blackburn (2002). "Identification and Characterization of Thymic Epithelial Progenitor Cells." Immunity **16**(6): 803-814.

Benz, C., K. Heinzel and C. C. Bleul (2004). "Homing of immature thymocytes to the subcapsular microenvironment within the thymus is not an absolute requirement for T cell development." Eur J Immunol **34**(12): 3652-3663.

Bhandoola, A., R. Cibotti, J. A. Punt, L. Granger, A. J. Adams, S. O. Sharrow and A. Singer (1999). "Positive Selection as a Developmental Progression Initiated by αβTCR Signals that Fix TCR Specificity prior to Lineage Commitment." Immunity **10**(3): 301-311.

Bhandoola, A., A. Sambandam, D. Allman, A. Meraz and B. Schwarz (2003). "Early T Lineage Progenitors: New Insights, but Old Questions Remain." The Journal of Immunology **171**(11): 5653-5658.

Bhandoola, A., H. von Boehmer, H. T. Petrie and J. C. Zuniga-Pflucker (2007). "Commitment and developmental potential of extrathymic and intrathymic T cell precursors: plenty to choose from." Immunity **26**(6): 678-689.

Blackburn, C. C., C. L. Augustine, R. Li, R. P. Harvey, M. A. Malin, R. L. Boyd, J. F. Miller and G. Morahan (1996). "The nu gene acts cell-autonomously and is required for differentiation of thymic epithelial progenitors." Proc Natl Acad Sci U S A **93**(12): 5742-5746.

Blair, H. C., A. J. Kahn, E. C. Crouch, J. J. Jeffrey and S. L. Teitelbaum (1986). "Isolated osteoclasts resorb the organic and inorganic components of bone." J Cell Biol **102**(4): 1164-1172.

Bleul, C. C., T. Corbeaux, A. Reuter, P. Fisch, J. S. Monting and T. Boehm (2006). "Formation of a functional thymus initiated by a postnatal epithelial progenitor cell." Nature **441**(7096): 992-996.

Blin-Wakkach, C., F. Bernard and G. F. Carle (2004). "[Osteopetrosis, from mouse to man]." Med Sci (Paris) **20**(1): 61-67.

Blin-Wakkach, C., M. Rouleau and A. Wakkach (2014). "Roles of osteoclasts in the control of medullary hematopoietic niches." Arch Biochem Biophys **561**: 29-37.

Blin-Wakkach, C., M. Rouleau and A. Wakkach (2014). "Roles of osteoclasts in the control of medullary hematopoietic niches." Arch Biochem Biophys.

Blin-Wakkach, C., M. Rouleau and A. Wakkach (2014). "Roles of osteoclasts in the control of medullary hematopoietic niches." Archives of Biochemistry and Biophysics **561**(0): 29-37.

Blin-Wakkach, C., A. Wakkach, P. M. Sexton, N. Rochet and G. F. Carle (2004). "Hematological defects in the oc/oc mouse, a model of infantile malignant osteopetrosis." Leukemia **18**(9): 1505-1511.

Boehm, T. and J. B. Swann (2013). "Thymus involution and regeneration: two sides of the same coin?" Nat Rev Immunol **13**(11): 831-838.

Boyle, W. J., W. S. Simonet and D. L. Lacey (2003). "Osteoclast differentiation and activation." Nature **423**(6937): 337-342.

Broxmeyer, H. E., S. Cooper, G. Hangoc and C. H. Kim (2005). "Stromal cell-derived factor-1/CXCL12 selectively counteracts inhibitory effects of myelosuppressive chemokines on hematopoietic progenitor cell proliferation in vitro." Stem Cells Dev **14**(2): 199-203.

Bunting, M. D., I. Comerford and S. R. McColl (2011). "Finding their niche: chemokines directing cell migration in the thymus." Immunol Cell Biol **89**(2): 185-196.

Burgess, T. L., Y. Qian, S. Kaufman, B. D. Ring, G. Van, C. Capparelli, M. Kelley, H. Hsu, W. J. Boyle, C. R. Dunstan, S. Hu and D. L. Lacey (1999). "The ligand for osteoprotegerin (OPGL) directly activates mature osteoclasts." J Cell Biol **145**(3): 527-538.

Burstein, A. H., J. M. Zika, K. G. Heiple and L. Klein (1975). "Contribution of collagen and mineral to the elastic-plastic properties of bone." J Bone Joint Surg Am **57**(7): 956-961.

Cai, A. Q., K. A. Landman, B. D. Hughes and C. M. Witt (2007). "T cell development in the thymus: From periodic seeding to constant output." Journal of Theoretical Biology **249**(2): 384-394.

Calvi, L. M. (2006). Osteoblastic activation in the hematopoietic stem cell niche. Skeletal Development and Remodeling in Health, Disease, and Aging. M. Zaidi. Oxford, Blackwell Publishing. **1068:** 477-488.

Calvi, L. M., G. B. Adams, K. W. Weibrecht, J. M. Weber, D. P. Olson, M. C. Knight, R. P. Martin, E. Schipani, P. Divieti, F. R. Bringhurst, L. A. Milner, H. M. Kronenberg and D. T. Scadden (2003). "Osteoblastic cells regulate the haematopoietic stem cell niche." Nature **425**(6960): 841-846.

Cappariello, A., A. Maurizi, V. Veeriah and A. Teti (2014). "Reprint of: The Great Beauty of the osteoclast." Arch Biochem Biophys **561**: 13-21.

Carotta, S., L. Wu and S. L. Nutt (2010). "Surprising new roles for PU.1 in the adaptive immune response." Immunol Rev **238**(1): 63-75.

Carsetti, R. (2000). "The development of B cells in the bone marrow is controlled by the balance between cell-autonomous mechanisms and signals from the microenvironment." J Exp Med **191**(1): 5-8.

Castaneda, B., Y. Simon, J. Jacques, E. Hess, Y. W. Choi, C. Blin-Wakkach, C. Mueller, A. Berdal and F. Lezot (2011). "Bone resorption control of tooth eruption and root morphogenesis: Involvement of the receptor activator of NF-kappaB (RANK)." J Cell Physiol **226**(1): 74-85.

Ceradini, D. J., A. R. Kulkarni, M. J. Callaghan, O. M. Tepper, N. Bastidas, M. E. Kleinman, J. M. Capla, R. D. Galiano, J. P. Levine and G. C. Gurtner (2004). "Progenitor cell trafficking is regulated by hypoxic gradients through HIF-1 induction of SDF-1." Nat Med **10**(8): 858-864.

Chalhoub, N., N. Benachenhou, V. Rajapurohitam, M. Pata, M. Ferron, A. Frattini, A. Villa and J. Vacher (2003). "Grey-lethal mutation induces severe malignant autosomal recessive osteopetrosis in mouse and human." Nat Med **9**(4): 399-406.

Chiusaroli, R., A. Sanjay, K. Henriksen, M. T. Engsig, W. C. Horne, H. Gu and R. Baron (2003). "Deletion of the gene encoding c-Cbl alters the ability of osteoclasts to migrate, delaying resorption and ossification of cartilage during the development of long bones." Developmental Biology **261**(2): 537-547.

Choi, K. Y., S. W. Lee, M. H. Park, Y. C. Bae, H. I. Shin, S. Nam, Y. J. Kim, H. J. Kim and H. M. Ryoo (2002). "Spatio-temporal expression patterns of Runx2 isoforms in early skeletogenesis." Exp Mol Med **34**(6): 426-433.

Choi, Y., J. R. Arron and M. J. Townsend (2009). "Promising bone-related therapeutic targets for rheumatoid arthritis." Nat Rev Rheumatol **5**(10): 543-548.

Choi, Y., J. R. Arron and M. J. Townsend (2009). "Promising bone-related therapeutic targets for rheumatoid arthritis." Nat Rev Rheumatol **5**(10): 543-548.

Chong, M. M., A. L. Cornish, R. Darwiche, E. G. Stanley, J. F. Purton, D. I. Godfrey, D. J. Hilton, R. Starr, W. S. Alexander and T. W. Kay (2003). "Suppressor of cytokine signaling-1 is a critical regulator of interleukin-7-dependent CD8+ T cell differentiation." Immunity **18**(4): 475-487.

Ciofani, M., T. M. Schmitt, A. Ciofani, A. M. Michie, N. Cuburu, A. Aublin, J. L. Maryanski and J. C. Zuniga-Pflucker (2004). "Obligatory role for cooperative signaling by pre-TCR and Notch during thymocyte differentiation." J Immunol **172**(9): 5230-5239.

Ciofani, M. and J. C. Zuniga-Pflucker (2007). "The thymus as an inductive site for T lymphopoiesis." Annu Rev Cell Dev Biol **23**: 463-493.

Coccia, P. F., W. Krivit, J. Cervenka, C. Clawson, J. H. Kersey, T. H. Kim, M. E. Nesbit, N. K. Ramsay, P. I. Warkentin, S. L. Teitelbaum, A. J. Kahn and D. M. Brown (1980). "Successful bone-marrow transplantation for infantile malignant osteopetrosis." N Engl J Med **302**(13): 701-708.

Cole, J. H. and M. C. van der Meulen (2011). "Whole bone mechanics and bone quality." Clin Orthop Relat Res **469**(8): 2139-2149.

Coudert, A. E., M. C. de Vernejoul, M. Muraca and A. Del Fattore (2015). "Osteopetrosis and its relevance for the discovery of new functions associated with the skeleton." **2015**: 372156.

Cummins, A. G. and F. M. Thompson (1997). "Postnatal changes in mucosal immune response: a physiological perspective of breast feeding and weaning." Immunol Cell Biol **75**(5): 419-429.
Cyster, J. G. (2009). "Settling the thymus: immigration requirements." J Exp Med **206**(4): 731-734.

Dalby, M. J., D. McCloy, M. Robertson, C. D. Wilkinson and R. O. Oreffo (2006). "Osteoprogenitor response to defined topographies with nanoscale depths." Biomaterials **27**(8): 1306-1315.

Daley, S. R., D. Y. Hu and C. C. Goodnow (2013). "Helios marks strongly autoreactive CD4+ T cells in two major waves of thymic deletion distinguished by induction of PD-1 or NF-kappaB." J Exp Med **210**(2): 269-285.

Danks, L. and H. Takayanagi (2013). "Immunology and bone." J Biochem **154**(1): 29-39.

David-Fung, E. S., R. Butler, G. Buzi, M. A. Yui, R. A. Diamond, M. K. Anderson, L. Rowen and E. V. Rothenberg (2009). "Transcription factor expression dynamics of early T-lymphocyte specification and commitment." Dev Biol **325**(2): 444-467.

Dazzi, F., R. Ramasamy, S. Glennie, S. P. Jones and I. Roberts (2006). "The role of mesenchymal stem cells in haemopoiesis." Blood Reviews **20**(3): 161-171.

de Barros, S. C., R. Vicente, K. Chebli, C. Jacquet, V. S. Zimmermann and N. Taylor (2013). "Intrathymic progenitor cell transplantation across histocompatibility barriers results in the persistence of early thymic progenitors and T-cell differentiation." Blood **121**(11): 2144-2153.

de Boer, J., A. Williams, G. Skavdis, N. Harker, M. Coles, M. Tolaini, T. Norton, K. Williams, K. Roderick, A. J. Potocnik and D. Kioussis (2003). "Transgenic mice with hematopoietic and lymphoid specific expression of Cre." Eur J Immunol **33**(2): 314-325.

De Obaldia, M. E., J. J. Bell, X. Wang, C. Harly, Y. Yashiro-Ohtani, J. H. DeLong, D. A. Zlotoff, D. A. Sultana, W. S. Pear and A. Bhandoola (2013). "T cell development requires constraint of the myeloid regulator C/EBP-[alpha] by the Notch target and transcriptional repressor Hes1." Nat Immunol **14**(12): 1277-1284.

Del Fattore, A., A. Teti and N. Rucci (2008). "Osteoclast receptors and signaling." Arch Biochem Biophys **473**(2): 147-160.

Delaisse, J. M. (2014). "The reversal phase of the bone-remodeling cycle: cellular prerequisites for coupling resorption and formation." Bonekey Rep **3**: 561.

Delogu, A., A. Schebesta, Q. Sun, K. Aschenbrenner, T. Perlot and M. Busslinger (2006). "Gene Repression by Pax5 in B Cells Is Essential for Blood Cell Homeostasis and Is Reversed in Plasma Cells." Immunity **24**(3): 269-281.

Dengler, H. S., G. V. Baracho, S. A. Omori, S. Bruckner, K. C. Arden, D. H. Castrillon, R. A. DePinho and R. C. Rickert (2008). "Distinct functions for the transcription factor Foxo1 at various stages of B cell differentiation." Nat Immunol **9**(12): 1388-1398.

Domon, T., Y. Yamazaki, A. Fukui, Y. Ohnishi, S. Takahashi, T. Yamamoto and M. Wakita (2002). "Three-dimensional distribution of the clear zone of migrating osteoclasts on dentin slices in vitro." Tissue Cell **34**(5): 326-336.

Donskoy, E., D. Foss and I. Goldschneider (2003). "Gated importation of prothymocytes by adult mouse thymus is coordinated with their periodic mobilization from bone marrow." J Immunol **171**(7): 3568-3575.

Dorsam, G., M. H. Graeler, C. Seroogy, Y. Kong, J. K. Voice and E. J. Goetzl (2003). "Transduction of multiple effects of sphingosine 1-phosphate (S1P) on T cell functions by the S1P1 G protein-coupled receptor." J Immunol **171**(7): 3500-3507.

Dougall, W. C., M. Glaccum, K. Charrier, K. Rohrbach, K. Brasel, T. De Smedt, E. Daro, J. Smith, M. E. Tometsko, C. R. Maliszewski, A. Armstrong, V. Shen, S. Bain, D. Cosman, D. Anderson, P. J. Morrissey, J. J. Peschon and J. Schuh (1999). "RANK is essential for osteoclast and lymph node development." Genes Dev **13**(18): 2412-2424.

Drake, P. M., C. M. Stock, J. K. Nathan, P. Gip, K. P. Golden, B. Weinhold, R. Gerardy-Schahn and C. R. Bertozzi (2009). "Polysialic acid governs T-cell development by regulating progenitor access to the thymus." Proc Natl Acad Sci U S A **106**(29): 11995-12000.

Driessen, R. L., H. M. Johnston and S. K. Nilsson (2003). "Membrane-bound stem cell factor is a key regulator in the initial lodgment of stem cells within the endosteal marrow region." Exp Hematol **31**(12): 1284-1291.

Dunn, C. D. (1971). "The differentiation of haemopoietic stem cells." Ser Haematol **4**(4): 1-71.
Egawa, T., K. Kawabata, H. Kawamoto, K. Amada, R. Okamoto, N. Fujii, T. Kishimoto, Y. Katsura and T. Nagasawa (2001). "The earliest stages of B cell development require a chemokine stromal cell-derived factor/pre-B cell growth-stimulating factor." Immunity **15**(2): 323-334.

Elefteriou, F., J. D. Ahn, S. Takeda, M. Starbuck, X. Yang, X. Liu, H. Kondo, W. G. Richards, T. W. Bannon, M. Noda, K. Clement, C. Vaisse and G. Karsenty (2005). "Leptin regulation of bone resorption by the sympathetic nervous system and CART." Nature **434**(7032): 514-520.

Ellmeier, W., L. Haust and R. Tschismarov (2013). "Transcriptional control of CD4 and CD8 coreceptor expression during T cell development." Cell Mol Life Sci **70**(23): 4537-4553.

Engel, I. and C. Murre (2004). "E2A proteins enforce a proliferation checkpoint in developing thymocytes." Embo j **23**(1): 202-211.

Epstein, J. A., J. Li, D. Lang, F. Chen, C. B. Brown, F. Jin, M. M. Lu, M. Thomas, E. Liu, A. Wessels and C. W. Lo (2000). "Migration of cardiac neural crest cells in Splotch embryos." Development **127**(9): 1869-1878.

Essabar, L., T. Meskini, S. Ettair, N. Erreimi and N. Mouane (2014). "Malignant infantile osteopetrosis: case report with review of literature." Pan Afr Med J **17**: 63.

Falahati-Nini, A., B. L. Riggs, E. J. Atkinson, W. M. O'Fallon, R. Eastell and S. Khosla (2000). "Relative contributions of testosterone and estrogen in regulating bone resorption and formation in normal elderly men." J Clin Invest **106**(12): 1553-1560.

Feng, C., K. J. Woodside, B. A. Vance, D. El-Khoury, M. Canelles, J. Lee, R. Gress, B. J. Fowlkes, E. W. Shores and P. E. Love (2002). "A potential role for CD69 in thymocyte emigration." Int Immunol **14**(6): 535-544.

Ferron, M., M. Boudiffa, M. Arsenault, M. Rached, M. Pata, S. Giroux, L. Elfassihi, M. Kisseleva, Philip W. Majerus, F. Rousseau and J. Vacher (2011). "Inositol Polyphosphate 4-Phosphatase B as a Regulator of Bone Mass in Mice and Humans." Cell Metabolism **14**(4): 466-477.

Foss, D. L., E. Donskoy and I. Goldschneider (2001). "The importation of hematogenous precursors by the thymus is a gated phenomenon in normal adult mice." J Exp Med **193**(3): 365-374.

Foster, K., J. Sheridan, H. Veiga-Fernandes, K. Roderick, V. Pachnis, R. Adams, C. Blackburn, D. Kioussis and M. Coles (2008). "Contribution of neural crest-derived cells in the embryonic and adult thymus." J Immunol **180**(5): 3183-3189.

Gallegos, A. M. and M. J. Bevan (2004). "Central tolerance to tissue-specific antigens mediated by direct and indirect antigen presentation." J Exp Med **200**(8): 1039-1049.

Garcia-Ojeda, M. E., R. G. Klein Wolterink, F. Lemaitre, O. Richard-Le Goff, M. Hasan, R. W. Hendriks, A. Cumano and J. P. Di Santo (2013). "GATA-3 promotes T-cell specification by repressing B-cell potential in pro-T cells in mice." Blood **121**(10): 1749-1759.

Gay, C. V. and J. A. Weber (2000). "Regulation of differentiated osteoclasts." Crit Rev Eukaryot Gene Expr **10**(3-4): 213-230.

Germar, K., M. Dose, T. Konstantinou, J. Zhang, H. Wang, C. Lobry, K. L. Arnett, S. C. Blacklow, I. Aifantis, J. C. Aster and F. Gounari (2011). "T-cell factor 1 is a gatekeeper for T-cell specification in response to Notch signaling." Proc Natl Acad Sci U S A **108**(50): 20060-20065.

Gerritsen, E. J., J. M. Vossen, A. Fasth, W. Friedrich, G. Morgan, A. Padmos, A. Vellodi, O. Porras, A. O'Meara, F. Porta and et al. (1994). "Bone marrow transplantation for autosomal recessive osteopetrosis. A report from the Working Party on Inborn Errors of the European Bone Marrow Transplantation Group." J Pediatr **125**(6 Pt 1): 896-902.

Giachelli, C. M. and S. Steitz (2000). "Osteopontin: a versatile regulator of inflammation and biomineralization." Matrix Biol **19**(7): 615-622.

Gill, J., M. Malin, G. A. Hollander and R. Boyd (2002). "Generation of a complete thymic microenvironment by MTS24(+) thymic epithelial cells." Nat Immunol **3**(7): 635-642.

Godfrey, D. I., A. Zlotnik and T. Suda (1992). "Phenotypic and functional characterization of c-kit expression during intrathymic T cell development." J Immunol **149**(7): 2281-2285.

Goldschneider, I. (2006). "Cyclical mobilization and gated importation of thymocyte progenitors in the adult mouse: evidence for a thymus-bone marrow feedback loop." Immunol Rev **209**: 58-75.

Gordon, J. and N. R. Manley (2011). "Mechanisms of thymus organogenesis and morphogenesis." Development **138**(18): 3865-3878.

Gossens, K., S. Naus, S. Y. Corbel, S. Lin, F. M. Rossi, J. Kast and H. J. Ziltener (2009). "Thymic progenitor homing and lymphocyte homeostasis are linked via S1P-controlled expression of thymic P-selectin/CCL25." J Exp Med **206**(4): 761-778.

Gruneberg, H. (1935). A New Sub-Lethal Colour Mutation in the House Mouse.
GRÜNEBERG, H. (1936). "GREY-LETHAL, A NEW MUTATION IN THE HOUSE MOUSE." Journal of Heredity **27**(3): 105-109.

Guerrini, M. M., C. Sobacchi, B. Cassani, M. Abinun, S. S. Kilic, A. Pangrazio, D. Moratto, E. Mazzolari, J. Clayton-Smith, P. Orchard, F. P. Coxon, M. H. Helfrich, J. C. Crockett, D. Mellis, A. Vellodi, I. Tezcan, L. D. Notarangelo, M. J. Rogers, P. Vezzoni, A. Villa and A. Frattini (2008). "Human Osteoclast-Poor Osteopetrosis with Hypogammaglobulinemia due to TNFRSF11A (RANK) Mutations." The American Journal of Human Genetics **83**(1): 64-76.

Guerrini, M. M., C. Sobacchi, B. Cassani, M. Abinun, S. S. Kilic, A. Pangrazio, D. Moratto, E. Mazzolari, J. Clayton-Smith, P. Orchard, F. P. Coxon, M. H. Helfrich, J. C. Crockett, D. Mellis, A. Vellodi, I. Tezcan, L. D. Notarangelo, M. J. Rogers, P. Vezzoni, A. Villa and A. Frattini (2008). "Human osteoclast-poor osteopetrosis with hypogammaglobulinemia due to TNFRSF11A (RANK) mutations." Am J Hum Genet **83**(1): 64-76.

Guerrini, M. M. and H. Takayanagi (2014). "The immune system, bone and RANKL." Archives of Biochemistry and Biophysics **561**(0): 118-123.

Gwin, K. A., M. B. Shapiro, J. J. Dolence, Z. L. Huang and K. L. Medina (2013). "Hoxa9 and Flt3 signaling synergistically regulate an early checkpoint in lymphopoiesis." J Immunol **191**(2): 745-754.

Hardy, R. R. and K. Hayakawa (2001). "B cell development pathways." Annu Rev Immunol **19**: 595-621.

Hardy, R. R., P. W. Kincade and K. Dorshkind (2007). "The Protean Nature of Cells in the B Lymphocyte Lineage." Immunity **26**(6): 703-714.

Harman, B. C., E. J. Jenkinson and G. Anderson (2003). "Microenvironmental regulation of Notch signalling in T cell development." Semin Immunol **15**(2): 91-97.

Hattori, K., B. Heissig, K. Tashiro, T. Honjo, M. Tateno, J. H. Shieh, N. R. Hackett, M. S. Quitoriano, R. G. Crystal, S. Rafii and M. A. Moore (2001). "Plasma elevation of stromal cell-derived factor-1 induces mobilization of mature and immature hematopoietic progenitor and stem cells." Blood **97**(11): 3354-3360.

Heraud, C., A. Griffiths, S. N. Pandruvada, M. W. Kilimann, M. Pata and J. Vacher (2014). "Severe neurodegeneration with impaired autophagy mechanism triggered by ostm1 deficiency." J Biol Chem **289**(20): 13912-13925.

Hirvonen, M. J., K. Fagerlund, P. Lakkakorpi, H. K. Vaananen and M. T. Mulari (2013). "Novel perspectives on the transcytotic route in osteoclasts." Bonekey Rep **2**: 306.

Ho, M. S., R. L. Medcalf, S. A. Livesey and K. Traianedes (2015). "The dynamics of adult haematopoiesis in the bone and bone marrow environment." Br J Haematol.

Hobeika, E., S. Thiemann, B. Storch, H. Jumaa, P. J. Nielsen, R. Pelanda and M. Reth (2006). "Testing gene function early in the B cell lineage in mb1-cre mice." Proceedings of the National Academy of Sciences **103**(37): 13789-13794.

Hollander, G. A., B. Wang, A. Nichogiannopoulou, P. P. Platenburg, W. van Ewijk, S. J. Burakoff, J. C. Gutierrez-Ramos and C. Terhorst (1995). "Developmental control point in induction of thymic cortex regulated by a subpopulation of prothymocytes." Nature **373**(6512): 350-353.

Horowitz, M. C., J. A. Fretz and J. A. Lorenzo (2010). "How B cells influence bone biology in health and disease." Bone **47**(3): 472-479.

Hosoya, T., T. Kuroha, T. Moriguchi, D. Cummings, I. Maillard, K. C. Lim and J. D. Engel (2009). "GATA-3 is required for early T lineage progenitor development." J Exp Med **206**(13): 2987-3000.

Hozumi, K., C. Mailhos, N. Negishi, K. Hirano, T. Yahata, K. Ando, S. Zuklys, G. A. Hollander, D. T. Shima and S. Habu (2008). "Delta-like 4 is indispensable in thymic environment specific for T cell development." J Exp Med **205**(11): 2507-2513.

Huang, Y., K. Sitwala, J. Bronstein, D. Sanders, M. Dandekar, C. Collins, G. Robertson, J. MacDonald, T. Cezard, M. Bilenky, N. Thiessen, Y. Zhao, T. Zeng, M. Hirst, A. Hero, S. Jones and J. L. Hess (2012). "Identification and characterization of Hoxa9 binding sites in hematopoietic cells." Blood **119**(2): 388-398.

Hughes, F. J., J. Collyer, M. Stanfield and S. A. Goodman (1995). "The effects of bone morphogenetic protein-2, -4, and -6 on differentiation of rat osteoblast cells in vitro." Endocrinology **136**(6): 2671-2677.

Igarashi, H., S. C. Gregory, T. Yokota, N. Sakaguchi and P. W. Kincade (2002). "Transcription from the RAG1 locus marks the earliest lymphocyte progenitors in bone marrow." Immunity **17**(2): 117-130.

Ikawa, T., K. Masuda, M. Lu, N. Minato, Y. Katsura and H. Kawamoto (2004). "Identification of the earliest prethymic T-cell progenitors in murine fetal blood." Blood **103**(2): 530-537.

Ikeda, K. and S. Takeshita (2014). "Factors and mechanisms involved in the coupling from bone resorption to formation: how osteoclasts talk to osteoblasts." J Bone Metab **21**(3): 163-167.

Inlay, M. A., D. Bhattacharya, D. Sahoo, T. Serwold, J. Seita, H. Karsunky, S. K. Plevritis, D. L. Dill and I. L. Weissman (2009). "Ly6d marks the earliest stage of B-cell specification and identifies the branchpoint between B-cell and T-cell development." Genes and Development **23**(20): 2376-2381.

Ishii, M., J. Kikuta, Y. Shimazu, M. Meier-Schellersheim and R. N. Germain (2010). "Chemorepulsion by blood S1P regulates osteoclast precursor mobilization and bone remodeling in vivo." J Exp Med **207**(13): 2793-2798.

Janas, M. L., G. Varano, K. Gudmundsson, M. Noda, T. Nagasawa and M. Turner (2010). "Thymic development beyond beta-selection requires phosphatidylinositol 3-kinase activation by CXCR4." J Exp Med **207**(1): 247-261.

Janeway, C. A., P. Travers, M. Walport and J. D. Capra (1999). Immunobiology: the immune system in health and disease, Current Biology Publications New York, NY;.

Jang, H. D., J. H. Shin, D. R. Park, J. H. Hong, K. Yoon, R. Ko, C. Y. Ko, H. S. Kim, D. Jeong, N. Kim and S. Y. Lee (2011). "Inactivation of glycogen synthase kinase-3beta is required for osteoclast differentiation." J Biol Chem **286**(45): 39043-39050.

Jenkinson, W. E., A. Bacon, A. J. White, G. Anderson and E. J. Jenkinson (2008). "An epithelial progenitor pool regulates thymus growth." J Immunol **181**(9): 6101-6108.

Jenkinson, W. E., E. J. Jenkinson and G. Anderson (2003). "Differential requirement for mesenchyme in the proliferation and maturation of thymic epithelial progenitors." J Exp Med **198**(2): 325-332.

Jotereau, F., F. Heuze, V. Salomon-Vie and H. Gascan (1987). "Cell kinetics in the fetal mouse thymus: precursor cell input, proliferation, and emigration." J Immunol **138**(4): 1026-1030.

Jotereau, F. V. and N. M. Le Douarin (1982). "Demonstration of a cyclic renewal of the lymphocyte precursor cells in the quail thymus during embryonic and perinatal life." J Immunol **129**(5): 1869-1877.

Kang, J. and S. D. Der (2004). "Cytokine functions in the formative stages of a lymphocyte's life." Curr Opin Immunol **16**(2): 180-190.

Kasper, D., R. Planells-Cases, J. C. Fuhrmann, O. Scheel, O. Zeitz, K. Ruether, A. Schmitt, M. Poet, R. Steinfeld, M. Schweizer, U. Kornak and T. J. Jentsch (2005). "Loss of the chloride channel ClC-7 leads to lysosomal storage disease and neurodegeneration." Embo j **24**(5): 1079-1091.

Kikuchi, K., A. Y. Lai, C. L. Hsu and M. Kondo (2005). "IL-7 receptor signaling is necessary for stage transition in adult B cell development through up-regulation of EBF." J Exp Med **201**(8): 1197-1203.

Kim, J. H., K. Kim, H. M. Jin, I. Song, B. U. Youn, S. H. Lee, Y. Choi and N. Kim (2010). "Negative feedback control of osteoclast formation through ubiquitin-mediated down-regulation of NFATc1." J Biol Chem **285**(8): 5224-5231.

Kim, J. H. and N. Kim (2014). "Regulation of NFATc1 in Osteoclast Differentiation." J Bone Metab **21**(4): 233-241.

Kimura, Y., B. Ding, N. Imai, D. J. Nolan, J. M. Butler and S. Rafii (2011). "c-Kit-mediated functional positioning of stem cells to their niches is essential for maintenance and regeneration of adult hematopoiesis." PLoS One **6**(10): e26918.

Kitazawa, H., K. Muegge, R. Badolato, J. M. Wang, W. E. Fogler, D. K. Ferris, C. K. Lee, S. Candeias, M. R. Smith, J. J. Oppenheim and S. K. Durum (1997). "IL-7 activates alpha4beta1 integrin in murine thymocytes." J Immunol **159**(5): 2259-2264.

Klein, L., B. Kyewski, P. M. Allen and K. A. Hogquist (2014). "Positive and negative selection of the T cell repertoire: what thymocytes see (and don't see)." Nat Rev Immunol **14**(6): 377-391.

Klug, D. B., C. Carter, E. Crouch, D. Roop, C. J. Conti and E. R. Richie (1998). "Interdependence of cortical thymic epithelial cell differentiation and T-lineage commitment." Proc Natl Acad Sci U S A **95**(20): 11822-11827.

Koble, C. and B. Kyewski (2009). "The thymic medulla: a unique microenvironment for intercellular self-antigen transfer." J Exp Med **206**(7): 1505-1513.

Koch, U., E. Fiorini, R. Benedito, V. Besseyrias, K. Schuster-Gossler, M. Pierres, N. R. Manley, A. Duarte, H. R. Macdonald and F. Radtke (2008). "Delta-like 4 is the essential, nonredundant ligand for Notch1 during thymic T cell lineage commitment." J Exp Med **205**(11): 2515-2523.

Kogianni, G. and B. S. Noble (2007). "The biology of osteocytes." Curr Osteoporos Rep **5**(2): 81-86.

Kollet, O., A. Dar, S. Shivtiel, A. Kalinkovich, K. Lapid, Y. Sztainberg, M. Tesio, R. M. Samstein, P. Goichberg, A. Spiegel, A. Elson and T. Lapidot (2006). "Osteoclasts degrade endosteal components and promote mobilization of hematopoietic progenitor cells." Nat Med **12**(6): 657-664.

Komatsu, N., K. Okamoto, S. Sawa, T. Nakashima, M. Oh-hora, T. Kodama, S. Tanaka, J. A. Bluestone and H. Takayanagi (2014). "Pathogenic conversion of Foxp3+ T cells into TH17 cells in autoimmune arthritis." Nat Med **20**(1): 62-68.

Kondo, M. (2010). "Lymphoid and myeloid lineage commitment in multipotent hematopoietic progenitors." Immunological Reviews **238**(1): 37-46.

Kondo, M., I. L. Weissman and K. Akashi (1997). "Identification of clonogenic common lymphoid progenitors in mouse bone marrow." Cell **91**(5): 661-672.

Kong, Y. Y., H. Yoshida, I. Sarosi, H. L. Tan, E. Timms, C. Capparelli, S. Morony, A. J. Oliveira-dos-Santos, G. Van, A. Itie, W. Khoo, A. Wakeham, C. R. Dunstan, D. L. Lacey, T. W. Mak, W. J. Boyle and J. M. Penninger (1999). "OPGL is a key regulator of osteoclastogenesis, lymphocyte development and lymph-node organogenesis." Nature **397**(6717): 315-323.

Kornak, U., D. Kasper, M. R. Bosl, E. Kaiser, M. Schweizer, A. Schulz, W. Friedrich, G. Delling and T. J. Jentsch (2001). "Loss of the ClC-7 chloride channel leads to osteopetrosis in mice and man." Cell **104**(2): 205-215.

Kronenberg, H. M. (2003). "Developmental regulation of the growth plate." Nature **423**(6937): 332-336.

Krueger, A. and H. von Boehmer (2007). "Identification of a T lineage-committed progenitor in adult blood." Immunity **26**(1): 105-116.

Krueger, A., S. Willenzon, M. Lyszkiewicz, E. Kremmer and R. Forster (2010). "CC chemokine receptor 7 and 9 double-deficient hematopoietic progenitors are severely impaired in seeding the adult thymus." Blood **115**(10): 1906-1912.

Kyewski, B. A. (1987). "Seeding of thymic microenvironments defined by distinct thymocyte-stromal cell interactions is developmentally controlled." J Exp Med **166**(2): 520-538.

Lacey, D. L., E. Timms, H. L. Tan, M. J. Kelley, C. R. Dunstan, T. Burgess, R. Elliott, A. Colombero, G. Elliott, S. Scully, H. Hsu, J. Sullivan, N. Hawkins, E. Davy, C. Capparelli, A. Eli, Y. X. Qian, S. Kaufman, I. Sarosi, V. Shalhoub, G. Senaldi, J. Guo, J. Delaney and W. J. Boyle (1998). "Osteoprotegerin ligand is a cytokine that regulates osteoclast differentiation and activation." Cell **93**(2): 165-176.

Lai, A. Y. and M. Kondo (2006). "Asymmetrical lymphoid and myeloid lineage commitment in multipotent hematopoietic progenitors." Journal of Experimental Medicine **203**(8): 1867-1873.

Lai, A. Y., A. Watanabe, T. O'Brien and M. Kondo (2009). "Pertussis toxin-sensitive G proteins regulate lymphoid lineage specification in multipotent hematopoietic progenitors." Blood **113**(23): 5757-5764.

Lam, J., S. Takeshita, J. E. Barker, O. Kanagawa, F. P. Ross and S. L. Teitelbaum (2000). "TNF-alpha induces osteoclastogenesis by direct stimulation of macrophages exposed to permissive levels of RANK ligand." J Clin Invest **106**(12): 1481-1488.

Lang, G., C. Mamalaki, D. Greenberg, N. Yannoutsos and D. Kioussis (1991). "Deletion analysis of the human CD2 gene locus control region in transgenic mice." Nucleic Acids Res **19**(21): 5851-5856.

Lang, G., D. Wotton, M. J. Owen, W. A. Sewell, M. H. Brown, D. Y. Mason, M. J. Crumpton and D. Kioussis (1988). "The structure of the human CD2 gene and its expression in transgenic mice." Embo j **7**(6): 1675-1682.

Lange, P. F., L. Wartosch, T. J. Jentsch and J. C. Fuhrmann (2006). "ClC-7 requires Ostm1 as a beta-subunit to support bone resorption and lysosomal function." Nature **440**(7081): 220-223.

Lapid, K., C. Glait-Santar, S. Gur-Cohen, J. Canaani, O. Kollet and T. Lapidot (2008). Egress and Mobilization of Hematopoietic Stem and Progenitor Cells: A Dynamic Multi-facet Process. StemBook. Cambridge (MA), Harvard Stem Cell Institute

Lapidot, T. and I. Petit (2002). "Current understanding of stem cell mobilization: the roles of chemokines, proteolytic enzymes, adhesion molecules, cytokines, and stromal cells." Exp Hematol **30**(9): 973-981.

Lecuyer, E., S. Herblot, M. Saint-Denis, R. Martin, C. G. Begley, C. Porcher, S. H. Orkin and T. Hoang (2002). "The SCL complex regulates c-kit expression in hematopoietic cells through functional interaction with Sp1." Blood **100**(7): 2430-2440.

Lee, Y., A. Gotoh, H. J. Kwon, M. You, L. Kohli, C. Mantel, S. Cooper, G. Hangoc, K. Miyazawa, K. Ohyashiki and H. E. Broxmeyer (2002). "Enhancement of intracellular signaling associated with hematopoietic progenitor cell survival in response to SDF-1/CXCL12 in synergy with other cytokines." Blood **99**(12): 4307-4317.

Lemaire, V., F. L. Tobin, L. D. Greller, C. R. Cho and L. J. Suva (2004). "Modeling the interactions between osteoblast and osteoclast activities in bone remodeling." J Theor Biol **229**(3): 293-309.

Lensch, M. W. and G. Q. Daley (2004). "Origins of mammalian hematopoiesis: In vivo paradigms and in vitro models." Stem Cells in Development and Disease **60**: 127-196.

Lévesque, J.-P., J. Hendy, I. G. Winkler, Y. Takamatsu and P. J. Simmons (2003). "Granulocyte colony-stimulating factor induces the release in the bone marrow of proteases that cleave c-KIT receptor (CD117) from the surface of hematopoietic progenitor cells." Experimental Hematology **31**(2): 109-117.

Lewinsohn, D. M., A. Nagler, N. Ginzton, P. Greenberg and E. C. Butcher (1990). "Hematopoietic progenitor cell expression of the H-CAM (CD44) homing-associated adhesion molecule." Blood **75**(3): 589-595.

Li, S., Q. Zhai, D. Zou, H. Meng, Z. Xie, C. Li, Y. Wang, J. Qi, T. Cheng and L. Qiu (2013). "A pivotal role of bone remodeling in granulocyte colony stimulating factor induced hematopoietic stem/progenitor cells mobilization." Journal of Cellular Physiology **228**(5): 1002-1009.

Lind, E. F., S. E. Prockop, H. E. Porritt and H. T. Petrie (2001). "Mapping precursor movement through the postnatal thymus reveals specific microenvironments supporting defined stages of early lymphoid development." J Exp Med **194**(2): 127-134.

Lorenzo, J., M. Horowitz and Y. Choi (2008). "Osteoimmunology: interactions of the bone and immune system." Endocr Rev **29**(4): 403-440.

Lotinun, S., R. Kiviranta, T. Matsubara, J. A. Alzate, L. Neff, A. Luth, I. Koskivirta, B. Kleuser, J. Vacher, E. Vuorio, W. C. Horne and R. Baron (2013). "Osteoclast-specific cathepsin K deletion stimulates S1P-dependent bone formation." J Clin Invest **123**(2): 666-681.

Love, P. E. and A. Bhandoola (2011). "Signal integration and crosstalk during thymocyte migration and emigration." Nat Rev Immunol **11**(7): 469-477.

Lu, M., R. Tayu, T. Ikawa, K. Masuda, I. Matsumoto, H. Mugishima, H. Kawamoto and Y. Katsura (2005). "The earliest thymic progenitors in adults are restricted to T, NK, and dendritic cell lineage and have a potential to form more diverse TCRbeta chains than fetal progenitors." J Immunol **175**(9): 5848-5856.

Lundberg, K., W. Heath, F. Kontgen, F. R. Carbone and K. Shortman (1995). "Intermediate steps in positive selection: differentiation of CD4+8int TCRint thymocytes into CD4-8+TCRhi thymocytes." J Exp Med **181**(5): 1643-1651.

Maier, H., R. Ostraat, H. Gao, S. Fields, S. A. Shinton, K. L. Medina, T. Ikawa, C. Murre, H. Singh, R. R. Hardy and J. Hagman (2004). "Early B cell factor cooperates with Runx1 and mediates epigenetic changes associated with mb-1 transcription." Nat Immunol **5**(10): 1069-1077.

Manilay, J. O. and M. Zouali (2014). "Tight relationships between B lymphocytes and the skeletal system." Trends in Molecular Medicine **20**(7): 405-412.

Manley, N. R. (2000). "Thymus organogenesis and molecular mechanisms of thymic epithelial cell differentiation." Semin Immunol **12**(5): 421-428.

Manley, N. R., E. R. Richie, C. C. Blackburn, B. G. Condie and J. Sage (2011). "Structure and function of the thymic microenvironment." Front Biosci (Landmark Ed) **16**: 2461-2477.

Mansour, A., G. Abou-Ezzi, E. Sitnicka, S. E. Jacobsen, A. Wakkach and C. Blin-Wakkach (2012). "Osteoclasts promote the formation of hematopoietic stem cell niches in the bone marrow." J Exp Med **209**(3): 537-549.

Mansour, A., A. Anginot, S. J. Mancini, C. Schiff, G. F. Carle, A. Wakkach and C. Blin-Wakkach (2011). "Osteoclast activity modulates B-cell development in the bone marrow." Cell Res **21**(7): 1102-1115.

Mansour, A., A. Wakkach and C. Blin-Wakkach (2012). "Role of osteoclasts in the hematopoietic stem cell niche formation." Cell Cycle **11**(11): 2045-2046.

Mansson, R., S. Zandi, E. Welinder, P. Tsapogas, N. Sakaguchi, D. Bryder and M. Sigvardsson (2010). "Single-cell analysis of the common lymphoid progenitor compartment reveals functional and molecular heterogeneity." Blood **115**(13): 2601-2609.

Maranda, B., G. Chabot, J. C. Decarie, M. Pata, B. Azeddine, A. Moreau and J. Vacher (2008). "Clinical and cellular manifestations of OSTM1-related infantile osteopetrosis." J Bone Miner Res **23**(2): 296-300.

Martins, V. C., K. Busch, D. Juraeva, C. Blum, C. Ludwig, V. Rasche, F. Lasitschka, S. E. Mastitsky, B. Brors, T. Hielscher, H. J. Fehling and H.-R. Rodewald (2014). "Cell competition is a tumour suppressor mechanism in the thymus." Nature **509**(7501): 465-470.

Martins, V. C., E. Ruggiero, S. M. Schlenner, V. Madan, M. Schmidt, P. J. Fink, C. von Kalle and H. R. Rodewald (2012). "Thymus-autonomous T cell development in the absence of progenitor import." J Exp Med **209**(8): 1409-1417.

Massa, S., G. Balciunaite, R. Ceredig and A. G. Rolink (2006). "Critical role for c-kit (CD117) in T cell lineage commitment and early thymocyte development in vitro." European Journal of Immunology **36**(3): 526-532.

Matsumoto, M., M. Kogawa, S. Wada, H. Takayanagi, M. Tsujimoto, S. Katayama, K. Hisatake and Y. Nogi (2004). "Essential role of p38 mitogen-activated protein kinase in cathepsin K gene expression during osteoclastogenesis through association of NFATc1 and PU.1." J Biol Chem **279**(44): 45969-45979.

Mazzolari, E., C. Forino, A. Razza, F. Porta, A. Villa and L. D. Notarangelo (2009). "A single-center experience in 20 patients with infantile malignant osteopetrosis." Am J Hematol **84**(8): 473-479.

McCaughtry, T. M., R. Etzensperger, A. Alag, X. Tai, S. Kurtulus, J. H. Park, A. Grinberg, P. Love, L. Feigenbaum, B. Erman and A. Singer (2012). "Conditional deletion of cytokine receptor chains reveals that IL-7 and IL-15 specify CD8 cytotoxic lineage fate in the thymus." J Exp Med **209**(12): 2263-2276.

Mebius, R. E., T. Miyamoto, J. Christensen, J. Domen, T. Cupedo, I. L. Weissman and K. Akashi (2001). "The fetal liver counterpart of adult common lymphoid progenitors gives rise to all lymphoid lineages, CD45+CD4+CD3- cells, as well as macrophages." J Immunol **166**(11): 6593-6601.

Medvinsky, A. L., N. L. Samoylina, A. M. Muller and E. A. Dzierzak (1993). "An early pre-liver intraembryonic source of CFU-S in the developing mouse." Nature **364**(6432): 64-67.

Mendelson, A. and P. S. Frenette (2014). "Hematopoietic stem cell niche maintenance during homeostasis and regeneration." Nat Med **20**(8): 833-846.

Mendes-da-Cruz, D. A., M. A. Stimamiglio, J. J. Muñoz, D. Alfaro, E. Terra-Granado, J. Garcia-Ceca, L. M. Alonso-Colmenar, W. Savino and A. G. Zapata (2012). "Developing T-cell migration: role of semaphorins and ephrins." The FASEB Journal **26**(11): 4390-4399.

Mendez-Ferrer, S., D. Lucas, M. Battista and P. S. Frenette (2008). "Haematopoietic stem cell release is regulated by circadian oscillations." Nature **452**(7186): 442-447.

Merchant, M. S. (2010). "Chaperoning the lympho-stromal dance." Blood **115**(12): 2334-2335.
Michie, A. M. and J. C. Zuniga-Pflucker (2002). "Regulation of thymocyte differentiation: pre-TCR signals and beta-selection." Semin Immunol **14**(5): 311-323.

Miller, J. F. (1961). "IMMUNOLOGICAL FUNCTION OF THYMUS." Lancet **2**(720): 748-&.
Misslitz, A., O. Pabst, G. Hintzen, L. Ohl, E. Kremmer, H. T. Petrie and R. Forster (2004). "Thymic T cell development and progenitor localization depend on CCR7." J Exp Med **200**(4): 481-491.

Miyamoto, K., S. Yoshida, M. Kawasumi, K. Hashimoto, T. Kimura, Y. Sato, T. Kobayashi, Y. Miyauchi, H. Hoshi, R. Iwasaki, H. Miyamoto, W. Hao, H. Morioka, K. Chiba, T. Kobayashi, H. Yasuda, J. M. Penninger, Y. Toyama, T. Suda and T. Miyamoto (2011). "Osteoclasts are dispensable for hematopoietic stem cell maintenance and mobilization." J Exp Med **208**(11): 2175-2181.

Miyamoto, T. (2011). "Regulators of osteoclast differentiation and cell-cell fusion." Keio J Med **60**(4): 101-105.

Miyamoto, T. (2013). "Role of osteoclasts in regulating hematopoietic stem and progenitor cells." World J Orthop **4**(4): 198-206.

Miyazaki, K., M. Miyazaki and C. Murre (2014). "The establishment of B versus T cell identity." Trends in Immunology **35**(5): 205-210.

Mohtashami, M., D. K. Shah, K. Kianizad, G. Awong and J. C. Zúñiga-Pflücker (2013). "Induction of T-cell development by Delta-like 4-expressing fibroblasts." International Immunology **25**(10): 601-611.

Mohtashami, M. and J. C. Zuniga-Pflucker (2006). "Three-dimensional architecture of the thymus is required to maintain delta-like expression necessary for inducing T cell development." J Immunol **176**(2): 730-734.

Monostori, E., G. Lang, D. Kioussis, D. A. Cantrell, R. Zamoyska, M. H. Brown and M. J. Crumpton (1991). "Human CD2 is functional in CD2 transgenic mice." Immunology **74**(3): 369-372.

Morrison, S. J., N. Uchida and I. L. Weissman (1995). "The biology of hematopoietic stem cells." Annual Review of Cell and Developmental Biology **11**: 35-71.

Morrison, S. J., A. M. Wandycz, H. D. Hemmati, D. E. Wright and I. L. Weissman (1997). "Identification of a lineage of multipotent hematopoietic progenitors." Development **124**(10): 1929-1939.

Mueller, C. G. and E. Hess (2012). "Emerging Functions of RANKL in Lymphoid Tissues." Front Immunol **3**: 261.

Mulcahy, L. E., D. Taylor, T. C. Lee and G. P. Duffy (2011). "RANKL and OPG activity is regulated by injury size in networks of osteocyte-like cells." Bone **48**(2): 182-188.

Mundy, G. R., B. Boyce, D. Hughes, K. Wright, L. Bonewald, S. Dallas, S. Harris, N. Ghosh-Choudhury, D. Chen, C. Dunstan and et al. (1995). "The effects of cytokines and growth factors on osteoblastic cells." Bone **17**(2 Suppl): 71s-75s.

Nagasawa, T. (2006). "Microenvironmental niches in the bone marrow required for B-cell development." Nat Rev Immunol **6**(2): 107-116.

Nakashima, T. and H. Takayanagi (2011). "New regulation mechanisms of osteoclast differentiation." Annals of the New York Academy of Sciences **1240**(1): E13-E18.

Negishi-Koga, T., M. Shinohara, N. Komatsu, H. Bito, T. Kodama, R. H. Friedel and H. Takayanagi (2011). "Suppression of bone formation by osteoclastic expression of semaphorin 4D." Nat Med **17**(11): 1473-1480.

Nicholls, B. M., R. G. M. Bredius, N. A. T. Hamdy, E. J. A. Gerritsen, A. C. Lankester, P. C. W. Hogendoorn, S. A. Nesbitt, M. A. Horton and A. M. Flanagan (2005). "Limited Rescue of Osteoclast-Poor Osteopetrosis After Successful Engraftment by Cord Blood From an Unrelated Donor." Journal of Bone and Mineral Research **20**(12): 2264-2270.

Nitta, T., S. Nitta, Y. Lei, M. Lipp and Y. Takahama (2009). "CCR7-mediated migration of developing thymocytes to the medulla is essential for negative selection to tissue-restricted antigens." Proc Natl Acad Sci U S A **106**(40): 17129-17133.

Olsen, B. R., A. M. Reginato and W. Wang (2000). "BONE DEVELOPMENT." Annual Review of Cell and Developmental Biology **16**(1): 191-220.

Omatsu, Y., T. Sugiyama, H. Kohara, G. Kondoh, N. Fujii, K. Kohno and T. Nagasawa (2010). "The essential functions of adipo-osteogenic progenitors as the hematopoietic stem and progenitor cell niche." Immunity **33**(3): 387-399.

Orchard, P. J., A. L. Fasth, J. Le Rademacher, W. He, J. J. Boelens, E. M. Horwitz, A. Al-Seraihy, M. Ayas, C. M. Bonfim, F. Boulad, T. Lund, D. K. Buchbinder, N. Kapoor, T. A. O'Brien, M. A. Perez, P. A. Veys and M. Eapen (2015). "Hematopoietic stem cell transplantation for infantile osteopetrosis." Blood **126**(2): 270-276.

Oreffo, R. O., C. Cooper, C. Mason and M. Clements (2005). "Mesenchymal stem cells: lineage, plasticity, and skeletal therapeutic potential." Stem Cell Rev **1**(2): 169-178.

Ott, C.-E., B. Fischer, P. Schröter, R. Richter, N. Gupta, N. Verma, M. Kabra, S. Mundlos, A. Rajab, H. Neitzel and U. Kornak (2013). "Severe neuronopathic autosomal recessive osteopetrosis due to homozygous deletions affecting OSTM1." Bone **55**(2): 292-297.

Oursler, M. J. (2010). "Recent advances in understanding the mechanisms of osteoclast precursor fusion." J Cell Biochem **110**(5): 1058-1062.

Pandruvada, S. N., J. Beauregard, S. Benjannet, M. Pata, C. Lazure, N. G. Seidah and J. Vacher (2015). "Role of Ostm1 Cytosolic Complex with Kinesin 5B in Intracellular Dispersion and Trafficking." Mol Cell Biol **36**(3): 507-521.

Pangrazio, A., B. Cassani, M. M. Guerrini, J. C. Crockett, V. Marrella, L. Zammataro, D. Strina, A. Schulz, C. Schlack, U. Kornak, D. J. Mellis, A. Duthie, M. H. Helfrich, A. Durandy, D. Moshous, A. Vellodi, R. Chiesa, P. Veys, N. Lo Iacono, P. Vezzoni, A. Fischer, A. Villa and C. Sobacchi (2012). "RANK-dependent autosomal recessive osteopetrosis: Characterization of five new cases with novel mutations." Journal of Bone and Mineral Research **27**(2): 342-351.

Pangrazio, A., P. L. Poliani, A. Megarbane, G. Lefranc, E. Lanino, M. Di Rocco, F. Rucci, F. Lucchini, M. Ravanini, F. Facchetti, M. Abinun, P. Vezzoni, A. Villa and A. Frattini (2006). "Mutations in OSTM1 (grey lethal) define a particularly severe form of autosomal recessive osteopetrosis with neural involvement." J Bone Miner Res **21**(7): 1098-1105.

Papathanasiou, P., J. L. Attema, H. Karsunky, N. Hosen, Y. Sontani, G. F. Hoyne, R. Tunningley, S. T. Smale and I. L. Weissman (2009). "Self-renewal of the long-term reconstituting subset of hematopoietic stem cells is regulated by Ikaros." Stem Cells **27**(12): 3082-3092.

Parfitt, A. M. (1994). "Osteonal and hemi-osteonal remodeling: the spatial and temporal framework for signal traffic in adult human bone." J Cell Biochem **55**(3): 273-286.

Pata, M., C. Heraud and J. Vacher (2008). "OSTM1 bone defect reveals an intercellular hematopoietic crosstalk." J Biol Chem **283**(45): 30522-30530.

Peaudecerf, L., S. Lemos, A. Galgano, G. Krenn, F. Vasseur, J. P. Di Santo, S. Ezine and B. Rocha (2012). "Thymocytes may persist and differentiate without any input from bone marrow progenitors." J Exp Med **209**(8): 1401-1408.

Pelus, L. M., H. Bian, A. G. King and S. Fukuda (2004). "Neutrophil-derived MMP-9 mediates synergistic mobilization of hematopoietic stem and progenitor cells by the combination of G-CSF and the chemokines GRObeta/CXCL2 and GRObetaT/CXCL2delta4." Blood **103**(1): 110-119.

Penit, C. (1987). "In vivo proliferation and differentiation of prothymocytes in the thymus." Immunol Res **6**(4): 271-278.

Penit, C. (1988). "Localization and phenotype of cycling and post-cycling murine thymocytes studied by simultaneous detection of bromodeoxyuridine and surface antigens." J Histochem Cytochem **36**(5): 473-478.

Perlot, T. and J. M. Penninger (2012). "Development and Function of Murine B Cells Lacking RANK." The Journal of Immunology **188**(3): 1201-1205.

Petrie, H. T. (2003). "Cell migration and the control of post-natal T-cell lymphopoiesis in the thymus." Nat Rev Immunol **3**(11): 859-866.

Petrie, H. T. and J. C. Zuniga-Pflucker (2007). "Zoned out: functional mapping of stromal signaling microenvironments in the thymus." Annu Rev Immunol **25**: 649-679.

Phee, H., B. B. Au-Yeung, O. Pryshchep, K. L. O'Hagan, S. G. Fairbairn, M. Radu, R. Kosoff, M. Mollenauer, D. Cheng, J. Chernoff and A. Weiss (2014). "Pak2 is required for actin cytoskeleton remodeling, TCR signaling, and normal thymocyte development and maturation." eLife **3**: e02270.

Phelan, J. D., I. Saba, H. Zeng, C. Kosan, M. S. Messer, H. A. Olsson, J. Fraszczak, D. A. Hildeman, B. J. Aronow, T. Moroy and H. L. Grimes (2013). "Growth factor independent-1 maintains Notch1-dependent transcriptional programming of lymphoid precursors." PLoS Genet **9**(9): e1003713.

Pillai, S. and A. Cariappa (2009). "The bone marrow perisinusoidal niche for recirculating B cells and the positive selection of bone marrow-derived B lymphocytes." Immunol Cell Biol **87**(1): 16-19.

Plotkin, J., S. E. Prockop, A. Lepique and H. T. Petrie (2003). "Critical role for CXCR4 signaling in progenitor localization and T cell differentiation in the postnatal thymus." J Immunol **171**(9): 4521-4527.

Porritt, H. E., K. Gordon and H. T. Petrie (2003). "Kinetics of steady-state differentiation and mapping of intrathymic-signaling environments by stem cell transplantation in nonirradiated mice." J Exp Med **198**(6): 957-962.

Porritt, H. E., L. L. Rumfelt, S. Tabrizifard, T. M. Schmitt, J. C. Zuniga-Pflucker and H. T. Petrie (2004). "Heterogeneity among DN1 prothymocytes reveals multiple progenitors with different capacities to generate T cell and non-T cell lineages." Immunity **20**(6): 735-745.

Porritt, H. E., L. L. Rumfelt, S. Tabrizifard, T. M. Schmitt, J. C. Zúñiga-Pflücker and H. T. Petrie (2004). "Heterogeneity among DN1 Prothymocytes Reveals Multiple Progenitors with Different Capacities to Generate T Cell and Non-T Cell Lineages." Immunity **20**(6): 735-745.

Prockop, S. E. and H. T. Petrie (2004). "Regulation of thymus size by competition for stromal niches among early T cell progenitors." J Immunol **173**(3): 1604-1611.

Pronk, C. J. H., D. J. Rossi, R. Månsson, J. L. Attema, G. L. Norddahl, C. K. F. Chan, M. Sigvardsson, I. L. Weissman and D. Bryder (2007). "Elucidation of the Phenotypic, Functional, and Molecular Topography of a Myeloerythroid Progenitor Cell Hierarchy." Cell Stem Cell **1**(4): 428-442.

Quarello, P., M. Forni, L. Barberis, C. Defilippi, M. F. Campagnoli, L. Silvestro, A. Frattini, N. Chalhoub, J. Vacher and U. Ramenghi (2004). "Severe malignant osteopetrosis caused by a GL gene mutation." J Bone Miner Res **19**(7): 1194-1199.

Radtke, F., H. R. MacDonald and F. Tacchini-Cottier (2013). "Regulation of innate and adaptive immunity by Notch." Nat Rev Immunol **13**(6): 427-437.

Rajapurohitam, V., N. Chalhoub, N. Benachenhou, L. Neff, R. Baron and J. Vacher (2001). "The mouse osteopetrotic grey-lethal mutation induces a defect in osteoclast maturation/function." Bone **28**(5): 513-523.

Ramirez, J., K. Lukin and J. Hagman (2010). "From hematopoietic progenitors to B cells: mechanisms of lineage restriction and commitment." Curr Opin Immunol **22**(2): 177-184.

Ramond, C., C. Berthault, O. Burlen-Defranoux, A. P. de Sousa, D. Guy-Grand, P. Vieira, P. Pereira and A. Cumano (2014). "Two waves of distinct hematopoietic progenitor cells colonize the fetal thymus." Nat Immunol **15**(1): 27-35.

Revest, J. M., R. K. Suniara, K. Kerr, J. J. Owen and C. Dickson (2001). "Development of the thymus requires signaling through the fibroblast growth factor receptor R2-IIIb." J Immunol **167**(4): 1954-1961.

Rickert, R. C., J. Roes and K. Rajewsky (1997). "B Lymphocyte-Specific, Cre-mediated Mutagenesis in Mice." Nucleic Acids Research **25**(6): 1317-1318.

Riddell, J., R. Gazit, B. S. Garrison, G. Guo, A. Saadatpour, P. K. Mandal, W. Ebina, P. Volchkov, G. C. Yuan, S. H. Orkin and D. J. Rossi (2014). "Reprogramming committed murine blood cells to induced hematopoietic stem cells with defined factors." Cell **157**(3): 549-564.

Rivera, J., R. L. Proia and A. Olivera (2008). "The alliance of sphingosine-1-phosphate and its receptors in immunity." Nat Rev Immunol **8**(10): 753-763.

Rodewald, H.-R., M. Ogawa, C. Haller, C. Waskow and J. P. DiSanto (1997). "Pro-Thymocyte Expansion by c-kit and the Common Cytokine Receptor γ Chain Is Essential for Repertoire Formation." Immunity **6**(3): 265-272.

Romas, E., M. T. Gillespie and T. J. Martin (2002). "Involvement of receptor activator of NFkappaB ligand and tumor necrosis factor-alpha in bone destruction in rheumatoid arthritis." Bone **30**(2): 340-346.

Rossi, F. M., S. Y. Corbel, J. S. Merzaban, D. A. Carlow, K. Gossens, J. Duenas, L. So, L. Yi and H. J. Ziltener (2005). "Recruitment of adult thymic progenitors is regulated by P-selectin and its ligand PSGL-1." Nat Immunol **6**(6): 626-634.

Rossi, S. W., M. Y. Kim, A. Leibbrandt, S. M. Parnell, W. E. Jenkinson, S. H. Glanville, F. M. McConnell, H. S. Scott, J. M. Penninger, E. J. Jenkinson, P. J. Lane and G. Anderson (2007). "RANK signals from CD4(+)3(-) inducer cells regulate development of Aire-expressing epithelial cells in the thymic medulla." J Exp Med **204**(6): 1267-1272.

Rothenberg, E. V. and D. D. Scripture-Adams (2008). "Competition and collaboration: GATA-3, PU.1, and Notch signaling in early T-cell fate determination." Seminars in Immunology **20**(4): 236-246.

Saltel, F., A. Chabadel, E. Bonnelye and P. Jurdic (2008). "Actin cytoskeletal organisation in osteoclasts: a model to decipher transmigration and matrix degradation." Eur J Cell Biol **87**(8-9): 459-468.

Sanchez-Fernandez, M. A., A. Gallois, T. Riedl, P. Jurdic and B. Hoflack (2008). "Osteoclasts control osteoblast chemotaxis via PDGF-BB/PDGF receptor beta signaling." PLoS One **3**(10): e3537.

Sato, K., A. Suematsu, K. Okamoto, A. Yamaguchi, Y. Morishita, Y. Kadono, S. Tanaka, T. Kodama, S. Akira, Y. Iwakura, D. J. Cua and H. Takayanagi (2006). "Th17 functions as an osteoclastogenic helper T cell subset that links T cell activation and bone destruction." J Exp Med **203**(12): 2673-2682.

Scadden, D. T. (2008). "Circadian rhythms: Stem cells traffic in time." Nature **452**(7186): 416-417.

Schachtner, H., S. D. Calaminus, S. G. Thomas and L. M. Machesky (2013). "Podosomes in adhesion, migration, mechanosensing and matrix remodeling." Cytoskeleton (Hoboken) **70**(10): 572-589.

Schatz, D. G. and P. C. Swanson (2011). "V(D)J recombination: mechanisms of initiation." Annu Rev Genet **45**: 167-202.

Schwarz, B. A. and A. Bhandoola (2006). "Trafficking from the bone marrow to the thymus: a prerequisite for thymopoiesis." Immunol Rev **209**: 47-57.

Scimone, M. L., I. Aifantis, I. Apostolou, H. von Boehmer and U. H. von Andrian (2006). "A multistep adhesion cascade for lymphoid progenitor cell homing to the thymus." Proc Natl Acad Sci U S A **103**(18): 7006-7011.

Seeman, E. (2009). "Bone modeling and remodeling." Crit Rev Eukaryot Gene Expr **19**(3): 219-233.

Seo, W., T. Ikawa, H. Kawamoto and I. Taniuchi (2012). "Runx1-Cbfbeta facilitates early B lymphocyte development by regulating expression of Ebf1." J Exp Med **209**(7): 1255-1262.

Shah, D. K. and J. C. Zuniga-Pflucker (2014). "An overview of the intrathymic intricacies of T cell development." J Immunol **192**(9): 4017-4023.

Shapiro-Shelef, M. and K. Calame (2005). "Regulation of plasma-cell development." Nat Rev Immunol **5**(3): 230-242.

Shinohara, T. and T. Honjo (1997). "Studies in vitro on the mechanism of the epithelial/mesenchymal interaction in the early fetal thymus." Eur J Immunol **27**(2): 522-529.

Shores, E. W., W. Van Ewijk and A. Singer (1994). "Maturation of medullary thymic epithelium requires thymocytes expressing fully assembled CD3-TCR complexes." Int Immunol **6**(9): 1393-1402.

Shortman, K. and L. Wu (1996). "Early T lymphocyte progenitors." Annu Rev Immunol **14**: 29-47.

Sigvardsson, M., D. R. Clark, D. Fitzsimmons, M. Doyle, P. Akerblad, T. Breslin, S. Bilke, R. Li, C. Yeamans, G. Zhang and J. Hagman (2002). "Early B-cell factor, E2A, and Pax-5 cooperate to activate the early B cell-specific mb-1 promoter." Mol Cell Biol **22**(24): 8539-8551.

Silver, I. A., R. J. Murrills and D. J. Etherington (1988). "Microelectrode studies on the acid microenvironment beneath adherent macrophages and osteoclasts." Exp Cell Res **175**(2): 266-276.

Sims, N., J. Quinn, T. Martin, J. Lorenzo, Y. Choi, M. Horowitz and H. Takayanagi "Coupling between immune and bone cells." Osteoimmunology: Interactions of the Immune and Skeletal Systems. 2nd ed. London: Academic Press (Forthcoming).

Sims, N. A. and T. J. Martin (2015). "Coupling Signals between the Osteoclast and Osteoblast: How are Messages Transmitted between These Temporary Visitors to the Bone Surface?" Front Endocrinol (Lausanne) **6**: 41.

Singer, A., S. Adoro and J. H. Park (2008). "Lineage fate and intense debate: myths, models and mechanisms of CD4- versus CD8-lineage choice." Nat Rev Immunol **8**(10): 788-801.

Sobacchi, C., A. Frattini, P. Orchard, O. Porras, I. Tezcan, M. Andolina, R. Babul-Hirji, I. Baric, N. Canham, D. Chitayat, S. Dupuis-Girod, I. Ellis, A. Etzioni, A. Fasth, A. Fisher, B. Gerritsen, V. Gulino, E. Horwitz, V. Klamroth, E. Lanino, M. Mirolo, A. Musio, G. Matthijs, S. Nonomaya, L. D. Notarangelo, H. D. Ochs, A. Superti Furga, J. Valiaho, J. L. van Hove, M. Vihinen, D. Vujic, P. Vezzoni and A. Villa (2001). "The mutational spectrum of human malignant autosomal recessive osteopetrosis." Hum Mol Genet **10**(17): 1767-1773.

Sobacchi, C., A. Schulz, F. P. Coxon, A. Villa and M. H. Helfrich (2013). "Osteopetrosis: genetics, treatment and new insights into osteoclast function." Nat Rev Endocrinol **9**(9): 522-536.

Staal, F. J., F. Weerkamp, M. R. Baert, C. M. van den Burg, M. van Noort, E. F. de Haas and J. J. van Dongen (2004). "Wnt target genes identified by DNA microarrays in immature CD34+ thymocytes regulate proliferation and cell adhesion." J Immunol **172**(2): 1099-1108.

Starr, T. K., S. C. Jameson and K. A. Hogquist (2003). "Positive and negative selection of T cells." Annu Rev Immunol **21**: 139-176.

Stefanova, I., J. R. Dorfman and R. N. Germain (2002). "Self-recognition promotes the foreign antigen sensitivity of naive T lymphocytes." Nature **420**(6914): 429-434.

Steffen, A., M. Ladwein, G. A. Dimchev, A. Hein, L. Schwenkmezger, S. Arens, K. I. Ladwein, J. Margit Holleboom, F. Schur, J. Victor Small, J. Schwarz, R. Gerhard, J. Faix, T. E. B. Stradal, C. Brakebusch and K. Rottner (2013). "Rac function is crucial for cell migration but is not required for spreading and focal adhesion formation." Journal of Cell Science **126**(20): 4572-4588.

Stritesky, G. L., Y. Xing, J. R. Erickson, L. A. Kalekar, X. Wang, D. L. Mueller, S. C. Jameson and K. A. Hogquist (2013). "Murine thymic selection quantified using a unique method to capture deleted T cells." Proc Natl Acad Sci U S A **110**(12): 4679-4684.

Suda, T., N. Takahashi, N. Udagawa, E. Jimi, M. T. Gillespie and T. J. Martin (1999). "Modulation of osteoclast differentiation and function by the new members of the tumor necrosis factor receptor and ligand families." Endocr Rev **20**(3): 345-357.

Surh, C. D., B. Ernst and J. Sprent (1992). "Growth of epithelial cells in the thymic medulla is under the control of mature T cells." J Exp Med **176**(2): 611-616.

Suzuki, H., J. A. Punt, L. G. Granger and A. Singer (1995). "Asymmetric signaling requirements for thymocyte commitment to the CD4+ versus CD8+ T cell lineages: a new perspective on thymic commitment and selection." Immunity **2**(4): 413-425.

Svensson, M., J. Marsal, H. Uronen-Hansson, M. Cheng, W. Jenkinson, C. Cilio, S. E. Jacobsen, E. Sitnicka, G. Anderson and W. W. Agace (2008). "Involvement of CCR9 at multiple stages of adult T lymphopoiesis." J Leukoc Biol **83**(1): 156-164.

Szewczyk, K. A., K. Fuller and T. J. Chambers (2013). "Distinctive subdomains in the resorbing surface of osteoclasts." PLoS One **8**(3): e60285.

Szydlowski, M., E. Jablonska and P. Juszczynski (2014). "FOXO1 transcription factor: a critical effector of the PI3K-AKT axis in B-cell development." Int Rev Immunol **33**(2): 146-157.

Tagaya, H., T. Kunisada, H. Yamazaki, T. Yamane, T. Tokuhisa, E. F. Wagner, T. Sudo, L. D. Shultz and S.-I. Hayashi (2000). "Intramedullary and extramedullary B lymphopoiesis in osteopetrotic mice." Blood **95**(11): 3363-3370.

Taghon, T., M. A. Yui, R. Pant, R. A. Diamond and E. V. Rothenberg (2006). "Developmental and molecular characterization of emerging beta- and gammadelta-selected pre-T cells in the adult mouse thymus." Immunity **24**(1): 53-64.

Tagliaferri, C., Y. Wittrant, M.-J. Davicco, S. Walrand and V. Coxam (2015). "Muscle and bone, two interconnected tissues." Ageing Research Reviews **21**: 55-70.

Takahama, Y. (2006). "Journey through the thymus: stromal guides for T-cell development and selection." Nat Rev Immunol **6**(2): 127-135.

Takayanagi, H. (2005). "Osteoimmunological insight into bone damage in rheumatoid arthritis." Mod Rheumatol **15**(4): 225-231.

Takayanagi, H. (2007). "Osteoimmunology: shared mechanisms and crosstalk between the immune and bone systems." Nat Rev Immunol **7**(4): 292-304.

Takeuchi, T., T. Tsuboi, M. Arai and A. Togari (2001). "Adrenergic stimulation of osteoclastogenesis mediated by expression of osteoclast differentiation factor in MC3T3-E1 osteoblast-like cells." Biochem Pharmacol **61**(5): 579-586.

Tan, J. T., B. Ernst, W. C. Kieper, E. LeRoy, J. Sprent and C. D. Surh (2002). "Interleukin (IL)-15 and IL-7 jointly regulate homeostatic proliferation of memory phenotype CD8+ cells but are not required for memory phenotype CD4+ cells." J Exp Med **195**(12): 1523-1532.

Tang, Y., X. Wu, W. Lei, L. Pang, C. Wan, Z. Shi, L. Zhao, T. R. Nagy, X. Peng, J. Hu, X. Feng, W. Van Hul, M. Wan and X. Cao (2009). "TGF-[beta]1-induced migration of bone mesenchymal stem cells couples bone resorption with formation." Nat Med **15**(7): 757-765.

Teague, T. K., C. Tan, J. H. Marino, B. K. Davis, A. A. Taylor, R. W. Huey and C. J. Van De Wiele (2010). "CD28 expression redefines thymocyte development during the pre-T to DP transition." International Immunology **22**(5): 387-397.

Teitelbaum, S. L. (2000). "Bone resorption by osteoclasts." Science **289**(5484): 1504-1508.
Teti, A. (2011). "Bone development: overview of bone cells and signaling." Curr Osteoporos Rep **9**(4): 264-273.

Teti, A. (2012). "Osteoclasts and hematopoiesis." Bonekey Rep **1**: 46.

Thompson, E. C., B. S. Cobb, P. Sabbattini, S. Meixlsperger, V. Parelho, D. Liberg, B. Taylor, N. Dillon, K. Georgopoulos, H. Jumaa, S. T. Smale, A. G. Fisher and M. Merkenschlager (2007). "Ikaros DNA-binding proteins as integral components of B cell developmental-stage-specific regulatory circuits." Immunity **26**(3): 335-344.

Titorencu, I., V. Pruna, V. V. Jinga and M. Simionescu (2014). "Osteoblast ontogeny and implications for bone pathology: an overview." Cell Tissue Res **355**(1): 23-33.

Tokoyoda, K., T. Egawa, T. Sugiyama, B. I. Choi and T. Nagasawa (2004). "Cellular niches controlling B lymphocyte behavior within bone marrow during development." Immunity **20**(6): 707-718.

Trampont, P. C., A. C. Tosello-Trampont, Y. Shen, A. K. Duley, A. E. Sutherland, T. P. Bender, D. R. Littman and K. S. Ravichandran (2010). "CXCR4 acts as a costimulator during thymic beta-selection." Nat Immunol **11**(2): 162-170.

Tran Van, P., A. Vignery and R. Baron (1982). "An electron-microscopic study of the bone-remodeling sequence in the rat." Cell Tissue Res **225**(2): 283-292.

Trapnell, C., A. Roberts, L. Goff, G. Pertea, D. Kim, D. R. Kelley, H. Pimentel, S. L. Salzberg, J. L. Rinn and L. Pachter (2012). "Differential gene and transcript expression analysis of RNA-seq experiments with TopHat and Cufflinks." Nat Protoc **7**(3): 562-578.

Trapnell, C., A. Roberts, L. Goff, G. Pertea, D. Kim, D. R. Kelley, H. Pimentel, S. L. Salzberg, J. L. Rinn and L. Pachter (2014). "Corrigendum: Differential gene and transcript expression analysis of RNA-seq experiments with TopHat and Cufflinks." Nat Protoc **9**(10): 2513.

Tussiwand, R., C. Engdahl, N. Gehre, N. Bosco, R. Ceredig and A. G. Rolink (2011). "The preTCR-dependent DN3 to DP transition requires Notch signaling, is improved by CXCL12 signaling and is inhibited by IL-7 signaling." Eur J Immunol **41**(11): 3371-3380.

Ueno, T., F. Saito, D. H. Gray, S. Kuse, K. Hieshima, H. Nakano, T. Kakiuchi, M. Lipp, R. L. Boyd and Y. Takahama (2004). "CCR7 signals are essential for cortex-medulla migration of developing thymocytes." J Exp Med **200**(4): 493-505.

Van De Wiele, C. J., J. H. Marino, B. W. Murray, S. S. Vo, M. E. Whetsell and T. K. Teague (2004). "Thymocytes between the β-Selection and Positive Selection Checkpoints Are Nonresponsive to IL-7 as Assessed by STAT-5 Phosphorylation." The Journal of Immunology **172**(7): 4235-4244.

van Ewijk, W., G. Hollander, C. Terhorst and B. Wang (2000). "Stepwise development of thymic microenvironments in vivo is regulated by thymocyte subsets." Development **127**(8): 1583-1591.

van Ewijk, W., B. Wang, G. Hollander, H. Kawamoto, E. Spanopoulou, M. Itoi, T. Amagai, Y.-F. Jiang, W. T. V. Germeraad, W.-F. Chen and Y. Katsura (1999). "Thymic microenvironments, 3-D versus 2-D?" Seminars in Immunology **11**(1): 57-64.

Vasseur, F., A. Le Campion and C. Pénit (2001). "Scheduled kinetics of cell proliferation and phenotypic changes during immature thymocyte generation." European Journal of Immunology **31**(10): 3038-3047.

Villa, A., M. M. Guerrini, B. Cassani, A. Pangrazio and C. Sobacchi (2009). "Infantile malignant, autosomal recessive osteopetrosis: the rich and the poor." Calcif Tissue Int **84**(1): 1-12.

von Andrian, U. H. and T. R. Mempel (2003). "Homing and cellular traffic in lymph nodes." Nat Rev Immunol **3**(11): 867-878.

von Boehmer, H. (2005). "Unique features of the pre-T-cell receptor [alpha]-chain: not just a surrogate." Nat Rev Immunol **5**(7): 571-577.

Wada, H., K. Masuda, R. Satoh, K. Kakugawa, T. Ikawa, Y. Katsura and H. Kawamoto (2008). "Adult T-cell progenitors retain myeloid potential." Nature **452**(7188): 768-772.

Wagner, J. E., J. N. Barker, T. E. DeFor, K. S. Baker, B. R. Blazar, C. Eide, A. Goldman, J. Kersey, W. Krivit, M. L. MacMillan, P. J. Orchard, C. Peters, D. J. Weisdorf, N. K. C. Ramsay and S. M. Davies (2002). "Transplantation of unrelated donor umbilical cord blood in 102 patients with malignant and nonmalignant diseases: influence of CD34 cell dose and HLA disparity on treatment-related mortality and survival." Blood **100**(5): 1611-1618.

Walker, E. C., N. E. McGregor, I. J. Poulton, M. Solano, S. Pompolo, T. J. Fernandes, M. J. Constable, G. C. Nicholson, J. G. Zhang, N. A. Nicola, M. T. Gillespie, T. J. Martin and N. A. Sims (2010). "Oncostatin M promotes bone formation independently of resorption when signaling through leukemia inhibitory factor receptor in mice." J Clin Invest **120**(2): 582-592.

Waskow, C., S. Paul, C. Haller, M. Gassmann and H. R. Rodewald (2002). "Viable c-Kit(W/W) mutants reveal pivotal role for c-kit in the maintenance of lymphopoiesis." Immunity **17**(3): 277-288.

Weerkamp, F., M. R. Baert, B. A. Naber, E. E. Koster, E. F. de Haas, K. R. Atkuri, J. J. van Dongen, L. A. Herzenberg and F. J. Staal (2006). "Wnt signaling in the thymus is regulated by differential expression of intracellular signaling molecules." Proc Natl Acad Sci U S A **103**(9): 3322-3326.

Wei, S., H. Kitaura, P. Zhou, F. P. Ross and S. L. Teitelbaum (2005). "IL-1 mediates TNF-induced osteoclastogenesis." J Clin Invest **115**(2): 282-290.

Weinreich, M. A. and K. A. Hogquist (2008). "Thymic emigration: when and how T cells leave home." Journal of immunology (Baltimore, Md. : 1950) **181**(4): 2265-2270.

Weissman, I. L. (2000). "Stem cells: Units of development, units of regeneration, and units in evolution." Cell **100**(1): 157-168.

Weissman, I. L. and J. A. Shizuru (2008). "The origins of the identification and isolation of hematopoietic stem cells, and their capability to induce donor-specific transplantation tolerance and treat autoimmune diseases." Blood **112**(9): 3543-3553.

Wiktor-Jedrzejczak, W., J. Grzybowski, A. Ahmed and L. Kaczmarek (1983). "Osteopetrosis associated with premature thymic involution in grey-lethal mice. In vitro studies of thymic microenvironment." Clin Exp Immunol **52**(3): 465-471.

Winandy, S., L. Wu, J. H. Wang and K. Georgopoulos (1999). "Pre-T cell receptor (TCR) and TCR-controlled checkpoints in T cell differentiation are set by Ikaros." J Exp Med **190**(8): 1039-1048.

Witt, C. M. and E. A. Robey (2004). "The ins and outs of CCR7 in the thymus." J Exp Med **200**(4): 405-409.

Wojciechowski, J., A. Lai, M. Kondo and Y. Zhuang (2007). "E2A and HEB are required to block thymocyte proliferation prior to pre-TCR expression." J Immunol **178**(9): 5717-5726.

Wong, B. R., R. Josien, S. Y. Lee, B. Sauter, H. L. Li, R. M. Steinman and Y. Choi (1997). "TRANCE (tumor necrosis factor [TNF]-related activation-induced cytokine), a new TNF family member predominantly expressed in T cells, is a dendritic cell-specific survival factor." J Exp Med **186**(12): 2075-2080.

Wong, S. H., J. A. Walker, H. E. Jolin, L. F. Drynan, E. Hams, A. Camelo, J. L. Barlow, D. R. Neill, V. Panova, U. Koch, F. Radtke, C. S. Hardman, Y. Y. Hwang, P. G. Fallon and A. N. J. McKenzie (2012). "Transcription factor ROR[alpha] is critical for nuocyte development." Nat Immunol **13**(3): 229-236.

Wright, D. E., A. J. Wagers, A. P. Gulati, F. L. Johnson and I. L. Weissman (2001). "Physiological migration of hematopoietic stem and progenitor cells." Science **294**(5548): 1933-1936.

Xi, H., R. Schwartz, I. Engel, C. Murre and G. J. Kersh (2006). "Interplay between RORgammat, Egr3, and E proteins controls proliferation in response to pre-TCR signals." Immunity **24**(6): 813-826.

Xian, L., X. Wu, L. Pang, M. Lou, C. J. Rosen, T. Qiu, J. Crane, F. Frassica, L. Zhang, J. P. Rodriguez, J. Xiaofeng, Y. Shoshana, X. Shouhong, E. Argiris, W. Mei and C. Xu (2012). "Matrix IGF-1 maintains bone mass by activation of mTOR in mesenchymal stem cells." Nat Med **18**(7): 1095-1101.

Xing, L., E. M. Schwarz and B. F. Boyce (2005). "Osteoclast precursors, RANKL/RANK, and immunology." Immunological Reviews **208**(1): 19-29.

Xing, L., Y. Xiu and B. F. Boyce (2012). "Osteoclast fusion and regulation by RANKL-dependent and independent factors." World J Orthop **3**(12): 212-222.

Xiong, J., M. A. Armato and T. M. Yankee (2011). "Immature single-positive CD8+ thymocytes represent the transition from Notch-dependent to Notch-independent T-cell development." Int Immunol **23**(1): 55-64.

Xu, M., A. Sharma, D. L. Wiest and J. M. Sen (2009). "Pre-TCR-induced beta-catenin facilitates traversal through beta-selection." J Immunol **182**(2): 751-758.

Xu, W., T. Carr, K. Ramirez, S. McGregor, M. Sigvardsson and B. L. Kee (2013). "E2A transcription factors limit expression of Gata3 to facilitate T lymphocyte lineage commitment." Blood **121**(9): 1534-1542.

Yagi, M., T. Miyamoto, Y. Sawatani, K. Iwamoto, N. Hosogane, N. Fujita, K. Morita, K. Ninomiya, T. Suzuki, K. Miyamoto, Y. Oike, M. Takeya, Y. Toyama and T. Suda (2005). "DC-STAMP is essential for cell-cell fusion in osteoclasts and foreign body giant cells." J Exp Med **202**(3): 345-351.

Yamashita, I., T. Nagata, T. Tada and T. Nakayama (1993). "CD69 cell surface expression identifies developing thymocytes which audition for T cell antigen receptor-mediated positive selection." International Immunology **5**(9): 1139-1150.

Yokota, T., J. Huang, M. Tavian, Y. Nagai, J. Hirose, J. C. Zuniga-Pflucker, B. Peault and P. W. Kincade (2006). "Tracing the first waves of lymphopoiesis in mice." Development **133**(10): 2041-2051.

Yokota, T., T. Sudo, T. Ishibashi, Y. Doi, M. Ichii, K. Orirani and Y. Kanakura (2013). "Complementary regulation of early B-lymphoid differentiation by genetic and epigenetic mechanisms." Int J Hematol **98**(4): 382-389.

Yu, Q., J. H. Park, L. L. Doan, B. Erman, L. Feigenbaum and A. Singer (2006). "Cytokine signal transduction is suppressed in preselection double-positive thymocytes and restored by positive selection." J Exp Med **203**(1): 165-175.

Yu, Y., J. Wang, W. Khaled, S. Burke, P. Li, X. Chen, W. Yang, N. A. Jenkins, N. G. Copeland, S. Zhang and P. Liu (2012). "Bcl11a is essential for lymphoid development and negatively regulates p53." J Exp Med **209**(13): 2467-2483.

Yui, M. A., N. Feng and E. V. Rothenberg (2010). "Fine-scale staging of T cell lineage commitment in adult mouse thymus." J Immunol **185**(1): 284-293.

Yui, M. A. and E. V. Rothenberg (2014). "Developmental gene networks: a triathlon on the course to T cell identity." Nat Rev Immunol **14**(8): 529-545.

Yun, T. J., M. D. Tallquist, A. Aicher, K. L. Rafferty, A. J. Marshall, J. J. Moon, M. E. Ewings, M. Mohaupt, S. W. Herring and E. A. Clark (2001). "Osteoprotegerin, a crucial regulator of bone metabolism, also regulates B cell development and function." J Immunol **166**(3): 1482-1491.

Zachariah, M. A. and J. G. Cyster (2010). "Neural crest-derived pericytes promote egress of mature thymocytes at the corticomedullary junction." Science **328**(5982): 1129-1135.

Zaidi, M., B. Troen, B. S. Moonga and E. Abe (2001). "Cathepsin K, osteoclastic resorption, and osteoporosis therapy." J Bone Miner Res **16**(10): 1747-1749.

Zepponi, V., V. Michaels Lopez, C. Martinez-Cingolani, A. Boudil, V. Pasqualetto, L. Skhiri, L. Gautreau, A. Legrand, J. Megret, F. Zavala and S. Ezine (2015). "Lymphoid Gene Upregulation on Circulating Progenitors Participates in Their T-Lineage Commitment." J Immunol **195**(1): 156-165.

Zhang, C., C. Dou, J. Xu and S. Dong (2014). "DC-STAMP, the Key Fusion-Mediating Molecule in Osteoclastogenesis." Journal of Cellular Physiology **229**(10): 1330-1335.

Zhang, J., C. Niu, L. Ye, H. Huang, X. He, W.-G. Tong, J. Ross, J. Haug, T. Johnson, J. Q. Feng, S. Harris, L. M. Wiedemann, Y. Mishina and L. Li (2003). "Identification of the haematopoietic stem cell niche and control of the niche size." Nature **425**(6960): 836-841.

Zhang, J. A., A. Mortazavi, B. A. Williams, B. J. Wold and E. V. Rothenberg (2012). "Dynamic transformations of genome-wide epigenetic marking and transcriptional control establish T cell identity." Cell **149**(2): 467-482.

Zhang, J. W., C. Niu, L. Ye, H. Y. Huang, X. He, W. G. Tong, J. Ross, J. Haug, T. Johnson, J. Q. Feng, S. Harris, L. M. Wiedemann, Y. Mishina and L. H. Li (2003). "Identification of the haematopoietic stem cell niche and control of the niche size." Nature **425**(6960): 836-841.

Zhao, C., N. Irie, Y. Takada, K. Shimoda, T. Miyamoto, T. Nishiwaki, T. Suda and K. Matsuo (2006). "Bidirectional ephrinB2-EphB4 signaling controls bone homeostasis." Cell Metab **4**(2): 111-121.

Zhao, Z., M. Zhao, G. Xiao and R. T. Franceschi (2005). "Gene transfer of the Runx2 transcription factor enhances osteogenic activity of bone marrow stromal cells in vitro and in vivo." Mol Ther **12**(2): 247-253.

Zhou, X. and J. Platt (2011). Molecular and Cellular Mechanisms of Mammalian Cell Fusion. Cell Fusion in Health and Disease. T. Dittmar and K. Zänker, Springer Netherlands. **713:** 33-64.

Zhu, J., R. Garrett, Y. Jung, Y. Zhang, N. Kim, J. Wang, G. J. Joe, E. Hexner, Y. Choi, R. S. Taichman and S. G. Emerson (2007). "Osteoblasts support B-lymphocyte commitment and differentiation from hematopoietic stem cells." Blood **109**(9): 3706-3712.

Zlotoff, D. A. and A. Bhandoola (2011). "Hematopoietic progenitor migration to the adult thymus." Ann N Y Acad Sci **1217**: 122-138.

Zlotoff, D. A., A. Sambandam, T. D. Logan, J. J. Bell, B. A. Schwarz and A. Bhandoola (2010). "CCR7 and CCR9 together recruit hematopoietic progenitors to the adult thymus." Blood **115**(10): 1897-1905.

Zuniga-Pflucker, J. C. (2009). "The original intrathymic progenitor from which T cells originate." J Immunol **183**(1): 3-4.

APPENDIX 3: COPYRIGHT LICENCE AGREEMENTS